

The Effect of Fuel on Automotive Lubricant Degradation

By

Peter Robert Hurst

A thesis submitted in partial fulfilment of the requirements for the degree
of Doctor of Philosophy

University of York
Department of Chemistry

March 2013

Abstract

Fuel is known to mix with automotive lubricants during cold starting of the engine, leading to fuel contamination in the sump. The effect that fuel contamination has on lubricant degradation is not well understood, so is investigated for this work. The effect of selected fuel components representative of naphthalenes and bioethanol on the degradation of partially formulated and model base oils has been examined by oxidation in bench top reactors under temperature conditions representative of those found in engines with fuel dilution levels representative of those found in the field.

The ethanol treatment of squalane samples containing 1% (w/w) dispersant promoted reverse micelle formation, confirmed by laser scattering and UV-VIS analysis using Nile red as a marker. The ethanol treated samples were found to be significantly more stable to oxidation in comparison to the untreated sample. It is proposed in the literature that the increased oxidative stability is due to the ability of the reverse micelle to act as an alkyl peroxide trap. This in turn reduces the bulk alkyl peroxide concentration which reduces the reaction rate of the radical chain mechanism.

A mechanism has been proposed in this work for the effect of reverse micelles on the autoxidation of branched hydrocarbons. In this work it is suggested that alkyl peroxides formed during autoxidation of the bulk hydrocarbon migrate to the reverse micelle. Once inside the alkyl peroxide can undergo decomposition in the presence of other alkyl peroxides away from the bulk hydrocarbon to form less reactive radicals. This work highlights the need to fully understand the effect of heterogeneity on the autoxidation of hydrocarbons.

1-methylnaphthalene was observed to inhibit the autoxidation of squalane at 150 °C while present in solution. A computational method has been devised to accurately calculate the carbon oxygen bond strength in the alkyl peroxy radical.

Contents

Abstract	iii
List of Figures	xi
List of Tables	xix
Acknowledgements.....	xxi
Author's Declaration	xxiii
1: Introduction.....	2
<i>Chapter Overview</i>	2
1.1: Lubrication Introduction	2
1.2: Engine Conditions Affecting Lubricant Degradation.....	4
1.3: Oxidation of Automotive Engine Lubricants	9
1.4: The Use of Antioxidants in Automotive Engine Lubricants.....	14
1.5: The Chemical Oxidation of Conventional Gasoline.....	16
1.6: Effect of Conventional Gasoline on Automotive Lubricant Degradation	21
1.7: Effect of Bioethanol on Automotive Lubricant Degradation.....	30
1.8: Conclusion and Thesis Aims	32
2: Experimental.....	34
2.1: Bench Top Oxidation Apparatus.....	34
2.1.1: Continuous Flow Reactor Set Up.....	34
2.1.2: Continuous Flow Reactor Set Up for Bio-Fuel Work.....	37
2.1.3: Continuous Flow Reactor Set Up for Conventional Fuel	38
2.2: Model Ethanol Fuel Dilution.....	38
2.2.1: Ethanol Treated Method.....	38
2.3: Chemical Analysis	40
2.3.1: Gas Chromatography (GC)	40
2.3.2: Gas Chromatography Coupled with Mass Spectrometry (GC-MS).....	41
2.3.3: Gel Permeation Chromatography (GPC).....	42
2.3.4: Laser Technique for Determining Scattering of Sample	42
2.3.5: UV-VIS Spectroscopy	43
2.3.6: Confocal Microscopy.....	44
2.3.7: Determination of Oxygen Uptake	44
2.3.8: Determination of Additive Additive Synergies.....	46

2.4: Materials Employed	47
3: Effect of Non-Antioxidant Additive Interactions on Lubricant Degradation	50
<i>Chapter Overview</i>	50
3.1: Introduction.....	50
3.2: Effect of Composition on the Antioxidant Properties of Aminic Antioxidants.....	52
3.2.1: Effect of Dispersant on the Autoxidation of Squalane Containing Aminic Antioxidant.....	52
3.2.2: Effect of Dispersant and Detergent on the Inhibition by Aminic Antioxidants on the Autoxidation of Squalane	59
3.2.3: Effect of Composition on the Properties of Aminic Antioxidants.....	60
3.3: Effect of Composition on the Antioxidant Properties of Phenolic Antioxidants..	63
3.3.1: Effect of Detergent on the Autoxidation of Squalane with Phenolic Antioxidant.....	64
3.3.2: Effect of Dispersant on the Autoxidation of Squalane with Phenolic Antioxidant.....	66
3.3.3: Effect of Dispersant and Detergent on the Autoxidation of a Squalane Sample Containing 0.25% (w/w) Phenolic Antioxidant	67
3.3.4: Effect of Composition on the Properties of Phenolic Antioxidants.....	68
3.4: Effect of Composition on the Autoxidation of Squalane Containing ZDDP	70
3.4.1: Effect of Coating on the Oxidative Stability of Model Lubricants	70
3.4.2: Effect of a Phenolic Antioxidant on the Autoxidation of Squalane Containing ZDDP	74
3.4.3: Effect of a Dispersant and Detergent on the Autoxidation of a Squalane Sample Containing ZDDP and Phenolic Antioxidant	75
3.4.4: Effect of Composition on the Antioxidant Properties of ZDDP	76
3.5: Conclusions.....	79
4: Effect of Ethanol on Model Automotive Lubricant Degradation.....	82
<i>Chapter Overview</i>	82
4.1: Introduction.....	82
4.2: Results	84
4.2.1: Effect of Ethanol on the Autoxidation of Squalane Samples Containing a Phenolic Antioxidant	84
4.2.2: Effect of Ethanol on the Autoxidation of Squalane Samples Containing a Diphenyl Aminic Antioxidant.....	94

4.2.3: Effect of Ethanol on the Autoxidation of Squalane Samples Containing ZDDP.....	98
4.3: Discussion.....	102
4.3.1: Effect of Ethanol on the Autoxidation of Model Lubricants Incorporating Primary Antioxidants.....	102
4.3.2: Effect of Ethanol on the Autoxidation of Model Lubricants Incorporating ZDDP.....	104
4.4: Conclusions.....	105
5: Characterisation of Reverse Micelles through Optical and Spectroscopic Methods.....	106
<i>Chapter Overview</i>	106
5.1: Introduction.....	106
5.2: Laser Scattering.....	110
5.3: Analysis of Samples Using Fluorescent Label for Reverse Micelle.....	114
5.3.1: UV-VIS Using Nile Red as a Fluorescent Label.....	114
5.3.2: Nile Red Analysis in Confocal Microscopy.....	118
5.4: Summary and Conclusions.....	123
6: Effect of Micellar Media on the Autoxidation of Hydrocarbons.....	126
<i>Chapter Overview</i>	126
6.1: Introduction.....	126
6.1.1: Previous Work on the Effect of Reverse Micelles on the Autoxidation of Hydrocarbons.....	126
6.1.2: Effect of Normal Micelles on the Efficiency of Antioxidants – The “Polar Paradox”.....	136
6.2: Similarities between Reverse Micelle Theory and the “Polar Paradox”.....	150
6.3: Relationship between the Work Presented in this Thesis and the Work in the Field.....	151
6.4: Micelle Mechanism with No Antioxidant.....	152
6.5: Micelle Mechanism in the Presence of a Bulk Antioxidant.....	156
6.6: Summary of the Proposed Mechanism.....	159
6.7: Evidence for the Phenolic Antioxidant Being a Bulk Additive.....	161
6.8: How this Mechanism Compares to Existing Literature.....	164

6.8.1: Comparisons to Bakunin’s Work on Reverse Micelles.....	164
6.8.2: Can the Proposed Mechanism be Utilised to Understand the “Polar Paradox”	165
6.9: Conclusions.....	167
7: Effect of 1-Methylnaphthalene on the Autoxidation of Squalane.....	170
<i>Chapter Overview</i>	170
7.1: Introduction.....	170
7.2: Results and Discussion	174
7.2.1: Effect of 1-Methylnaphthalene on the Autoxidation of Squalane.....	174
7.2.2: Product Identification.....	177
7.3: Possible 1-Methylnaphthalene Autoxidation Mechanism	184
7.4: Ab-initio Thermocalculations of Ceiling Temperatures	184
7.4.1: Ceiling Temperature Determination.....	185
7.4.2: Gaussian Method Development	186
7.4.3: Testing the Model for the Level of Theory	186
7.4.4: Thermochemical Calculations of Selected 1-methylnaphthalene Adducts	188
7.4.5: Ceiling Temperature Calculation	189
7.4.6: 1-Ethylnaphthalene as a Model for Polyalkylated Naphthalene Base Oils	193
7.5: Conclusions.....	195
8: Summary and Conclusions	198
<i>Chapter Overview</i>	198
8.1: Conclusions.....	198
8.2: Recommendations for Future Work	199
8.2.1: Effect of Surfactant on Reverse Micelle Formation.....	199
8.2.2: Effect of Altering the Bulk Additive Package.....	199
8.2.3: More Robust Imaging Methods	200
Appendix.....	202
A.1: Volatile Loss and Lifetime of 1-Methylnaphthalene	202
A.1.1: Determination of Volatile Loss by Calculation.....	203
A.1.2: 1-Methylnaphthalene Volatility under an Inert Atmosphere at 150 °C	208
A2: Effect of 2 nd Generation Bio-fuel on Automotive Lubricant Degradation	213

<i>Chapter Overview</i>	213
A2.1: Introduction	213
A2.2: Results.....	215
A2.2.1: Calculated Loss of 2 nd Generation Bio-Fuels Due to Volatility at 150 °C	215
A2.2.2: Calculated Loss of 2 nd Generation Bio-Fuels due to Volatility at 100 °C.	217
A2.3: Discussion	219
A2.4: Conclusions	222
Abbreviations.....	224
References	226

List of Figures

Figure 1.1: Schematic Diagram of a Spark Ignition Engine (http://www.radford.edu/~wkovarik/papers/fuel.html#auto).....	6
Scheme 1.1: Free Radical Mechanism of Hydrocarbon Oxidation [13, 31, 32].....	10
Figure 1.2: 2,6,10,14 tetramethylpentadecane (Pristane, C ₁₉ H ₄₀).....	11
Figure 1.3: 2,6,10,15,19,23 hexamethyltetracosane (Squalane, C ₃₀ H ₆₂).....	12
Figure 1.4: An Example of an Radical Scavenging 2,4,6-tritert-butylphenol,.....	14
Figure 1.5: An Example of an Radical Scavenging 4-tert-butyl-N-(4-tert-butylphenyl)aniline.....	14
Figure 1.6: 2-(1-cyano-1-methyl-ethyl)azo-2-methyl-propanenitrile (azobisisobutyronitrile, C ₈ H ₁₂ N ₄).....	17
Scheme 1.4: Addition of Peroxyl Radical to 1-methylnaphthalene Ring Leading to the Formation of Non-Radical Products [46].....	18
Scheme 1.5: Oxidation Mechanism of 1-methylnaphthalene at 927 °C Proposed by Shaddix [47].....	19
Scheme 1.6: The Proposed Mechanism for the Formation of 3-methyl-1(3H)- isobenzofuranone by Ehrhardt [48].....	20
Figure 1.7: Pyrene (C ₁₆ H ₁₀).....	22
Figure 1.8: Phenanthrene (C ₁₄ H ₁₀).....	24
Figure 1.9: Fluoranthene (C ₁₆ H ₁₀).....	24
Figure 1.10: Benzo[ghi]perylene (C ₂₂ H ₁₂).....	25
Scheme 1.7: Oxidation of 1-methylnaphthalene via Hydrogen Abstraction [46].....	27
Scheme 1.8: Mechanism for the Addition of the Alkyl Peroxide to 1-Methylnaphthalene [46].....	28
Scheme 1.9: The Hydroperoxyl Alkylperoxyl Cross Reaction [46].....	29
Scheme 1.10: The Hydroperoxyl Self Reaction [46].....	29
Figure 1.11: Phthalic Acid [46].....	30
Figure 1.12: 2-Acetylbenzoic Acid [46].....	30
Figure 2.1: Picture of stainless steel reactor with 49 cm ³ internal volume.....	34
Figure 2.2: Schematic Diagram of the Stainless Steel High Temperature Oxidation Reactor.....	36
Figure 2.3: The effect of ethanol dilution on a commercially available automotive lubricant, before mixing (A), mixed (B) and settled (C).....	40

Figure 2.4: Laser Scattering of Untreated (Left Hand Side) and Ethanol Treated (Right Hand Side) Squalane Sample Containing 1% (w/w) Dispersant, 1% (w/w) Detergent and 0.25% (w/w) Phenolic Antioxidant 43

Figure 3.1: 4-(1,1,3,3-tetramethylbutyl)-N-[4-(1,1,3,3-tetramethylbutyl)phenyl]aniline (Commercial name Irganox L01, called here in abbreviation AmAO) 52

Figure 3.2: Effect of 0.18 % (w/w) Aminic Antioxidant on the Autoxidation of Squalane at 180 °C and 1 Bar of O₂..... 53

Figure 3.3: Succinimide Dispersant..... 54

Figure 3.4: Effect of 1% (w/w) Dispersant on the Oxidative Stability of a Model Lubricant Composing 0.18% (w/w) Aminic Antioxidant at 180 °C and 1 Bar of O₂..... 54

Figure 3.5: Effect of 1% (w/w) Dispersant on the Chemical Degradation of Squalane at 180 °C and 1 Bar of O₂..... 55

Figure 3.6: Determination of the Synergistic Effect between 1% (w/w) Succinimide Dispersant and 0.18% (w/w) Aminic Antioxidant at 180 °C..... 56

Figure 3.7: Effect of Succinimide Dispersant and Aminic Antioxidant on the Autoxidation of Squalane at 180 °C and 1 Bar of O₂ 57

Figure 3.10: Effect of 1% (w/w) Detergent (Det) and Dispersant (Disp) on the Autoxidation of 0.18 % (w/w) Aminic Antioxidant (AmAO) Containing Squalane (Squ) Samples at 180 °C and 1 Bar of O₂..... 60

Figure 3.11: octadecyl 3-(3,5-ditert-butyl-4-hydroxyphenyl)propanoate (Irganox L107, PhAO)..... 63

Figure 3.12: Effect of 0.25% (w/w) Phenolic Antioxidant on the Autoxidation of Squalane at 180 °C and 1 Bar of O₂..... 64

Figure 3.13: Neutral Calcium Detergent..... 65

Figure 3.14: Effect of 1% (w/w) Detergent on the Autoxidation of Squalane Containing 0.25% (w/w) Phenolic Antioxidant at 180 °C and 1 Bar of O₂ 66

Figure 3.18: Zincdialkyldithiophosphate (ZDDP) 71

Figure 3.19: Effect of ZDDP Tribofilm Formation on the Autoxidation of Squalane Consisting of Repeated Runs Using 1% (w/w) ZDDP at 180 °C and 1 Bar of O₂..... 72

Figure 3.20: Effect of ZDDPTribofilm Formation on the Autoxidation of Squalane at 180 °C and 1 Bar of O₂ Compared to that of Squalane with 0.25% (w/w) Phenolic Antioxidant in a Clean Reactor..... 73

Figure 3.21: Effect of 1% (w/w) ZDDP on the Autoxidation of Squalane Containing 0.25% (w/w) Phenolic Antioxidant at 180 °C and 1 Bar of O₂ 74

Figure 3.22: Determination of the Synergistic Effect Between a Phenolic Antioxidant and ZDDP.....	74
Figure 3.23: Effect of 1% (w/w) Dispersant and 1% (w/w) Detergent on the Autoxidation of Squalane Consisting of 1% (w/w) ZDDP and 0.25% (w/w) Phenolic Antioxidant at 180 °C and 1 Bar of O ₂	75
Figure 3.24: Effect of 1% (w/w) Detergent (Det) Dispersant (Disp) and ZDDP on the Autoxidation of 0.25% (w/w) Phenolic Antioxidant (PhAO) Containing Squalane (Squ) Samples at 180 °C and 1 Bar of O ₂	76
Figure 3.25: Schematic Diagram of ZDDP Tribofilm Structure and Composition [78] ..	77
Figure 3.26: Diagram of Comparison Between a ZDDP Coated Reactor (Left Hand Side) and a Non-Coated Reactor (Right Hand Side).....	78
Figure 4.1: GC Analysis of the Ethanol Treated Sample Before and After the Heating Period.....	86
Figure 4.2: Effect of Ethanol on the Autoxidation of Squalane at 180 °C and 1 Bar of O ₂	87
Figure 4.3: Effect of Ethanol on the Autoxidation of Squalane with 0.25% (w/w) Phenolic Antioxidant at 180 °C and 1 Bar of O ₂	88
Figure 4.4: Effect of Ethanol on the Autoxidation of Squalane with 1% (w/w) Detergent at 180 °C and 1 Bar of O ₂	89
Figure 4.5: Effect of Ethanol on the Autoxidation of Squalane with 0.25% (w/w) Phenolic Antioxidant and 1% (w/w) Detergent at 180 °C and 1 Bar of O ₂	90
Figure 4.6: Effect of Ethanol on the Autoxidation of Squalane with 1% (w/w) Dispersant at 180 °C and 1 Bar of O ₂	91
Figure 4.9: 4-(1,1,3,3-tetramethylbutyl)-N-[4-(1,1,3,3-tetramethylbutyl)phenyl]aniline (Irganox L01, AmAO).....	94
Figure 4.10: Effect of Ethanol on the Autoxidation of Squalane with 0.18% (w/w) Aminic Antioxidant at 180 °C and 1 Bar of O ₂	95
Figure 4.11: Effect of Ethanol on the Autoxidation of Squalane with 0.18% (w/w) Aminic Antioxidant and 1% (w/w) Dispersant at 180 °C and 1 Bar of O ₂	96
Figure 4.14: Effect of Ethanol on the Autoxidation of Squalane with 1% (w/w) ZDDP and 0.25% Phenolic Antioxidant (PhAO) at 180 °C and 1 Bar of O ₂	100
Figure 4.21: Effect of Ethanol on Model Lubricants with Phenolic Antioxidant (PhAO) as the Primary Antioxidant and ZDDP as the Secondary Antioxidant at 180 °C and 1 Bar of O ₂	104

Figure 5.3: 9-diethylamino-5-benzo[α]phenoxazinone (Nile Red, Nile Blue Oxazone) 107

Figure 5.1: Schematic of a Typical Laser Scanning Confocal Microscope, [104] 109

Figure 5.2: Process for Reducing Background Haze in Confocal Microscopy, [104].. 110

Figure 5.4: Photograph Showing the Level of Light Scattering in Undiluted by Ethanol (Left), Ethanol Diluted (Middle) and Ethanol Treated (Right) Squalane Samples Containing 1% (w/w) Dispersant, 1% (w/w) Detergent and 0.25% (w/w) Phenolic Antioxidant 112

Figure 5.6: UV-VIS Spectra Showing the Absorbances of Nile Red in Polar (Ethanol and Propan-2-ol) and Non Polar Solvents (Squalane and Hexane), Nile Red:Lubricant Ratio 1:1x10⁶ 115

Figure 5.7: UV-VIS Spectra of Nile Red Doped Untreated and Ethanol Treated Squalane Samples Containing 1% (w/w) Dispersant, 1% (w/w) Detergent and 0.25% (w/w) Phenolic Antioxidant (L107), Nile Red Employed in a Ratio of 1:1x10⁶ (Nile Red:Lubricant) 116

Figure 5.8: Comparison of Nile Red Colouring of Squalane (1), Squalane with 1% (w/w) Dispersant, 1% (w/w) Detergent and 0.25% (w/w) Phenolic Antioxidant (L107) Untreated (2), Ethanol Diluted (3) and Ethanol Treated (4), Nile Red Employed in a Ratio of 1:1x10⁶ (Nile Red:Lubricant) 118

Figure 5.9: Confocal Microscopy of Ethanol Diluted Squalane Sample Containing 10% (w/w) Dispersant, 10% (w/w) Detergent and 2.5% (w/w) Phenolic Antioxidant (L107) with Nile Red Marker..... 120

Figure 5.10: Confocal Microscopy of Ethanol Diluted Squalane Sample Containing 10% (w/w) dispersant, 10% (w/w) Detergent and 2.5% (w/w) Phenolic Antioxidant (L107) with Nile Red Marker..... 121

Figure 5.12: Confocal Microscopy of Ethanol Diluted 100% (w/w) Squalane with Nile Red Marker 123

Figure 6.1: Sodium 4-[(E)-(4-dimethylaminophenyl)azo]benzenesulfonate 127 (Methyl Orange)..... 127

Figure 6.2: Bakunin’s Proposed Mechanism for the Introduction of Reverse Micelles into a Lubricant [100, 119, 121, 123]..... 129

Figure 6.3: Heterolytic Decomposition of a Secondary Alkyl Peroxide into Non-Radical Products [158]..... 130

Figure 6.4: Heterolytic Decomposition of a Secondary Alkyl Peroxide into Non-Radical Products 130

Figure 6.5: Bakunin's Proposed Three Phase System upon Addition of Reverse Micelles into a Non Polar Medium [117].....	131
Figure 6.6: Sodium 1,4-bis(2-ethylhexoxy)-1,4-dioxobutane-2-sulfonate (AOT)	132
Figure 6.7: Sodium N,N-diethylcarbamodithioate (DTC- C ₂)	132
Figure 6.8: 2,6-ditert-butyl-3-[(2,4-ditert-butyl-3-hydroxy-phenyl)methyl]phenol	135
Figure 6.9: Butylatedhydroxytoluene (BHT)	138
Figure 6.10: 3,4,5-Trihydroxybenzoic acid (Gallic Acid)	138
Figure 6.11: Butylatedhydroxytoluene (BHT)	140
Figure 6.12: 4-Hydroxymethyl-2,6-ditertiarybutylphenol	140
Figure 6.13: 2,5,7,8-Tetramethyl-2-(1,5,9,13-tetramethyltetradecyl)chroman-6-ol (α tocopherol).....	140
Figure 6.14: 2,7-Dimethyl-2-(1,5,9,13-tetramethyltetradecyl)chroman-6-ol (δ tocopherol).....	141
Figure 6.16: [(2S)-2-[(2R)-4,5-Dihydroxy-3-oxo-2-furyl]-2-hydroxy-ethyl] Hexadecanoate (ascorbyl palmitate).....	143
Figure 6.17: (2R)-2-[(1S)-1,2-Dihydroxyethyl]-3,4-dihydroxy-2H-furan-5-one (ascorbic acid).....	143
Figure 6.18: 6-Hydroxy-2,5,7,8-tetramethyl-chromane-2-carboxylic acid (Trolox®)...	143
Figure 6.19: Antioxidant Activity of Ascorbic Acid and Ascorbyl Palmitate in Stripped Corn Oil [122]	144
Figure 6.20: Antioxidant Activity of Trolox and α -Tocopherol in Stripped Corn Oil [122]	145
Figure 6.21: Antioxidant Activity of Gallic Acid and Lauryl Gallate in Stripped Corn Oil [122]	145
Figure 6.22: Antioxidant Activity of Epigallocatechin Gallate (EGCG) and EGCG-C18 in Stripped Corn Oil [122]	145
Figure 6.23: Example of Antioxidant Concentration Reaching Maximum Efficiency at 180 °C and O ₂ Pressure of 1 Bar, see Chapter 3	146
Figure 6.24: [5,7-Dihydroxy-2-(3,4,5-trihydroxyphenyl)chroman-3-yl] 3,4,5-trihydroxybenzoate (epigallocatechin gallate, EGCG)	147
Figure 6.24: 2-Octadecoxyethanol (Brij 76).....	148
Figure 6.25: Reverse Micelle Autoxidation Mechanism	153
Figure 6.26: Alkyl Peroxide Decomposition inside a Peroxide Rich Environment i.e. Reverse Micelle [149]	154
Figure 6.27: Net Reaction for the Bulk Decomposition of Alkyl Peroxides.....	155

Figure 6.28: Net Reaction for the Reverse Micelle Decomposition of Alkyl Peroxide. 155

Figure 6.31 & 6.32: Effect of Ethanol on the Autoxidation of Squalane with 0.25% (w/w) Phenolic Antioxidant (PhAO), 0.3% (w/w) Aminic Antioxidant (AmAO), 1% (w/w) Dispersant (Disp) and 1% (w/w) Detergent (Det) at 180 °C and 1 Bar of O₂ (AmAO, Det Not Carried Out)..... 157

Figure 6.33: Reverse Micelle Autoxidation Mechanism in the Presence of an Antioxidant..... 158

Figure 6.35: Effect of 1% (w/w) Dispersant on the Chemical Degradation of Squalane at 180 °C and 1 Bar of O₂..... 160

Figure 6.36: Effect of Phenolic Antioxidant (PhAO), Dispersant (Disp) and Detergent (Det) on Reverse Micelle Formation using Nile Red as a Marker in UV-VIS, using a Nile Red:Lubricant Ratio of 1:1x10⁶ 162

Figure 6.37: Effect of Reverse Micelle Formation on the Break Point of Ethanol Treated Squalane Samples Containing 1% (w/w) Dispersant (Disp), Detergent (Det) and 0.25% (w/w) Phenolic Antioxidant (PhAO) at 180 °C and 1 bar O₂..... 163

Figure 7.1: Autoxidation Mechanism of 1-methylnaphthalene Proposed by Ingold [45, 46] 172

Figure 7.2: Mechanism for the Addition of the Alkyl Peroxide to the 1-methylnaphthalene [45 & 46] 173

Figure 7.3: Hydroperoxyl-alkylperoxyl Cross Termination Reaction 173

Figure 7.4: Hydroperoxyl-hydroperoxyl Termination Reaction..... 173

Figure 7.5: Effect of 5% (v/v) 1-methylnaphthalene on the Autoxidation of Squalane at 150 °C and an Oxygen Flow Rate of 0.1 dm³ min⁻¹ at a O₂ Pressure of 1 Bar 174

Figure 7.6: Effect of 5% (v/v) 1-methylnaphthalene on the Autoxidation of Squalane at 150 °C and an Oxygen Flow rate of 0.03 dm³ min⁻¹ at a O₂ Pressure of 1 Bar..... 175

Figure 7.7: Effect of 5% (v/v) 1-methylnaphthalene on the Autoxidation of Squalane at 130 °C and a Oxygen Flow Rate of 0.1 dm³ min⁻¹ at an O₂ Pressure of 1 Bar 176

Figure 7.8: Effect of 5% (v/v) 1-methylnaphthalene on the Autoxidation of Squalane at 130 °C and an Oxygen Flow rate of 0.03 dm³ min⁻¹ at an O₂ Pressure of 1 Bar..... 177

Figure 7.9: GC-MS(EI) Analysis of Starting Material at T=0, Performed on an Agilent DB5-HT Column (30m x 0.32mm)..... 178

Figure 7.10: GC-MS(EI) Analysis of Oxidised 100% 1-methylnaphthalene at 150 °C and Sealed Reaction, Performed on an Agilent DB5-HT Column (30m x 0.32mm) 179

Figure 7.11: GC-MS(EI) Analysis of Oxidised 100% 1-methylnaphthalene after 240 Minutes at 150 °C in a Sealed Reaction at 1 Bar Pressure of O ₂ , Performed on an Agilent DB5-HT Column (30m x 0.32mm)	179
Figure 7.12: GC-MS(EI) Fragmentation Pattern of Peak with Retention Time 35 Minutes Proposed to be a 1-methylnaphthalene Dehydrodimer, Performed on an Agilent DB5-HT Column (30m x 0.32mm)	180
Figure 7.14: GPC Analysis of Squalane with 5% (v/v) 1-methylnaphthalene Prior to Oxidation (t=0)	182
Figure 7.15: GPC Analysis of Squalane with 5% (v/v) 1-methylnaphthalene after 90 Minutes at a Temperature of 150 °C and a Gas Flow Rate of 0.1 dm ³ min ⁻¹	182
Figure 7.16: GPC Polystyrene Standard Weight Calibration Curve Run on a Phenomenex Phenogel 50Å Column (300 x 4.6mm) with a Tetrahydrofuran Flow Rate of 0.350 ml min ⁻¹	183
Figure 7.17: Formation of the methylnaphthylperoxyl Radical	189
Figure 7.18: Ceiling Temperatures of 1-methylnaphthalene (Square), Toluene (Triangle), Allyl (Diamond) and Ethane (Cross) Calculated using the DFT B3PW91 6-311G ++ (3df) Method	190
Table 7.5: Thermochemical Data for the Para Resonance 1-methylnaphthyl Structure Calculated using Gaussian 09w Running the DFT B3PW91 6-311G ++(3df) Method and Basis Set	191
Table 7.6: Estimated Ceiling Temperature for Reaction R + O ₂ → R-OO Employing the DFT B3PW91 6-311G ++(3df) Method.....	191
Figure 7.20: 1-ethylnaphthalene	194
Figure 7.25: R-OO Bond Formation on the Two Resonance Structures of 1-ethylnaphthalene	195
Figure A1.2: Calculated volatile loss of 1-methylnaphthalene compared to observed experimental loss of 1-methylnaphthalene at 130 °C with an O ₂ flow rate of 0.1 dm ³ min ⁻¹ at a O ₂ pressure of 1 bar	205
Figure A1.3: First order plot of the observed loss of 1-methylnaphthalene with the volatile loss at 150 °C, 0.1 dm ³ min ⁻¹ and 1 bar absolute.....	206
Figure A1.4: First order plot of the observed loss of 1-methylnaphthalene with the volatile loss at 130 °C, 0.1 dm ³ min ⁻¹ and 1 bar absolute.....	206
Figure A1.5: Effect on squalane concentration of 5% 1-methylnaphthalene dilution at 150 °C with 0.1 dm ³ min ⁻¹ N ₂ flow rate at 1 bar absolute	208

Figure A1.6: Difference in the rate of loss of 1-methylnaphthalene under an nitrogen atmosphere with the loss observed under an oxygen atmosphere at 150 °C, 0.1 dm³min⁻¹ and 1 bar absolute 209

Figure A1.7: Plot of the difference in the rate of loss of 1-methylnaphthalene under an nitrogen atmosphere with the loss observed under an oxygen atmosphere at 150 °C, 0.03 dm³ min⁻¹ and 1 bar absolute 211

Figure A2.1: 2,5-dimethylfuran 214

Figure A2.2: butanol..... 214

Figure A2.3: ethyl valerate 214

Figure A2.4: The calculated volatile loss of 2,5-dimethylfuran, ethyl valerate, butanol and 1-methylnaphthalene at 150 °C and a gas flow rate of 0.03 dm³ min⁻¹ 216

Figure A2.5: The calculated volatile loss of 2,5-dimethylfuran, ethyl valerate, butanol and 1-methylnaphthalene at 100 °C and a gas flow rate of 0.03 dm³ min⁻¹ 218

Figure A2.12: Laser scattering of butanol treated squalane sample containing 0.25% (w/w) Phenolic Antioxidant, 1% (w/w) Dispersant and 1% (w/w) Detergent 221

Figure A2.13: Laser scattering of ethyl valerate treated squalane sample containing 0.25% (w/w) Phenolic Antioxidant, 1% (w/w) Dispersant and 1% (w/w) Detergent ... 221

Figure A2.14: Laser scattering of 2,5-dimethylfuran treated squalane sample containing 0.25% (w/w) Phenolic Antioxidant, 1% (w/w) Dispersant and 1% (w/w) Detergent ... 222

List of Tables

Table 1.1: Typical Carbon-Hydrogen Dissociation Energies [36].....	11
Table 1.2: Bond Dissociation Energies of Typical C-H's [36].....	26
Table 2.1: Table of Specific Reactor Details	35
Table 2.2: Table Showing Equipment Specifics	37
Table 3.1: Determination of Synergistic Effect Observed for Aminic Antioxidants and Dispersant used in this Study using Equation 2.3	58
Table 3.2: The effect of dispersant on the break point and reaction rate constant of the autoxidation of squalane at 180 °C	70
Table 5.1: Results of the Laser Scattering Analysis of the Effect of Ethanol Treatment on Squalane Containing 1% (w/w) Dispersant, 1% (w/w) Detergent, 0.3% (w/w) Aminic Antioxidant and 0.25% (w/w) Phenolic Antioxidant.....	113
Table 7.1: R-OO Bond Dissociation Energies of C ₂ H ₅ -OO, C ₃ H ₅ -OO and (C ₆ H ₅)CH ₂ OO Calculated using Different Methods and Basis Sets Based on Published Experimental Values. [159] Values in Brackets Display the Deviance From the Mean	187
Table 7.2: R-H Bond Dissociation Energies of C ₂ H ₅ -H, C ₃ H ₅ -H and (C ₆ H ₅)CH ₂ -H Calculated using Different Methods and Basis Sets Based on Published Experimental Values. [85, 159-161] Values in Brackets Display the Deviance From the Mean	187
Table 7.3: Thermochemical Data for 1-methylnaphthalene Calculated Using Gaussian 09w Running the DFT B3PW91 6-311G ++(3df) Method and Basis Set	188
Table 7.4: Estimated Ceiling Temperature for Reaction R + O ₂ → R-OO Employing the DFT B3PW91 6-311G ++(3df) Method.....	189
Table 7.7: Thermochemical data for 1-ethylnaphthalene Calculated using Gaussian 09w Running the DFT B3PW91 6-311G ++(3df) Method and Basis Set	194
Table 7.8: Estimated Ceiling Temperature for Reaction R + O ₂ → R-OO Employing the DFT B3PW91 6-311G ++(3df) Method.....	195
Table A1.1: Calculation of rate of reaction k_r	207
Table A1.2: Comparison of the two methods employed to calculate the rate constant for the volatile loss of 1-methylnaphthalene at 150 °C and a gas flow rate of 0.1 dm ³ min ⁻¹	210
Table A2.1: Model reaction details used to calculate the rate of volatile loss of the model fuel component	215
Table A2.2: Model reaction details used to calculate the rate of volatile loss of the model fuel component	217

Table A2.3: Calculated pseudo first order rate constant for the volatile loss of the fuel component at a flow rate of $0.03 \text{ dm}^3\text{min}^{-1}$ 219

Acknowledgements

To start with I would like to thank Dr Moray Stark for his excellent supervision and encouragement during the research programme.

I would also like to thank my industrial supervisor Dr Robert Ian Taylor at Shell Global Solutions for his support and would also like to thank Dr Chris Padden and Dr Dennis Kruchinin for their valuable input during the early stages of this work. Thanks also go to Prof. Martin Priest, Dr Peter Lee and Prashan De Silva who provided many helpful comments and suggestions during the regular project meetings. I am indebted to Shell Global Solutions for their financial support during this project.

Thanks go to Gareth, Jimbo and Bernadeta who were always supportive and made the last four years fun. I would also like to thank everyone in Green Chemistry past and present, too many to name but I hope to see you soon, who have made these four years enjoyable. However many thanks must go to Dr Andy Hunt and Dr Rob McElroy for proof reading my chapters and offering valuable advice and encouragement during the writing up stage. I would also like to thank my friends from back home Rick, Martin and Sarah who have always been supportive during this period of my life. I would also like to thank Paul Elliott for his bad jokes and assistance it was greatly appreciated.

Finally I would like to thank my family and in particular my Dad who has been so supportive during these years. He did not just proof read my thesis but was also a sounding board during the hard times, I don't think words can express my gratitude.

Author's Declaration

I declare that this PhD thesis entitled “The Effect of Fuel on Automotive Lubricant Degradation” has been compiled by myself under the supervision of Dr Moray Stark.

The confocal microscopy analysis present in chapter 5 was performed by K. Hodgkinson at the Technology Facility in the Department of Biology at the University of York.

1: Introduction

Chapter Overview

In this chapter a literature review on the effect of fuel dilution on engine lubricant degradation will be presented. The topics will cover the autoxidation of the lubricant under laboratory conditions, the mechanism of fuel dilution and the main areas of the automotive engine where the lubricant functions.

1.1: Lubrication Introduction

Lubricants are required in most machinery, from high temperature applications in for example, internal combustion engines to low temperature applications for example, disk drives. Their use is critical in reducing the energy losses due to friction, therefore resulting in more efficient machinery. For automotive lubricants a reduction in friction results in less CO₂ being emitted from the exhaust per kilometre travelled, and, with ever tighter CO₂ emissions regulations due to the European emissions standards, this will be beneficial. [1, 2] In September (2009) the Euro 5 standard was implemented, that limited the level of CO₂ from new car emissions to 120 g/km. [3]

One way of reducing the CO₂ emissions of cars currently on the road is by improving the lubricant lifetime and therefore reducing the friction for longer. [4, 5] The advantages are not as great as would be from improving aerodynamics but gains can be made. There therefore has been a lot of interest in the automotive lubrication field recently in the degradation processes of the lubricant, and in improving the lubricant formulation. [4] Automotive lubricants are also employed to combat wear in an engine, and are required wherever any surfaces are in contact. [6] If there was no lubricant present in the engine it would rapidly stop working due to damage to the engine.

One of the important properties of the lubricant is the viscosity; it is required to be sufficiently viscous enough to provide a protective film between moving parts, however if the viscosity is too high this can also increase the friction

between moving parts of an engine. [6] A lubricant, particularly for an engine, is also required to be resistant to oxidation, thought to be the main cause of lubricant degradation. [7] The oxidative degradation of automotive lubricants is detrimental to the viscosity of the lubricant, as if the lubricant undergoes degradation the viscosity can increase, resulting in increased friction, a decrease in efficiency and hence an increase in CO₂ emissions into the atmosphere. [6]

Lubricants are often complex mixtures of chemicals, with the main component typically being a hydrocarbon base oil. [8] Base oils are usually derived from mineral oil and classified in terms of their quality, from group I through to IV, the standards for which are defined by the American Petroleum Institute. The higher the group number the more refined the base oil will be, [9] typically group I are derived from petroleum cracking. Group IV are synthetic base oils and are generally molecules which are known to have a high oxidative stability.

In addition to the base oil a lubricant will also contain an additive package incorporated into the finished product. [10] The additive package typically contains an antioxidant which will compete against and prevent the oxidative degradation of the lubricant. [6] There will also be dispersants as well as detergents which will clean the engine during use; they keep any solid degradation products suspended in a solution therefore preventing their aggregation. Those are two types of additives which are incorporated into the lubricant formulation but there are many others which are employed. These include friction and viscosity modifiers, corrosion and rust inhibitors and metal deactivators. [11]

The process of formulating an automotive lubricant which provides protection against oxidation while also delivering an optimum viscosity throughout the lifetime of the lubricant requires a considerable skill. An automotive lubricant has to undergo many tests before it is brought onto the market. [12] The first stage of testing is generally in the lab in bench top reactors that aim to simulate in some way conditions in an engine.[12] An example of such test is the

Robotest which evaluates the effect of pour point depressants on the low temperature properties of used oils. In a Robotest the lubricant is combined with a small amount of iron catalyst and is placed in a 1 litre reactor. The sample is then reacted with air and nitrogen dioxide for a period of 40 hours at 170 °C, after which the lubricant is cooled and tested. Any formulations which show positive results in the laboratory are then taken onto the next testing stage which is a static engine test. [12] However, just because there is a positive outcome in the lab does not necessarily mean it will correlate with the engine test. There is a significant interest in improving the bench top techniques so that they mimic the static engine tests more closely. This would result in a cost reduction in the testing of lubricant formulations.

The next stage of the testing formulation is field engine tests of a new lubricant formulation, these are more realistic, but less controlled than the static engine tests, which are highly controlled; once it passes the fleet test stage the lubricant will then be able to go onto the market. [12] There are a number of stages in the testing procedure and by improving certain aspects one could significantly reduce costs.

There has been a significant level of research investigating the degradation pathways of model lubricant base oils in the laboratory. [2, 13, 14] This allows a detailed understanding of the mechanisms which cause the degradation of the lubricant by oxidation to be understood. In comparison, the chemical effects of fuel on automotive lubricant degradation are generally less well understood in the lab, with most of the research undertaken in research engines. [15-21]

1.2: Engine Conditions Affecting Lubricant Degradation

Before bench top tests can be undertaken an understanding of the physical conditions that the lubricant is exposed to in an engine is required, which will allow a bench top test to be more representative. There are three distinct areas in the engine where the lubricant is in operation, the sump, valve train and the piston ring pack, where the lubricant is applied between the cylinder wall and

the piston to reduce friction, Figure 1.1. [7, 22-24] The lubricant can undergo degradation in both these areas; however, it is the piston ring pack where the majority of the degradation occurs [24] due to the very harsh conditions the lubricant is exposed too, which can be chemical and physical, in the combustion chamber.

In an internal combustion engine the energy is produced via the compression of an air-fuel mixture in the combustion chamber which, followed by combustion, results in high temperatures as well as a gaseous mixture of carbon oxides and hydrocarbons. [25] Most internal spark ignition combustion engines are four stroke therefore having four basic steps during its operation. [26] The first of these steps is the intake step where the inlet valve opens allowing the air fuel mixture to be drawn into the combustion chamber, by the piston moving down the cylinder. [26] Once a sufficient volume has been drawn in the inlet valve closes and the mixture is then compressed, the compression step. [26] This high pressure mixture is then ignited which forces the piston down driving the crank which allows a portion of the fuel's chemical energy to be released as work, the final step is the exhaust step where the outlet valve opens allowing the gaseous mixture of carbon dioxide, carbon monoxide and fuel or oxygen to go through to the exhaust. In order to seal the combustion chamber rings are attached to the piston (called the piston ring pack) and this ring pack also regulates the oil consumption, while also supporting heat transfer from the piston to the cylinder. [7] As these rings are subjected to the harsh environments it has been suggested that the majority of lubricant degradation occurs here. [23, 24, 27]

While the lubricant is in the sump it is in large volume and under relatively mild conditions, when compared to the piston ring pack, therefore it could be expected to undergo slow oxidation. [24] When the lubricant is pumped through to the piston ring pack it is exposed to high temperatures, typically between 115 and 180 °C, high pressures and blow-by gases (a compressed air and fuel mixture) from the combustion process all of which can affect lubricant

degradation. [24] Therefore by analysing the transport of the lubricant between the sump and the piston ring pack a greater understanding can be gained.

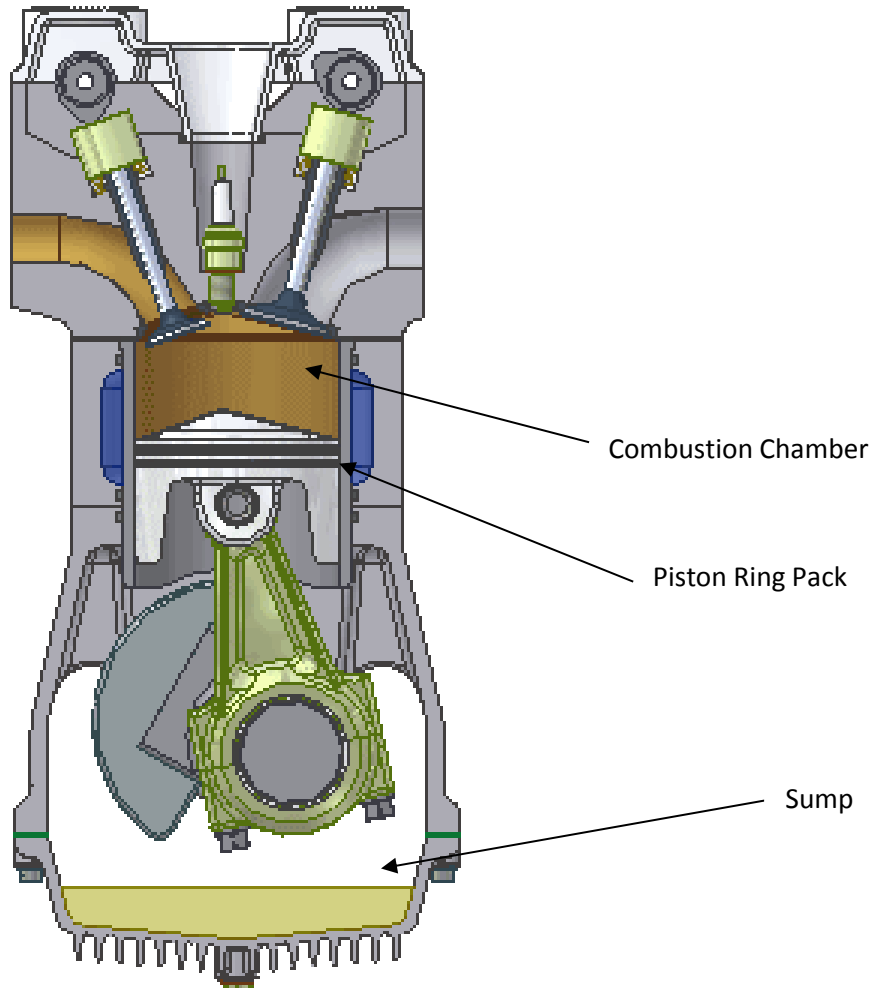


Figure 1.1: Schematic Diagram of a Spark Ignition Engine
(<http://www.radford.edu/~wkovarik/papers/fuel.html#auto>)

This area has seen some research activity, particularly investigating the chemical processes which are involved in the lubricants degradation of which oxidation. [14, 28, 29] The work typically investigates possible components which can compete against the chemical rate determining steps in the degradation pathway, either inhibiting the degradation or promoting it.

Saville et al studied the lubricant condition in the piston ring pack of a single cylinder diesel engine. [30] This was achieved by removing samples directly

from the piston ring pack through a PTFE tube which was connected to the inside of the piston. Another study was undertaken by Stark who investigated the composition of the lubricant in the piston ring pack, using the same sampling technique as Saville. [30] This was to ascertain how long the lubricant stayed in the ring pack before flowing back to the sump and how much of the oil was in the ring pack. The tests were undertaken using a modified gasoline engine where two systems of lubricant supply were employed. One system was supplying the camshafts and the second system supplied oil to the rest of the engine. The sump was maintained externally at 70 °C to ensure little oxidation occurred in the sump and thus the degradation seen would only be due to the ring pack environment.

To ensure rapid degradation the lubricant did not have any antioxidants added to it and to measure the flow of the lubricant a marker was used which was less prone to oxidation than the lubricant. [20] This was achieved by using a molecule which contains no tertiary hydrogen atoms (which are more likely to be abstracted by a radical the marker used was octadecane and an internal standard of hexadecane was employed. Thus the ratio of marker to internal standard in the ring pack would be able to be measured and the residence time could be ascertained. In this paper it was found that the sump residence time being 185 ± 5 hours litre⁻¹cylinder⁻¹ and the flow rate of 0.36 ± 0.02 cm³ min⁻¹ cylinder⁻¹ from ring pack to sump. [20] This paper gives an insight into where the main areas of degradation occur (being the ring pack).

Further work by Moritani investigated the degradation of lubricating oil in the second land region of a gasoline engine piston. [24] To monitor the lubricant degradation Moritani employed three methods, Total Acid Number (TAN), which is the amount of Potassium Hydroxide to neutralize the acids in one gram of oil, Total Base Number (TBN), a measure of the basic content of the lubricant and Infra Red (IR) spectroscopy, monitoring the carbonyl content. [24] They found that oxidation of the lubricant was occurring at a faster rate in the piston region of the engine assembly where the lubricant is exposed to high temperatures and oxidising gases, O₂ and NOx's. [24] This leads to an increase in oxidation

products resulting in an increase in TAN. To compete against the formation of the oxidation products a lubricant will have a number of antioxidants added to the mixture, the TBN is a measure of the antioxidant content in the lubricant. Therefore as the TAN is increasing the TBN should decrease as the antioxidants are depleted in trying to halt the oxidation of the lubricant. The increase in the degradation of the lubricant in the land region was suggested by Moritani to be due to the increase in temperature in the crankcase and the harsh conditions it endures. This is an example of the data one can get from engine tests, it is not as detailed chemically and is generally quantifying the effects of the harsh conditions on the lubricant.

The composition of blow-by gases was also investigated by Moritani. [24] Gas samples were taken at the same time as the oil sample, which were then analyzed for hydrocarbon, NO_x and oxygen content. Hydrocarbons were measured by directly connecting the sample tube to the gas chromatogram. It was found that the blow-by gases influenced the degradation of the lubricant while the concentration of the hydrocarbons tended to increase at higher rotational speeds and loads and by comparison the extent of lubricant degradation in the second land region was found to be higher than in the crankcase. This part of the research is interesting as it links the effect of blow-by gases to the rate of degradation, however it does not give any mechanisms or products which are produced.

It can be seen that from the work undertaken by Moritani that the degradation of the lubricant is occurring predominately in the piston assembly where the lubricant is exposed to high temperatures, resulting in a decrease in TBN and an increase in TAN. [24] The temperature of the piston ring pack was also measured by Moritani and found to be 115 °C to 160 °C, which compares well to work undertaken by Taylor which suggests 180 °C. [24] Therefore, for any bench top test to be representative of the conditions observed in the engine, the temperature range stated by Moritani should be employed.

1.3: Oxidation of Automotive Engine Lubricants

As mentioned previously, it is understood that the primary cause for the chemical degradation of the lubricant is by oxidation at high temperatures in the piston ring pack. [24] The reaction of the lubricant with oxygen is an example of a free radical reaction which is initiated by the abstraction by an oxygen molecule of a hydrogen atom from the base oil, which is usually a long chain branched hydrocarbon, reaction 1 in Scheme 1.1. [31, 32]

The alkyl radical, $R\cdot$, will undergo propagation reactions predominately by addition of an oxygen molecule to form an alkylperoxyl radical, $RO_2\cdot$; reaction 2. [31, 32] The alkylperoxyl radical can abstract a hydrogen atom from another molecule of the hydrocarbon resulting in the formation of another alkyl radical and an alkylperoxide, reaction 3. [31, 32] This step is often referred to as the chain reaction step and it is this reaction for which antioxidants are designed to compete against. [33] Other radicals can also abstract a hydrogen atom, for example, reactions 4 and 5 are also chain reactions resulting in the formation of additional alkyl radicals. [31, 32] The resultant alkylperoxide formed in the chain reaction step, Scheme 1.1 reaction 3, can undergo homolysis due to the weak oxygen-oxygen bond, Scheme 1.1 reaction 6, forming the alkoxy, $RO\cdot$, and hydroxyl, $OH\cdot$, radicals, this step is called the chain branching step as it increases the number of radicals present, and hence the rate of reaction, also the alkoxy radical is the precursor to the majority of the degradation products observed during hydrocarbon oxidation. [31, 32] For the radical chain reactions to not grow exponentially indefinitely two radicals must come together and form non-radical products, this is the termination step. [31, 32]

Phase	Reaction	Reaction Number
Initiation	$\text{RH} + \text{O}_2 \rightarrow \text{R}\cdot + \cdot\text{OOH}$	1
Propagation	$\text{R}\cdot + \text{O}_2 \rightarrow \text{ROO}\cdot$	2
	$\text{ROO}\cdot + \text{RH} \rightarrow \text{R}\cdot + \text{ROOH}$	3
Branching	$\text{ROOH} \rightarrow \text{RO}\cdot + \cdot\text{OH}$	4
	$\text{RO}\cdot + \text{RH} \rightarrow \text{ROH} + \text{R}\cdot$	5
	$\cdot\text{OH} + \text{RH} \rightarrow \text{HOH} + \text{R}\cdot$	6
	$\text{HOO}\cdot + \text{RH} \rightarrow \text{HOOH} + \text{R}\cdot$	7
Termination	$\text{R}\cdot + \text{R}'\cdot \rightarrow \text{RR}'$	8
	$\text{R}\cdot + \text{R}'\text{OO}\cdot \rightarrow \text{R}'\text{OOR}$	9
	$\text{ROO}\cdot + \text{R}'\text{OO}\cdot \rightarrow \text{Products}$	10

Scheme 1.1: Free Radical Mechanism of Hydrocarbon Oxidation [13, 31, 32]

Jensen and Korcek studied the autoxidation of hexadecane in a bench top reactor at temperatures ranging from 160-180 °C, where hydroperoxides were identified as the primary oxidation products. [34] But under the relatively high temperatures employed the hydroperoxides decompose by cleaving across the weak oxygen-oxygen bond producing the alkoxy and hydroxyl radicals which further oxidise on to secondary oxidation products, such as ketones, alcohols, carboxylic acids and esters. Later work by Blaine and Savage [14] on the autoxidation of n-hexadecane are derived from this mechanism.

The work by Blaine et al and Jensen et al on the oxidation of a long chain unbranched hydrocarbon is not completely representative of a base oil degradation. [14,34] As described earlier base oils are typically branched long

chain hydrocarbons, thus the radical attack can occur at one of three sites as branched hydrocarbon possesses three hydrogen sites, primary, secondary and tertiary C-H sites, that have differing C-H bond dissociation energies. The resulting bond dissociation energies and the stability of the radical are directly related, the more stable the radical formed the lower the bond dissociation energy. [35] So from analysis of the bond dissociation energies of the three hydrogen sites, Table 1.1, it can be seen that the radical attack would be expected to occur mainly at the tertiary site, resulting in a tertiary alkyl radical.

Table 1.1: Typical Carbon-Hydrogen Dissociation Energies [36]

C-H Bond	C-H Bond	Bond Dissociation Energy (kJ mol ⁻¹)
CH ₃ -CH ₂ -CH ₂ -CH ₂ -H	Primary C-H	421.3
CH ₃ -CH(CH ₂ CH ₃)-H	Secondary C-H	411 ± 2
CH ₃ CH(CH ₃)C(CH ₃) ₂ -H	Tertiary C-H	399 ± 14

Stark et al, examined the mechanisms of pristane (2,6,10,14 tetramethylpentadecane, C₁₉H₄₀), Figure 1.2, and squalane (2,6,10,15,19,23-hexamethyltetracosane, C₃₀H₆₂), Figure 1.3, oxidation to investigate the selectivity of the oxidation reaction, as tertiary, secondary and primary hydrogens are present in ratios resembling a typical base oil. [13]

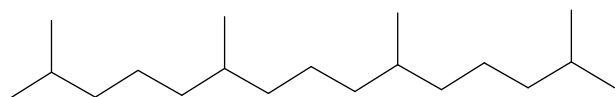


Figure 1.2: 2,6,10,14 tetramethylpentadecane (Pristane, C₁₉H₄₀)

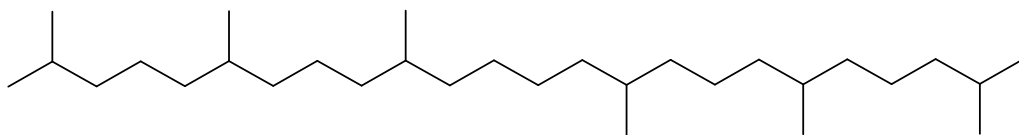
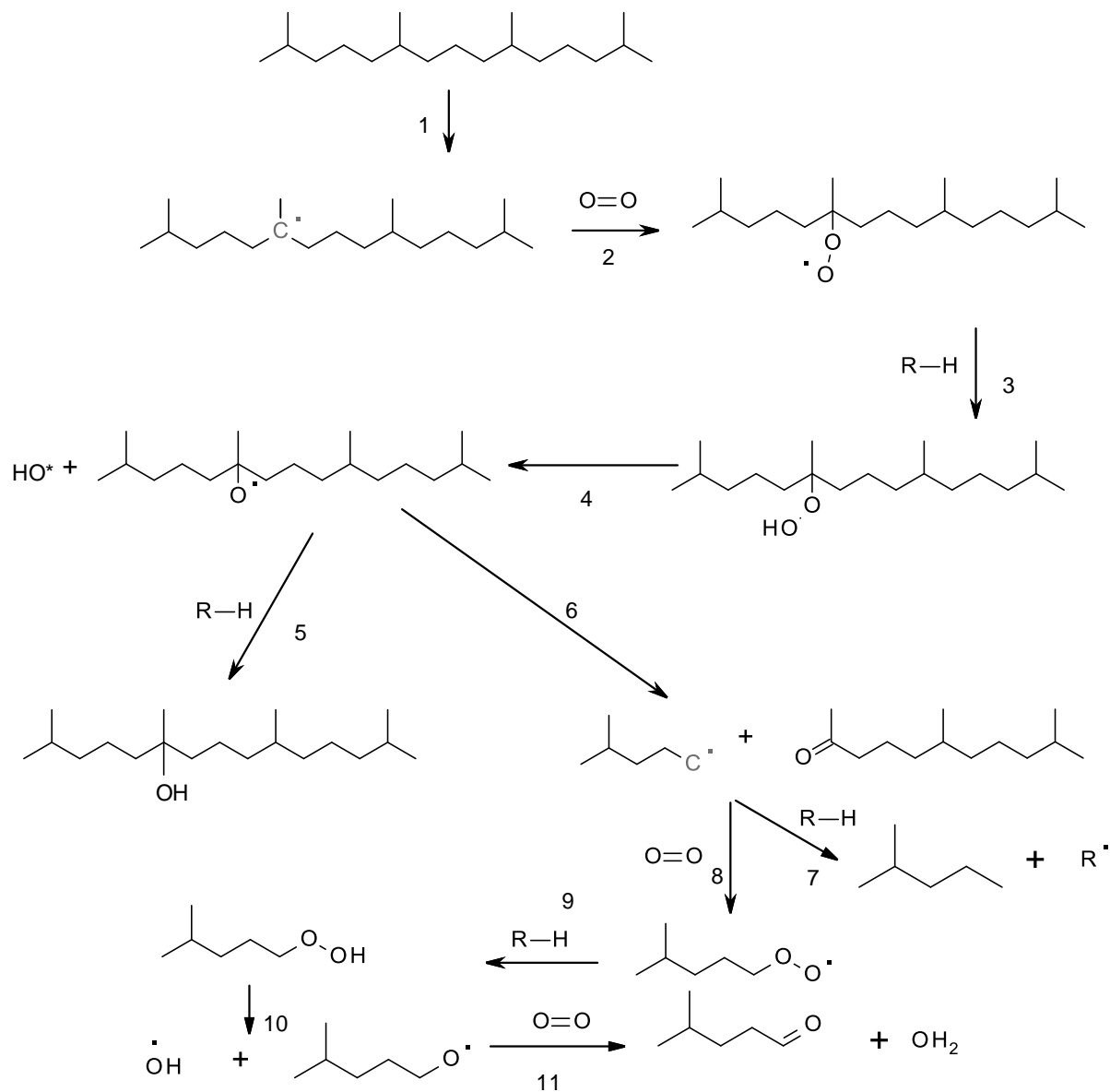


Figure 1.3: 2,6,10,15,19,23 hexamethyltetracosane (Squalane, C₃₀H₆₂)

Thus one could determine the key mechanisms while also measuring the preference of radical attack on tertiary, secondary or primary hydrogens. The reaction was undertaken in a bench top reactor, with temperature of 170 °C under oxygen. The temperature was representative of what would be expected in the piston assembly of a gasoline engine. [7, 24] In total 23 products were identified with 16 being due to the further reaction of the tertiary alkoxy radical, that has been formed via radical attack of the tertiary hydrogen resulting in the formation of the tertiary hydroperoxide, Scheme 1.2 reactions 1-3. The tertiary alcohols were the most significant products of autoxidation, via abstraction of a hydrogen atom from another base oil molecule by tertiary alkoxy radicals, Scheme 1.2 reactions 1-5.



Scheme 1.2: The Oxidation of Pristane Forming Typical Oxidation Products, [13]

The information which can be gained from bench top tests can be limited in that it can only investigate one reaction, whereas in an engine there are a multitude

of reactions occurring. [8, 24] Therefore a component which has a positive effect on the lubricant in bench top test, may not give the same results in a static engine test. [12]

1.4: The Use of Antioxidants in Automotive Engine Lubricants

To compete against the chain reaction, Scheme 1.1 reaction 3, in the oxidative degradation of the lubricant, antioxidants are incorporated in to the formulation. [37] One of the properties the antioxidant must possess is a low bond dissociation energy, which would result in a very fast rate of reaction with peroxy radicals and a long-lived, relatively unreactive radical due to its stability. [33] Radical scavenging antioxidants employed in lubricant formulations tend to be hindered phenols, Figure 1.4, or diphenylamines, Figure 1.5, which due to the aromaticity, possess low O-H or N-H bond dissociation energies.

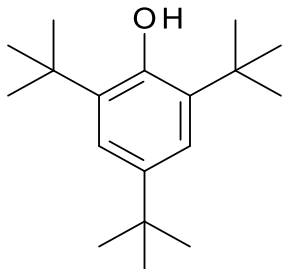


Figure 1.4: An Example of an Radical Scavenging 2,4,6-tri-tert-butylphenol,

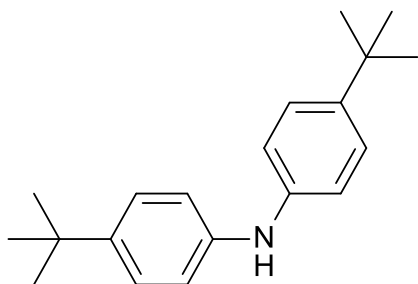
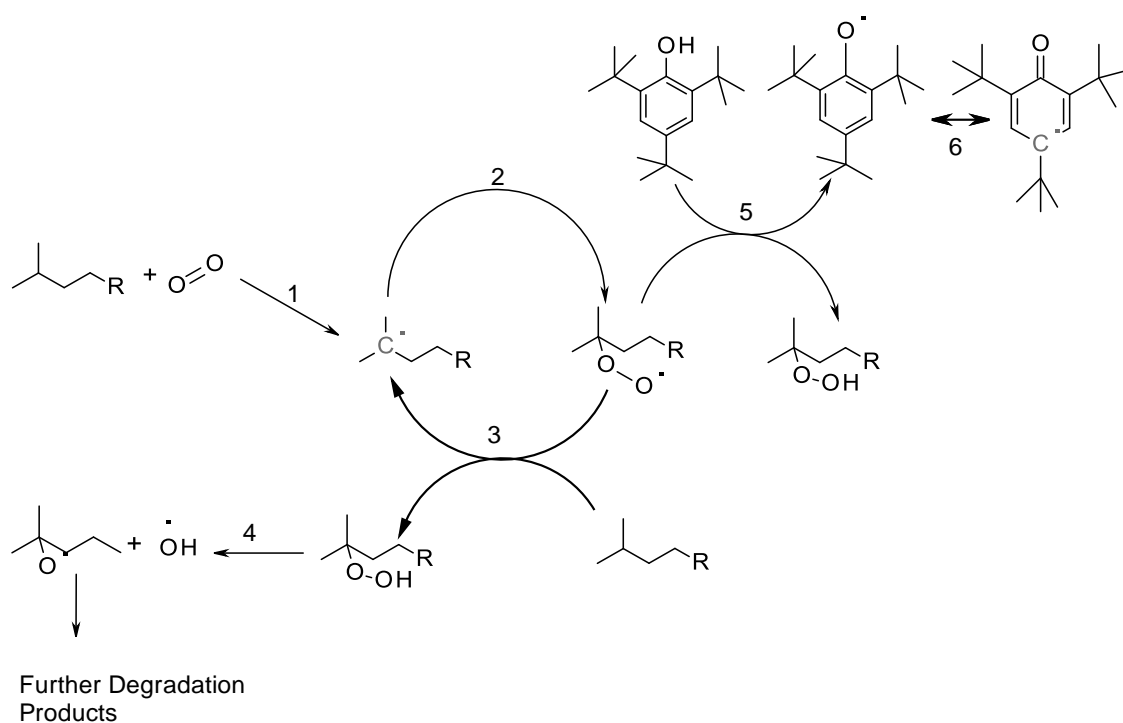


Figure 1.5: An Example of an Radical Scavenging 4-tert-butyl-N-(4-tert-butylphenyl)aniline

Therefore they compete against the chain reaction step shown in Scheme 1.3, reaction 5, which results in the retarding of the degradation of the base oil by oxidation. The resultant aromatic radical is very stable when compared to the alkyl radical formed during the chain reaction step. The area of antioxidants has seen a significant level of research recently, [38], to investigate the potential of new antioxidants or improving synergies between existing antioxidants and hence provide a lubricant which will last longer in an engine and therefore increasing the time between oil changes while reducing vehicle emissions.



Scheme 1.3: The effect of phenolic antioxidants on base oil degradation

The oxidation of automotive lubricants is thought to be the major cause for the chemical degradation of the lubricant. [24] However, as described earlier while the lubricant is in use it can be degraded by other processes, in an engine the lubricant can be exposed to fuel, blow by gases which include NO_x as well as oxygen. The interaction of the lubricant with oxygen is well known and the key papers demonstrating the work undertaken have been described earlier. The effect of fuel and NO_x are less well understood chemically, but could have as an

important effect as the oxidation process, with the majority of the work being undertaken by use of engine testing.

1.5: The Chemical Oxidation of Conventional Gasoline

Gasoline/petrol is a product of petroleum distillation and hydrocracking and has been the primary source of fuel for internal spark ignition combustion engines for many years. [39] It is a highly volatile combination of aliphatic and aromatic hydrocarbons, predominately ranging from C4 to C12 and a mixture of additives in low concentrations. [40] During the early years of gasoline fuelled cars its only purpose was to provide the energy to allow the movement of the piston in the cylinder. Today with ever tighter emissions legislation, fuel has been designed to be more efficient. [1, 3] This has resulted in gasoline becoming more complex, with many additives incorporated into the fuel to improve its characteristics and as well as its octane rating.

The octane rating is used to measure the quality of the gasoline, by rating the efficiency of the combustion under specified conditions. [41] A fuel which possesses an octane rating of 95 has the same combustion properties as a mixture of 95% iso-octane and 5% heptane, and this relates directly to the efficiency of the fuel during combustion. [41] Iso-octane is defined as having an octane number of one hundred while heptane has a rating of zero and this allows the octane rating to be calculated, typically by use of engine tests. [41] The need for fuels to possess high octane ratings has lead fuels to have a number of additives incorporated into the composition.

In the summer when the ambient temperatures are higher the fuel will be more aromatic in composition making the fuel less volatile. [42] During the cooler months when the ambient temperatures are lower the fuel will consist of lighter fractions increasing the volatility of the fuel, typically short chain alkanes. [42] What can be seen here is that unlike the lubricant formulation, which stays constant throughout the year, the fuel formulations are changing on a seasonal

basis. Therefore the components which can interact with the lubricant could be many and varied.

While fuel is in the compressed air fuel mixture it can undergo chemical oxidation reactions. [43] As described above the fuel composition is very complex in nature and therefore to analyse the effects of conventional fuel on lubricant degradation a model component had to be identified. Work by Stark investigating the free radicals and aromatic species which were present in a sample of lubricant extracted from the piston ring pack identified a component of interest. [44] The component in question is 1-methylnaphthalene where it was observed both in the fuel and lubricant GC (gas chromatography) samples. While it is also a member of the methylated PAH (polycyclic aromatic hydrocarbon) group, therefore it should be representative of the rest of the group.

The oxidation reactions of 1-methylnaphthalene in the liquid and gas phase have been previously examined by Jensen in 1992 and Shaddix, while the photo-oxidation of 1-methylnaphthalenes in sea water, was investigated by Ehrhardt. [45,46,47,48] Jensen was investigating the autoxidation of alkylnaphthalenes employing azobisisobutyronitrile, Figure 1.6, as the initiator at temperatures between 30 and 60 °C. [45]

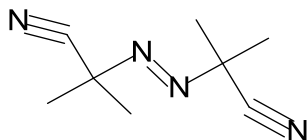
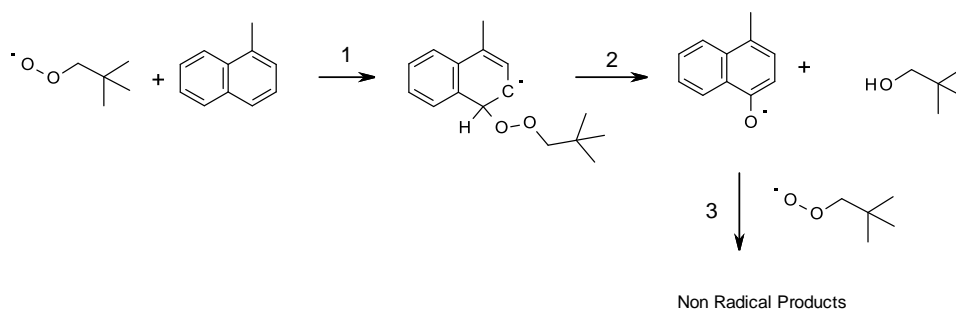


Figure 1.6: 2-(1-cyano-1-methyl-ethyl)azo-2-methyl-propanenitrile (azobisisobutyronitrile, C₈H₁₂N₄)

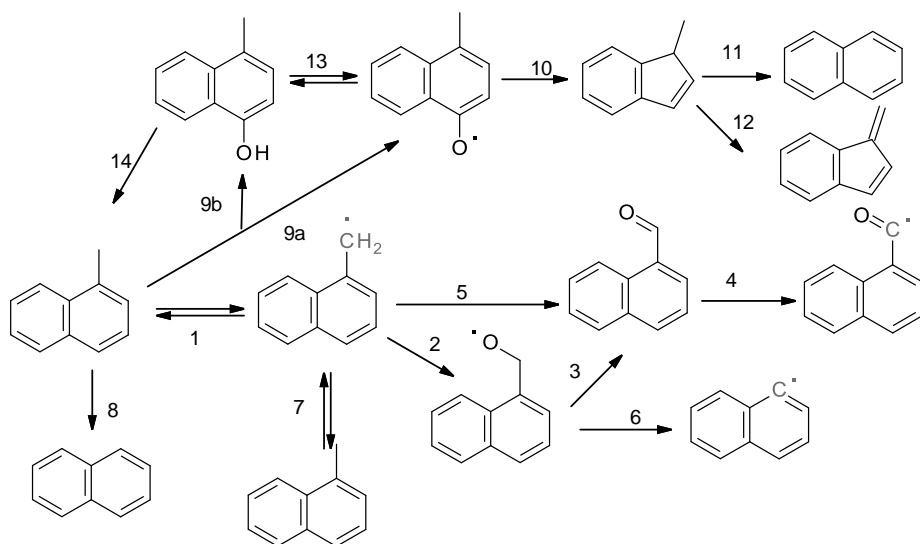
It was previously reported by Larsen that alkylnaphthalenes are more resistant to oxidation than the corresponding alkyl benzene. [31] This was in part due to the chemical radical reactions it can undergo and the products they form, 1-methylnaphthalene can undergo chemical reactions with oxygen at two sites,

same as toluene, either abstraction of an H atom from the methyl group or, through peroxy radical addition to the aromatic ring. [45] Of the two mechanisms the abstraction reaction was the dominant mechanism. [46] Interestingly it is the second addition mechanism, Scheme 1.6, that Igarashi suggests gives the 1-methylnaphthalene its self inhibiting properties. [45] The radical formed by the addition process can undergo further oxidation and continue chain propagation or, it can decompose to form a tert-butyl alkoxy radical and a methylnaphthoxy radical. Igarashi proposed that the decomposition reaction is responsible for the first order chain termination step, by reaction with a peroxy radical resulting in the formation of stable oxidation products, Scheme 1.4. Later work by Jensen investigated the effect of 1-methylnaphthalene on the autoxidation of hexadecane. [46]



Scheme 1.4: Addition of Peroxyl Radical to 1-methylnaphthalene Ring Leading to the Formation of Non-Radical Products [46]

The work undertaken by Shaddix investigated the oxidation reaction of 1-methylnaphthalene at 927 °C, simulating combustion conditions. [47] By identification of the stable intermediate species, a chemical mechanism was proposed, Scheme 1.5. In this mechanism three competing reactions were present; these were the abstraction of a benzylic H atom by H/O radical system, Scheme 1.5 reaction 1, and molecular oxygen, homolysis which lead to the formation of the naphthyl methyl radical, Scheme 1.5 reaction 9, addition of oxygen to the ring system, Scheme 1.5 reaction 9b. [47]

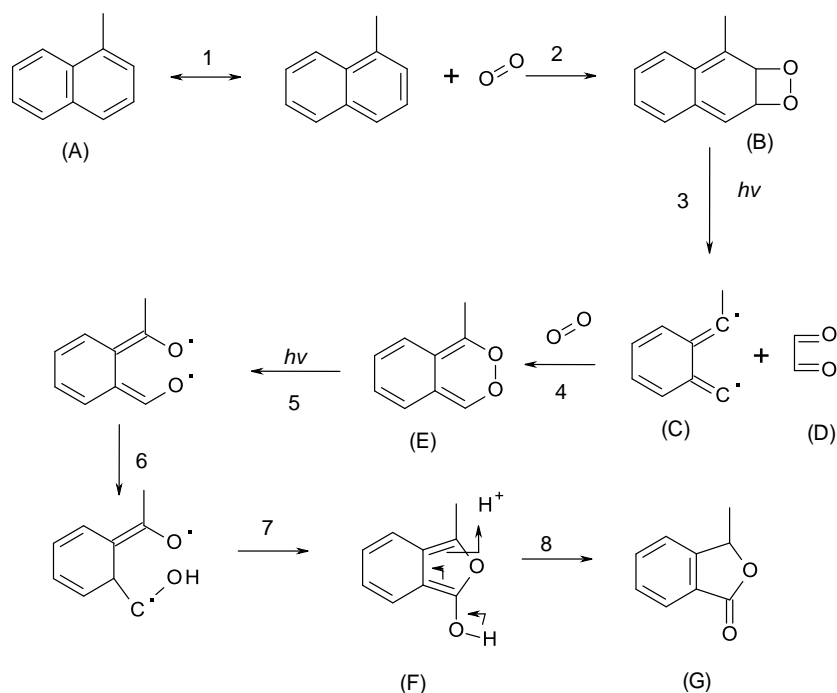


**Scheme 1.5: Oxidation Mechanism of 1-methylnaphthalene at 927 °C
Proposed by Shaddix [47]**

Due to the high temperatures involved in the work by Shaddix it is possible that some of the products will not form at lower temperatures. [47] For instance it is very unlikely that the methyl group will be removed from the 1-methylnaphthalene, Scheme 1.5 reaction 8, due to energy restrictions. Therefore the two products which are likely to form will be the 1-methyl-4-naphthol, Scheme 1.5 reaction 9b and the 1-naphthaldehyde, Scheme 1.5 reaction 5, at lower temperatures (employed in typical bench top oxidation tests). A more representative oxidation mechanism was proposed by Ehrhardt. [48]

Ehrhardt investigated the photo-oxidation decay routes of 1-methylnaphthalene in sea water at ambient temperature. [48] The basis of this work was with 1-methylnaphthalene being present in fuel, it could be emitted from engine exhausts tail pipe, which would mean it could enter sea water upon cooling. For this work 1-methylnaphthalene was mixed with sea water samples in varying concentrations and was photo-oxidised in sunlight. Five products were identified by GC analysis of the samples two of which were typical oxidation products 1-naphthaldehyde and 1-naphthalenemethanol, derived from the abstraction of hydrogen from the methyl group. The three other products were methyl

benzofuranones of which they proposed a mechanism for their formation from 1-methylnaphthalene, Scheme 1.6 molecule G, which included the oxygen adding to the aromatic ring, Scheme 1.6 reaction 2.



Scheme 1.6: The Proposed Mechanism for the Formation of 3-methyl-1(3H)-isobenzofuranone by Ehrhardt [48]

Ehrhardt proposed that Scheme 1.6 could be used to describe the formation of 3-methyl-1(3H)-isobenzofuranone it was tentatively proposed due to the presence of glyoxal in the GC analysis, which Ehrhardt proposed was due to the cleaving of the oxygen in the formation of the diradical species, Scheme 1.6 reaction 3. [48] The formation of 3-methyl-1(3H)-isobenzofuranones will be unlikely at lower temperatures or at all, this is in part due to the conversion from 3-methyl-2a,8a-dihydronaphtho[2,3-c]dioxete, Scheme 1.6 molecule B, to the diradical, Scheme 1.6 molecule c, in Scheme 1.6 reaction 3. In this step to form the glyoxal and the naphthyl radical a photon is required, which would not be possible in a sealed flow reactor. While it is highly unlikely that the mechanism in Scheme 1.6 can be used to describe the formation of 3-methyl-1(3H)-isobenzofuranones, this is in part due to the addition of oxygen across the

double bond to form 3-methyl-2a,8a-dihydronaphtho[2,3-c]dioxete in Scheme 1.6, this is very unlikely due to steric hindrance. Therefore from the work by Ehrhardt the products of 1-methylnaphthalene oxidation which are formed are the 1-naphthaldehyde and the 1-naphthalenemethanol. [48] While Shaddix and Ehrhardt have found possible 1-methylnaphthalene oxidation products, they were not directly applicable to the products which could be formed in this work. [47, 48] A more directly related investigation was the work undertaken by Jensen in 1992. [45, 46]

1.6: Effect of Conventional Gasoline on Automotive Lubricant Degradation

In a combustion chamber the fuel and the lubricant can interact, typically during cold starting of the engine and in particular during the compression stroke, during which fuel can condense on the metallic surfaces of the cylinder and absorb into the lubricant film. [19, 49] Once absorbed into the lubricant the fuel could potentially inhibit or promote certain degradation pathways of the lubricant. [50] This area has seen increasing interest due to tighter emissions legislations, and the need for engines to be more efficient. One of the ways of improving the efficiency of the engine apart from increasing the compressions ratio is from investigating the fuel-lubricant interactions. [5] By understanding the chemistry of the fuel and lubricant interactions new formulations could be made producing synergies which decrease the piston friction observed in the engine and power loss, therefore reducing emissions.

The typical type of test that is employed in analysing the effects of fuel on lubricant degradation are engine tests. Work by Lieberzeit is an example where he investigated the use of polymers to detect chemical changes in the oil. [51] Lieberzeit was investigating the use of polymers as an alternative to the established TBN and TAN methods for monitoring the degradation of oil, as used for example by Moritani. [24] The polymers showed good correlation with TBN therefore indicating their possible use as sensors in lubricant degradation. Of greater significance to this project is the investigation on the influence of fuel and water. Using fuel and water it was found that viscosity decreases to around

a third of the initial value when the contaminants were added to 15% (v/v). However in this paper no aspects of the cause of this reduction of viscosity were investigated. The decrease in viscosity may have a detrimental effect on the lubricant, potentially leaving the lubricant with insufficient film thickness to fully lubricate in the piston ring pack, therefore increasing piston friction and wear.

There is a body of work centred on the effect of traditional gasoline, the components of fuel which researchers are most interested in are the aromatics, due to their use as fuel additives. [51, 52] This centred on investigating the polycyclic aromatic hydrocarbons (PAH's) which are in small quantities in the fuel as a by-product of the cracking process, these molecules are fused aromatic rings which contain no heteroatom or substituent's. They are known to be lipophilic and thus are more likely to be found in oil rather than water. An example of a PAH is Pyrene ($C_{16}H_{10}$) Figure 1.7.

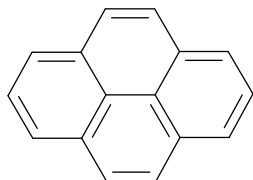


Figure 1.7: Pyrene ($C_{16}H_{10}$)

The main increase of PAH in fuel is due to the halt in the use of lead in fuels to improve the octane number, leading to the use of aromatics which can increase the octane number. A few investigations have researched how the lubricant can affect the PAH exhaust emission rate. Pedersen in 1980 researched the effect of the lubricant on the PAH emission in the exhaust. [51] In this study it was found that the PAH's accumulated in the lubricant which leads to their subsequent emission. The PAH rate of addition to the lubricant was found to be 10 times as high as in the exhaust emission rates which suggests that PAH could have a sink effect in the sump, i.e. the PAH will accumulate in the sump and increase in concentration.

Further research by Brandenberger investigated the effect of lubricating oil on the diesel particulate emissions, which found PAH concentrations to be six times higher in lubricating oil than the diesel exhaust. [52] It was found that non-combusted PAH's from the fuel are then transported with the combustion gases, which then accumulate in the lubricating oil.

The work undertaken by Brandenberger and Pedersen investigated the effect of the lubricant on exhaust emissions; the area which has not been covered in this review is how fuel absorption can affect the lubricant. [52,53] Shayler investigated the fuel losses to the crankcase, leading to a description of the absorption and desorption properties of the fuel into the lubricant. [19, 49] These tests were undertaken using a Ford engine and a Ford branded lubricant with a standard gasoline. It was found that the bulk of the blow-by gases were formed during the power stroke. The hydrocarbon mass flow rate in the crankcase was dependent strongly on the rate of the blow-by. The absorption efficiency of the fuel in the oil was found to be highest at lower temperatures.

The absorption efficiency gives an indication of how much fuel is being absorbed by the oil. [19] When the oil and fuel arrive in the crankcase at low temperature the fuel is easily absorbed into the oil. However when the temperature is increased the fuel is less easily absorbed into the oil. In these conditions the blow by gases go straight through to the ventilation chamber with the lighter hydrocarbons absorbed (during warm up) by the oil, desorbing and going through exhaust vents with the blow by gases. [19] This leaves the oil in the sump containing a proportion of the heavier PAH's. This is due to the decreased solubility of the lighter fractions so they will volatise out of solution.

The problem of blow-by gases absorbing into the oil is increased at low temperatures, cold starting of the engine, and this should have an effect on the lubricant. Shayler investigated the absorption and desorption characteristics of the fuel in oil however it does not go into detail about the products formed, only that they are hydrocarbons. [19, 49] This work suggests that at lower temperatures it is more likely that the fuel will enter the lubricant and this is what

Shayler found during his work investigating the cold start properties of the lubricant in the top ring zone.

In the work by Shayler describing the process of fuel absorbing and desorbing from fuel there was no identification of the fuel components which were present in the oil only that they were large in size (if still present in lubricant at high temperatures). [19, 49] However, work by Reardon investigated the molecules present in used oil and which increase with the age of the oil. [53] The tests involved different car engines, from different manufacturers, which were supplied with oils again from different manufacturers. The research analysed the new oils, bought from over the counter, and analysed the used oils, which were of differing ages and used under different conditions. From the total ion chromatogram an extracted ion profile was undertaken to compare concentrations of differing PAH's. The work concluded that from the extracted ion profile that pyrene, Figure 1.7, phenanthrene ($C_{14}H_{10}$), Figure 1.8, fluoranthene ($C_{16}H_{10}$), Figure 1.9, and benzo[ghi]perylene ($C_{22}H_{12}$), Figure 1.10, were found to increase in concentration with increasing oil age, for all the oils from the differing manufacturers.

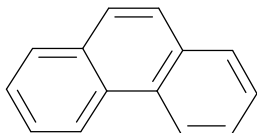


Figure 1.8: Phenanthrene ($C_{14}H_{10}$)

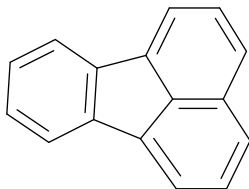


Figure 1.9: Fluoranthene ($C_{16}H_{10}$)

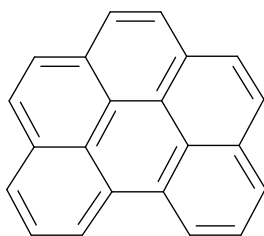


Figure 1.10: Benzo[ghi]perylene (C₂₂H₁₂)

This work compliments the findings of Shayler who suggested that the heavier molecules stay in the lubricant, due to not being able to be desorbed from the engine oil, when compared to the lighter compounds. [19, 49] This is what can be seen here with the subsequent build up of these molecules with increasing oil age.

It is known that while the lubricant is in the piston ring pack it undergoes oxidation reactions. Thus from this analogy it can be assumed that when a fuel is absorbed into the lubricant that the fuel will undergo the same oxidation reactions and contribute either positively or negatively to the degradation process. This is the basis behind work by Stark which was a computational model trying to describe the trends observed in earlier work undertaken by Cracknell. [44,55] The earlier work was investigating differing fuel compositions and their effect on the lubricant, of the fuels tested it was found that highly aromatic content had a detrimental effect on the lubricant, while a fuel high in short chain alkanes had little effect on the lubricant. This can be explained by the work undertaken by Shayler on fuel absorption efficiency, where it was suggested that heavier components are more likely to stay in the lubricant. [19, 49] Therefore a fuel which is rich in alkanes, it could be suggested that once the engine is up to fully warmed conditions that the fuel components will volatilise out of solution and have very little effect on the degradation of the lubricant

In the later work Stark computer modelled the effect of certain fuel components on a model lubricant trying to explain the trends. [44] The interesting point of the research was the difference in rates of oxidation dependent on what component was added. Aromatics were found to increase the rate of oxidation

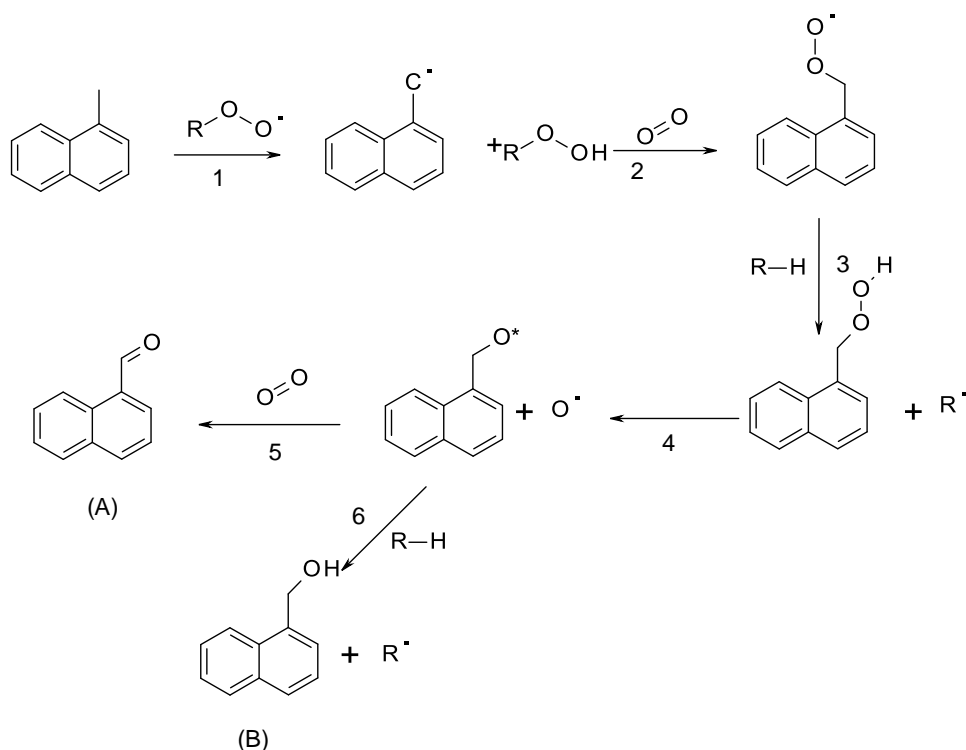
with the more substituted components (Xylene>Toluene>Benzene) promoting the effect even more due to beneficial hydrogen abstraction from the methyl substituent, this was in good agreement with the earlier engine tests. While alkanes, alkenes and ethanol were predicted to slow down the oxidation reaction. This work is showing how the effects observed in the engine can be described by chemical mechanisms, however it would be beneficial for a lab based technique to be designed which could incorporate the fuel components.

As described earlier in the text for this work 1-methylnaphthalene will be used as the model fuel component, of which there has been some work undertaken on its effect on hexadecane oxidation, while Yoshida has a patent describing the use of monoalkylnaphthalenes as a major or minor component in a synthetic lubricant. [54] Jensen suggested that methylnaphthalenes have an inhibiting effect on the oxidation of hexadecane, this is in contrast to work by Stark which suggest that aromatics increase the rate of oxidation. [44,45] In Jensens work it is suggested that methylnaphthalenes have two potential reactions with the peroxy radicals one of which can inhibit, but not halt, the autoxidation of hexadecane. [46] The first mechanism which was suggested was the abstraction of a hydrogen atom from the methyl group. This is not unexpected due to the C-H bond strength of the methyl group will be lower than that for the secondary hydrogen atom on hexadecane, Table 1.2. [36]

Table 1.2: Bond Dissociation Energies of Typical C-H's [36]

C-H Bond		Bond Dissociation Energy (kJ mol⁻¹)
CH ₃ -CH ₂ -CH ₂ -CH ₂ -H	Primary	421.3
CH ₃ -CH(CH ₂ CH ₃)-H	Secondary	411 ± 2
CH ₃ CH(CH ₃)C(CH ₃) ₂ -H	Tertiary	399 ± 14
C ₁₀ H ₇ -CH ₂ -H	Methyl group on 1-methylnaphthalene	356 ± 6

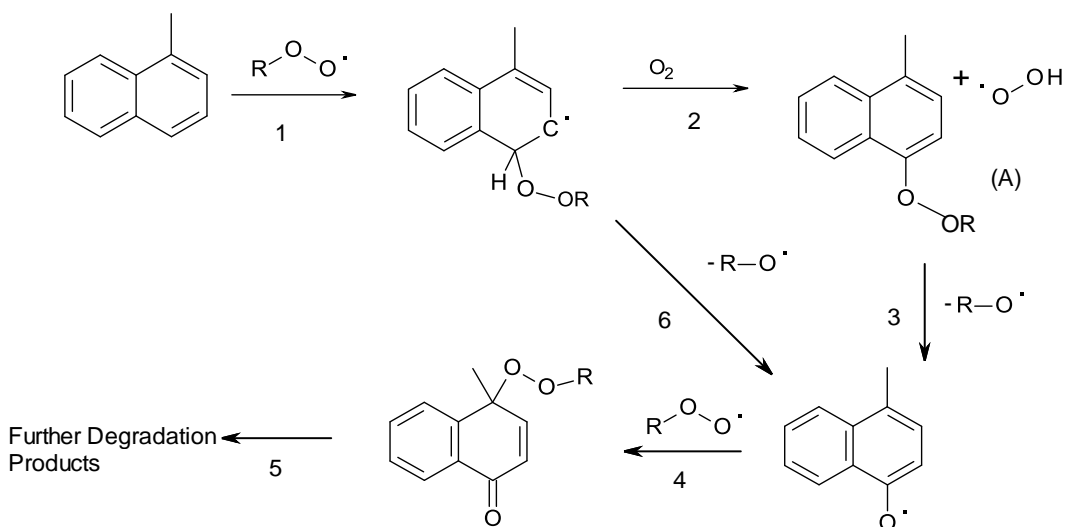
Therefore in a system where the lowest energy pathway is preferred the alkylperoxyl radical will abstract a hydrogen atom from the methylnaphthalene, leading to the formation of a methylnaphthyl radical, Scheme 1.7 reaction 1, that can undergo subsequent reactions to form the corresponding naphthaldehyde (A), Scheme 1.7 reactions 1-5, and naphthalenemethanol (B) Scheme 1.7 reactions 1-4 and 6, both of which were identified by GC analysis.



Scheme 1.7: Oxidation of 1-methylnaphthalene via Hydrogen Abstraction [46]

By inspection of the mechanism shown in Scheme 1.7, it can be seen that by the formation of the naphthalenemethanol (A) two alkyl radicals are formed, while the formation of naphthaldehyde (B) leads to the formation of one alkyl radical. This would suggest that by the abstraction of hydrogen from the methyl group of the methylnaphthalene that it is acting as a pro-oxidant, increasing the degradation of hexadecane. A second proposed route for the inhibiting effect of methylnaphthalene was suggested by [46]

This alternative route involves an addition reaction onto the aromatic ring, Scheme 1.8, this can go through further reactions forming phthalic anhydrides and acids, Scheme 1.8 reactions 1-5.

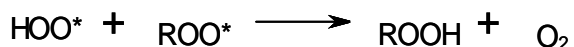


Scheme 1.8: Mechanism for the Addition of the Alkyl Peroxide to 1-Methylnaphthalene [46]

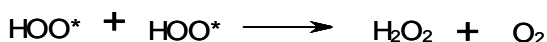
Igarashi proposed that the addition reaction was the cause of the inhibiting effect of methylnaphthalene on the oxidation of hexadecane. This is due to the formation of the hydroperoxyl radical (a) in Scheme 1.8 reactions 1,2,3 and 5, the formation of which increases the second order rate constant for the chain termination reaction by undergoing subsequent fast cross, Scheme 1.9, and self reactions, Scheme 1.10. While a kinetically first order chain termination step was established by the effective trapping of the alkyl peroxy radical by (methyl)naphthoxyl radicals, Scheme 1.8 reactions 1,4 and 5, which Igarashi had earlier found in previous work. [45]

It is proposed that in the early stages of oxidation the first order chain termination step effectively reduces the overall kinetic chain length, therefore providing methylnaphthalene with its antioxidant properties. [46] However as the reaction progresses the hydroperoxide concentration was found to rise which increased the steady state concentration of peroxy radicals and therefore

increasing the importance of the second order chain termination step. This increase was found to reduce the effectiveness of methylnaphthalene as an inhibitor of hexadecane oxidation.



Scheme 1.9: The Hydroperoxyl Alkylperoxyl Cross Reaction [46]



Scheme 1.10: The Hydroperoxyl Self Reaction [46]

The addition of alkylperoxyl radicals to the 1-methylnaphthalene ring was suggested due to an increase in the concentration of hydrogen peroxide (H_2O_2) being formed during the reaction. This increase will be due to the formation of hydroperoxides from the self reaction mechanism, Scheme 1.10. Therefore, in the presence of methylnaphthalene, the hydroperoxide concentration should be higher than when there is no 1-methylnaphthalene present, due to the increased formation of hydroperoxides in Scheme 1.8, which Igashari saw.

As another check on the addition mechanism Ingold undertook product analysis of potential ring opened products resulting from further reaction of the product of Scheme 1.8, which were found to be phthalic acid, Figure 1.11, and 2-Acetylbenzoic acid, Figure 1.12. During the product analysis it was found that there were higher concentrations of products due to hydrogen abstraction at the methyl group, therefore indicating that the abstraction mechanism is the dominant mechanism.

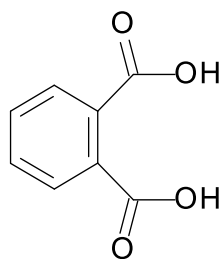


Figure 1.11: Phthalic Acid [46]

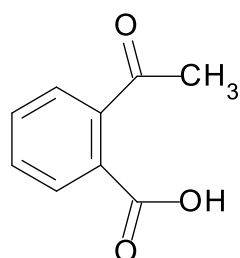


Figure 1.12: 2-Acetylbenzoic Acid [46]

What is apparent from this section is that while the chemical lubricant degradation by oxidation is well understood by bench top oxidation tests, fuel-lubricant interactions are less well understood, with the majority of the work undertaken by the use of engine tests. To obtain a greater knowledge of fuel-lubricant interactions a suitable bench top test is required, which will allow detailed chemical mechanisms to be determined like the work undertaken by Jensen [46].

1.7: Effect of Bioethanol on Automotive Lubricant Degradation

With the increasing demand for greener fuels and lower greenhouse emissions bio-ethanol and biodiesel have found increasing importance in today's fuel formulations. The European Union set the target that by 2010, automotive fuel will contain 5.75% bio-fuels,[1] while American car manufacturers have agreed, as part of the 2008 government bailout, that 50% of their fleet will be flexible

fuel vehicles (FFV), which can run on conventional gasoline or high ethanol fuel (E95), by 2012. [55-57]

Ethanol has been established as the primary fuel in Brazil. It has only been relatively recent, due to uncertainties in oil reserves and supply, that ethanol has been used as a fuel in other territories. [58-61] At present the United States sell ethanol fuel at E85, the term E85 describes the amount of ethanol in the fuel. For example a fuel with a rating of E85 will have an ethanol content of 85% with the remaining 15% made up of conventional fuel. [50] The use of ethanol as a fuel brings its own benefits one of which being the reduced need for aromatics to improve the octane rating. [62] They also have their disadvantages, one being the lower air fuel ratio for ethanol therefore the need to use additives in the fuel composition. This will improve the combustion process, thus improving the fuel economy to nearer that of a gasoline engine.

There have been patents discussing inventions and formulations of ethanol fuel [63] describing additives which have been incorporated into the formulation. These additives range from diethyl ethers and dimethyl ethers which are added to improve the combustion properties, particularly the cold start properties of ethanol. Other additives include dispersants which can disperse the deposits which occur during fuel combustion thus reducing the rate of sludge formation.

A potential problem with ethanol as a fuel is its interaction with the lubricant. [15] The majority of automotive lubricants will be designed for use in a non-polar environment. Thus when conventional fuel components interact with the lubricant it will directly affect the degradation. [64] Ethanol however, is polar and therefore there is a potential problem when the fuel enters the lubricant, it might not be soluble in the lubricant. [18, 65-67] It could in theory remove the more polar additives from the lubricant into a polar ethanol layer or microemulsion. [68, 69] Depending on the additives which are removed the stability of the lubricant could be affected.

Another problem with the use of ethanol as a fuel is its hygroscopic properties when compared to gasoline. This could lead to a high level of water in the

lubricant therefore potentially affecting the lubricant properties. [70] The potential problem with the hygroscopic properties of ethanol was the basis behind Boons work where a fleet test was undertaken to assess the affect of ethanol on the lubricant. [50] Boons observed a large amount of water contamination in the lubricant and this was due to the hygroscopic nature of the ethanol. [50] This can be assumed to be attributed to the incomplete combustion of ethanol during the cold start conditions, producing water which then absorbs into the lubricant. [50] Due to the hygroscopic nature of ethanol, one would expect more water to be retained in the lubricant when compared to gasoline. It is predicted that these effects only have an influence under cold start conditions, where the ethanol will not be able to evaporate, however when most car journeys involve cold start and short drive times, this dilution effect should be looked into, especially how it affects lubricant viscosity. This could have an effect on certain additives in the lubricant which could ultimately result in chemical changes. The increase in use of ethanol as a fuel has made the area of ethanol lubricant interactions very interesting.

The most current work in this field of ethanol fuel dilution is by Besser. [71] In the work undertaken by Besser lubricant samples were diluted with 1% (v/v) ethanol and subsequently oxidised at 160 °C. No effect on the oxidative stability of the lubricant was observed upon addition of 1% ethanol to the lubricant. This would suggest that ethanol has little effect on the lubricants degradation mechanism.

1.8: Conclusion and Thesis Aims

In an engine the lubricant is exposed to two very different environments, the piston ring pack and the sump, where the majority of the degradation is observed in the hot ring pack.[24] There are a variety of routes for the chemical degradation of the lubricant whilst it is in the ring pack, with oxidation thought to be the major route for the chemical degradation of the lubricant. This has lead to detailed chemical mechanisms being derived for the process of lubricant oxidative degradation. The oxidation products formed will take the form of

ketones, carboxylic acids, alcohols and esters, with preferential attack at tertiary hydrogen on the lubricant. [13, 14] However, the effect of fuel on the chemical degradation of the lubricant is less well known chemically, with the majority of the research employing engine tests.

Typical bench top oxidation tests mimic the fully operational piston temperature which is estimated to be around 140-180 °C, however, the piston is not always operating at that temperature. [7, 24] There are times when the piston will never reach that temperature (during short cold start conditions) thus the bench top tests only show degradation at fully warmed temperatures, which can provide problems when correlating data with engine test data.

What is apparent from this section is that while the degradation of the lubricant by oxidation is well understood through use of bench top oxidation tests, fuel lubricant interactions are less well understood, with the majority of the work undertaken by the use of engine tests. To obtain a greater knowledge of fuel lubricant interactions a suitable bench top test is required, which will allow detailed chemical mechanisms to be determined and provide cheaper and more effective tests which can monitor lubricant degradation.

The aim of this thesis is to further the knowledge of both interactions, by investigating the mechanism of the oxidation of certain fuel components and their interaction with the lubricant. This could allow fuel and lubricant formulations to be produced which complement each other, and result in a decrease in friction observed in the engine, therefore reducing the level of fuel required to provide the energy to move the piston, therefore increasing fuel economy. Fuel components from conventional gasoline to 1st and 2nd generation biofuels will be investigated to examine how they affect the lubricant chemistry.

2: Experimental

2.1: Bench Top Oxidation Apparatus

2.1.1: Continuous Flow Reactor Set Up

Oxidation reactions were undertaken in a stainless steel bench top reactor, Figure 2.1, which was made in-house at the Department of Chemistry at the University of York. The reactor had an internal volume of 49 cm³ with an inlet and outlet pipe for the continuous flow of gas through the reactor. Reactor specifications are shown in Table 2.1.



Figure 2.1: Picture of stainless steel reactor with 49 cm³ internal volume

Table 2.1: Table of Specific Reactor Details

Reactor Specifics		
Total Reactor Volume (cm ³)	49	42
Maximum Substrate Volume (cm ³)	7	5
Inlets	6	6
Sampling	Suba Seal	Suba Seal
Temperature Stability (°C)	±0.1	±0.1
Temperature Measurement	Sample via Stainless Steel BS316 Thermocouple	Sample via Stainless Steel BS316 Thermocouple
Surface Material	Stainless Steel BS 304	Stainless Steel BS 304
Stirring Rate (RPM)	600	600
Burst Disk	Yes	Yes
Reactor Number	2	5

The conditions inside the reactor were measured directly using the equipment listed in Table 2.1. An analogue to digital converter was used to record the data from the reaction into an electronic file, which was transferred to a spreadsheet program (excel) for manipulation. The only measurement which was not recorded directly from the reactor is the oxygen concentration, which was recorded after the exhaust gas after it had gone through two traps, solvent (to trap volatile hydrocarbons) and cold (to trap the volatile products), this is to protect the sensor from hydrocarbons and other volatile products. A picture of the set up used can be seen in Figure 2.2 & 2.3.

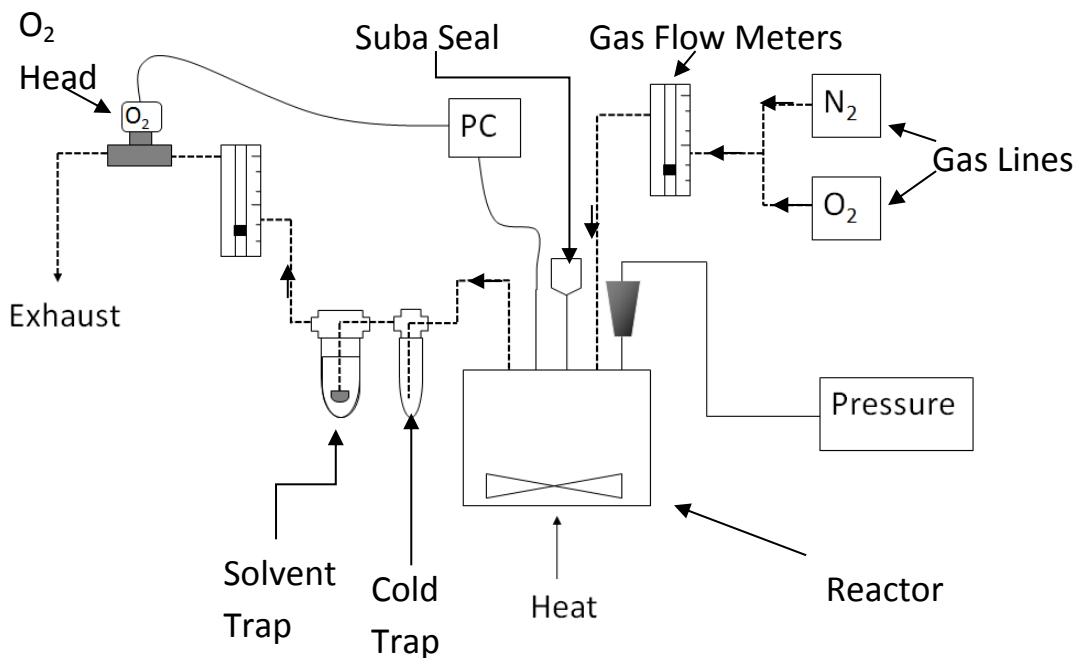


Figure 2.2: Schematic Diagram of the Stainless Steel High Temperature Oxidation Reactor

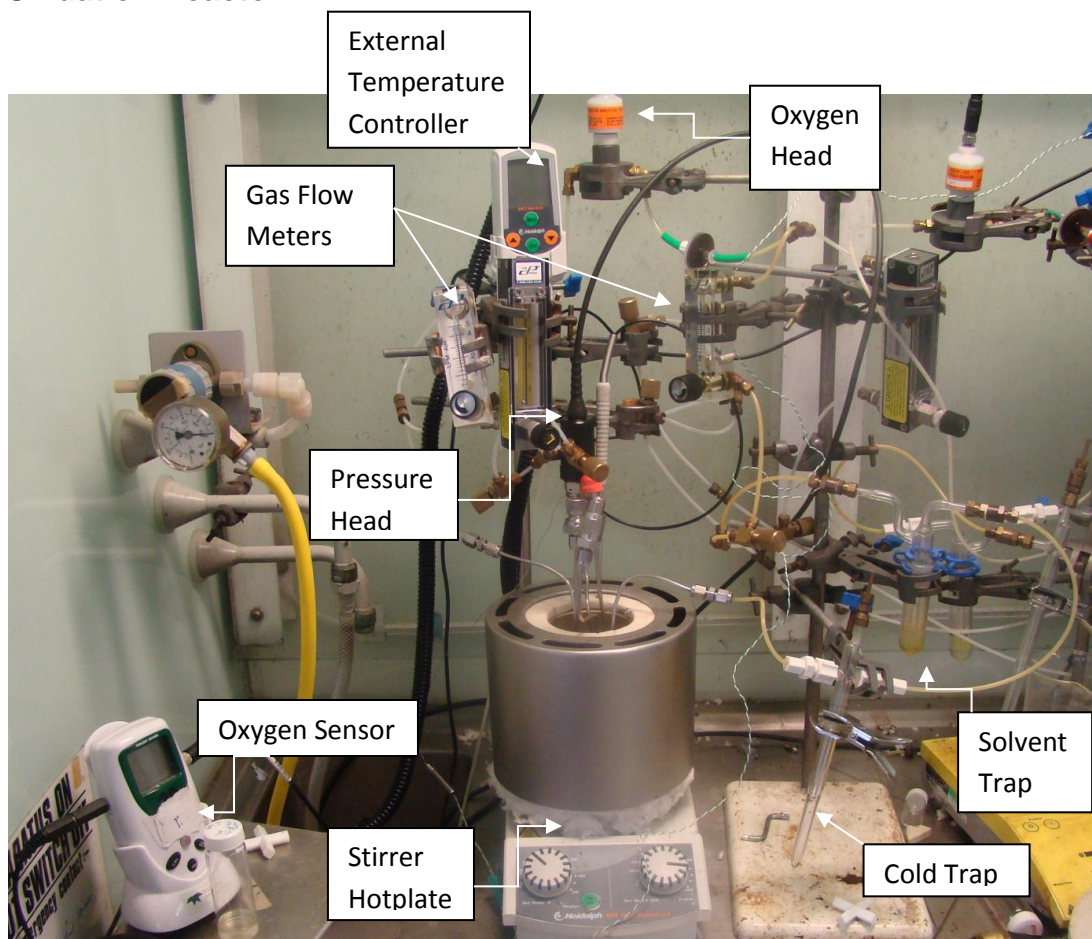


Figure 2.3: Picture of Stainless Steel High Temperature Oxidation Reactor Set-Up Highlighting Equipment Detail

Table 2.2: Table Showing Equipment Specifics

Measurement	Equipment Details
Oxygen	Sensor – Teledyne R-17a Head – Teledyne AX300i
Temperature	Labfacility – Stainless Steel (BS316) Type K thermocouple 150mm length and 0.5mm diameter
Pressure	Varian – Head No. 6543-25-038 Range – 1-2000 (± 0.5) mbar
Gas Flow Meters	Cole Parmer – 0.05-0.50 (± 0.02) $\text{dm}^3\text{min}^{-1}$ Cole Parmer – 0.008-0.050 (± 0.002) $\text{dm}^3\text{min}^{-1}$
Stirrer Hotplate	Heidolph – MR-Hei Standard with external temperature controller (EKT- Hei Con)
Stirrer Bar	Fisher Scientific – 1 ½ Inch PTFE Crosshead
Analogue to Digital Converter	Picotech – ADC-20 running Picolog software 20 bit software

2.1.2: Continuous Flow Reactor Set Up for Bio-Fuel Work

Flow reactions were undertaken by adding a known volume of the substrate into a cold reactor with a PTFE-coated magnetic cross stirrer bar. To ensure that there was a gas tight seal between the reactor lid and base an BS033 Viton o ring was placed inside an embedded groove inside the lid before it was screwed hand tight onto the base. The pressure head (Varian Model No. 6543-25-038) was then attached to the reactor and switched on before attaching the gas inlet and exhaust lines. The cold reactor was then placed inside a cold heating block,

the nitrogen valve turned on with the gas flow meters set at $0.1 \text{ dm}^3\text{min}^{-1}$ until the oxygen concentration is at zero, indicating that the reactor and substrate are oxygen free. At the desired oxygen concentration the stirrer bar speed was set to 600 rpm and the oven set to the desired temperature and left for 50 minutes. This method is to ensure that there is no remaining ethanol in the lubricant before oxidation. After 50 minutes the stirrer bar was switched off and the gas is changed from nitrogen to oxygen. When the oxygen concentration has reached $100\% \pm 1\%$ the stirrer bar is switched back on and the reaction is monitored by the concentration of oxygen in the exhaust line and samples taken from the reactor via the suba seal inlet port. The start of the reaction was taken as when the stirrer bar was turned back on with oxygen present.

2.1.3: Continuous Flow Reactor Set Up for Conventional Fuel

Flow reactions were undertaken using similar method to that described above, however due to the volatility of the substrate (1-methylnaphthalene) the following method was designed to ensure as little 1-methylnaphthalene was lost during the warm up period. Before the substrate was injected into the reactor the reactor was preheated under a flow of nitrogen set at a flow of $0.030 \pm 0.001 \text{ dm}^3\text{min}^{-1}$. When the reactor was at the desired temperature the substrate was inserted into the reactor via the suba seal inlet port and the gases were switched over. After the substrate was at the correct temperature and the oxygen concentration reached $100\% \pm 1\%$ the stirrer bar was set at 600 rpm and the reaction was started.

2.2: Model Ethanol Fuel Dilution

2.2.1: Ethanol Treated Method

The work in this study investigated the effect of ethanol fuel dilution in lubricant sumps of automotive engines. It has been reported in the literature that ethanol fuel dilution can be significant with the ethanol concentration in the sump lubricant reaching 10%(v/v). [50] For this work it was assumed that at high

temperatures found in the piston assembly (temperature range 150-200 °C) ethanol (boiling point 78.37 °C) should have little or no direct effect on the degradation of the lubricant due to oxidation, due to ethanol being in the gas phase. As this work is investigating the liquid autoxidation of lubricants, ethanol should have little effect on the rate of autoxidation in the liquid phase. It is most likely to have an effect in the sump lubricant, however ethanol is still likely to have a short residence time due to the reasonably high volatility. A model mixing regime was therefore devised to mimic ethanol fuel dilution in the sump and its effect once evaporated on the oxidative stability of the lubricant, i.e. an indirect effect.

To model ethanol fuel dilution in automotive sumps and its subsequent evaporation a lab scale model method was devised. This method was designed to mimic the extreme case of ethanol dilution in the sump due to cold weather starts and short drive times. The lubricant substrate was diluted with 10% (v/v) ethanol (Aldrich) prepared using 25 cm³ measuring cylinders with 18 cm³ sample of the substrate was made up to 20 cm³ by the addition of 2 cm³ of ethanol resulting in the formation of a polar ethanol layer and a non polar lubricant layer. The mixture was then shaken for a period of 1 minute resulting in the formation of an unstable emulsion which was then allowed to settle, with the cylinder stoppered, until two distinct layers were formed, a lower lubricant layer and an upper polar, ethanol rich layer; this took typically 2-3 days. The lower lubricant layer, ethanol diluted sample, was then employed in subsequent flow oxidation reactions and both layers were analysed by GC for additive content and ethanol content. The mixing procedure can be seen graphically below, Figure 2.3

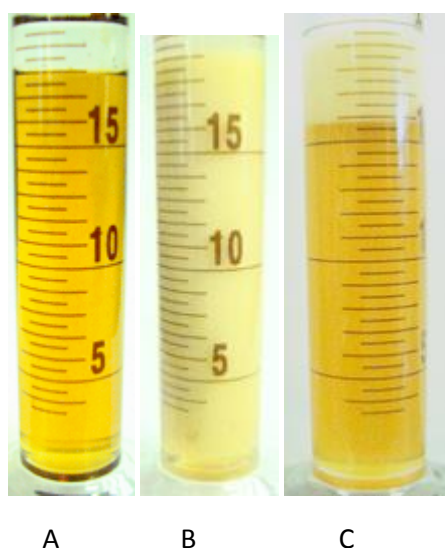


Figure 2.3: The effect of ethanol dilution on a commercially available automotive lubricant, before mixing (A), mixed (B) and settled (C)

After the emulsion is allowed to settle in a stoppered cylinder the sample is shaken again so that the unstable emulsion is reformed and then is allowed to settle again. However during the settling period the cylinder was unstoppered allowing the ethanol to volatise out of solution therefore resulting in only a lubricant layer remaining, which was analysed and used in experiments. The remaining lubricant layer is used in subsequent oxidation reactions and termed ethanol treated. This procedure modelling the evaporation of ethanol in the sump during operation and investigating the effect of ethanol on the remaining lubricant.

2.3: Chemical Analysis

2.3.1: Gas Chromatography (GC)

Gas chromatographic analysis of the substrates were undertaken using a Shimadzu GC-17a with a flame ionisation detector. The column was a 5% phenyl 95% dimethylpolysiloxane (Zebron ZB-5HT Inferno, Phenomenex) column (30 m x 0.25 mm x 0.25 μ m). The GC was fitted with a Shimadzu AOC-20a autosampler. Samples were diluted in a sample to solvent (typically

toluene) ratio of 1:5 with the injection volume set at $0.3 \mu\text{m}^3$ with a 10:1 split injection. The injector and detector temperatures were set at $360 \text{ }^\circ\text{C}$ while the initial column temperature was set at $50 \text{ }^\circ\text{C}$ increased to $350 \text{ }^\circ\text{C}$ at a rate of $5 \text{ }^\circ\text{C min}^{-1}$ with a hold of twenty minutes at $350 \text{ }^\circ\text{C}$. The GC data manipulation was undertaken using the Shimadzu software with quantification carried out by using calibration graphs of authentic standards and if no standards were available the effective carbon number method was employed. [74]

Gas chromatographic analysis of the ethanol samples required direct injection which was performed on Varian 3380 GC with the same column and a flame ionisation detector. The injection volume used was $0.3 \mu\text{m}^3$ employing a $0.5 \mu\text{m}^3$ micro syringe (SGE Australia). GC data manipulation was performed using JCL6000 software for Windows 2.0 chromatography data system. Quantification of ethanol was by a calibration of known concentrations of ethanol in isopropanol. All calibrations were performed using direct injections and isopropanol was chosen as the two peaks were identifiable and was soluble in ethanol. From the calibration the concentration of ethanol in the lubricant treated and diluted samples could be ascertained.

2.3.2: Gas Chromatography Coupled with Mass Spectrometry (GC-MS)

Gas chromatography-mass spectrometric analysis of the substrates was undertaken using a Perkin Elmer Clarus 500 gas chromatograph coupled to a Perkin Elmer Clarus 560s mass spectrometer with a was a 5% phenyl 95% dimethylpolysiloxane (Zebron ZB-5HT Inferno, Phenomenex) column ($30 \text{ m} \times 0.25 \text{ mm} \times 0.25 \mu\text{m}$). Samples were diluted in a sample to solvent ratio of 1:5 with the injection volume set at $0.3 \mu\text{m}^3$ with a 10:1 split injection. The injector and detector temperatures were set at $360 \text{ }^\circ\text{C}$ while the initial column temperature was set at $60 \text{ }^\circ\text{C}$ increased to $360 \text{ }^\circ\text{C}$ at a rate of $8 \text{ }^\circ\text{C min}^{-1}$ with a hold of twenty minutes at $360 \text{ }^\circ\text{C}$. Data analysis was performed using Perkin Elmers Turbomass Gas chromatography-mass spectrometry software. Method of charging the molecules in the mass spectrometer was by electron ionisation.

2.3.3: Gel Permeation Chromatography (GPC)

GPC analysis of the substrates were undertaken using a Hewlett Packard series 1090 liquid chromatograph with a 5 μm narrow bore 300 mm column with a column diameter of 4.6 mm and 50 Angstrom pore size capable of separating a mass range of 100-10000 g mol^{-1} (Phenomenex Phenogel 50Å gel permeation column with a Phenogel guard column) The column temperature was maintained at 40 °C with a flow rate of the mobile phase (tetrahydrofuran) set at 0.35 $\text{cm}^3 \text{min}^{-1}$ and a run time of 20 minutes. Tetrahydrofuran was chosen as the appropriate mobile phase due to its lack of UV absorption therefore not masking any potential product peaks. Detection was undertaken using a photo diode array detector which allowed acquisition of up to eight simultaneous channels between 280 and 560 nm. Samples were diluted with tetrahydrofuran and a sample of 25 μm^3 was injected via an autosampler. Data acquisition and manipulation was undertaken using HP Chemstation designed for liquid chromatography.

2.3.4: Laser Technique for Determining Scattering of Sample

A quick method to test the homogeneity of the samples treated with ethanol a qualitative laser technique was used. The sample was placed in front of a red diode laser in a white box (the white box is to provide a stable white background for photographs) and a picture taken. Any suspended micelles that are comparable or larger than the wavelength of the red diode laser (ca. 0.6 μm) will deflect the beam causing scattering and make the beam visible. Samples which show scattering in the photo were later analysed by standard spectroscopic methods to help determine the components in the micelles, Figure 2.4.

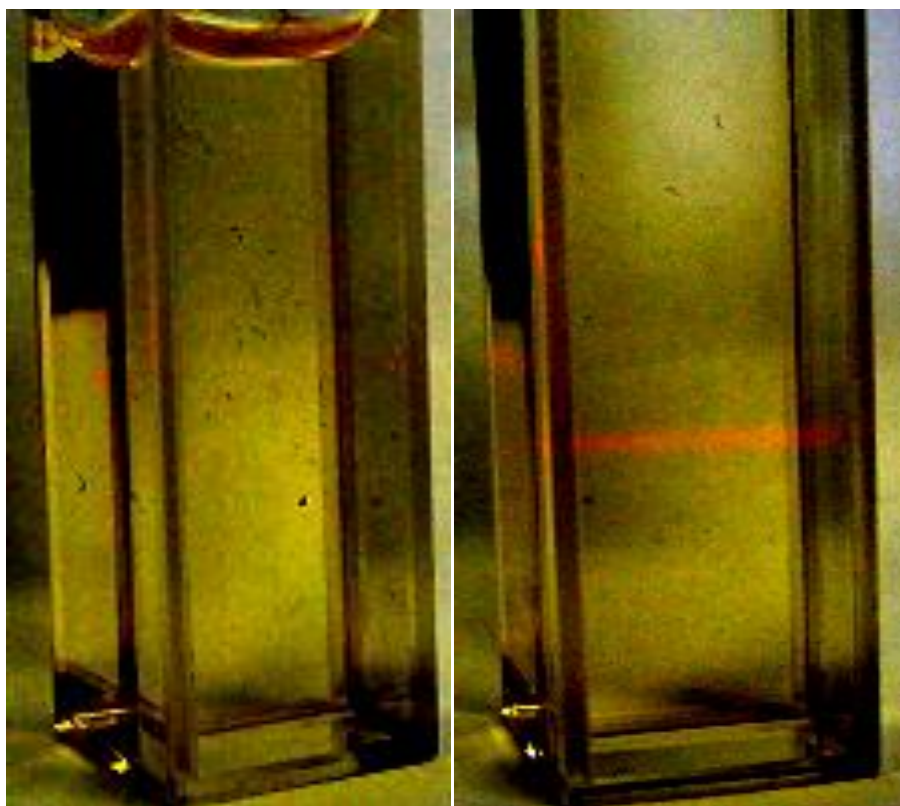


Figure 2.4: Laser Scattering of Untreated (Left Hand Side) and Ethanol Treated (Right Hand Side) Squalane Sample Containing 1% (w/w) Dispersant, 1% (w/w) Detergent and 0.25% (w/w) Phenolic Antioxidant

2.3.5: UV-VIS Spectroscopy

UV analysis of substrates was undertaken employing a Jasco 550 UV-VIS spectrophotometer with liquid and solid analysis modules. The spectrometer scans between 200 and 900 nm with a total collection time of around 1 minute, with samples diluted in a 1:50 (Substrate:Solvent) ratio. Dichloromethane was used as the solvent in UV analyses due to its ability to solubilise the lubricant sample and galvinol dye. No solvent was used in the analysis employing Nile red as a fluorescent label. Data manipulation and acquisition was performed using the Jasco Spectra software (32 bit). Both the liquid and solid sample modules were employed in this study.

UV-VIS analysis of the ethanol treated additive containing squalane samples was undertaken to determine their homogeneity. This work was based on the

assumption that if reverse micelles were forming due to ethanol treatment then the sample would be heterogeneous, and scattering of the UV beam should occur. As a consequence of the scattering there should be an absorption at all wavelengths which should follow the principles of Rayleigh scattering. The level of heterogeneity was determined by the level of baseline drift. Information can also be gathered about the components which take part in micelle formation. This is based on the assumption that any particles which cause scattering should see a decrease in absorbance as not all of the beam reaches the detector.

2.3.6: Confocal Microscopy

Confocal microscopy of the samples was undertaken using a Zeiss LSM 510 meta on an Axiovert 200M fully automated microscope. Imaging and remote operation was undertaken using Zeiss ZenLE software, which has the potential to analyse samples that have structure down to a minimum diameter of approx 1 μm . Samples were used undiluted with a UV active marker (Galvinol or Nile Red) incorporated into the lubricant composition. A drop of the sample was placed between two cover glasses before analysis. The microscopy was undertaken employing the wavelength at which the marker will fluoresce, for Galvinol it was 405 nm and for Nile red it was 561 nm.

2.3.7: Determination of Oxygen Uptake

Oxygen uptake was determined by the use of an AX300i electrochemical automotive oxygen sensor (Teledyne analytical instruments) which measures the percentage of oxygen present in the exhaust gas of the reactor. A series of calculations were employed to convert the raw oxygen percentage from the sensor into the concentration of oxygen taken up by the liquid,

The first equation converts the oxygen percentage into that of a volume,

$$O_2 \text{ uptake (dm}^{-3} \text{ min}^{-1}) = O_2 \text{ actual uptake (\%)} \times O_2 \text{ flow rate} \frac{(\text{dm}^{-3} \text{ min}^{-1})}{100}$$

Equation 2.1

The volume is then converted into a concentration

$$O_2 \text{ uptake (mol min}^{-1}) = (\text{pressure (mbar)} \times 100) \times \frac{O_2 \text{ uptake in dm}^{-3} \text{ min}^{-1}}{(R \times \text{absolute temperature})}$$

Equation 2.2

As the time between data collection on the analogue to digital converter was every second the time difference between data points is calculated by equation.

$$\text{Time Difference (min)} = \frac{1}{60}$$

Equation 2.3

The integral is calculated using equation 2.4.

$$\text{Integral (mol)} = O_2 \text{ uptake (mol min}^{-1}) \times \text{time difference (min)}$$

Equation 2.4

Equation 2.5, sums the values together

$$\text{Sum (mol)} = \text{latter sum cell} + \text{adjacent integral cell}$$

Equation 2.5

The concentration of oxygen is calculated by dividing the sum of moles by the volume, equation 2.6.

$$[\text{O}_2](\text{mol dm}^{-3}) = \frac{\text{sum(mol)}}{\text{substrate volume (dm}^{-3}\text{)}}$$

Equation 2.6

The oxygen concentration is then plotted against time. To determine the break point of the lubricant i.e. where oxidation starts, a line is drawn from the steepest gradient back to the x axis.

2.3.8: Determination of Additive Additive Synergies

To determine whether the interaction of additives was synergistic or just additive equation 2.7 was employed.

$$\text{Synergism} = \frac{\text{Formulated Break Point}}{\text{Combined Break Point}}$$

Equation 2.7: Calculation to Determine Level of Synergy

In this study the formulated break point is defined as the period of inhibition of the final formulated lubricant. The combined break point is defined as the predicted break point determined by summation of the break points for the individual additives. For these calculations the period of inhibition of squalane was deemed to be zero thus to calculate the break points equation 2.8 was employed

$$\text{Break Point} = \text{Additive Break Point} - \text{Squalane Break Point}$$

Equation 2.8: Equation to Determine Lubricant Break Point

2.4: Materials Employed

IUPAC name	Alternative Name	CAS number	Purity (%) or grade	Supplier
-	Calcium alkyl sulphonate	Proprietary	-	Shell Global Solutions
-	Succinimide dispersant	Proprietary	-	Shell Global Solutions
1-methylnaphthalene	-	90-12-0	95 +	Acros Organics
naphthalene-1-carbaldehyde	-	66-77-3	95	Aldrich
1-naphthylmethanol	-	4780-79-4	98	Aldrich
2,6,10,15,19,23-Hexamethyltetracosane	Squalane	111-01-3	99	Aldrich
N-[4-(1,1,3,3-tetramethylbutyl)phenyl]-4-(1,3,3-trimethylcyclobutyl)aniline	Irganox L01	Proprietary	N/A	BASF
octadecyl 3-(3,5-ditert-butyl-4-hydroxyphenyl)propionate	Irganox L107	Proprietary	N/A	BASF
Tetrahydrofuran	-	109-99-9	HPLC	Fisher Scientific
	Zinc dithiophosp	Proprietary	N/A	Shell

	hate			
9-diethylamino-5-benzo[α]phenoxazinone	Nile Red	7385-67-3	98	Sigma Aldrich
4-[[3,5-Bis(1,1-dimethylethyl)-4-hydroxyphenyl]methylene]-2,6-bis(1,1-dimethylethyl)-2,5-cyclohexadien-1-one	Galvinol	4359-97-1	N/A	Labotest
4-dimethylaminoazobenzene-4'-sulfonic acid sodium salt	Methyl Orange	547-58-0	Reagent Grade	Sigma Aldrich
Ethanol	-	64-17-9	99	Sigma Aldrich
Nonacosanol	-	6624-76-6	GC	In House
-	Shell Helix Super (HX5)	Proprietary	N/A	Shell Global Solutions
-	Shell Helix Plus (HX7)	Proprietary	N/A	Shell Global Solutions
-	Shell Helix Ultra	Proprietary	N/A	Shell Global Solutions
-	Shell Helix Red	Proprietary	N/A	Shell Global Solutions

3: Effect of Non-Antioxidant Additive Interactions on Lubricant Degradation

Chapter Overview

This chapter discusses the effect of lubricant composition on their oxidative stability. In particular, the effects of succinimide dispersant and neutral calcium detergent on a series of primary and secondary antioxidants is examined. These effects have received little attention to date, with the majority of the previous work centring on the effect of additives when used individually, whereas in formulated lubricants they are almost always used in combination. The aim of this chapter is to develop a clearer understanding of key additive - additive chemical interactions and the resultant effect on the oxidative stability of the lubricant, allowing for the development of improved lubricant additive packages.

3.1: Introduction

Automotive lubricants are complex formulations designed to give long-lasting protection against degradation and thus maintaining initial performance for as long as possible. [8] This is typically achieved through the introduction of an additive package consisting of a number of key species with specific functions and which is present in small concentrations typically ranging upto 20% (w/w). The chemical mechanisms for the action of each individual component is typically quite well understood. However, the effect of the chemical interactions between the additives when used together in a package and the effects on the chemical degradation of the lubricant are less well understood. This chapter will focus on the effect of two surfactants (dispersants and detergents) on the effectiveness of three different antioxidants in inhibiting the chemical degradation of lubricants.

In the literature the mechanisms for the antioxidant inhibited hydrocarbon oxidation are comparatively well understood. [28, 75, 76] Antioxidants can be

divided into two classes; radical scavenging and hydroperoxide decomposers. Radical scavengers, also called primary antioxidants, halt the radical chain process by possessing a labile hydrogen which upon removal, form the alkyl peroxide, a long-lived radical species, chapter 1 scheme 1.3. [33] Hydroperoxide decomposers, also called secondary antioxidants, decompose the resultant alkylperoxide into non-radical products halting the branching stage of autoxidation. [77] Most commercial lubricant additive packages will possess a radical scavenger and a hydroperoxide decomposer, as they act in synergy to provide improved antioxidancy in comparison with their use individually. [78] Synergism or synergy can be defined as the co-operation between two or more species to create a total period of inhibition which is greater than the sum of the individual effects.

There is little work on the effectiveness of antioxidants in the presence of non-antioxidant additives, there being just two reports on the interactions of aminic antioxidants with succinimide dispersants, Vipper and Alfadhli. [82,83] In both pieces of work it is suggested that dispersants can improve the effectiveness of aminic antioxidants when used in combination. A tentative explanation provided by Alfadhli is that the dispersant can disperse the aminic antioxidant more evenly around the lubricant. [82]

3.2: Effect of Composition on the Antioxidant Properties of Aminic Antioxidants

Aminic antioxidants (AmAO) are a class of radical scavenging antioxidants that are typically incorporated into automotive lubricant formulations to improve oxidative stability. The mechanism for their action has been studied when used in isolation. However, there has been little work reported on the effectiveness of aminic antioxidants in the presence of other classes of lubricant additives. The aminic antioxidant employed in this study is an example of a allyl substituted diphenyl aminic antioxidant, benzenamine 4-(1,1,3,3-tetramethylbutyl)-N-[4-(1,1,3,3-tetramethylbutyl)phenyl] (BASF, Irganox L01), Figure 3.1.

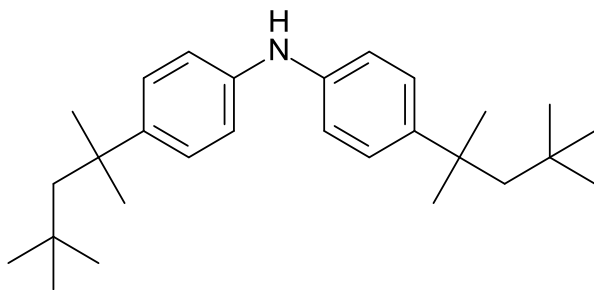


Figure 3.1: 4-(1,1,3,3-tetramethylbutyl)-N-[4-(1,1,3,3-tetramethylbutyl)phenyl]aniline (Commercial name Irganox L01, called here in abbreviation AmAO)

3.2.1: Effect of Dispersant on the Autoxidation of Squalane Containing Aminic Antioxidant

Effect of 0.18% (w/w) Aminic Antioxidant on the Autoxidation of Squalane

The next set of experiments were designed to assess the ability of an aminic antioxidant to inhibit squalane autoxidation. Upon addition of the aminic antioxidant to a level of 0.18% (w/w) (1.4×10^{-4} mol dm⁻³), the inhibition period of the system was increased by 8.0 ± 0.5 minutes from 3 minutes to 11 minutes, Figure 3.2. The error bars in Figure 3.2 and subsequent figures represent the

deviance from the mean from between two and four runs but typically three. In Figure 3.2 oxygen concentration is the amount of oxygen taken up by the liquid substrate and is a good measure of oxidation.

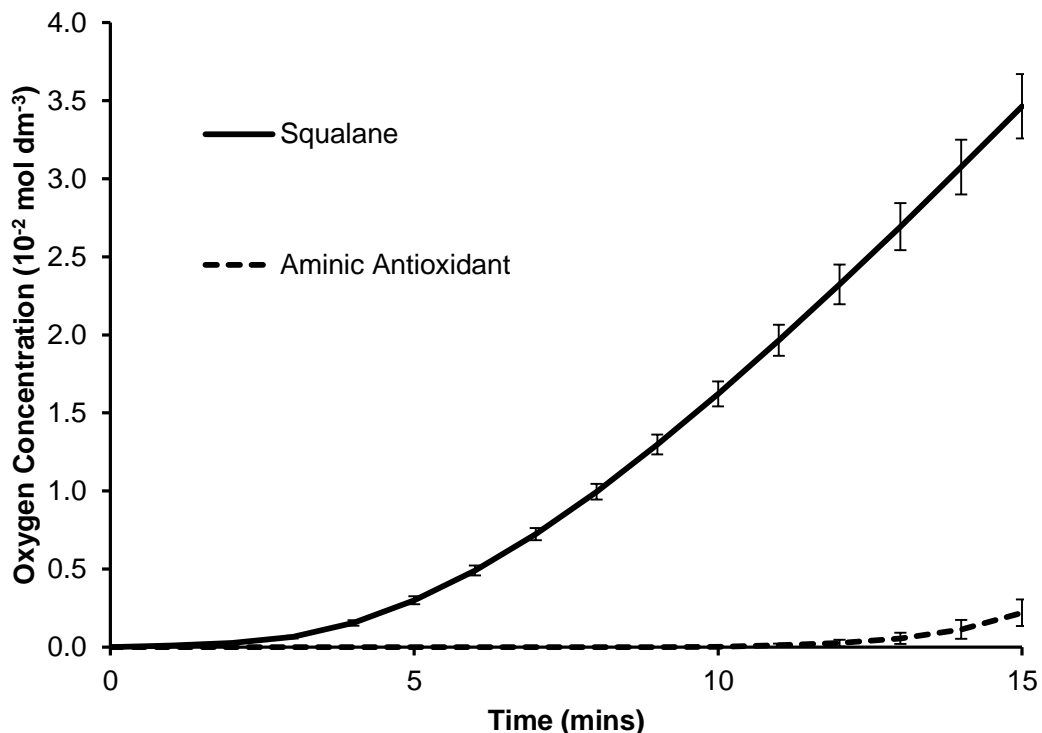


Figure 3.2: Effect of 0.18 % (w/w) Aminic Antioxidant on the Autoxidation of Squalane at 180 °C and 1 Bar of O₂

Effect of 1% (w/w) Dispersant on the Autoxidation of a Squalane Sample Containing 0.18% (w/w) Aminic Antioxidant

The next set of experiments were designed to assess the effect of a non-antioxidant additive in this case a succinimide dispersant, Figure 3.3, on the ability of the aminic antioxidant to inhibit squalane autoxidation.

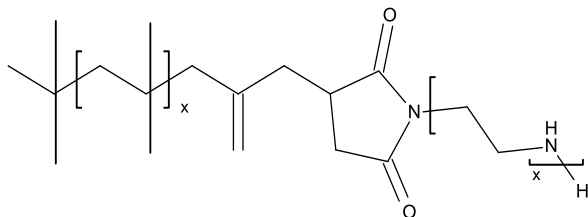


Figure 3.3: Succinimide Dispersant

It can be seen that addition of 1% (w/w) dispersant on its own to a sample of squalane had little effect on the inhibition of squalane autoxidation, Figure 3.4.

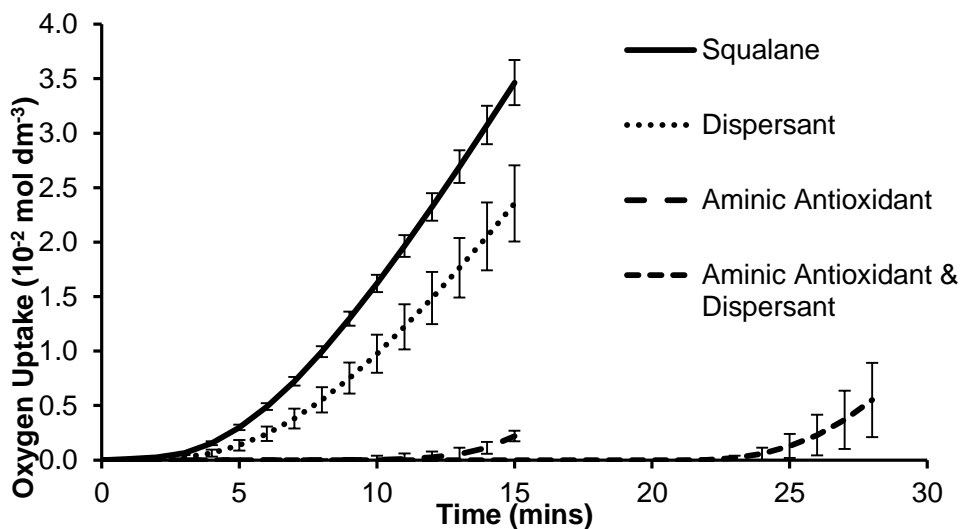


Figure 3.4: Effect of 1% (w/w) Dispersant on the Oxidative Stability of a Model Lubricant Composing 0.18% (w/w) Aminic Antioxidant at 180 °C and 1 Bar of O₂

There is a slight decrease in the rate of autoxidation once the lubricant is oxidising. This can be seen in Figure 3.5 where a slight decrease in the rate of squalane degradation was observed in the sample with 1% (w/w) dispersant present. It could be suggested that the dispersant is reducing the rate of reaction.

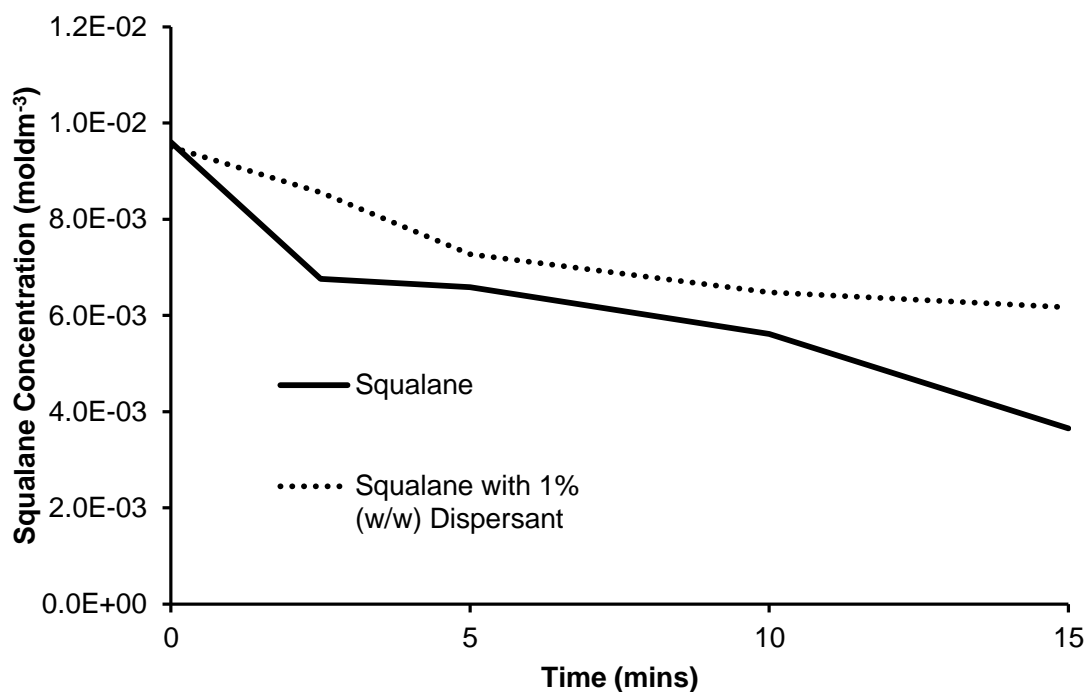


Figure 3.5: Effect of 1% (w/w) Dispersant on the Chemical Degradation of Squalane at 180 °C and 1 Bar of O₂

However, adding both dispersant and aminic antioxidant a significant increase in the antioxidancy of the lubricant was obtained upon addition of 1% (w/w) dispersant to this system. The inhibition period of the system was increased by 10 ± 1 minutes through addition of 1% (w/w) dispersant resulting in a lubricant which was stable to oxidation for 22 ± 1 minutes, Figure 3.4.

The degree of synergism was calculated as outlined in the experimental, section 2.3.9 Equation 2.7, and determined to be 2.50 ± 0.02 for the interaction of 1% (w/w) dispersant and 0.3% (w/w) aminic antioxidant. This is significant as it can be seen that with the addition of dispersant the lubricant is noticeably more stable to autoxidation as can be seen in Figure 3.6.

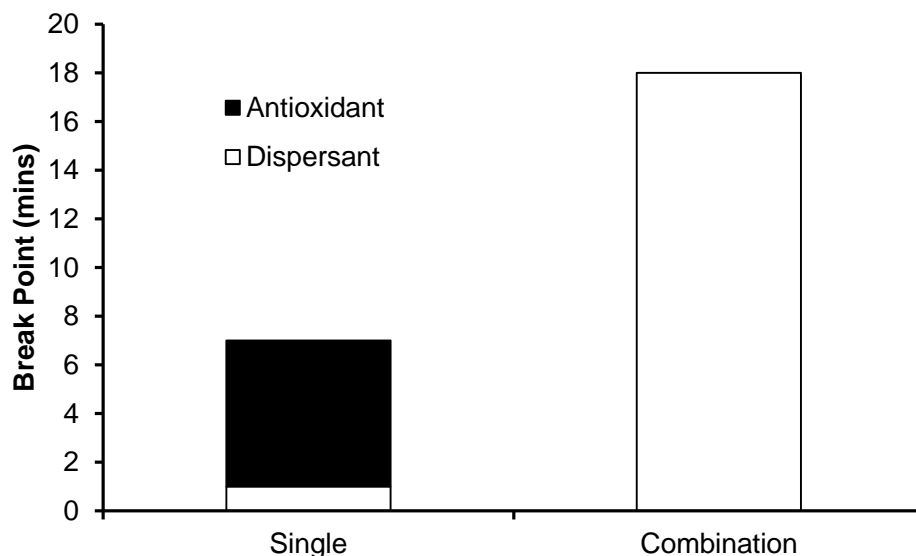


Figure 3.6: Determination of the Synergistic Effect between 1% (w/w) Succinimide Dispersant and 0.18% (w/w) Aminic Antioxidant at 180 °C

To investigate this clear synergism, further reactions were undertaken employing differing concentrations of dispersant and aminic antioxidant, Figures 3.7 & 3.8, Table 3.1. Figure 3.8 is a surface plot fitted to the observed values with each point being a repeat.

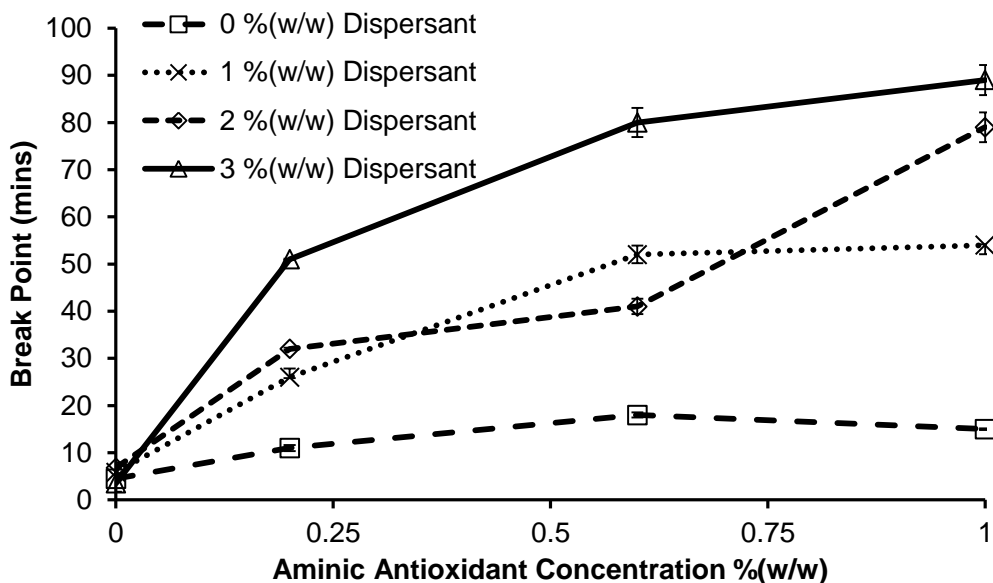


Figure 3.7: Effect of Succinimide Dispersant and Aminic Antioxidant on the Autoxidation of Squalane at 180 °C and 1 Bar of O₂

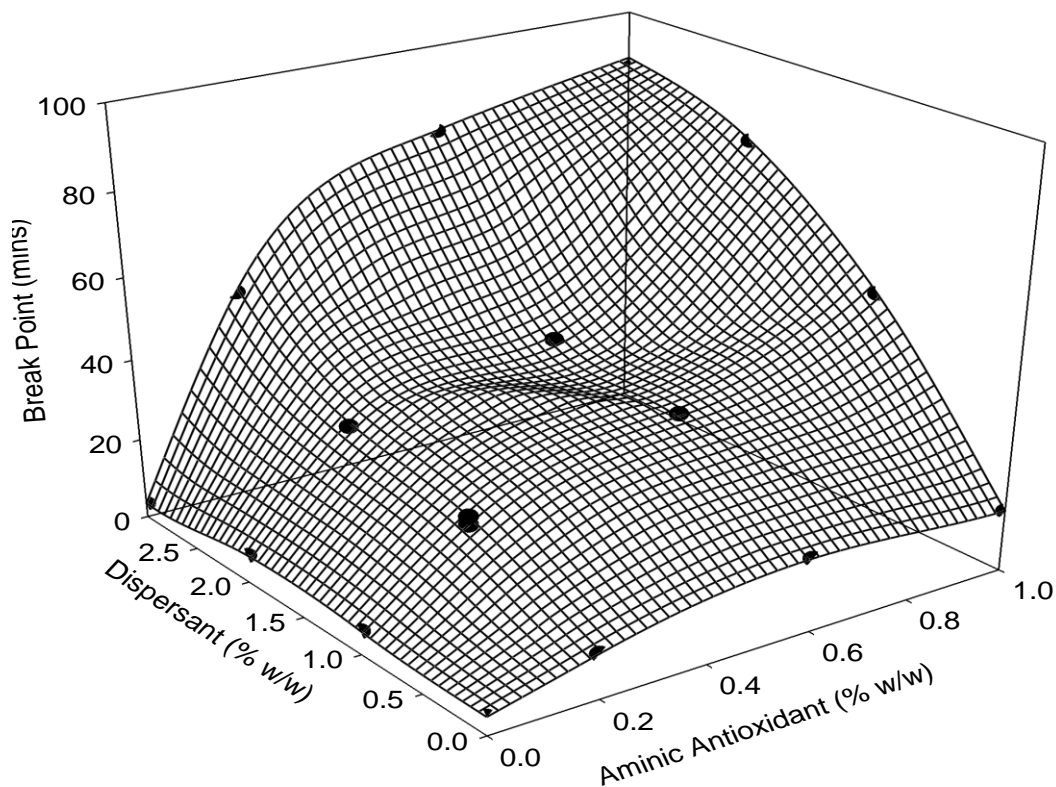


Figure 3.8: Effect of Succinimide Dispersant and Aminic Antioxidant on the Autoxidation of Squalane at 180 °C and 1 Bar of O₂

Table 3.1: Determination of Synergistic Effect Observed for Aminic Antioxidants and Dispersant used in this Study using Equation 2.3

Dispersant (% w/w)	Break Point (mins)	Aminic Antioxidant (% w/w)	Break Point (mins)	Calculated Break Point (mins)	Measured Break Point (mins)	Synergistic Effect
0.0	0.0	0.0	0.0	0.0	0.0	1
0.0	0.0	0.2	8.0	8.0	8.0	1
0.0	0.0	0.6	15.0	15.0	15.0	1
0.0	0.0	1.0	12.0	12.0	12.0	1
1.0	2.9	0.0	0.0	2.9	2.9	1
1.0	2.9	0.2	8.0	10.9	21.0	1.9
1.0	2.9	0.6	15.0	17.9	49.0	2.7
1.0	2.9	1.0	12.0	14.9	51.0	3.4
2.0	3.8	0.0	0.0	3.8	3.8	1
2.0	3.8	0.2	8.0	11.8	29.0	2.5
2.0	3.8	0.6	15.0	18.8	38.0	2.0
2.0	3.8	1.0	12.0	15.8	76.0	4.8
3.0	0.5	0.0	0.0	0.5	0.5	1
3.0	0.5	0.2	8.0	8.5	48.0	5.6
3.0	0.5	0.6	15.0	15.5	77.0	5.0
3.0	0.5	1.0	12.0	12.5	86.0	6.9

Figures 3.7 & 3.8 show that by increasing the dispersant concentration from 0 – 3% (w/w), in squalane samples containing no aminic antioxidant, little or no difference in the inhibition period of the lubricant is observed. Upon addition of aminic antioxidant to the samples, the break point is increased significantly, up to a period of 86 minutes with 3% (w/w) dispersant and 1% (w/w) aminic antioxidant, Figure 3.7 & 3.8. This would suggest that there is a significant synergistic effect between the dispersant and aminic antioxidant, Table 3.1.

3.2.2: Effect of Dispersant and Detergent on the Inhibition by Aminic Antioxidants on the Autoxidation of Squalane

The next set of experiments were designed to study the effect of two non-antioxidant additives, detergent and dispersant, on the ability of an aminic antioxidant to inhibit squalane autoxidation. The addition of detergent and dispersant to a sample containing 0.18 % (w/w) aminic antioxidant significantly increases the break point to a time of nearly 32 ± 0.5 minutes, Figure 3.9. This relates to an increase of 20 minutes over the sample containing only the aminic antioxidant, break point of 12 ± 1 minutes, Figure 3.9. It would also suggest that aminic antioxidants have a strong synergistic effect when used in conjunction with both detergent and dispersant surfactants used in this study.

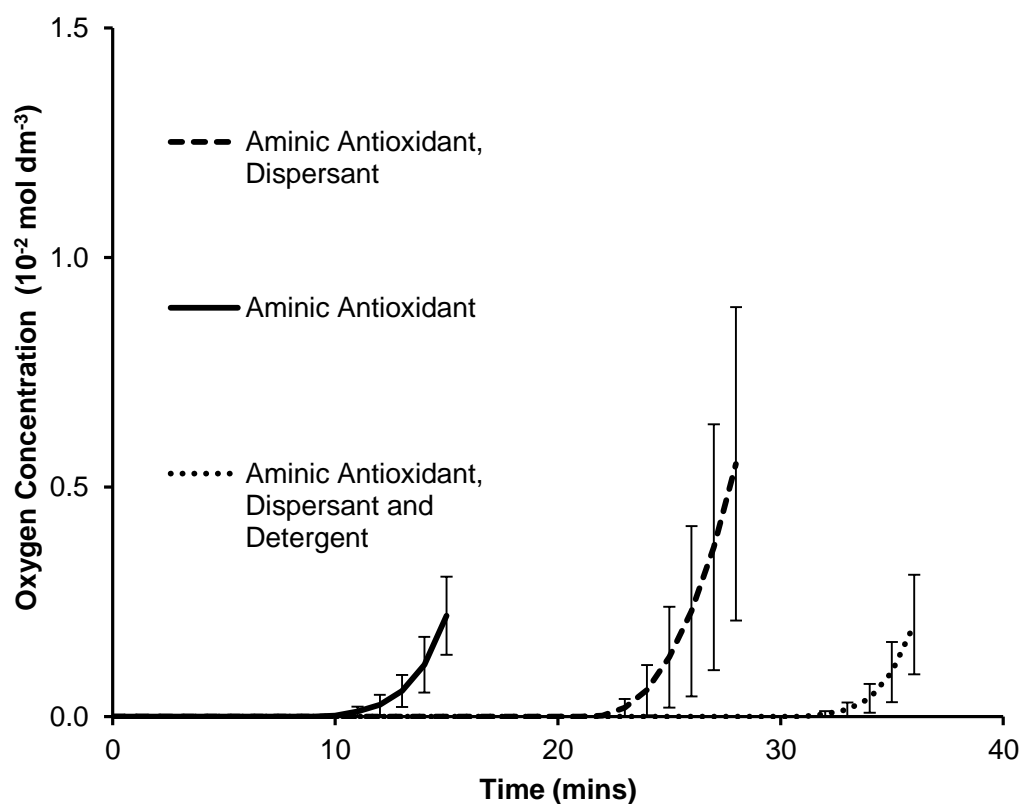


Figure 3.9: Effect of 1% (w/w) Dispersant and 1% (w/w) Detergent on the Autoxidation of Squalane Containing 0.18% (w/w) Aminic Antioxidant at 180 °C and 1 Bar of O₂

3.2.3: Effect of Composition on the Properties of Aminic Antioxidants

Summary of key observations

- Strong synergism between aminic antioxidants and detergent and dispersant surfactants, Figure 3.7 & 3.8

Figure 3.10 shows that with increasing complexity in the lubricant additive package, the lubricant becomes more stable to oxidation resulting in a break point of 35 minutes with a composition of 1% (w/w) dispersant, 1% (w/w) detergent and 0.18% (w/w) aminic antioxidant.

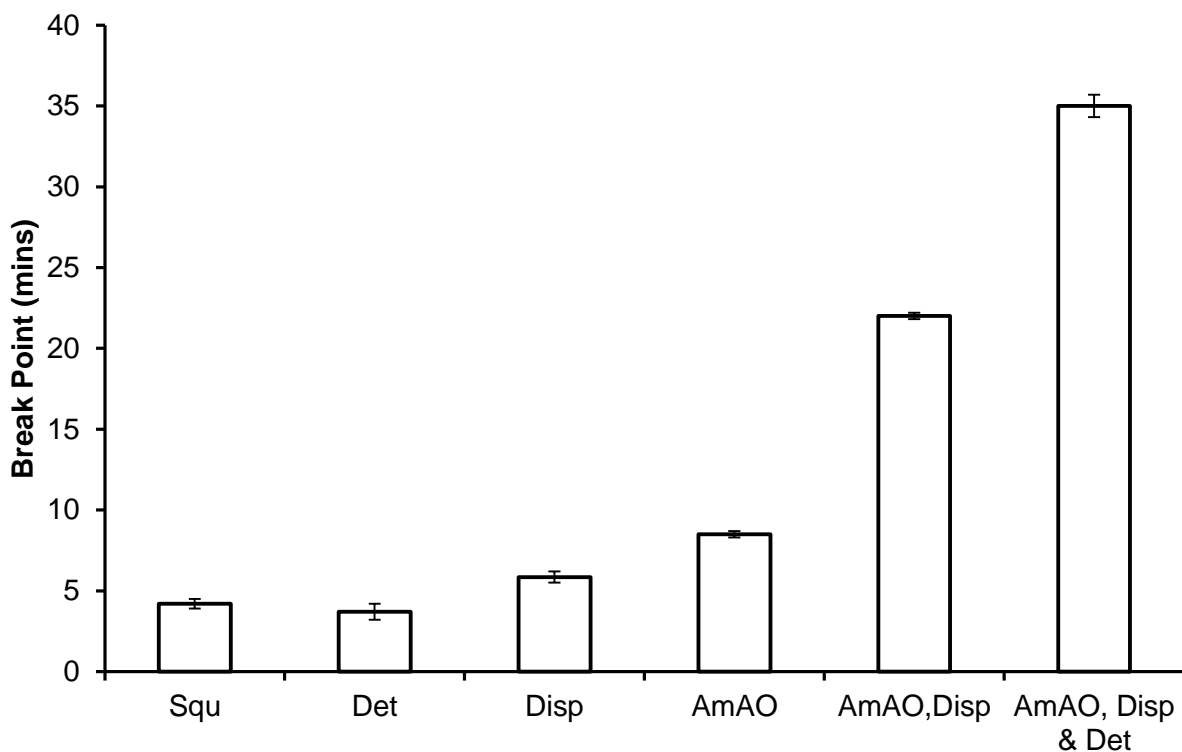
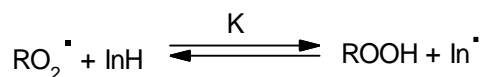


Figure 3.10: Effect of 1% (w/w) Detergent (Det) and Dispersant (Disp) on the Autoxidation of 0.18 % (w/w) Aminic Antioxidant (AmAO) Containing Squalane (Squ) Samples at 180 °C and 1 Bar of O₂

From the results it can be seen that the lifetime of aminic antioxidants is greatly enhanced in the presence of dispersants. In the literature there is a body of

work investigating the effect of reverse micelles on the autoxidation of branched and unbranched hydrocarbons. Bakunin proposed that reverse micelles can inhibit hydrocarbon oxidation by acting as a trap for alkyl peroxides, the mechanism of which will be described in more detail in chapter 6. During operation dispersants are designed to form reverse micelles in order to solubilise highly oxidised material. It is suggested in this work that dispersants can form reverse micelles around alkyl peroxides and hence can act as oxidative inhibitors.

Figure 3.10 summarises the results in Figures 3.2, 3.4 and 3.8 and indicates that the addition of 1% (w/w) dispersant to a squalane sample consisting 0.18 % (w/w) aminic antioxidant increases the oxidative stability of the lubricant to such a degree that it could be described as synergistic, Figure 3.7 & 3.8. Previous work suggests that the abstraction of a hydrogen from the aminic antioxidant by a alkyl peroxide radical could be reversible. [79]



Scheme 3.1: Abstraction of a Hydrogen from an Aminic Antioxidant (InH)

Varlamov arrived to this conclusion by calculating the equilibrium constant for the forward and reverse reactions of the peroxide radical with diphenylamine. [79] In comparison the aminic antioxidant used in this work is alkyl substituted. Their experiments were carried out at 348.5 ± 0.1 K in a bubbling cell reactor with the rate of oxidation being determined by the change in optical density. Cumyl hydroperoxide was employed as the source of alkyl peroxide in the reactions undertaken by Varlamov. [79] Through calculation the equilibrium constant for scheme 3.1 was found to be 3.00 at 349 K. It could therefore be suggested that this effectiveness of inhibition by aminic antioxidants, Scheme 3.1, is dependent on the concentration of alkyl peroxides and thus by reducing the concentration of alkyl peroxides an increased oxidative stability is observed. Other work has also shown aminic antioxidants to be less effective than their

phenolic counterparts even though the reaction mechanism is thought to be similar. [80, 81]

Existing Theories in the Literature

There is an alternative argument in the literature regarding the effect on dispersants on aminic antioxidants, Vipper suggests that the aminic antioxidant is being dispersed around the lubricant by the dispersant and thus allowing the antioxidant to be more evenly distributed. [82] It was suggested that this would allow the antioxidant to be present at high levels of oxidation. Vipper arrived at this conclusion through observing an increase in the oxidative stability of lubricants containing both aminic antioxidant and dispersant. This conclusion was also reached by Alfadhil who studies a similar system. [83] If this were the case for the system studied in this work then a decrease in the oxidative stability of the lubricant should have been observed, due to the removal of aminic antioxidant from the bulk resulting in a decrease in the level of the bulk antioxidant. This would result in a lower concentration of aminic antioxidant in the bulk phase, with a reduced ability to inhibit the oxidation process. In Vipper's and Alfadhil's work there is no suggestion that reverse micelles have an effect on the oxidative stability of the lubricant.

In summary it is suggested that the increase in oxidative stability of the lubricant upon addition of additives to aminic antioxidants is due to the formation of reverse micelles. The reverse micelles act as alkyl peroxide traps effectively controlling the bulk alkyl peroxide concentration. This is significant for the aminic antioxidants as their effectiveness is dependent on the alkyl peroxide concentration, due to the equilibrium constant of 3.00 found by Varlamov. [79] In the presence of reverse micelles the aminic antioxidant will give better protection against autoxidation.

3.3: Effect of Composition on the Antioxidant Properties of Phenolic Antioxidants

Phenolic antioxidants (PhAO) are typically incorporated into automotive lubricant formulations to improve the oxidative stability. The mechanism for this action is comparatively well understood in the literature when used in isolation. However, there is no work on the effectiveness of phenolic antioxidants in the presence of non-antioxidant additives in this field. The phenolic antioxidant employed in this study is the hindered phenolic antioxidant octadecyl 3-(3,5-ditert-butyl-4-hydroxyphenyl)propanoate (BASF, Irganox L107), Figure 3.11.

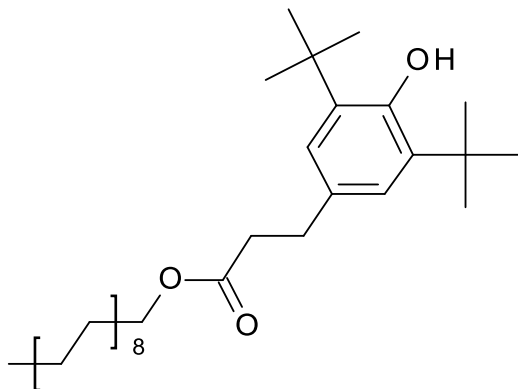


Figure 3.11: octadecyl 3-(3,5-ditert-butyl-4-hydroxyphenyl)propanoate (Irganox L107, PhAO)

3.3.1: Effect of Detergent on the Autoxidation of Squalane with Phenolic Antioxidant

Effect of 0.25% (w/w) Phenolic Antioxidant on the Oxidative Stability of Squalane

To provide a reference point for the effectiveness of phenolic antioxidants in the presence of additives, the series of reactions was started with a sample consisting of the phenolic antioxidant as a single additive at a temperature of 180 °C, Figure 3.12. Upon addition of the phenolic antioxidant, 0.25% (w/w), the inhibition period, determined by extrapolating back from the gradient, as shown in Figure 3.12, was increased by a period of 8 minutes, with no significant differences in the subsequent rate of reaction. The inhibition period for squalane alone is 5 minutes. The error bars in Figure 3.12 and subsequent Figures represent the deviance from the mean of between two and four runs but typically from three runs. In Figure 3.12 oxygen concentration is the amount of oxygen taken up by the liquid substrate and is a good measure of oxidation.

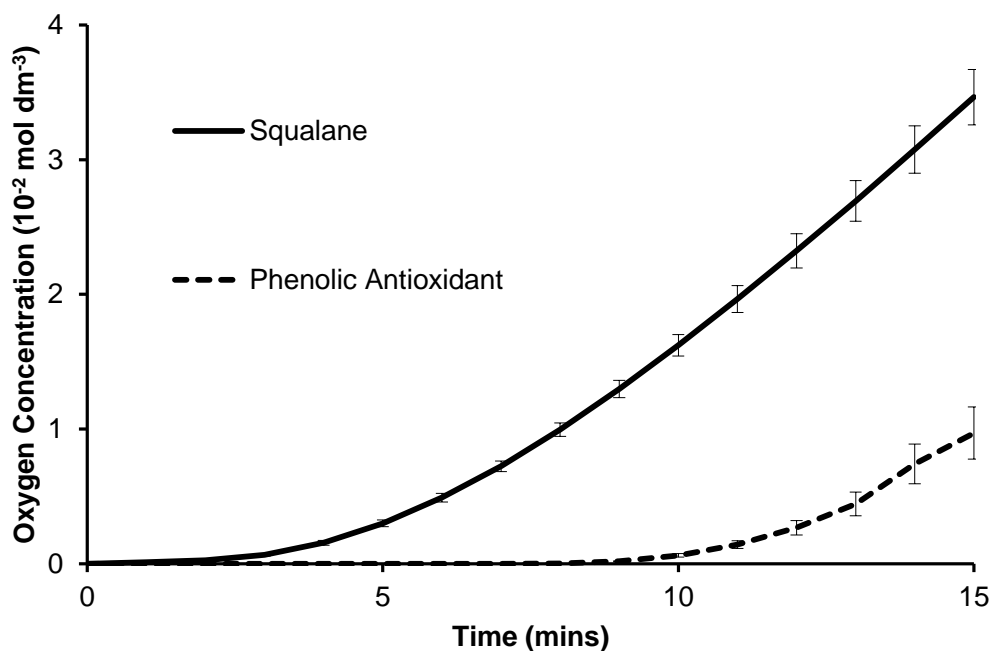


Figure 3.12: Effect of 0.25% (w/w) Phenolic Antioxidant on the Autoxidation of Squalane at 180 °C and 1 Bar of O₂

Effect of 1% (w/w) Detergent on the Oxidative Stability of a Squalane Sample Containing 0.25% (w/w) Phenolic Antioxidant

The next set of experiments were designed to study the effect of a non-antioxidant additive (detergent) on the ability of the phenolic antioxidant to inhibit squalane autoxidation. Upon addition of 1% (w/w) neutral calcium sulfonate detergent (diluted in diluent oil, concentrations of detergent and dispersant include the diluents oil), Figure 3.13, to a sample containing 0.25% (w/w) phenolic antioxidant the oxidative stability of the system is noticeably reduced, Figure 3.14.

The period of inhibition of the system is 6 ± 2 minutes, which corresponds to a decrease of 4 ± 2 minutes, suggesting that the addition of a detergent to a phenolic antioxidant results in a decrease in the oxidative stability of the lubricant. In comparison the addition of 1% (w/w) detergent to a sample of squalane had little effect on the period of inhibition, a break point of 3 ± 1 minutes, Figure 3.14.

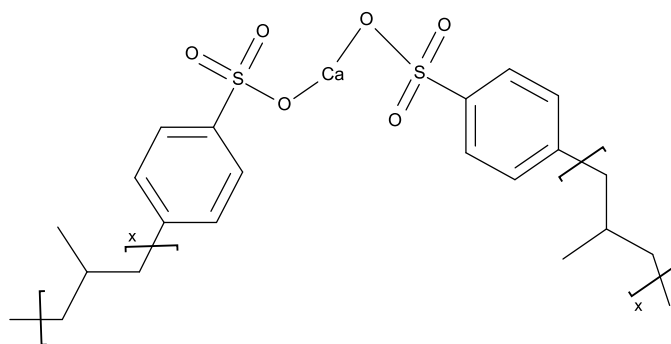


Figure 3.13: Neutral Calcium Detergent

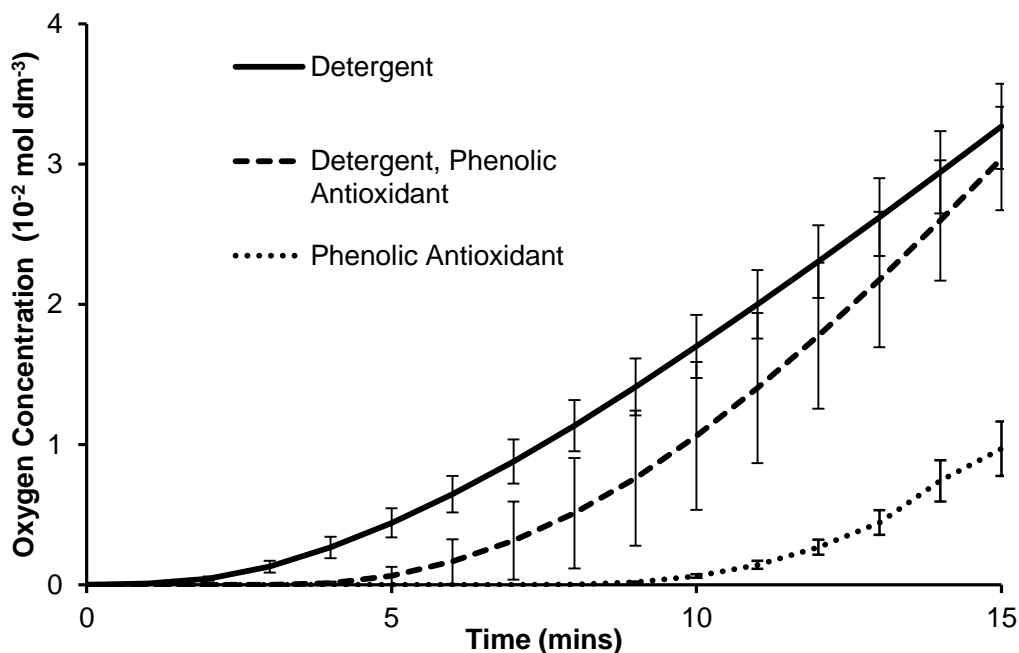


Figure 3.14: Effect of 1% (w/w) Detergent on the Autoxidation of Squalane Containing 0.25% (w/w) Phenolic Antioxidant at 180 °C and 1 Bar of O₂

3.3.2: Effect of Dispersant on the Autoxidation of Squalane with Phenolic Antioxidant

Effect of 1% (w/w) Dispersant on the Oxidative Stability of a Squalane Sample containing 0.25% (w/w) Phenolic Antioxidant

The next set of experiments investigates the effect of interactions between a phenolic antioxidant and a dispersant on the rate of squalane autoxidation. Upon addition of 1% (w/w) dispersant to a sample containing 0.25% (w/w) phenolic antioxidant the inhibition period is decreased slightly, Figure 3.15, but this is effectively within the error of the reaction while the rate of reaction is significantly reduced. This effect is in contrast to the addition of detergent which resulted in a decrease in the effectiveness of the phenolic antioxidant, with no difference in the rate of reaction, Figure 3.14.

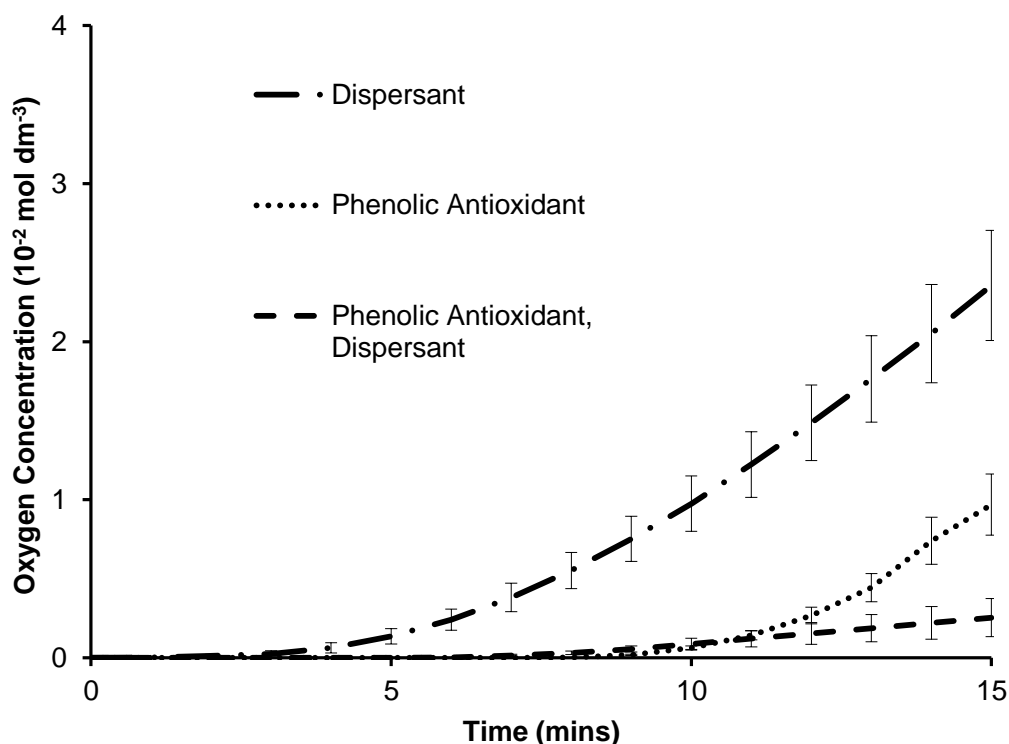


Figure 3.15: Effect of 1% (w/w) Dispersant on the Autoxidation of Squalane Containing 0.25% (w/w) Phenolic Antioxidant at 180 °C and 1 Bar of O₂

3.3.3: Effect of Dispersant and Detergent on the Autoxidation of a Squalane Sample Containing 0.25% (w/w) Phenolic Antioxidant

A dispersant and detergent were incorporated at 1% (w/w) levels to a squalane sample containing 0.25% (w/w) phenolic antioxidant. This was to assess the effect of two non antioxidant additives on the useful lifetime of the phenolic antioxidant. It can be seen that this three component model lubricant possesses similar antioxidancy as the phenolic antioxidant by itself, Figure 3.16. This would suggest that the addition of dispersant and detergent have little or no effect on the consumption of the phenolic antioxidant. However the subsequent rate of reaction is reduced which again suggests that the oxidative degradation mechanism has been altered.

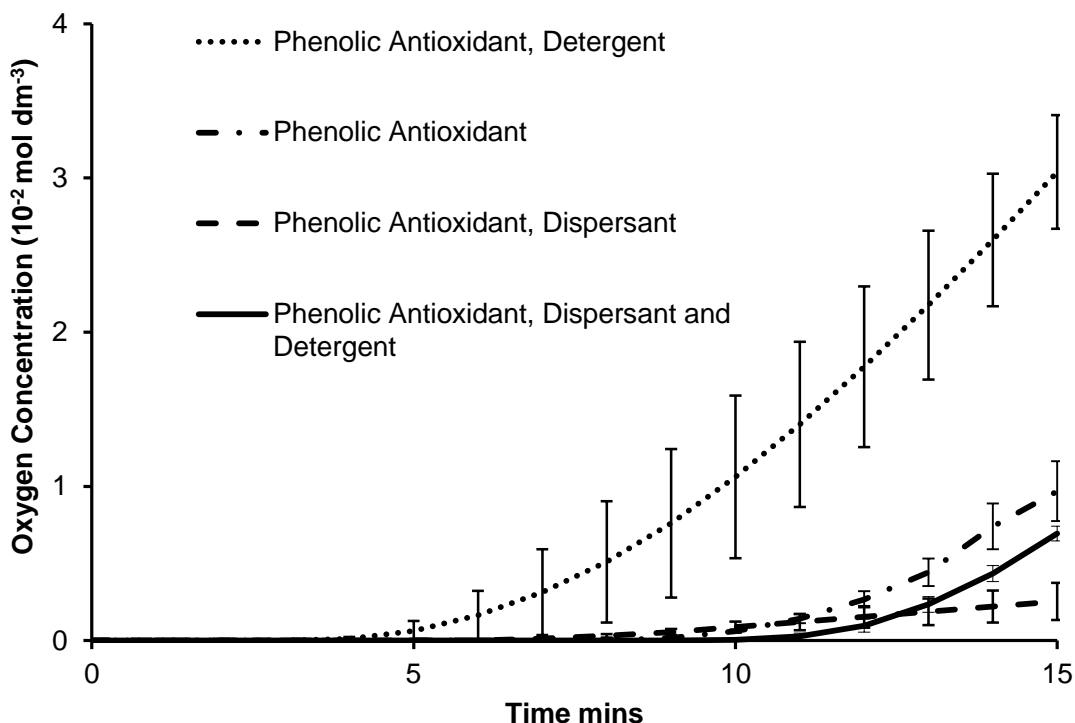


Figure 3.16: Effect of 1% (w/w) Dispersant and 1% (w/w) Detergent on the Autoxidation of Squalane Containing 0.25% (w/w) Phenolic Antioxidant at 180 °C and 1 Bar of O₂

3.3.4: Effect of Composition on the Properties of Phenolic Antioxidants

Summary of key observations

- Slight decrease in the effectiveness of phenolic antioxidants upon addition of a surfactant, Figure 3.17

Figure 3.17 shows that dispersants and detergents slightly decrease the effectiveness of the phenolic antioxidant when added as single components in a two component system, reducing the inhibition period of the system. It is only when the dispersant and detergent are incorporated into a three component

system that the lubricant reaches similar levels of protection that would be expected by the addition of a phenolic antioxidant on its own.

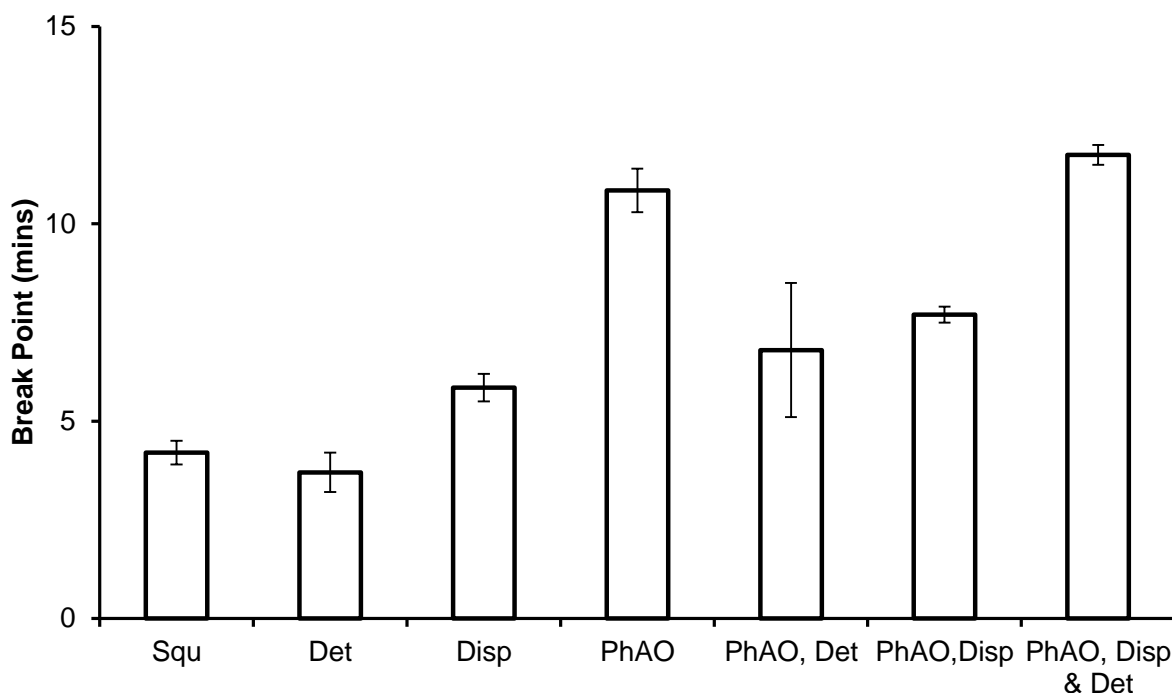


Figure 3.17: Effect of 1% (w/w) Detergent (Det) and Dispersant (Disp) on the Autoxidation of 0.25% (w/w) Phenolic Antioxidant (PhAO) Containing Squalane (Squ) Samples at 180 °C and 1 bar of O₂

A different conclusion is reached by inspecting the rate of reaction, Table 3.2, calculated assuming pseudo first order rate law. This was calculated by using a pseudo first order plot for the decay of squalane, from Figure 3.5. Despite no difference being observed in the break point there were slight changes in the reaction rate. The squalane only reaction rate was 3 times faster than with dispersant present.

Table 3.2: The effect of dispersant on the break point and reaction rate constant of the autoxidation of squalane at 180 °C

Sample	Break Point (minutes)	Reaction Rate Constant (mins ⁻¹)
Squalane	4.2 ± 0.3	(3.0 ± 0.2) × 10 ⁻²
Squalane and Dispersant	5.9 ± 0.4	(1.0 ± 0.1) × 10 ⁻²

The reduction in rate of reaction due to the addition of a dispersant is proposed to be due to the formation of reverse micelles. In the literature there is a theory which suggests that reverse micelles can act as traps for alkyl peroxides. A detailed discussion on the mechanism which results in the reduced rate of squalane autoxidation in the presence of surfactants can be read in chapter 6.

3.4: Effect of Composition on the Autoxidation of Squalane Containing ZDDP

Zinc dialkyldithiophosphate (ZDDP) are a different class of antioxidant to the previously discussed radical scavenging phenolic and aminic antioxidants studied earlier in the chapter in that it acts as a hydroperoxide decomposer. [77, 78, 84, 85] The mechanism by which it inhibits hydrocarbon oxidation in isolation and in combination with radical scavenging antioxidants has been studied extensively. [77, 78, 84, 85] In this work the effects of non-antioxidant additives on the effectiveness of ZDDP will be studied.

3.4.1: Effect of Coating on the Oxidative Stability of Model Lubricants

To test the effectiveness of the peroxide decomposing antioxidant ZDDP, a sample of 1% (w/w) ZDDP in squalane, Figure 3.18, was autoxidised at 180 °C as described in the experimental chapter.

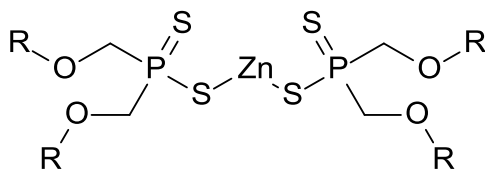


Figure 3.18: Zincdialkyldithiophosphate (ZDDP)

It has been reported that during normal operation the metal surfaces of the engine will become coated with a ZDDP tribofilm. [86] A tribofilm is a solid deposit formed due to sliding contact in machinery and can act as a barrier to reduce wear and friction. The effect of this film on the oxidative stability of ZDDP lubricants is not well understood but is believed to play a role in the inhibition of the chemical degradation of the lubricant. [78] Before work was carried out on ZDDP, the reactor was conditioned by undertaking repeated autoxidation runs; this was to provide a stable reproducible coating on the stainless steel surface. Four conditioning runs were required before the reactor gave a relatively stable period of inhibition, Figures 3.19. This would suggest that the effect of coating the reactor does indeed have an effect on the oxidative stability of the lubricant.

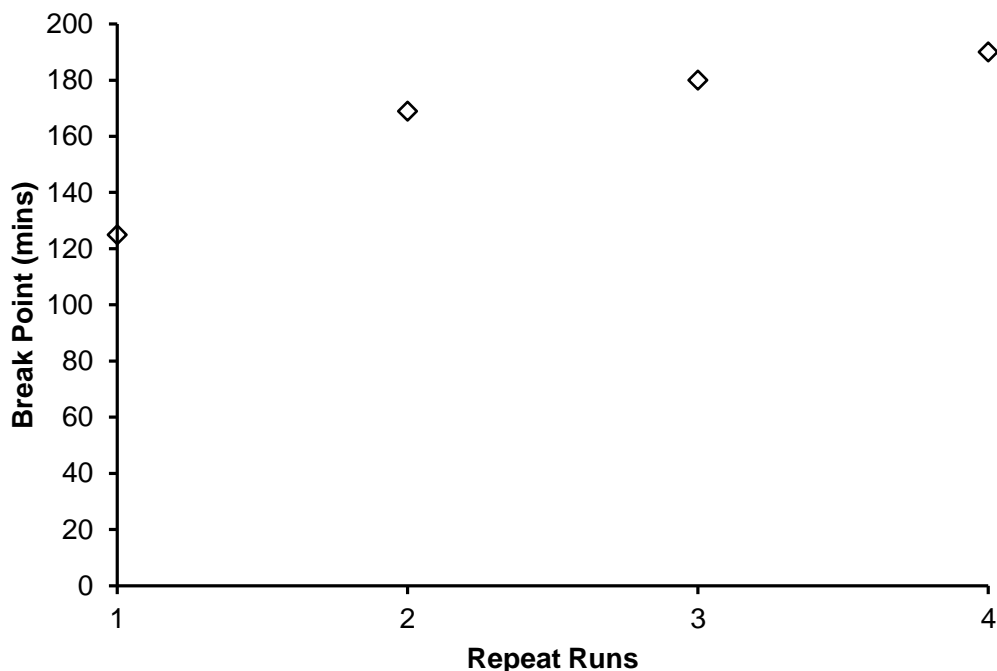


Figure 3.19: Effect of ZDDP Tribofilm Formation on the Autoxidation of Squalane Consisting of Repeated Runs Using 1% (w/w) ZDDP at 180 °C and 1 Bar of O₂

The first run had a break point of 125 minutes and in subsequent runs this increased by a further ca 60 minutes. Therefore the effect of coating is so great that upon oxidation of pure squalane at 180 °C in a ZDDP coated reactor the resultant inhibition period is increased to the same level as that achieved with the addition of 0.25% (w/w) phenolic antioxidant, Figure 3.20. The only difference between the two squalane samples in Figure 3.20 is the coating on the reactor surface. It could therefore be suggested that the surface chemistry does have a noticeable effect as the lubricant composition.

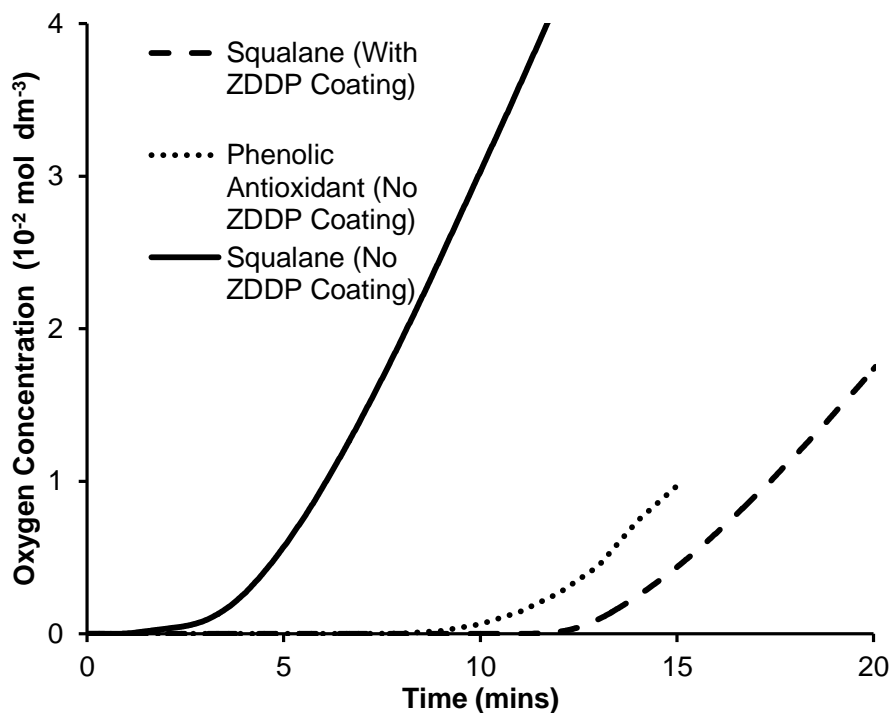


Figure 3.20: Effect of ZDDP Tribofilm Formation on the Autoxidation of Squalane at 180 °C and 1 Bar of O₂ Compared to that of Squalane with 0.25% (w/w) Phenolic Antioxidant in a Clean Reactor

3.4.2: Effect of a Phenolic Antioxidant on the Autoxidation of Squalane Containing ZDDP

With the addition of 1% (w/w) ZDDP to 0.25% (w/w) phenolic antioxidant, the break point doubled from 200 minutes (ZDDP only) to 400 minutes (ZDDP and phenolic antioxidant), Figure 3.21, suggesting a synergistic effect of 1.9 ± 0.1 , Figure 3.22.

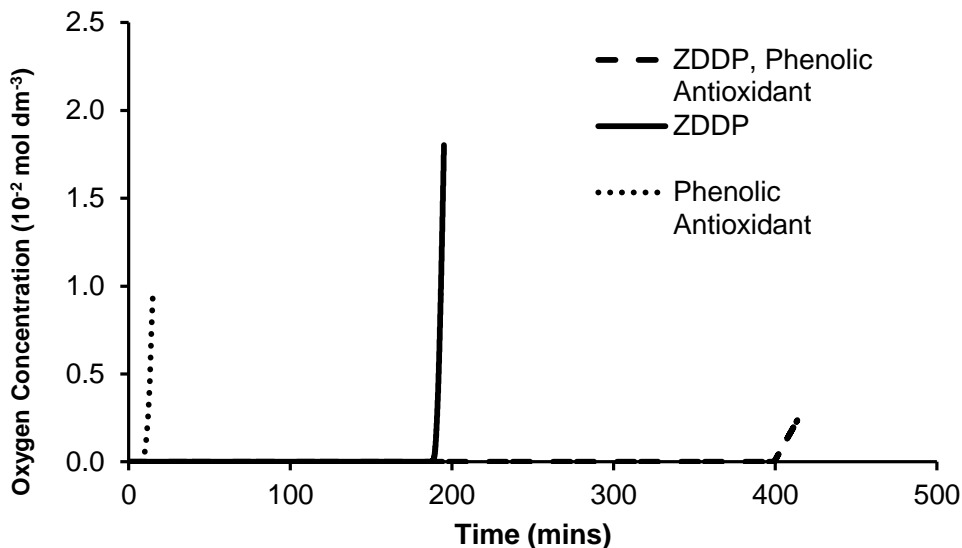


Figure 3.21: Effect of 1% (w/w) ZDDP on the Autoxidation of Squalane Containing 0.25% (w/w) Phenolic Antioxidant at 180 °C and 1 Bar of O₂

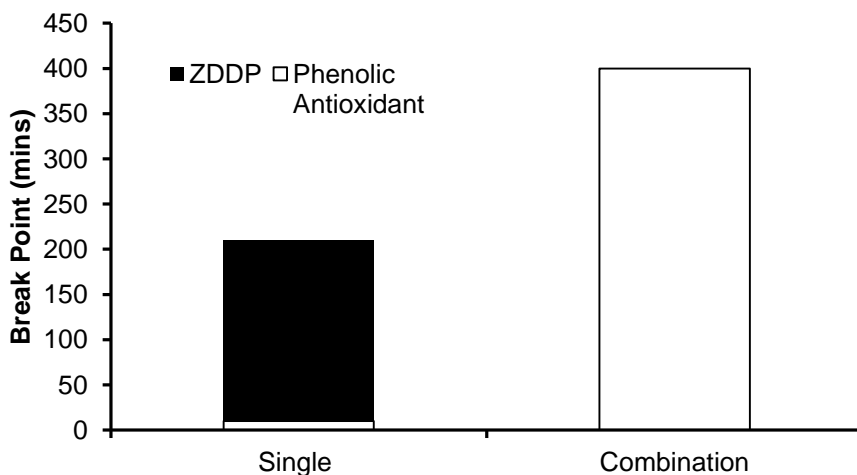


Figure 3.22: Determination of the Synergistic Effect Between a Phenolic Antioxidant and ZDDP

3.4.3: Effect of a Dispersant and Detergent on the Autoxidation of a Squalane Sample Containing ZDDP and Phenolic Antioxidant

The next set of experiments were designed to assess the effect of non antioxidant additives on the properties of ZDDP. It can be seen upon addition of 1% (w/w) dispersant and 1% (w/w) detergent, together, to a squalane sample containing 1% (w/w) ZDDP and 0.25% (w/w) phenolic antioxidant that the oxidative stability of the lubricant is reduced by 60 minutes, Figure 3.23. This shows that dispersants and detergents have a negative effect on ZDDP and the phenolic antioxidant.

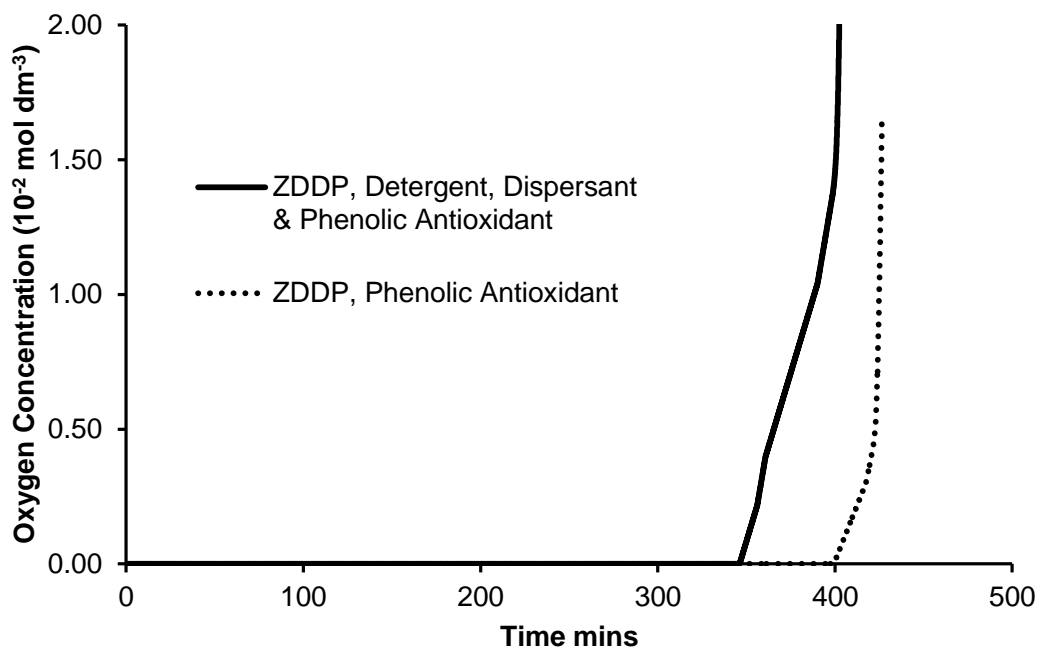


Figure 3.23: Effect of 1% (w/w) Dispersant and 1% (w/w) Detergent on the Autoxidation of Squalane Consisting of 1% (w/w) ZDDP and 0.25% (w/w) Phenolic Antioxidant at 180 °C and 1 Bar of O₂

3.4.4: Effect of Composition on the Antioxidant Properties of ZDDP

Summary of key observations

- ZDDP coated reactor results in an increased oxidative stability of base oil
- Strong synergy when phenolic and ZDDP used together
- Addition of detergent and dispersant reduces the oxidative stability of the lubricant

Unsurprisingly, addition of a secondary antioxidant (ZDDP) to a primary antioxidant (phenolic antioxidant) results in a lubricant which is more stable to oxidation, Figure 3.24. [87] This is in part due to the ZDDP acting as a peroxide decomposer.

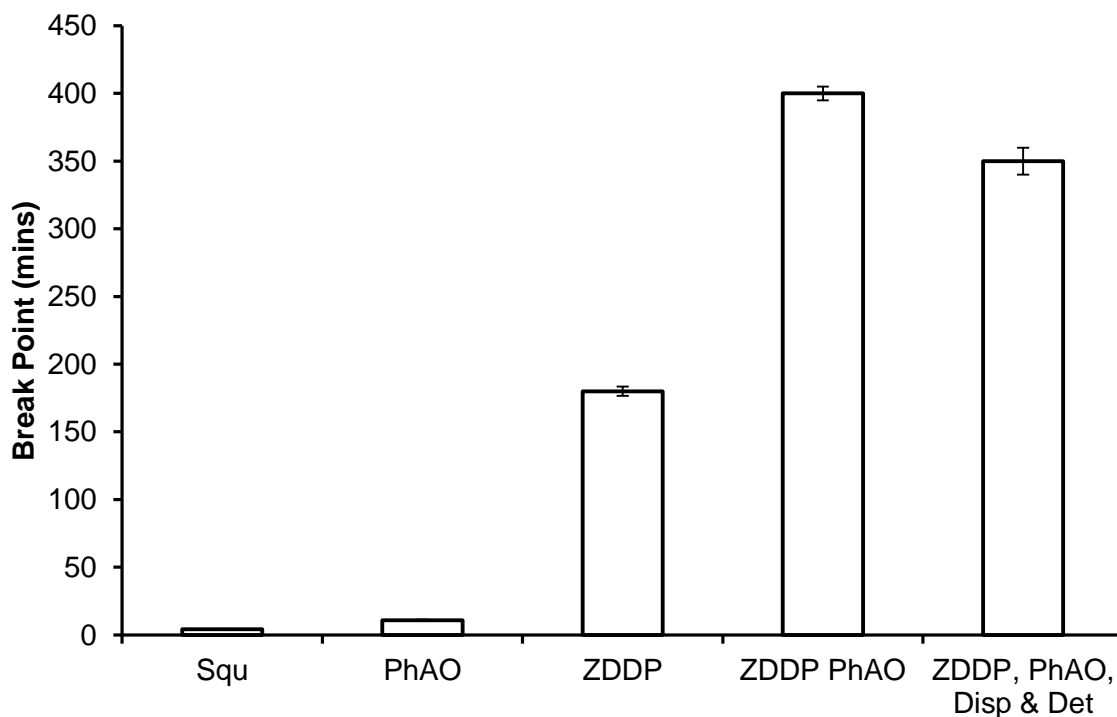


Figure 3.24: Effect of 1% (w/w) Detergent (Det) Dispersant (Disp) and ZDDP on the Autoxidation of 0.25% (w/w) Phenolic Antioxidant (PhAO) Containing Squalane (Squ) Samples at 180 °C and 1 Bar of O₂

In theory, the rate of alkyl peroxide formation during the autoxidation of squalane is reduced by the incorporation of phenolic antioxidant. With the addition of ZDDP the alkyl peroxide undergoes decomposition into non-radical products and thus disrupts the radical chain mechanism. This however cannot explain the increased oxidative stability observed in the ZDDP coated reactor.

Effect of ZDDP Coating on Autoxidation of Squalane

The majority of recent research activity into ZDDP has centred on the properties and formation of a tribofilm by it. A considerable amount has been learnt about its composition and structure. Tribofilm formation can occur at reasonably low temperatures, 50 °C, with the rate of formation increasing with temperature and on a steel surface the film can grow to a thickness of between 50 nm and 150 nm. [88, 89] Initial stages of formation occur in patches which gradually develop to form a pad like structure separated by valleys. [90] The pad like structure is thought to consist mainly of a glass-like sulphate, with a thin outer layer of zinc polyphosphate and ZnDTP's (ZDDP), Figure 3.25. [91, 92]

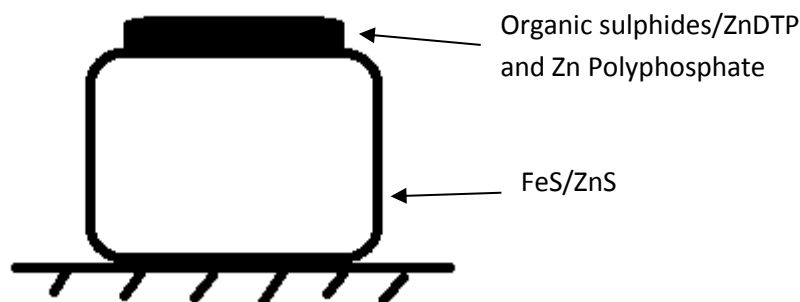


Figure 3.25: Schematic Diagram of ZDDP Tribofilm Structure and Composition [78]

From inspection of Figure 3.26 which shows the reactor bases used in this study, a coating can be seen to be forming on the non-sliding contacts.



Figure 3.26: Diagram of Comparison Between a ZDDP Coated Reactor (Left Hand Side) and a Non-Coated Reactor (Right Hand Side)

Considering the composition of the coating, a mechanism can be proposed to explain the increased oxidative stability in the coated reactor. From Figure 3.24 it can be seen that coating formation traps a small concentration of ZDDP on the surface of the pad. It is assumed that it can still act as a peroxide decomposing antioxidant explaining the increased oxidative stability of the squalane only sample in the coated reactor. In essence, the coated reactor has a small concentration of antioxidant in the coating which in turn increases the oxidative stability of the squalane sample to beyond the levels of a traditional antioxidant, as can be seen in Figure 3.20. This result shows the effect of surface chemistry on the oxidative stability of the lubricant as this is the only difference between the two reactors. The addition of surfactants to a squalane sample containing ZDDP and phenolic antioxidant reduced the effectiveness of ZDDP as can be seen in Figure 3.24. It can be suggested that this is due to the surfactants trapping a portion of phenolic antioxidant in a reverse micelle and hence not being available to decompose peroxides in the bulk, homogeneous phase.

3.5: Conclusions

The effect of two lubricant surfactants, dispersants and detergents on the ability of three antioxidants, phenolic, aminic and ZDDP to inhibit autoxidation has been studied in squalane at a temperature of 180 °C. All three antioxidants were affected by the presence of a dispersant and/or detergent, but in different ways.

Addition of 1% (w/w) dispersant to squalane resulted in no significant alteration in the break point, Figure 3.16. However, there was a reduction in the subsequent rate of reaction, Table 3.2. This is attributed to the dispersants forming reverse micelles around the polar molecules formed from the autoxidation of the squalane. Once these reverse micelles are formed they can then act as alkylperoxide traps. This effectively removes the alkylperoxide from the bulk phase, resulting in a reduction in the rate of reaction.

Aminic antioxidants were seen to exhibit a strong synergistic effect with dispersants, Figure 3.5 & Table 3.1. Again, this is attributed to the formation of reverse micelles that effectively reduce the bulk alkyl peroxide concentration by acting as alkyl peroxide traps. It is suggested that aminic antioxidants are susceptible to alkylperoxide concentration based on the assumption that dispersants form reverse micelles which act as alkyl peroxide traps.

The peroxide decomposer antioxidant, ZDDP, used in this study provided the expected good levels of protection and the previously observed synergistic effect with a radical scavenging antioxidant, Figure 3.22. Of interest was the effect of coating the reactor with a film of ZDDP as this gave greater levels of oxidative stability on subsequent reactions in this reactor. This is attributed to the formation of a tribofilm which trapped ZDDP on the top layer and in effect provided the surface with a level of antioxidancy.

It can be seen that non-antioxidant additives and surface chemistry do have a significant effect on the ability of antioxidant to inhibit autoxidation. It is proposed that it is the formation of reverse micelles and more importantly their

composition which provide the greatest effect, while the surface make up can also play a significant role.

This in turn introduces the idea of heterogeneous lubricant systems. Both the effect of reverse micelles and surface coatings on lubricant stability highlights the influence of the heterogeneity of the lubricant.

4: Effect of Ethanol on Model Automotive Lubricant Degradation

Chapter Overview

In this chapter the effect of ethanol fuel dilution on the oxidative stability of model lubricants is studied. The key aim of this chapter is to provide a description of the effect of ethanol on the key additive interactions outlined in the previous chapter between primary antioxidants (phenolic and aminic) and surfactants (dispersant and detergent).

4.1: Introduction

Lubricants are employed to protect the moving parts of automotive engines to reduce component wear and energy loss due to friction as described in chapter 1. An area of interest is the chemistry of the lubricant in the piston assembly where the lubricant is exposed to high temperature, O₂, NO_x and unburnt and partially combusted fuel. [22, 24, 30, 93] In the work of Moritani and Naidu it has been suggested that the majority of lubricant degradation occurs in the piston assembly, with the chemical degradation due to autoxidation being the major cause. [24, 94] The lubricant is only exposed to these harsh conditions for a relatively short time, ca 3 minutes, or less than 1 minute and in small volumes, where it is degraded before returning to the lubricant sump. [30, 95]

During typical operation of an automotive engine, uncombusted fuel can dissolve in the lubricant in the piston assembly, before returning into the sump. [7, 19] Temperatures in the sump are relatively low (ambient to ca. 80 °C) in comparison to the combustion chamber which is typically higher (110-160 °C). [7, 19, 24] The sump is the area of the engine where the lubricant spends the longest time.

Dilution of the lubricant with fuel is higher during the starting and warm-up period of the engine, particularly in winter, where the metal surfaces of the

cylinder are cold leading to fuel accumulating in the lubricant in the sump at significant concentrations, with up to 13% (v/v) reported for conventional gasoline in used oil samples being reported for gasoline engines. [19,50, 54]

When using fuel containing ethanol the concentrations observed in the sump are lower than that reported for gasoline at up to 10% (v/v), due in part to its higher volatility than conventional gasoline. [50] It has therefore been of interest to investigate whether having fuel in the sump can affect the degradation of the lubricant. Any increase in lubricant degradation could result in altered engine friction and hence result in reduced fuel economy, hence increased atmospheric carbon dioxide emissions from the engine and also affect the usable lifetime and hence cost of the lubricant, so this is worthy of investigation.

The bulk of the previous published research on the effect of oxygenated fuels on lubricants has centered on the effect of methanol and methyl-tert-butyl-ether (MTBE) on lubricant performance. [15, 64, 67, 71] During the oil crisis of the 1970's methanol was seen as an alternative to traditional gasoline due to its ready availability and relatively competitive cost. [96] It was still employed as an alternative to gasoline in North America until the early 1990's, leading to research into the effect of methanol on lubricant performance being undertaken. [97-99]

Moritani employed engine tests to investigate the effect of oxygenated fuels on lubricants and found that methanol had a beneficial effect by decreasing the rate of sludge formation. [100] In more recent history ethanol has replaced methanol as the main alternative to gasoline due to better green and safety credentials. One of the potential issues with ethanol dilution into lubricants is phase separation, as observed with methanol, which is of concern to gasoline suppliers who want to dilute gasoline fuel with ethanol. [70] It has also been observed that ethanol partitions into a polar and a non-polar phase when diluted with gasoline and used as a fuel and stored for a period of time. [101]

Shah developed a bench-scale test designed to evaluate the suitability of lubricants for use with methanol fuelled cars. [70, 71] It was also observed that the methanol contaminated lubricants undergo a liquid-liquid extraction, due to

the polar methanol being almost immiscible in lubricants, which consist predominantly of relatively non-polar hydrocarbons. The methanol soluble additives migrated into the methanol layer, with methanol-insoluble additives remaining in the lubricant layer. After this extraction procedure it was observed that methanol had a negative effect on the oxidative stability of the remaining lubricant; however a detailed chemical analysis of the chemistry behind this effect was not undertaken. [70]

More recent studies on the effect of ethanol on lubricant performance have been undertaken, with the formation of lubricant-water micro emulsions being observed in the sump with E85 (85% ethanol 15% gasoline) fuelled cars which were run for short drive cycles therefore not allowing the engine to reach normal operating temperature. [50] There was little chemical analysis of the emulsion carried out. A laboratory based study identified no effect on the lubricants degradation with ethanol dilution. [73]

The study reported here will present work on the effect of ethanol on the oxidative stability of model lubricants using a bench top reactor at piston ring pack temperatures.

4.2: Results

4.2.1: Effect of Ethanol on the Autoxidation of Squalane Samples Containing a Phenolic Antioxidant

Phenolic antioxidants (PhAO) are typically incorporated into automotive lubricant formulations to improve the oxidative stability. [33] The mechanism for this action is well understood in the literature and described in section 3.3, when they are used in isolation. However, there is little or no work on the effectiveness of phenolic antioxidants in the presence of ethanol fuel dilution. The hindered phenolic antioxidant employed in this study is octadecyl 3-(3,5-ditert-butyl-4-hydroxyphenyl)propanoate (BASF's Irganox L107).

Effect of Ethanol Treatment on Phenolic Antioxidant Containing Squalane Samples

Samples of squalane containing various additives were treated with ethanol to simulate the effect of cold starting the engine followed by a long run as described in the experimental. The treated lubricant was then used in subsequent autoxidation runs. The treatment method was designed to model the effect on the autoxidation of automotive lubricant that has had 10% (v/v) ethanol mixed through it and then subsequently evaporated. Due to ethanol's high volatility it will have a comparatively short residence time in the sump at normal operating temperature so the lubricant was mixed like it would in the sump and the ethanol allowed to evaporate at room temperature. The remaining lubricant should have no ethanol present in the lubricant and is referred to in the rest of this thesis as 'treated'. It is assumed that at piston ring pack temperatures ethanol will most likely be in the gas phase and have little effect on the lubricant degradation as a dilution effect and therefore this treatment method is thought to be more representative. The lubricants treated with ethanol in this way should have had little or no ethanol present in the lubricant prior to oxidation. This was confirmed by gas chromatography analysis, Figure 4.1, as no ethanol is present in the lubricant after heating but prior to the start of autoxidation with an upper limit of 0.01% (v/v) ethanol.

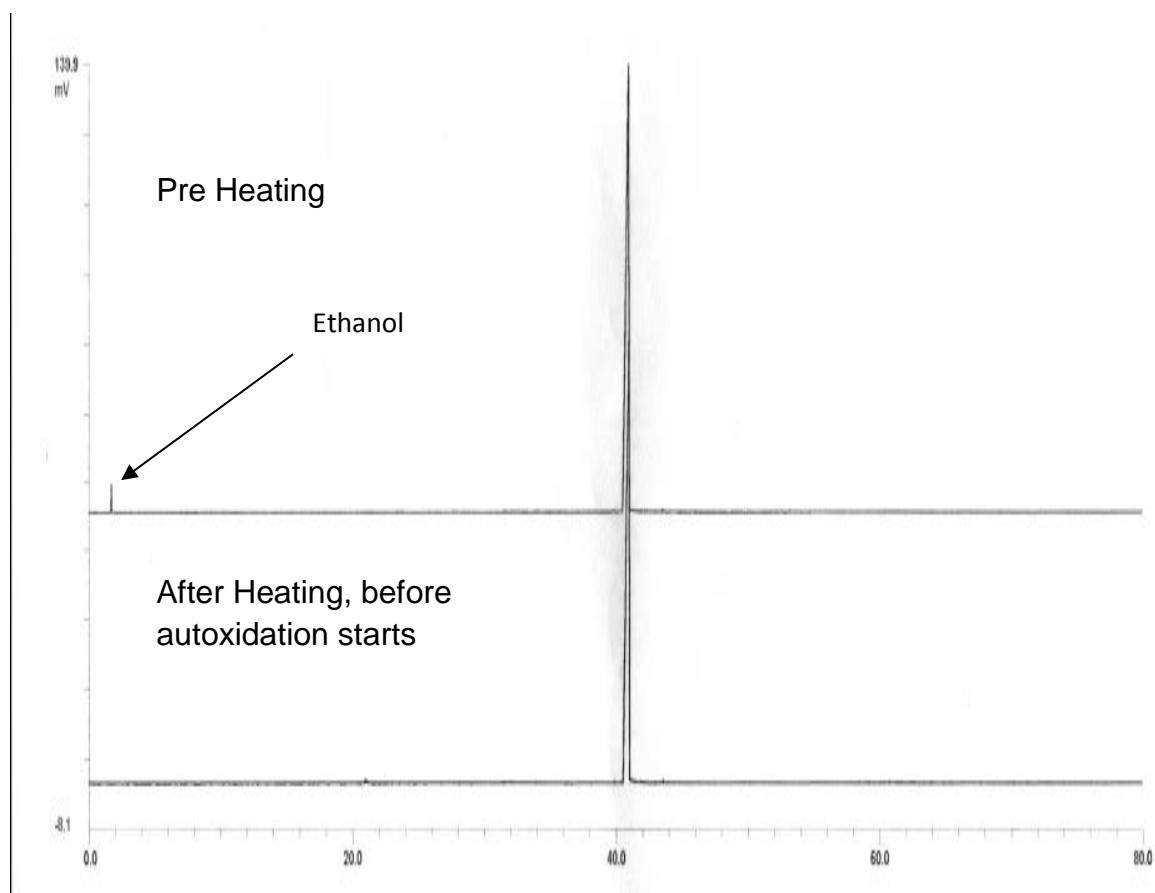


Figure 4.1: GC Analysis of the Ethanol Treated Sample Before and After the Heating Period.

Effect of Ethanol Treatment on the Autoxidation of a 100 % (w/w) Squalane Sample

The effect of this ethanol treatment on the autoxidation of squalane was examined and is shown in Figure 4.2, in this and subsequent figures the error bars represent the range of values from the mean of between two and four runs with the average being three and it is clear that ethanol treatment has little effect on the break point of squalane when no additives are present. However, there is a slight difference in the subsequent rate of autoxidation with an increased rate observed in the treated sample.

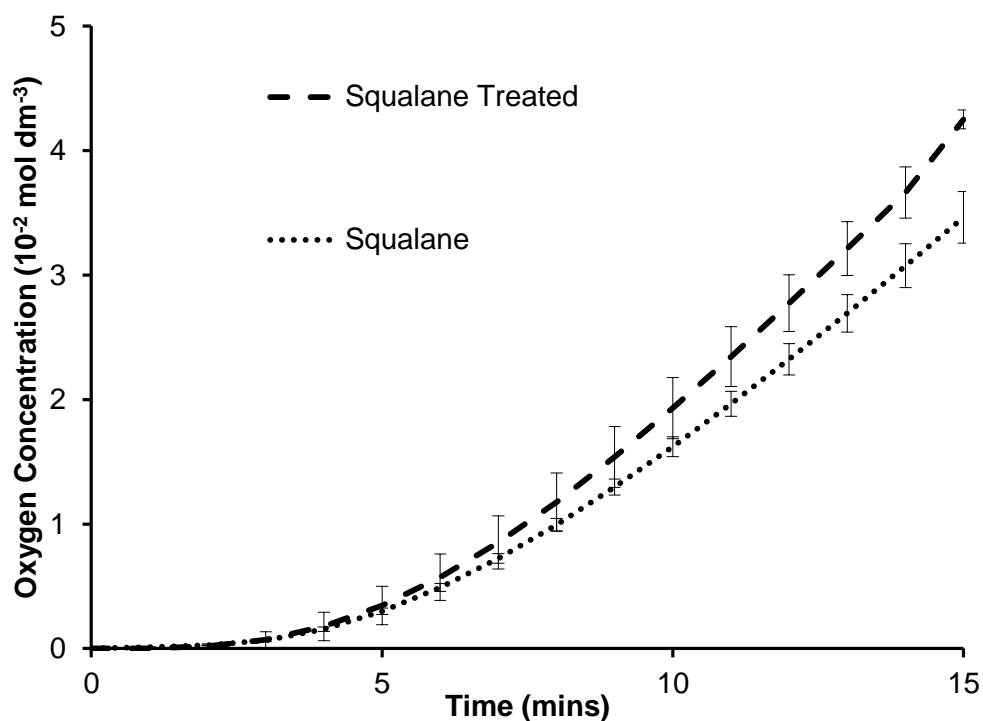


Figure 4.2: Effect of Ethanol on the Autoxidation of Squalane at 180 °C and 1 Bar of O₂

Effect of Ethanol Treatment on the Autoxidation of a Squalane Sample Consisting of 0.25% (w/w) Phenolic Antioxidant

The next series of experiments were designed to assess the effect of ethanol treatment on phenolic antioxidants. A squalane sample containing 0.25% (w/w) phenolic antioxidant was also treated with ethanol and it can be seen from Figure 4.3, that there is also little or no effect on the break point of the lubricant within experimental error. However, again there is an increase in the rate of autoxidation in the treated sample.

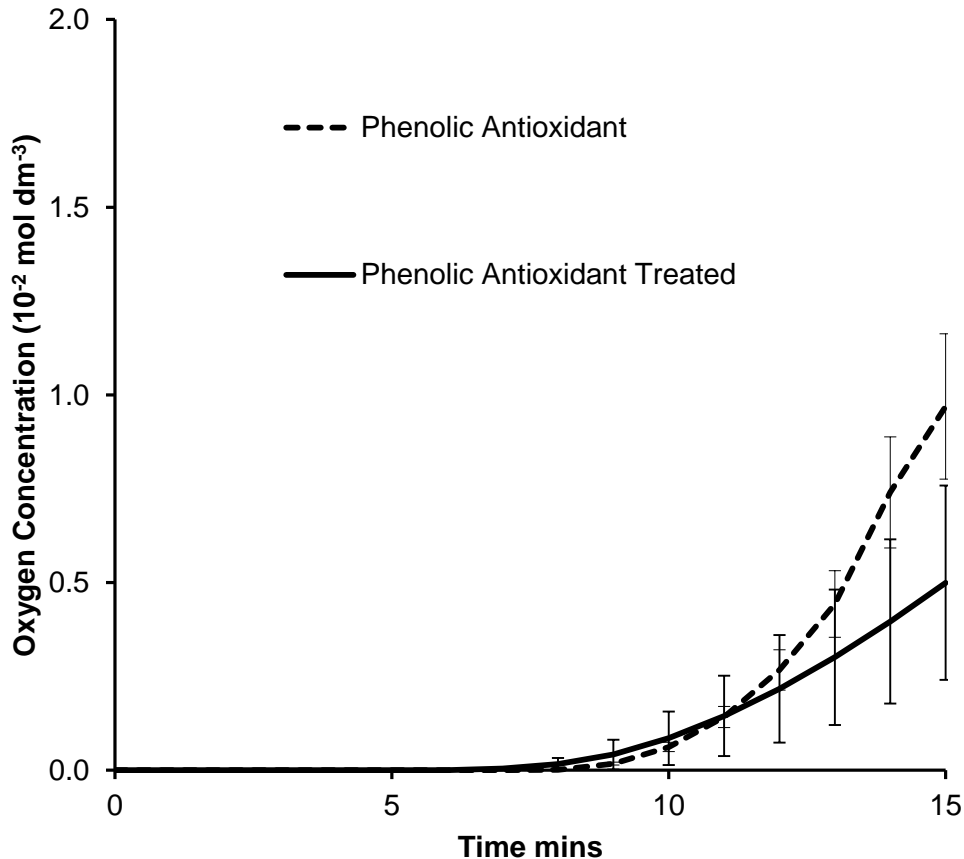


Figure 4.3: Effect of Ethanol on the Autoxidation of Squalane with 0.25% (w/w) Phenolic Antioxidant at 180 °C and 1 Bar of O₂

Effect of Ethanol Treatment on the Autoxidation of a Squalane Sample Consisting 1% (w/w) Detergent

The next series of experiments were designed to assess the effect of ethanol treatment on a neutral calcium detergent. A sample of squalane with 1% (w/w) detergent was treated with ethanol. Upon treatment it can be seen, Figure 4.4, that there was an increase in break point of 2 minutes. The ability of a detergent to inhibit the autoxidation of squalane can be said to be improved by ethanol treatment when they are used as single additives.

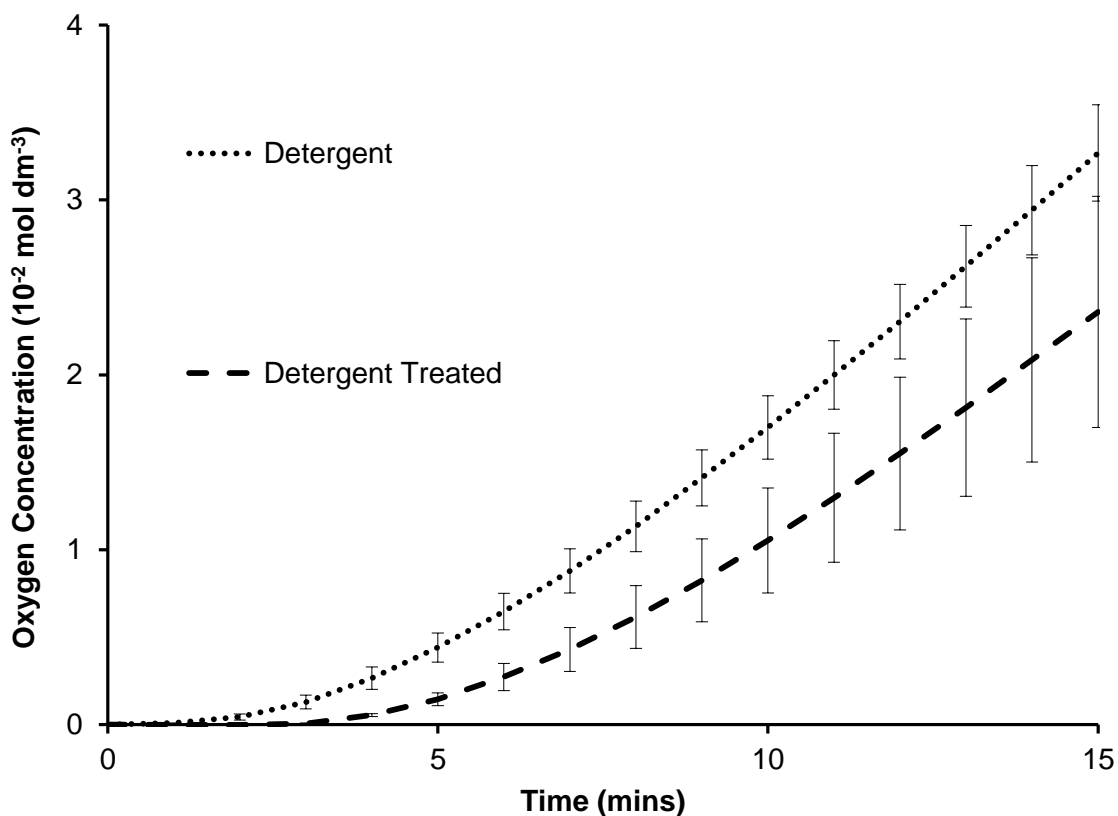


Figure 4.4: Effect of Ethanol on the Autoxidation of Squalane with 1% (w/w) Detergent at 180 °C and 1 Bar of O₂

Effect of Ethanol Treatment on the Autoxidation of a Squalane Sample Consisting 1% (w/w) Detergent and 0.25% (w/w) Phenolic Antioxidant

The next series of experiments were designed to assess the effect of ethanol treatment on a two component additive system. By adding ethanol and then allowing ethanol to volatilize out of squalane containing 0.25% (w/w) phenolic antioxidant and 1% (w/w) detergent it can be seen that the oxidative properties were noticeably improved, Figure 4.5. This can be seen in the observed increase in break point of the treated sample and the reduced rate of reaction. Of interest is the reduced error bars for the ethanol treated sample.

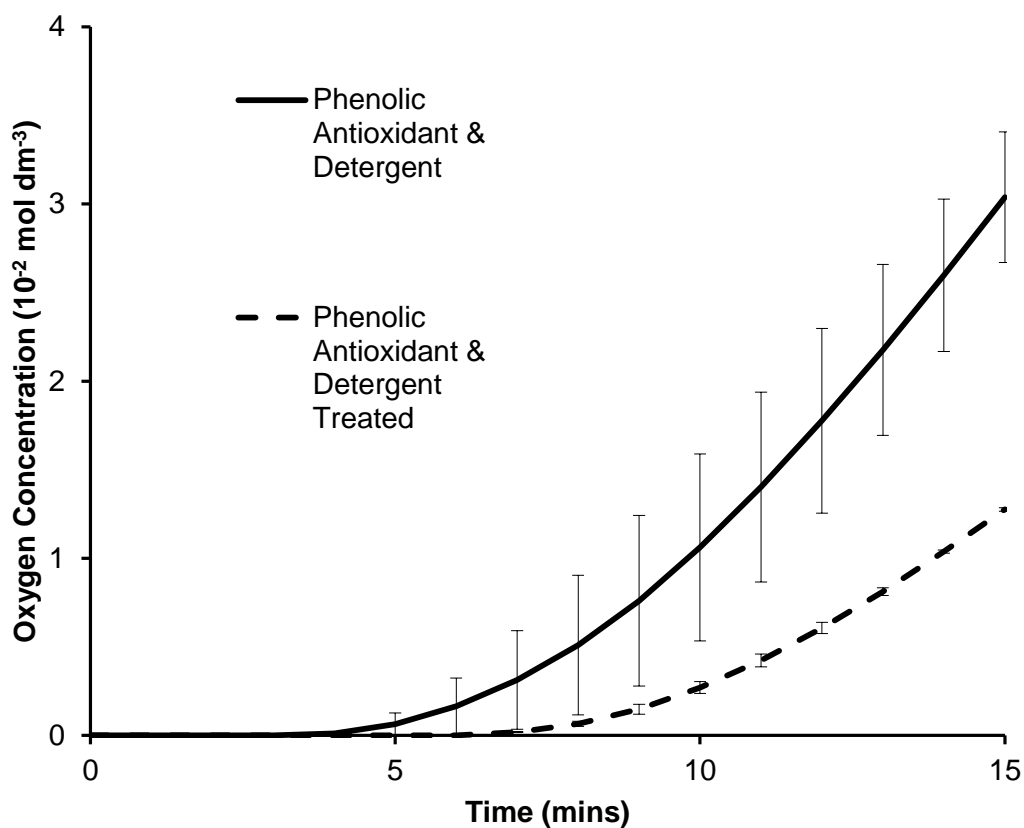


Figure 4.5: Effect of Ethanol on the Autoxidation of Squalane with 0.25% (w/w) Phenolic Antioxidant and 1% (w/w) Detergent at 180 °C and 1 Bar of O₂

Effect of Ethanol Treatment on the Autoxidation of a Squalane Sample Consisting 1% (w/w) Dispersant

The next series of experiments were designed to assess the effect of ethanol treatment on a succinimide dispersant. With 1% (w/w) dispersant in a squalane sample the effect of ethanol treatment a slight increase in the induction time was noted, but not much beyond the limits of reproducibility, Figure 4.6. The subsequent rate of oxidation was slightly lowered, following a similar trend to detergents. It is also apparent that the reproducibility of the treated sample is greater than the untreated sample. Again this is thought to be due to the introduction of reverse micelles into the lubricant formulation.

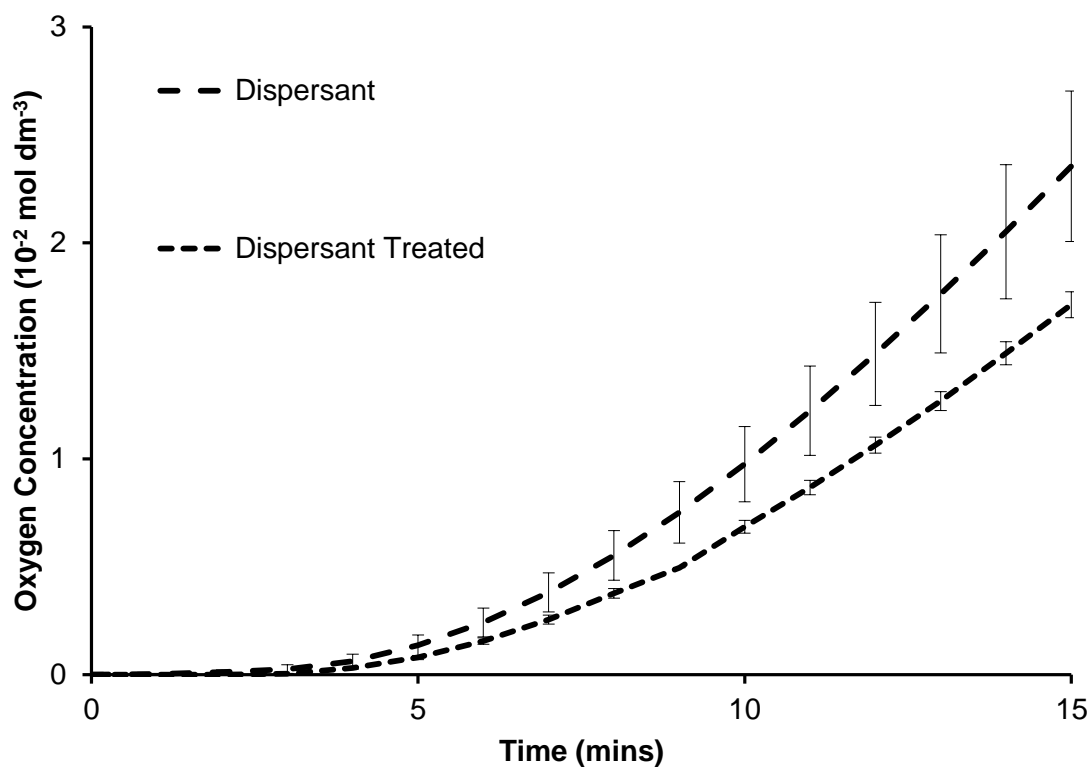


Figure 4.6: Effect of Ethanol on the Autoxidation of Squalane with 1% (w/w) Dispersant at 180 °C and 1 Bar of O₂

Effect of Ethanol Treatment on the Autoxidation of a Squalane Sample Consisting 1% (w/w) Dispersant and 0.25% (w/w) Phenolic Antioxidant

The next series of experiments were designed to assess the effect of ethanol treatment on a two component system consisting of a succinimide dispersant and a phenolic antioxidant. Upon the addition of 0.25% (w/w) phenolic antioxidant to a squalane sample incorporating 1% (w/w) dispersant resulted in a fluid which had noticeably greater oxidative stability upon ethanol treatment, Figure 4.7. This increased the induction time by a factor of 3.5 (15 minutes) over the untreated sample and is both statistically and actually significant. It is pertinent to highlight that while the additive concentration is not altered during the ethanol treatment process; the oxidative stability of the lubricant had risen, thus suggesting that the additive package was being modified during ethanol treatment in some way even though the overall fluid composition has not altered. The treated experiments were not carried further due to a lack of liquid in the reactor.

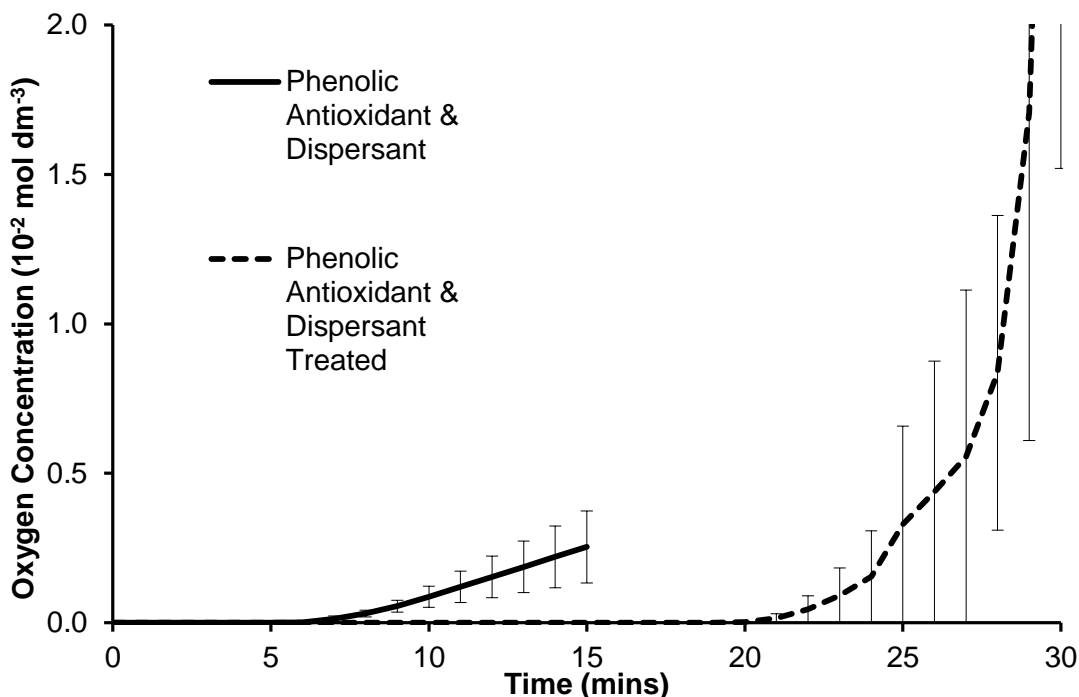


Figure 4.7: Effect of Ethanol on the Autoxidation of Squalane with 0.25% (w/w) Phenolic Antioxidant and 1% (w/w) Dispersant at 180 °C and 1 Bar of O₂

Effect of Ethanol Treatment on the Autoxidation of a Squalane Sample Consisting 1% (w/w) Detergent, 1% (w/w) Dispersant and 0.25% (w/w) Phenolic Antioxidant

The next series of experiments were designed to assess the effect of ethanol treatment on a semi formulated squalane sample containing a phenolic antioxidant, calcium detergent and a succinimide dispersant. It can be seen from Figure 4.8 that upon addition and subsequent volatilisation of ethanol, the oxidative stability of the lubricant was enhanced resulting in an increase in the induction time by a factor of 3.2 (22 minutes), again a significant increase in inhibition. The treated sample was not run further to assess the different rates of reaction due to lack of sample in the reactor. The error bars are again far greater in the treated sample and this could be due to the structure of the reverse micelle.

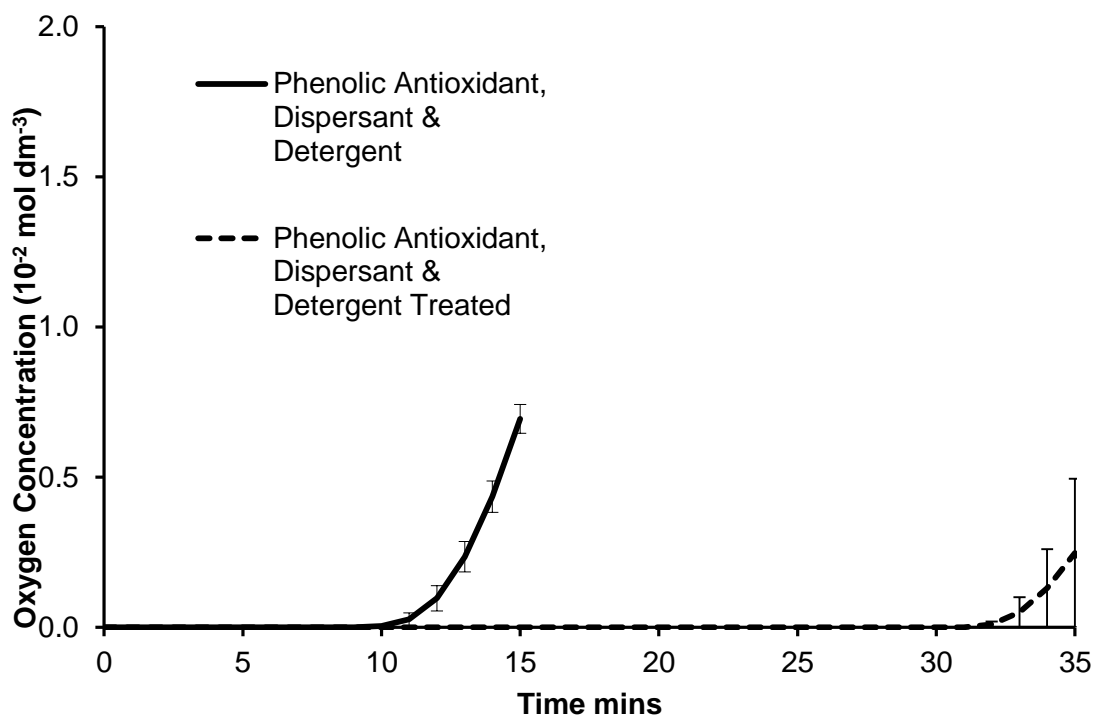


Figure 4.8: Effect of Ethanol on the Autoxidation of Squalane with 0.25% (w/w) Phenolic Antioxidant, 1% (w/w) Dispersant and 1% (w/w) Detergent at 180 °C and 1 Bar O₂

4.2.2: Effect of Ethanol on the Autoxidation of Squalane Samples Containing a Diphenyl Aminic Antioxidant

Aminic antioxidants (AmAO) are often incorporated into automotive lubricant formulations to improve the oxidative stability. The mechanism for this action has been described in the literature when used in isolation and is discussed in section 3.2. However, there has been no investigation into the effectiveness of aminic antioxidants in the presence of ethanol fuel dilution. The aminic antioxidant employed in this study is an example of a commercial diphenyl aminic antioxidant, benzenamine 4-(1,1,3,3-tetramethylbutyl)-N-[4-(1,1,3,3-tetramethylbutyl)phenyl] (BASF Irganox L01), Figure 4.9.

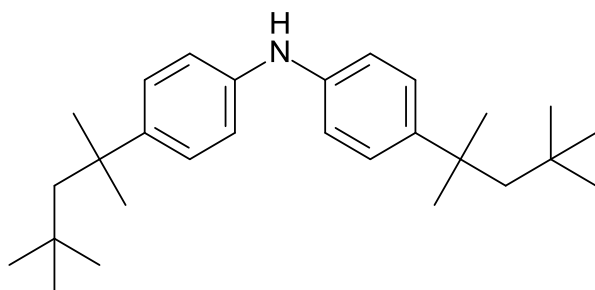


Figure 4.9: 4-(1,1,3,3-tetramethylbutyl)-N-[4-(1,1,3,3-tetramethylbutyl)phenyl]aniline (Irganox L01, AmAO)

Effect of Ethanol Treatment on the Autoxidation of a Squalane Sample Consisting 0.18% (w/w) Aminic Antioxidant

To assess the effect of ethanol treatment on aminic antioxidants a sample of squalane with 0.18% (w/w) aminic antioxidant (AmAO) was treated with ethanol, as described in section 2.2.1. Upon treatment it can be seen, Figure 4.10, that the induction time of the lubricant was decreased by 3 minutes.

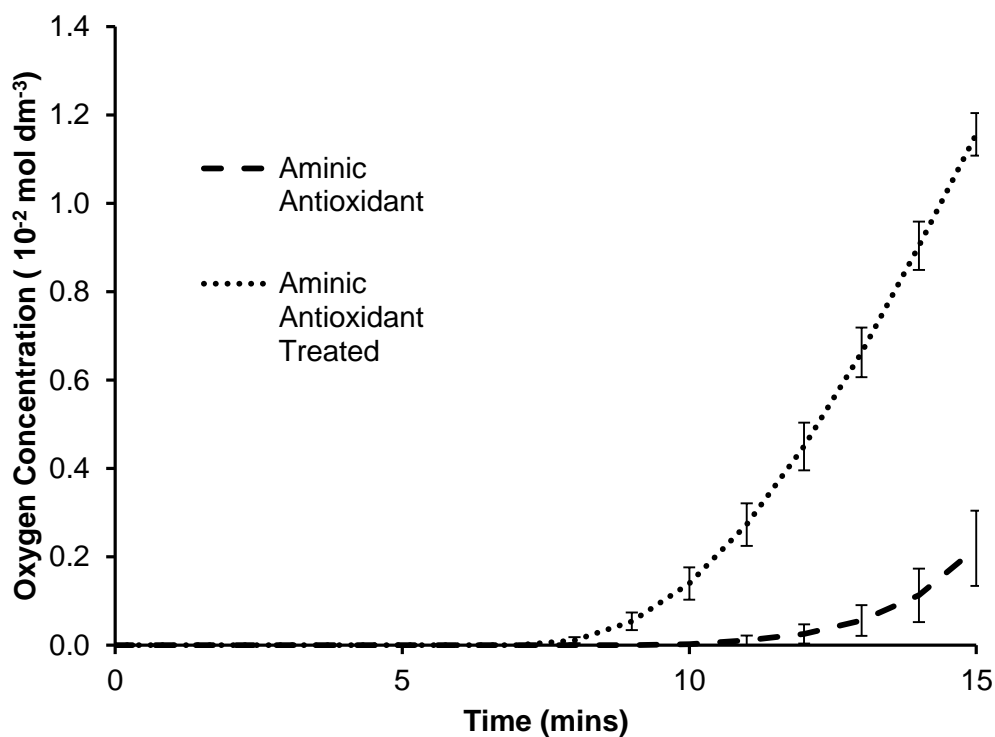


Figure 4.10: Effect of Ethanol on the Autoxidation of Squalane with 0.18% (w/w) Aminic Antioxidant at 180 °C and 1 Bar of O₂

Effect of Ethanol Treatment on the Autoxidation of a Squalane Sample Consisting 0.18% (w/w) Aminic Antioxidant and 1% (w/w) Dispersant

The next set of experiments were designed to assess the effect of ethanol treatment on aminic antioxidants in combination with dispersants. Ethanol treatment of squalane with both of 1% (w/w) dispersant and 0.18 % (w/w) aminic antioxidant resulted in a lubricant with enhanced oxidative stability, Figure 4.11. With ethanol treatment the induction period was increased from 22 minutes to a period of 32 minutes and thus suggested that aminic antioxidants oxidative properties are improved significantly as a result of ethanol treatment.

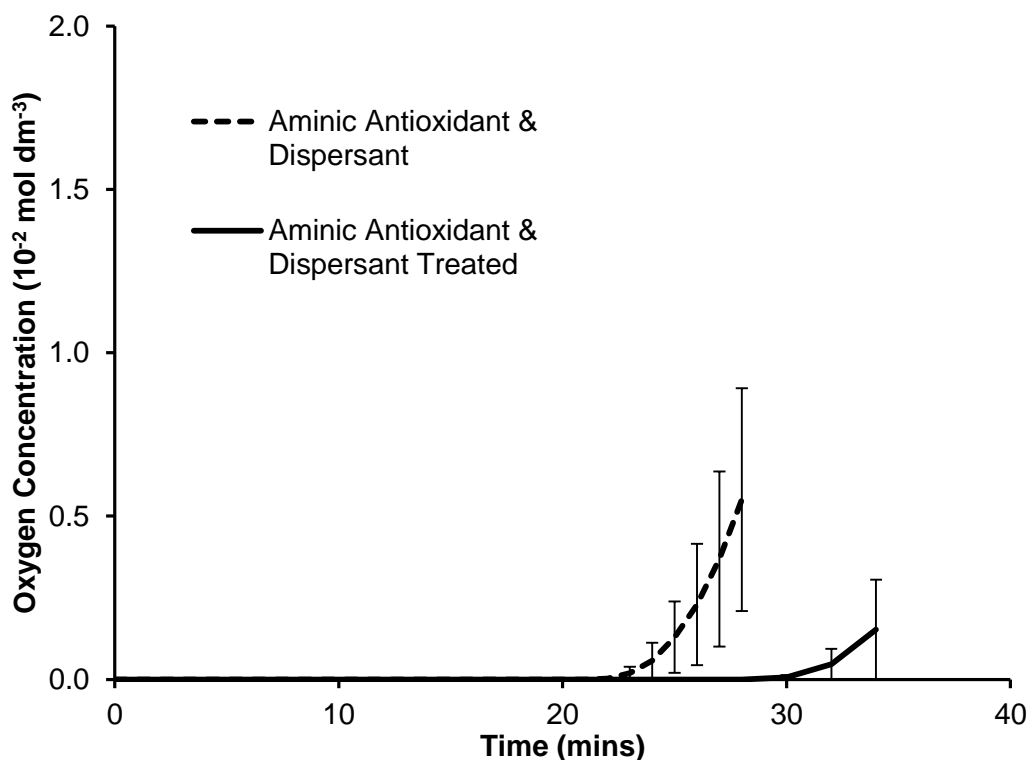


Figure 4.11: Effect of Ethanol on the Autoxidation of Squalane with 0.18% (w/w) Aminic Antioxidant and 1% (w/w) Dispersant at 180 °C and 1 Bar of O₂

Effect of Ethanol Treatment on the Autoxidation of a Squalane Sample Consisting 0.18% (w/w) Aminic Antioxidant, 1% (w/w) Dispersant and 1% (w/w) Detergent

A three component model lubricant comprising of 0.18% (w/w) aminic antioxidant, 1% (w/w) detergent and 1% (w/w) dispersant was also investigated to assess the effect of ethanol on a three component system. It can be seen from Figure 4.12 that upon addition and subsequent volatisation of ethanol, the oxidative stability of the lubricant was enhanced resulting in a factor of 1.6 (from 32 minutes to a period of 52 minutes) increase in the induction time. The treated samples were not run further due to a lack of liquid in the reactor.

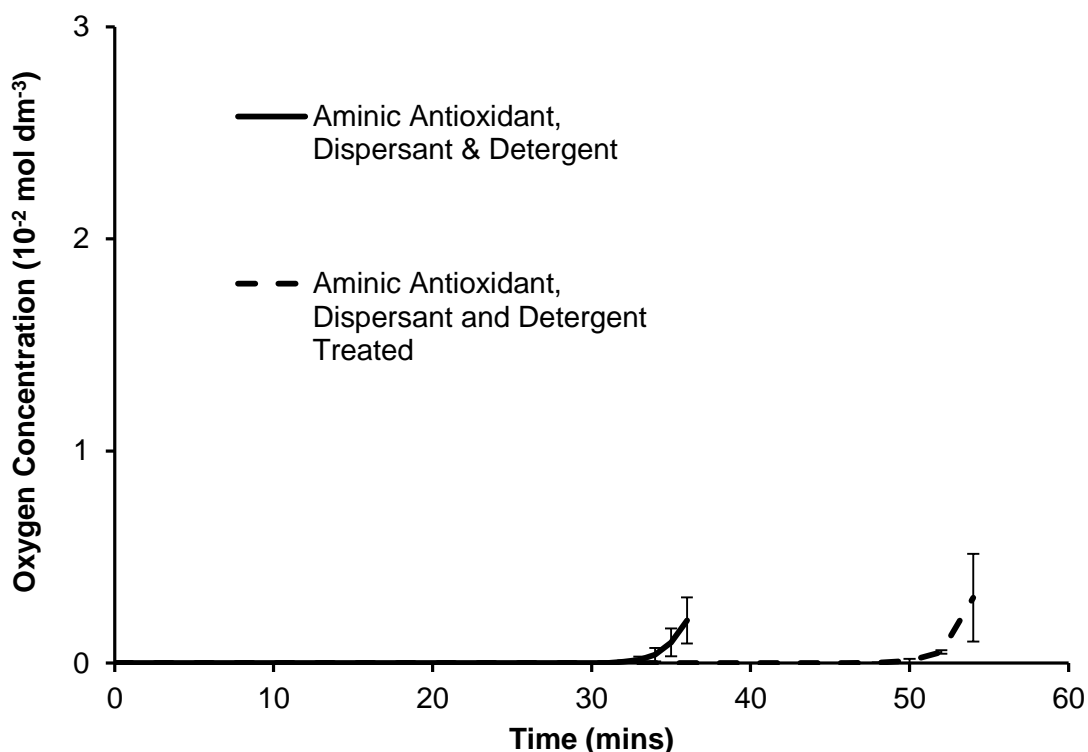


Figure 4.12: Effect of Ethanol on the Autoxidation of Squalane with 0.18% (w/w) Aminic Antioxidant, 1% (w/w) Dispersant and 1% (w/w) Detergent at 180 °C and 1 Bar of O₂

4.2.3: Effect of Ethanol on the Autoxidation of Squalane Samples Containing ZDDP

Effect of Ethanol Treatment on the Autoxidation of a Squalane Sample Consisting 1% (w/w) ZDDP

The next series of experiments were designed to assess the effect of ethanol treatment on ZDDP. Ethanol treatment of squalane containing 1% (w/w) ZDDP in squalane resulted in a sample with reduced oxidative stability, Figure 4.13, from 180 minutes to 135 minutes. Upon inspection of the treated lubricant there was a clear droplet at the bottom of the cylinder, consistent with their being some ZDDP that had gone into the ethanol phase, but not redissolved when the ethanol was removed. It was thought that this contained the remaining ZDDP, as the reverse micelles which are formed with ZDDP could be too dense to remain in solution and as a result fall to the bottom of the sample. To investigate this theory the sample was reshaken to allow the redistribution of ZDDP into the lubricant. It can be seen that once recombined the ethanol treated sample gave greater oxidative stability than the original sample, Figure 4.13. Note that in this section reactions were not repeated due to the issues regarding ZDDP and coating the reactor.

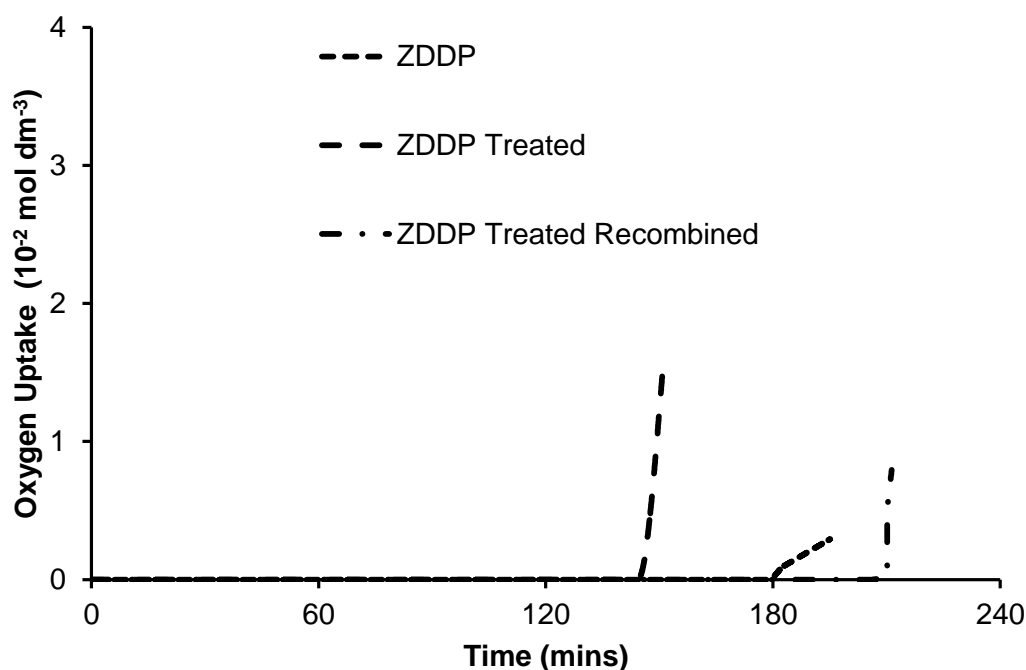


Figure 4.13: Effect of Ethanol on the Autoxidation of Squalane with 1% (w/w) ZDDP at 180 °C and 1 Bar of O₂

Effect of Ethanol Treatment on the Autoxidation of a Squalane Sample Consisting 1% (w/w) ZDDP and 0.25% (w/w) Phenolic Antioxidant

The next series of experiments were designed to assess the effect of ethanol treatment on a two component system consisting of a phenolic antioxidant and ZDDP. Ethanol treatment of a sample consisting of 0.25% (w/w) phenolic antioxidant and 1% (w/w) ZDDP resulted in reduced oxidative stability from 400 minutes to 360 minutes, Figure 4.14, suggesting that ethanol treatment has a detrimental effect on the oxidative stability on the composition of ZDDP and phenolic antioxidant, it was noted that no droplets were observed at the bottom of the treated sample.

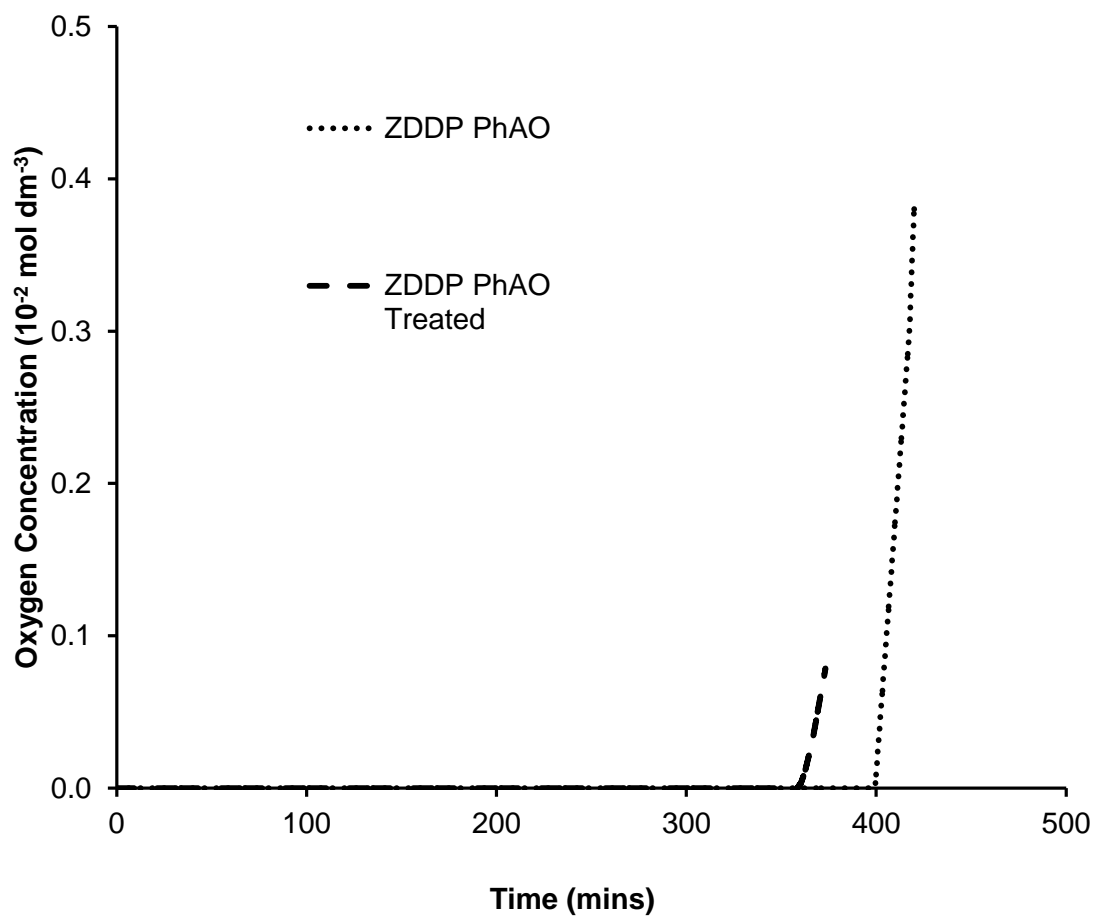


Figure 4.14: Effect of Ethanol on the Autoxidation of Squalane with 1% (w/w) ZDDP and 0.25% Phenolic Antioxidant (PhAO) at 180 °C and 1 Bar of O_2

Effect of Ethanol Treatment on the Autoxidation of a Squalane Sample Consisting 1% (w/w) ZDDP, 0.25% (w/w) Phenolic antioxidant, 1% (w/w) Dispersant and 1% (w/w) Detergent

The next series of experiments were designed to assess the effect of ethanol treatment on a semi formulated squalane sample consisting of 1% (w/w) ZDDP, 1% (w/w) dispersant, 1% (w/w) detergent and 0.25% (w/w) phenolic antioxidant. Following ethanol treatment of this sample the oxidative stability of the lubricant was enhanced from 360 minutes to 500 minutes (140 minutes), Figure 4.15. This would indicate that ethanol treatment of multiple component lubricants results in increased oxidative stability, of the lubricant.

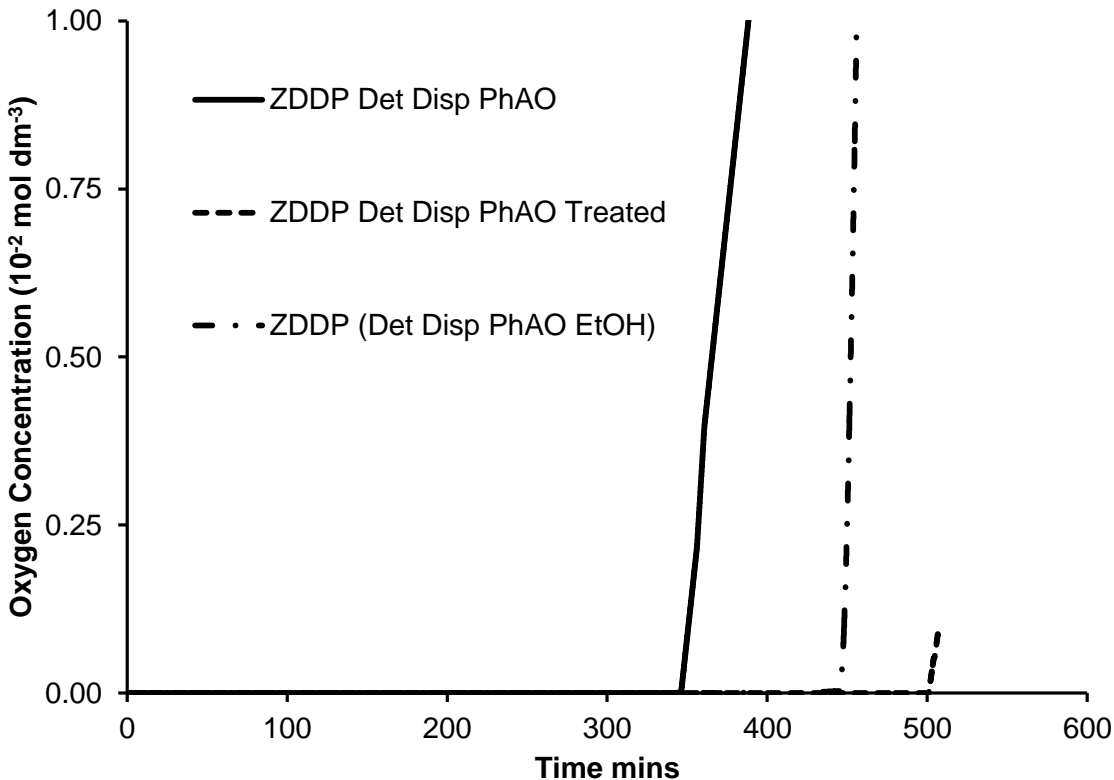


Figure 4.15: Effect of Ethanol Treatment on the Autoxidation of Squalane with 1% (w/w) ZDDP, 1% Dispersant and 1% (w/w) Detergent at 180 °C and 1 bar of O₂. (ZDDP (Det Disp PhAO EtOH) is Sample Where the Package in Brackets was Treated with Ethanol Before the Addition of ZDDP.)

To investigate whether the ethanol treatment of model lubricants could be used as a formulation step in the formulation of automotive lubricants a final experiment was undertaken. A three component sample consisting of 1% (w/w) dispersant, 1% (w/w) detergent and 0.25% (w/w) phenolic antioxidant was treated with ethanol. After the treatment process 1% (w/w) ZDDP was added to make it a four component sample. This is modelling the effect of ethanol treatment as an actual additive package. It can be seen that this sample labelled ZDDP (Det Disp PhAO EtOH) Figure 4.15, had decreased oxidative stability over the ethanol treated sample. This would suggest that there could be a possibility of using the ethanol treatment process as a step in the formulation of lubricants.

4.3: Discussion

From the previous sections it can be seen that ethanol fuel dilution can affect the lubricant in different ways. This is mostly dependent on the lubricant composition.

4.3.1: Effect of Ethanol on the Autoxidation of Model Lubricants Incorporating Primary Antioxidants

The effect of ethanol treatment on the oxidative stability of different formulations containing primary antioxidants is summarised in Figures 4.17 and 4.18. It can be seen through examination of the results presented in Figures 4.17 and 4.18, that the rate of autoxidation of automotive lubricants can be affected by ethanol treatment, leading to the positive effect of significantly increased induction times. The induction times lengthened as the complexity of the additive package increased. These results are in contradiction to previous work that presented a decreased lubricant performance upon oxygenated fuel dilution. [70, 71, 73, 101]

This is an unusual but significant observation, since the concentrations of the additives do not change during ethanol dilution and subsequent evaporation, but the period of inhibition is increased in comparison with what would be

expected upon addition of an antioxidant, e.g. Figure 3.9. A possible explanation for the increased oxidative stability observed for detergents and dispersants is that ethanol is potentially altering the distribution of the additives in the lubricant by promoting the formation of reverse micelles. The mechanism by which reverse micelles interact with the autoxidation mechanism will be discussed in detail in chapter 6.

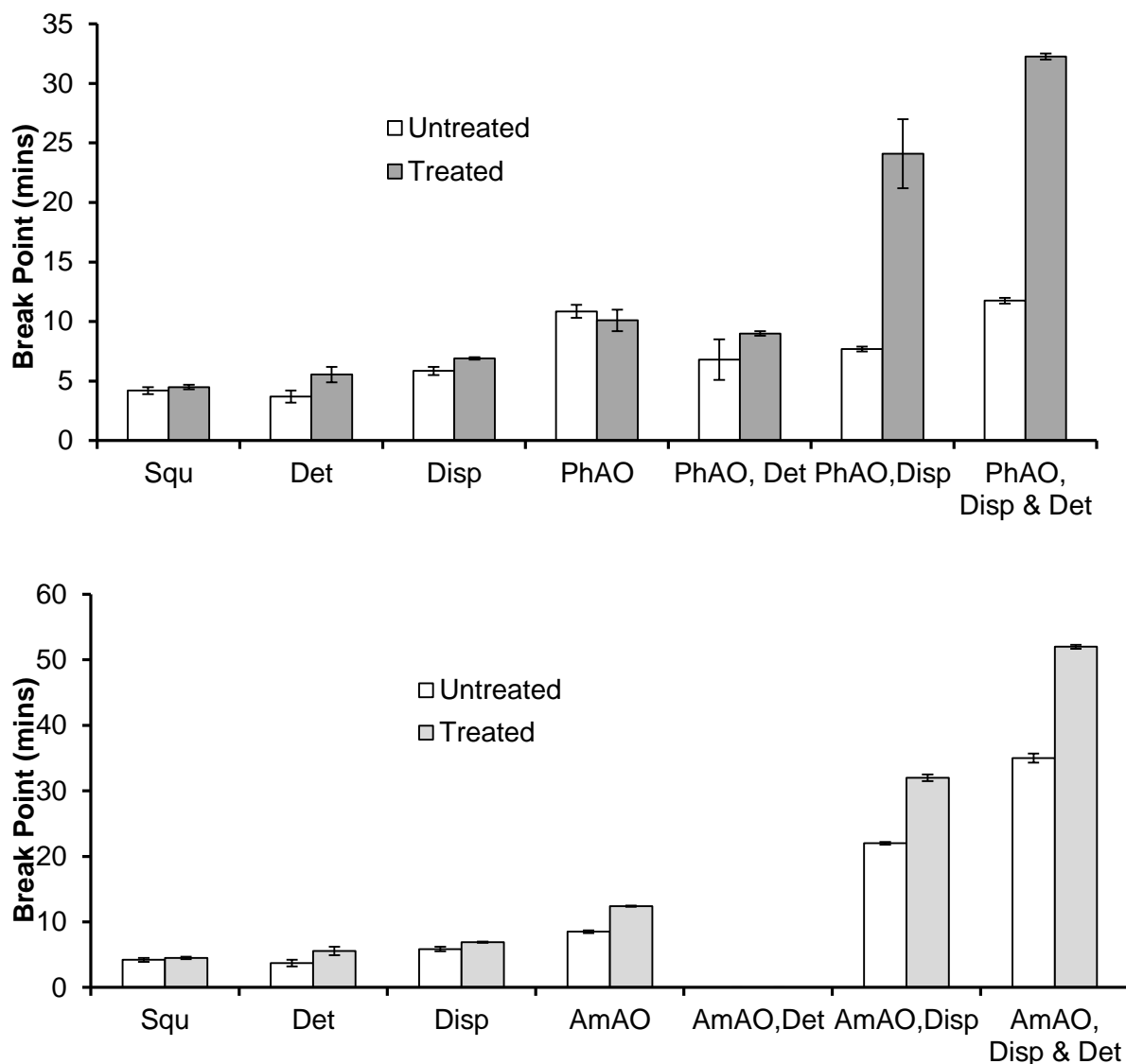


Figure 4.17 & 4.18: Effect of Ethanol on the Autoxidation of Squalane with 0.25% (w/w) Phenolic Antioxidant (PhAO), 0.3 % (w/w) Aminic Antioxidant (AmAO), 1% (w/w) Dispersant (Disp) and 1% (w/w) Detergent (Det) at 180 °C and 1 Bar of O₂

4.3.2: Effect of Ethanol on the Autoxidation of Model Lubricants Incorporating ZDDP

It can be seen by summarising the results that ethanol treatment has little or no effect on model lubricants which possess only ZDDP and phenolic antioxidants, Figure 4.21. It is only with the addition of 1% (w/w) dispersant and 1% (w/w) detergent to the lubricant that greater oxidative stability is achieved upon ethanol treatment. This is in contrast to the untreated result which is far less stable to oxidation in comparison to the ZDDP phenolic antioxidant composition.

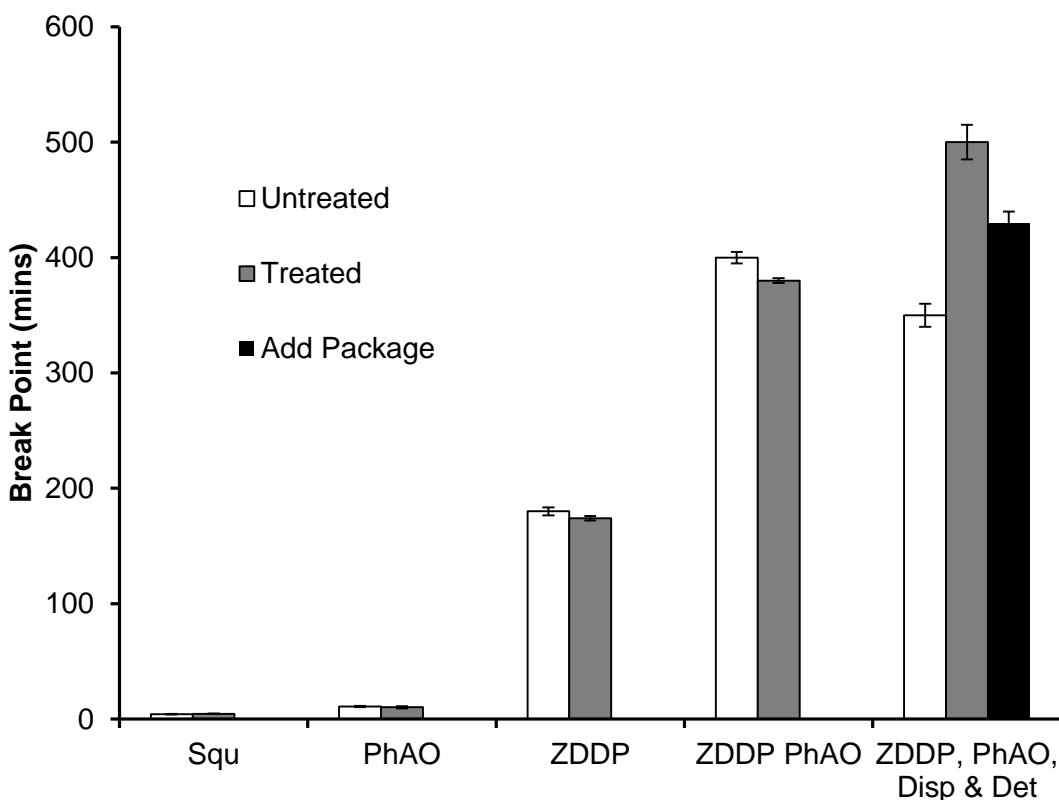


Figure 4.21: Effect of Ethanol on Model Lubricants with Phenolic Antioxidant (PhAO) as the Primary Antioxidant and ZDDP as the Secondary Antioxidant at 180 °C and 1 Bar of O₂

The interesting result in this section is when ethanol treatment process is treated as an additive package. A sample of 0.25% (w/w) phenolic antioxidant, 1% (w/w) dispersant and 1% (w/w) detergent was treated with ethanol prior to

the addition of 1% (w/w) ZDDP. In effect the treatment process is incorporated as an additive package. The oxidative stability of this lubricant, (Add Package) Figure 4.21, was greater than the untreated sample. However it was less than what was achieved with the ethanol treated sample.

4.4: Conclusions

By using model lubricants, the oxidative stability of lubricants incorporating detergents, dispersants and antioxidants (phenolic, aminic and ZDDP) have been shown to be enhanced upon ethanol fuel dilution and subsequent evaporation, as demonstrated by Figures 4.16, 4.17 & 4.21.

It can be seen that squalane samples consisting of aminic or phenolic antioxidants as single additives are largely unaffected by ethanol treatment, Figures 4.16 & 4.17. However, upon addition of 1% (w/w) dispersant and ethanol dilution to samples containing aminic and phenolic antioxidants results in lubricants which have far greater oxidative stability, Figures 4.16 & 4.17. Dispersants when in the presence of an antioxidant are most affected by ethanol treatment.

5: Characterisation of Reverse Micelles through Optical and Spectroscopic Methods

Chapter Overview

In the previous chapters it has been seen that squalane containing dispersant displayed increased oxidative stability in both untreated and ethanol treated samples. The proposition used to explain these effects is through the formation of reverse micelles which can act as alkyl peroxide traps. This chapter examines optical and spectroscopic methods to achieve two aims; firstly to identify the formation of reverse micelles and secondly, upon their identification, explore physical evidence of their possible structure.

5.1: Introduction

This chapter discusses the results from analytical tools employed to examine the presence, structure and size of the reverse micelles discussed in the previous chapters.

In the literature, two techniques have been identified as the key analysis techniques for the identification and characterisation of heterogeneity in solutions. These are light scattering and microscopy.

Light Scattering

Heterogeneity of a solution can be established through laser scattering. If structure present is comparable larger than the wavelength of the light source the beam can be highly scattered and become visible. A particle size analyser works on the same principles with the degree of scattering being measured. From the degree of scattering the particle radius can be determined, unfortunately a particle analyser was not available for this study.

Once structure has been identified by light scattering methods the components which are present in the micelle can be analysed. UV-VIS can be employed to

determine the heterogeneity of the sample and the components causing the structure using the fluorescent marker Nile Red, Figure 5.3 (9-diethylamino-5-benzo[α]phenoxazinone, Nile blue oxazine).

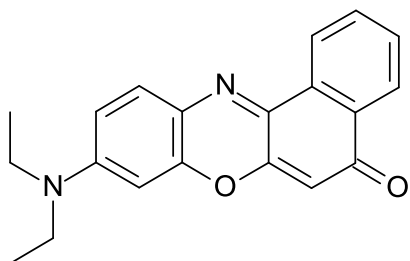


Figure 5.3: 9-diethylamino-5-benzo[α]phenoxazinone (Nile Red, Nile Blue Oxazine)

Several workers have employed Nile Red to label intercellular lipid droplets for analysis using confocal microscopy. [109-118] An example of this work is that undertaken by Greenspan where Nile Red was employed to distinguish between normal cells and cells containing lysosomal accumulations of phospholipids. The cells containing phospholipids consisted of triacylglycerol and cholesteryl esters and were shown to emit a brilliant yellow gold colour once stained with Nile Red. Of interest however is work by Datta where Nile Red was found to have two distinct absorbances which depend on the chemical environment of the dye. [111] Datta proposed that the absorbance in the region of 490nm is due to Nile Red present in non polar media and the absorbance in the region of 520nm is due to the dye present in a polar (reverse micelle) media. It is this technique which will be used in this work to examine reverse micelle structure.

Microscopy

Microscopy is typically used to determine the size and shape of the micelle with many research groups using microscopes with different sources of light employed to illuminate the sample. The key to choosing the appropriate

microscope depends on the sample in question. Typically, for micelle identification, polarized light microscopy is normally the technique of choice. [103] This is due to the ability of studying the micelle structure accurately. Polarized light microscopy utilises polarised light to enhance the quality of images when studying birefringent materials. [103] A birefringent material is one which its refractive index is dependent on the polarization and propagation direction of the light. The birefringent material will interact with the plane polarized light and result in an image contrast. To achieve this, the microscope must be fitted with a polariser, positioned below the sample but above the light source, that polarises the light source and an analyser, a second polariser positioned above the sample. [103] Image contrast comes from the difference between the polarised light source before interaction with the sample and afterwards. In the case of the samples in this study it is likely that they are not birefringent and therefore polarised microscopy was not effective and instead confocal microscopy was employed.

Confocal microscopes bridge the gap between bright field, where illumination is provided by white light and is one of the most simple forms of microscopy, and transmission electron microscopy and its major application is in the imaging of fixed or living tissues labelled with a fluorescent probe. [104] The advantage over wide field techniques is the ability to reduce or eliminate out of focus flare from highly fluorescently labelled specimens. This is achieved through two methods the first is by introducing a dichroic mirror which reflects light that is shorter than a certain wavelength and allows light through at wavelengths longer than that set wavelength, Figure 5.1. As a result the detector will only see the emitted light from the fluorescent dye without any scattered light. [104] This technique utilises the microscope objective to illuminate the sample, epi-fluorescence, instead of bathing the sample from below with light.

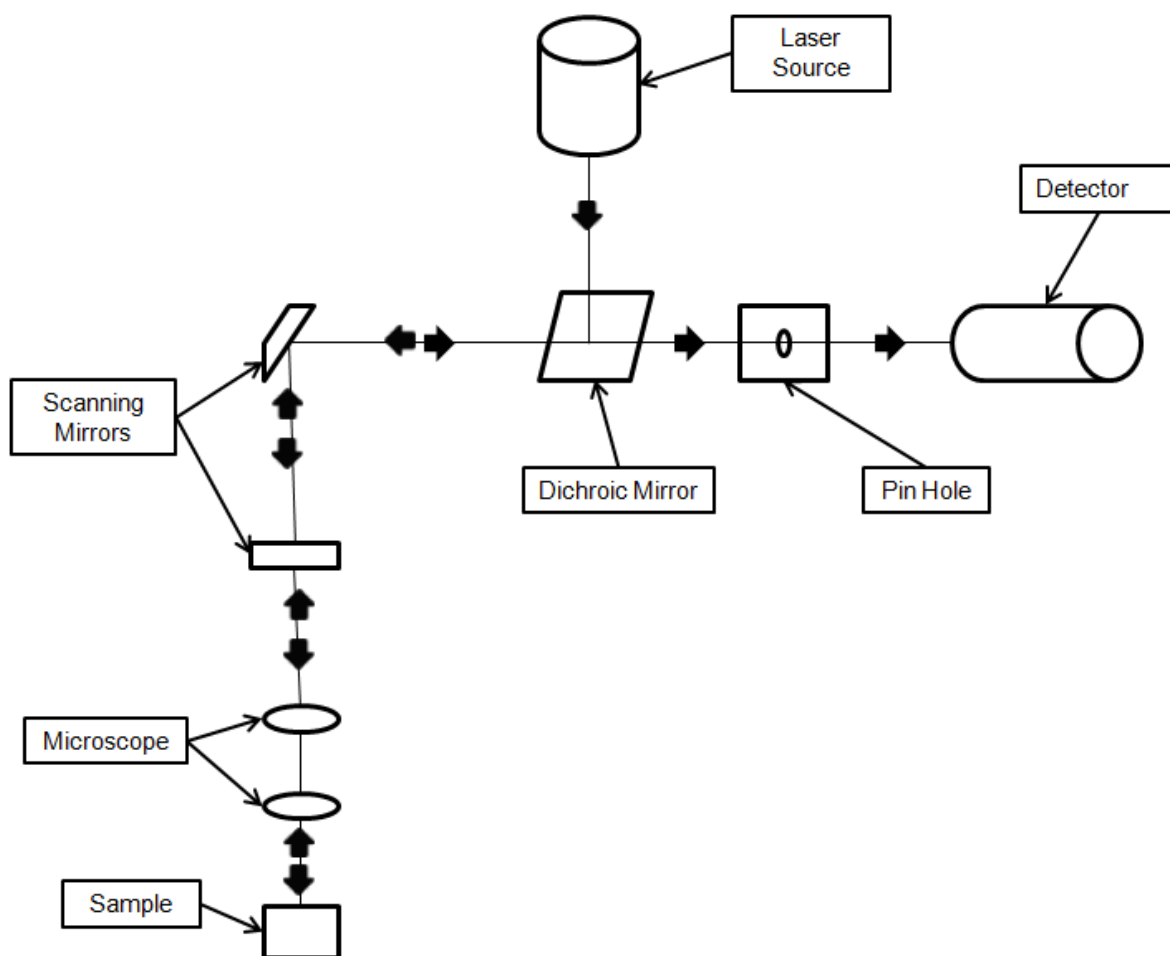


Figure 5.1: Schematic of a Typical Laser Scanning Confocal Microscope, [104]

The detector will only see fluorescence at a certain wavelength; however confocal microscopy has a second technique by which background haze is eliminated, a common problem with fluorescence microscopy. [104] Background haze is typically formed due to the whole sample being bathed by light and hence the whole sample is fluorescing. In confocal microscopy the focal point is set by two objective lenses like the technique used in typical fluorescence microscopes. The difference with confocal microscopy is the introduction of a pin hole in front of the detector which only allows light from a certain focus through. An example of this can be seen in Figure 5.2, with the introduction of a pin hole only light emitted from the circle is focused in the hole.

It can be seen that light emitted from the triangle is mostly eliminated as the focal point is after the pin hole aperture. Without the pin hole then the light emitted from the triangle would be observed as background haze. The introduction of the pin hole aperture increases contrast by decreasing the background noise. The term confocal microscopy is derived from the introduction of two conjugate points, the pin hole and the objective lens, with the pin hole being conjugate to the focal plane and hence confocal microscopy. [104] This increased sensitivity should allow the identification of the reverse micelles in solution, if present, providing the appropriate fluorescent label is employed. It has to be noted due to a lack of contrast in molecular weight between squalane and the reverse micelles that electron microscopy was deemed to be inappropriate.

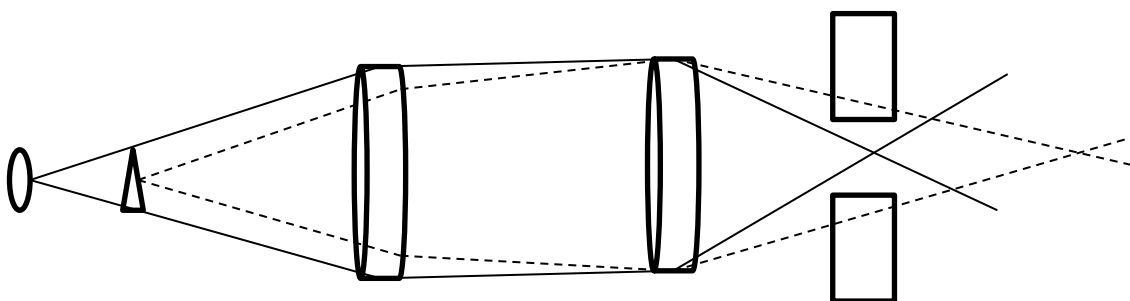


Figure 5.2: Process for Reducing Background Haze in Confocal Microscopy, [104]

The aim of this chapter is to answer two key questions; firstly, are reverse micelles formed as a consequence of ethanol treatment of squalane samples containing additives, and secondly, if they do, which lubricant additives take part in reverse micelle formation.

5.2: Laser Scattering

The proposition to be tested in this chapter is that whether through the ethanol treatment process that reverse micelles are formed. A straight forward method was used to identify reverse micelle formation in the ethanol treated samples, employing light scattering. A scattering effect should be seen if any particles are

present in the sample which have a diameter comparable to, or larger than, the wavelength of the chosen beam. All samples were heated at 180 °C, and stirred at 600 rpm under an N₂ atmosphere for a period of 50 minutes prior to analysis. This was to ensure that there was no residual ethanol present in the treated lubricant prior to analysis, apart from the ethanol diluted sample. A red diode laser, of wavelength ca 600 nm was employed to illuminate the untreated, treated and diluted samples and scattering should be observed in samples which possess particles greater than ca 0.3 μm in diameter.

From the results in the previous chapter the sample which provided the greatest increase in oxidative stability was a squalane sample with 1% (w/w) dispersant, 1% (w/w) detergent and 0.25% (w/w) phenolic antioxidant and should show scattering if reverse micelles were present. The untreated sample showed no scattering, as shown in Figure 5.4. However, it should be noted that there could still be structure present at a far smaller scale than the wavelength of the red diode laser. The diluted sample displays great scattering of the incident laser beam indicating a great deal of structure with size greater than the wavelength of the red diode laser and this is assumed to be ethanol suspended in reverse micelles.

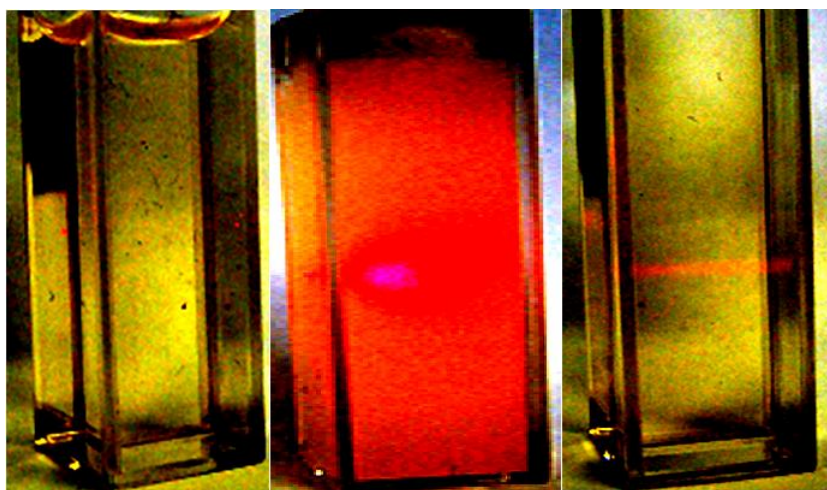


Figure 5.4: Photograph Showing the Level of Light Scattering in Undiluted by Ethanol (Left), Ethanol Diluted (Middle) and Ethanol Treated (Right) Squalane Samples Containing 1% (w/w) Dispersant, 1% (w/w) Detergent and 0.25% (w/w) Phenolic Antioxidant

In the treated sample the laser beam was visible, consistent with scattering due to inhomogeneity in the sample, and these were assumed to be reverse micelles, Figure 5.4. This provided evidence that the lubricants physical structure of the additive package had been altered, but with no alteration in the average additive concentration.

To ensure that the observed scattering in the treated sample was simply not due to residual ethanol in the sample gas chromatography (GC) analysis was undertaken before and after heating. It can be seen from GC analysis that the treated sample is ethanol free. In the pre heated sample, ethanol was present with a retention time of 2 minutes. After the heating period the sample had no detectable ethanol, with an upper limit of 0.01% (v/v), Figure 4.2.

This laser scattering method was repeated for all the samples which were treated with ethanol in the primary antioxidant section of the previous chapter. It can be seen that the majority of the samples which display scattering have a surfactant in solution, Table 5.1, consistent with the conclusions gained from the experimental data.

Table 5.1: Results of the Laser Scattering Analysis of the Effect of Ethanol Treatment on Squalane Containing 1% (w/w) Dispersant, 1% (w/w) Detergent, 0.3% (w/w) Aminic Antioxidant and 0.25% (w/w) Phenolic Antioxidant

	Scatters Red Diode Laser Beam	
	Untreated	Ethanol Treated
Squalane	No	No
Phenolic Antioxidant	No	No
Aminic Antioxidant	No	No
Dispersant	No	Yes
Detergent	No	Yes
Phenolic Antioxidant & Dispersant	No	Yes
Phenolic Antioxidant & Detergent	No	Yes
Aminic Antioxidant & Dispersant	No	Yes
Phenolic Antioxidant, Dispersant & Detergent	No	Yes
Aminic Antioxidant, Dispersant & Detergent	No	Yes

This method is informative and was able to provide information on the formation of reverse micelles upon ethanol treatment. However, it is likely to be quite crude and more quantifiable optical methods were investigated.

5.3: Analysis of Samples Using Fluorescent Label for Reverse Micelle

5.3.1: UV-VIS Using Nile Red as a Fluorescent Label

This next set of analysis was designed to investigate the chemical composition of the reverse micelles. Model lubricant samples were analysed by UV-VIS employing Nile Red as a dye marker. Datta employed the characteristic absorbances in the 450-500 nm region of the Nile Red spectrum to examine/conform reverse micelle formation, as can be seen in Figure 5.6. [111] The analyses using Nile Red in this study followed the procedure of Datta where Nile Red was incorporated into the lubricant with a ratio of $1:1 \times 10^6$ (Nile Red:lubricant ratio). [111] It can be seen that the Nile Red absorbances differ quite significantly between the non-polar and polar solvent. These clear differences are due to the changes in permittivity which affect the $\pi \pi^*$ transition probabilities. In the non-polar solvent two absorbances can be seen in the region of 450-500 nm. The polar solvent differs by having a broad stronger absorbance at 550 nm. This increase in absorbance when in a polar solvent is due to the Nile Red being more soluble as it is a lipophilic dye with concentration being kept constant. Due to these clear differences the UV-VIS analysis using Nile Red were undertaken in undiluted samples.

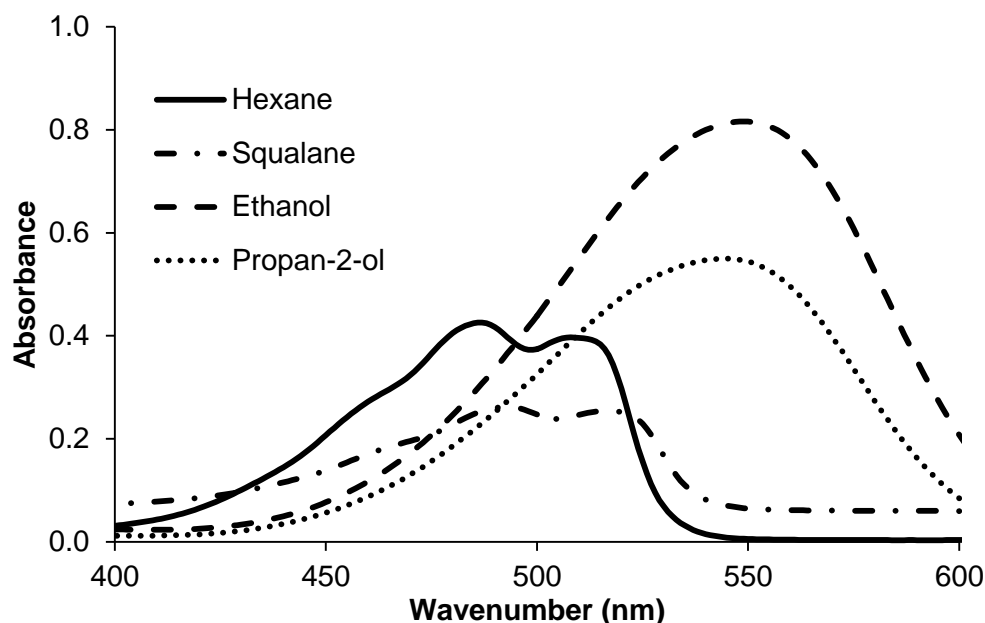


Figure 5.6: UV-VIS Spectra Showing the Absorbances of Nile Red in Polar (Ethanol and Propan-2-ol) and Non Polar Solvents (Squalane and Hexane), Nile Red:Lubricant Ratio $1:1 \times 10^6$

If reverse micelles are formed during the ethanol treatment of additive containing squalane samples, one would expect the absorbance at 520 nm to increase with 490 nm decreasing, when compared to the untreated sample. The aim of this analysis is to analyse the differences in absorbances at 520 and 490 nm. If the lubricant is unaffected by ethanol treatment then there should be no difference between the treated and untreated samples.

After ethanol treatment there are noticeable changes in the absorption spectrum for squalane samples containing surfactant additives, Figure 5.7. In all analysis Nile Red was added after ethanol treatment. It can be seen in the untreated sample that the absorbances at 490 and 520 nm are very similar, this would suggest that there could be reverse micelles present in the sample prior to treatment, or that Nile Red is being suspended in solution.

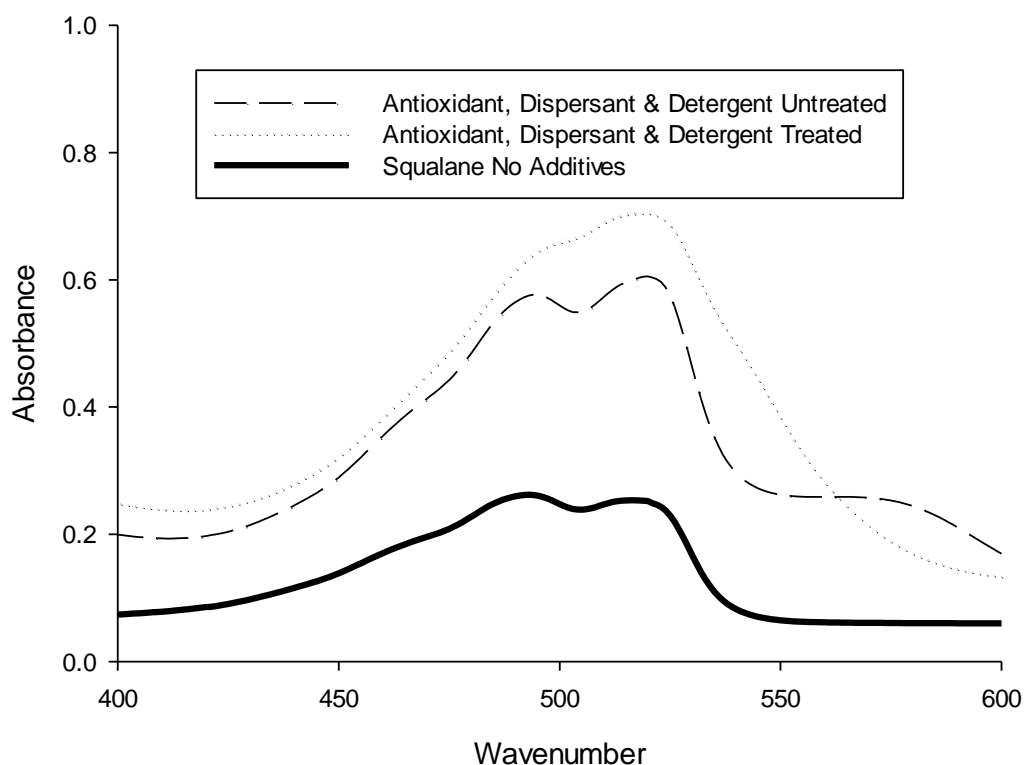


Figure 5.7: UV-VIS Spectra of Nile Red Doped Untreated and Ethanol Treated Squalane Samples Containing 1% (w/w) Dispersant, 1% (w/w) Detergent and 0.25% (w/w) Phenolic Antioxidant (L107), Nile Red Employed in a Ratio of $1:1 \times 10^6$ (Nile Red:Lubricant)

It can be seen by comparing the untreated sample, Figure 5.7, with squalane containing no additives, Figure 5.7, that the absorbance at 520 nm is higher in the treated sample than that in the squalane sample. Comparing the treated and untreated sample, the treated sample displayed a noticeable increase in the absorption at 520 nm which can be attributed to formation of reverse micelles. This is due to the absorbance at 520 nm being attributed to Nile Red being in a reverse micelle core. In the treated sample the peak at 520 nm is broadened and this is thought to be due to reverse micelle formation as the observation is consistent with more Nile Red was present in the polar media than in the non polar media as the general peak heights increase as the solvent becomes more polar. [111]

This analysis provides supporting evidence that reverse micelle formation is additive specific and is highly dependent on the presence of a surfactant in the lubricant, Table 5.2. There is negligible difference between the ratio of the peak heights at 497 nm and 520 nm in the sample containing only phenolic antioxidant after ethanol treatment. It is only in the presence of a dispersant that after ethanol treatment more reverse micelles are present and hence the increase in the absorbance at 520 nm, Table 5.2. Both the treated and untreated samples show a hump in the region of 500-590nm which Datta suggests is another indication of reverse micelle formation. [111] It can be seen that the overall absorption of Nile red increases as the polarity of the solvent increases. This is consistent with Nile red being more soluble in polar media not an increase in Nile red concentration.

Table 5.2: Nile Red Analysis of Treated and Untreated Squalane Samples Containing 1% (w/w) Dispersant, 1% (w/w) Detergent and 0.25% (w/w) Phenolic Antioxidant (L107), Nile Red Employed in a Ratio of 1:1x10⁶ (Nile Red:Lubricant). Ratio is (Non Micelle : Micelle)

		Non Micelle 497 nm	Micelle 520 nm	Ratio
Phenolic Antioxidant	Untreated	0.438	0.429	1.021
	Treated	0.736	0.723	1.018
Dispersant	Untreated	0.374	0.368	1.016
	Treated	1.240	1.288	0.963
Phenolic Antioxidant & Dispersant	Untreated	0.519	0.510	1.012
	Treated	0.893	0.916	0.975
Phenolic Antioxidant, Dispersant & Detergent	Untreated	0.578	0.606	0.953
	Treated	0.632	0.705	0.896

This analysis has provided evidence of reverse micelle formation as a result of ethanol treatment in squalane samples which contain dispersants.

5.3.2: Nile Red Analysis in Confocal Microscopy

To assess whether structure is present and to gain direct evidence of reverse micelle formation Nile Red doped samples were viewed using confocal microscopy to examine any structure present. Nile Red is a lipophilic dye which is extensively used to stain cells in biological systems. [106-110] In non polar solvents Nile Red emits a yellow-gold colour and changes to pink in slightly polar media as can be seen in Figure 5.8 which displays squalane samples used in this study. Typically, Nile Red is excited at 485 nm and fluoresces at 525 nm; these wavelengths were used to study the structure in selected samples using confocal microscopy. If reverse micelles are present in the ethanol samples then Nile Red should reside in the core and enable their identification. Even though Nile Red is lipophilic there are examples in the literature where it has been seen to migrate into reverse micelle cores. [111] A lipophilic compound is one that dissolves in non polar solvents. Nile Red was incorporated into neat squalane samples without the addition of any solvent, as previously achieved for the UV-VIS analysis.

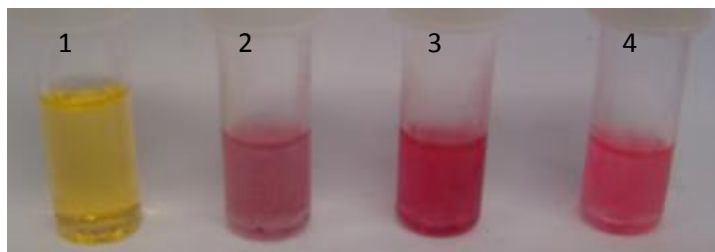


Figure 5.8: Comparison of Nile Red Colouring of Squalane (1), Squalane with 1% (w/w) Dispersant, 1% (w/w) Detergent and 0.25% (w/w) Phenolic Antioxidant (L107) Untreated (2), Ethanol Diluted (3) and Ethanol Treated (4), Nile Red Employed in a Ratio of 1:1x10⁶ (Nile Red:Lubricant)

For microscopy, to ensure that the reverse micelles formed upon ethanol dilution were of significant size and number the additive concentration was

increased by a factor of 10 (10% (w/w) dispersant, 10% (w/w) detergent and 2.5% (w/w) phenolic antioxidant). The squalane samples were ethanol diluted and not treated as the reverse micelles are expected to be larger in the diluted sample. This is due to the ethanol still present in the sample where it is suspended by the dispersant molecules. To recap on the ethanol dilution process the lubricant is diluted with 10% (v/v) ethanol and mixed until an unstable emulsion is formed. The sample is then allowed to settle until the unstable emulsion destabilises into a polar ethanol and non polar hydrocarbon layer. Confocal analysis was undertaken on the non polar hydrocarbon layer.

Nile red was incorporated into the lubricant in a ratio of 1:1x10⁶ (nile red: sample) and analysed in an undiluted sample using the microscope, as shown in Figure 5.9.

The ethanol-diluted, additive-rich sample, provided observable droplets ranging from 4 µm up to 25 µm in diameter, Figure 5.9. It is thought that these are suspended ethanol droplets in the lubricant, suspended by the surfactants in the lubricant i.e. reverse micelle formation.

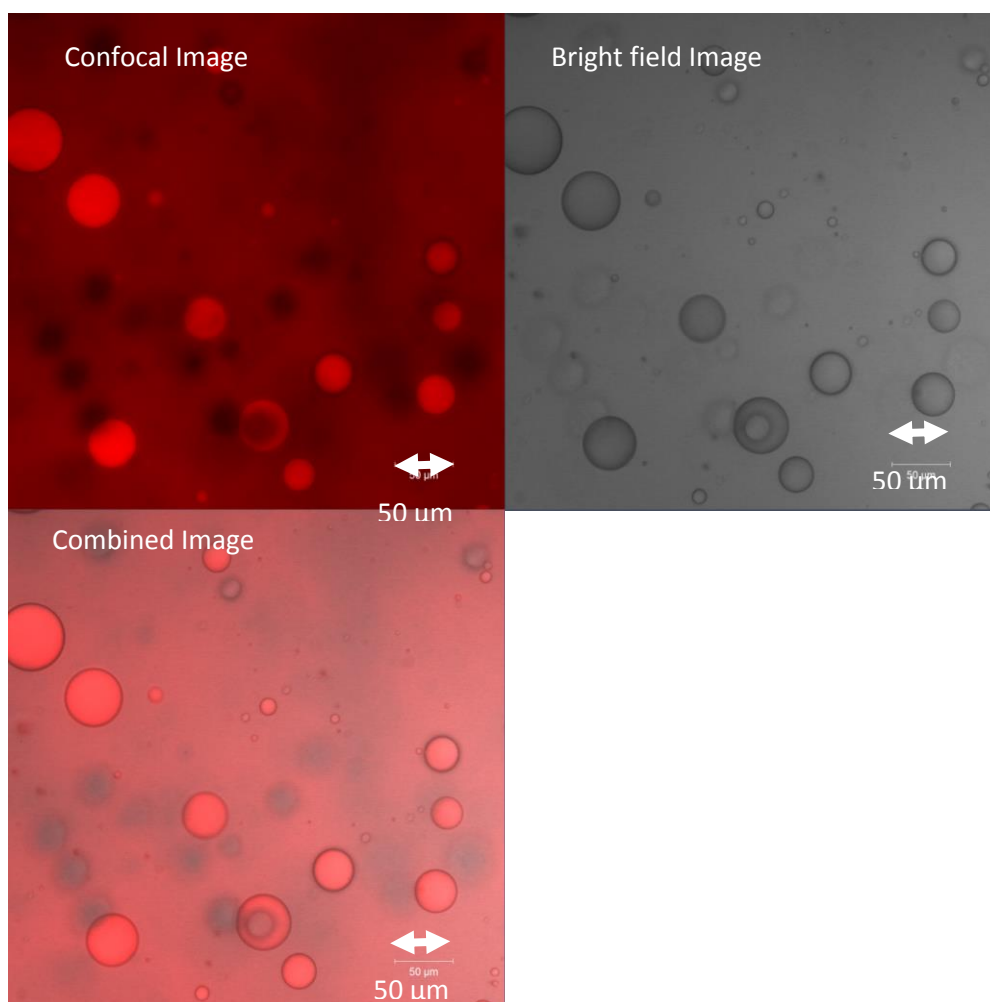


Figure 5.9: Confocal Microscopy of Ethanol Diluted Squalane Sample Containing 10% (w/w) Dispersant, 10% (w/w) Detergent and 2.5% (w/w) Phenolic Antioxidant (L107) with Nile Red Marker

Smaller droplets could be seen with increased magnification with a typical diameter of between 1 - 3 μm , Figure 5.10.

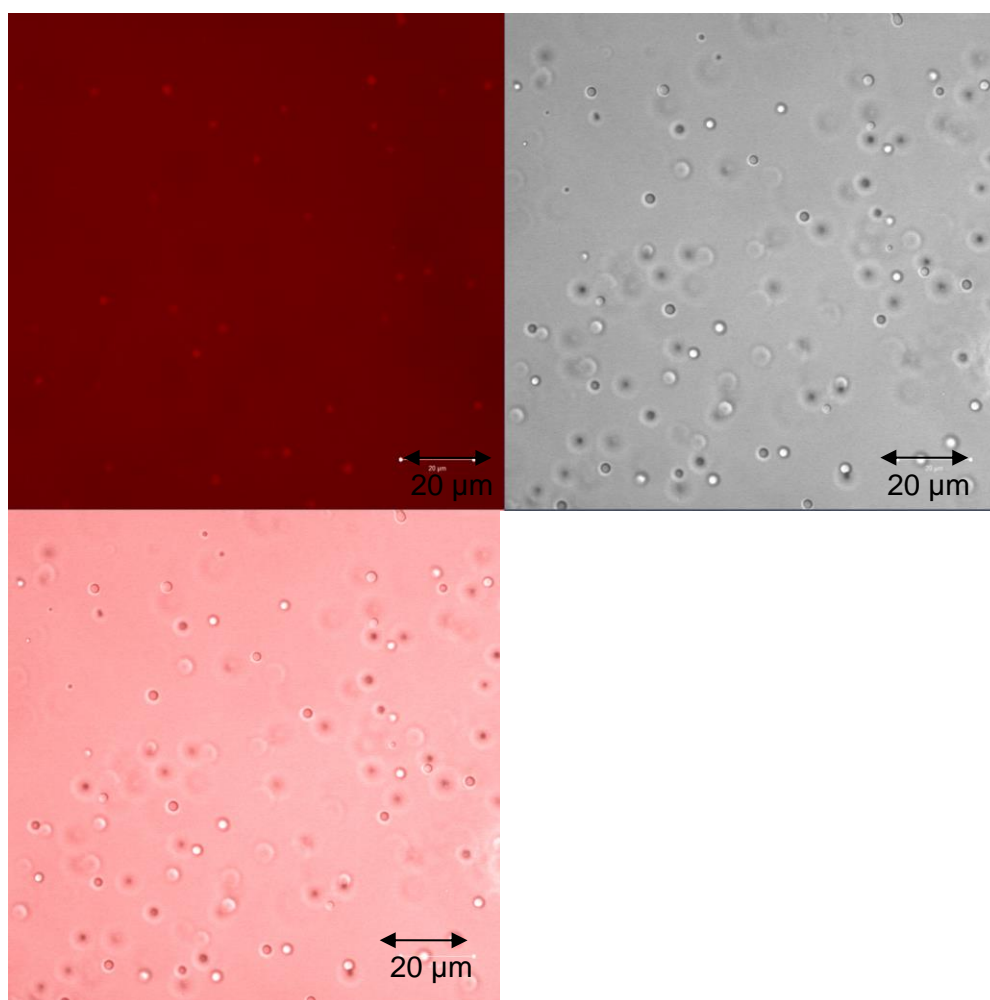


Figure 5.10: Confocal Microscopy of Ethanol Diluted Squalane Sample Containing 10% (w/w) dispersant, 10% (w/w) Detergent and 2.5% (w/w) Phenolic Antioxidant (L107) with Nile Red Marker

The untreated sample showed no signs of reverse micellar structure. This would suggest that reverse micelle formation is as a consequence of ethanol dilution/treatment. However it has to be noted that structure might be present but at a size beyond the lower limits of detection. It is only upon ethanol dilution that the reverse micelles increase in size to above the limits of detection.

The ethanol treated samples were prepared by diluting with 10% (v/v) ethanol a squalane sample containing additives. This sample is then shaken until an unstable emulsion is formed and is allowed to settle whilst sealed. Once the emulsion has settled into a polar ethanol and non polar hydrocarbon layer the

solution was shook again to reform the emulsion. The emulsion is then allowed to settle in an open environment at room temperature, thus allowing the ethanol to volatise out of solution. Once the ethanol layer is fully removed the samples is then termed ethanol treated. This preparation method was designed to closely mimic ethanol fuel dilution and subsequent evaporation in the sump.

Reverse micelles were not identified in the ethanol treated squalane sample containing 10% (w/w) dispersant, 10% (w/w) detergent and 2.5% (w/w) phenolic antioxidant (L107), even though this sample provided scattering when illuminated with a laser. It is thought that the reverse micelle size has contracted upon the volatisation of ethanol to a size which is below the detection limit of the microscope.

The formation of reverse micelles in the ethanol diluted samples can be confirmed as an additive effect as little structure was present in the ethanol diluted sample of squalane, Figure 5.12. It is assumed that the structure which is present is suspended ethanol droplets in the squalane sample.

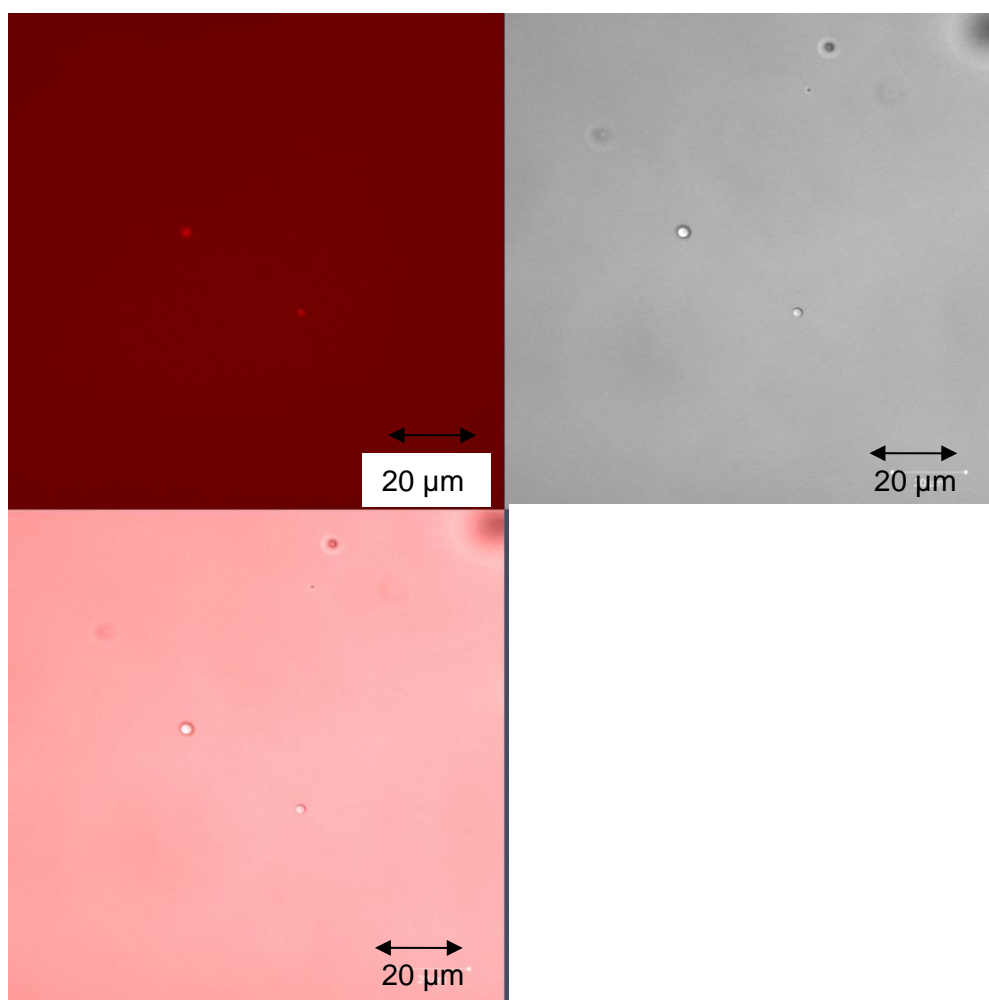


Figure 5.12: Confocal Microscopy of Ethanol Diluted 100% (w/w) Squalane with Nile Red Marker

5.4: Summary and Conclusions

Ethanol treated samples scattered a laser beam demonstrating that there is structure present in the lubricant, Figure 5.4. Upon UV-VIS analysis with Nile Red it could be seen that the chemical environment was altered upon ethanol treatment, due to changes in peak heights at 490 and 520 nm consistent with the findings of Datta. [111] The additives which have the greatest effect are surfactants, while the phenolic antioxidant did not promote reverse micelle formation, this was most evident in the UV-VIS analysis employing Nile Red as a

fluorescent marker, Table 5.2. Upon ethanol treatment samples containing surfactants (both with and without surfactant additives) showed decreased non micelle:micelle ratios, while the sample containing just phenolic antioxidant showed little change upon treatment, Table 5.2.

The radius of reverse micelles in the ethanol diluted samples ranged up to 5 μm measured using confocal microscopy with Nile red labelled samples. The radius of the ethanol treated samples was significantly decreased as can be seen in the laser scattering images, Figure 5.4.

To conclude, the presence of reverse micelles in additive containing squalane samples has been identified by a range of optical and spectroscopic methods. It can be seen that the crucial additives in the formation of reverse micelles are the dispersants and detergents, while antioxidants do not promote reverse micelle formation.

6: Effect of Micellar Media on the Autoxidation of Hydrocarbons

Chapter Overview

This chapter will review the key literature on the effect of micellar media on the autoxidation of hydrocarbons. A mechanism for the micelle induced autoxidation mechanism will be proposed which will be critically evaluated against the current level of understanding in the area of hydrocarbon autoxidation and lipid oxidation.

6.1: Introduction

From the results in chapters 3 and 4 it can be seen that the addition of a surfactant had a great effect on the autoxidative stability of hydrocarbons containing antioxidants. This was particularly apparent with aminic antioxidants where a significant synergistic effect was observed see Table 3.6. A noticeable effect was also observed when model lubricants containing surfactants were treated with ethanol with the lubricant lifetime increased by a factor of 3, see Figure 4.17. In the literature there are few examples in the field of hydrocarbon autoxidation on the effect of micellar media on the autoxidation of hydrocarbons, with only Bakunin's group actively researching this area. [100, 117-122]

6.1.1: Previous Work on the Effect of Reverse Micelles on the Autoxidation of Hydrocarbons

The increased stability to autoxidation of surfactant containing hydrocarbons were suggested to be due to the formation of reverse micelles which subsequently act as alkyl peroxide traps. It was proposed that the dispersants will form reverse micelles that act as traps for alkyl peroxides which can then act as oxidative inhibitors. This chapter will discuss the effect of reverse micelles on the autoxidation of hydrocarbons from a literature review and propose a new mechanism for the inhibition.

Identification of Reverse Micelle Media in Autoxidation of Non-Additive Containing Hydrocarbon Samples

The first published discussion of reverse micelle formation and the effect on the autoxidation of hydrocarbons was reported in a high temperature, 170 °C, autoxidation of hexadecane, which showed a decrease in the rate of autoxidation during the later stages of oxidation. [100] This was attributed to the formation of reverse micelles due to the agglomeration of highly polar oxidised products.

The identification of reverse micelles was undertaken employing the indicator methyl orange, Figure 6.1, which is insoluble in non-polar, i.e. hydrocarbon-rich, media but is soluble in polar media, i.e. a polar reverse micelle core. [102]

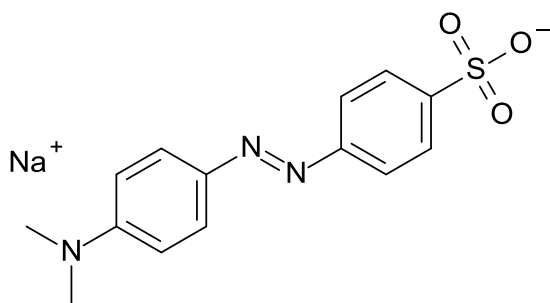


Figure 6.1: Sodium 4-[(E)-(4-dimethylaminophenyl)azo]benzenesulfonate (Methyl Orange)

Bakunin proposed that the observed increase with time in the solubility of methyl orange during hexadecane oxidation should be attributed to the formation of reverse micelles which are formed from the agglomeration of polar oxidised hydrocarbons. [100]

Later work by Bakunin also suggested evidence for the formation of reverse micelles in branched hydrocarbon media during the autoxidation of squalane at 170 °C. [120] The identification of reverse micelles in the oxidised squalane samples was again achieved through the use of methyl orange indicator. During the initial stages of oxidation, <5 minutes, it was reported that methyl orange

was insoluble in the hydrocarbon. [120] There was however an increase in the absorption at all wavelengths of the UV spectrum which they assumed to be an indication for formation of a dispersed reverse micelle polar phase, which can scatter light. After 10 minutes the concentration of methyl orange increased with time until a maximum was reached at 30 minutes, after which the sample were too viscous for the solubilisation of methyl orange into the sample.

Bakunin's choice of indicator, methyl orange, suggested by Bakunin to indicate the formation of reverse micelles could be flawed. During the oxidation of hexadecane and squalane Bakunin reported an increase in methyl orange concentration in oxidised hydrocarbon samples during the reaction. It was proposed that this increase was due to methyl orange being solubilised in polar reverse micelle cores.

An alternative explanation is that the solubility of methyl orange is indeed an indicator of the polarity of the medium becoming more soluble as the solvent polarity increases. If one looks at the polarity of the hydrocarbon feedstock it can be seen that polarity would be expected to increase during oxidation, i.e. alkanes going to form peroxides, alcohols and ketones, *even if these species remained solubilised*. As the sample is becoming more polar due to oxidation the increase in methyl orange concentration could simply be due to the increase in polarity of the sample. At present the positive methyl orange result is Bakunin's only analytical method for reverse micelle formation. This suggests a potential shortcoming in Bakunin's analytical methods and also suggests a need for a more suitable method of investigation of reverse micelle formation.

Proposed Mechanism for the Autoxidation of Hexadecane in the Presence of Reverse Micelles

Bakunin proposed a mechanism for the decrease in the rate of oxidation of hexadecane, Figure 6.2, in the presence of reverse micelles. [100] Bakunin proposes that reverse micelles can form due to the agglomeration of polar products during hydrocarbon autoxidation.

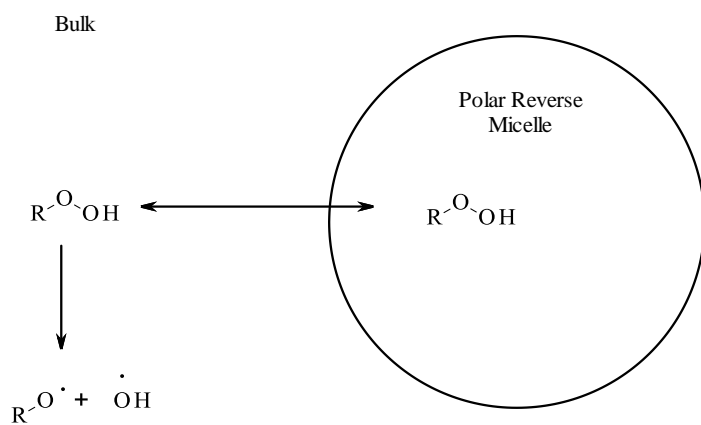


Figure 6.2: Bakunin's Proposed Mechanism for the Introduction of Reverse Micelles into a Lubricant [100, 119, 121, 123]

During the reaction Bakunin proposes that the alkyl peroxides produced during the oxidation reaction being polar, will tend to migrate into the polar reverse micelle core. Bakunin further suggested that the reverse micelle core has the ability to promote heterolytic decomposition of alkyl peroxides, produced during the propagation step of the autoxidation mechanism, into non-radical molecular products. [100] This in effect competes against the traditional, homolytic decomposition of peroxides in the bulk phase into radical products. The reverse micelle was in effect suggested to act as an alkyl peroxide trap, reducing the bulk concentration and as a result reducing the overall rate of autoxidation. Bakunin does not specify the reaction for the heterolytic decomposition of

peroxides into non radical products, but an example of such a reaction is shown in Figure 6.3. [158]

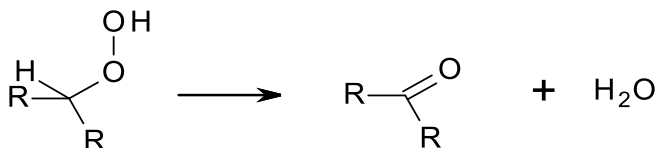


Figure 6.3: Heterolytic Decomposition of a Secondary Alkyl Peroxide into Non-Radical Products [158]

Bakunin's theory, that alkyl peroxides once inside the reverse micelle core can undergo heterolytic decomposition could be valid for hexadecane. [100, 122] This is due to autoxidation occurring primarily at secondary hydrocarbon sites, which is the lowest energy pathway. It is however not plausible for squalane for which Bakunin also reported reverse micelle formation and inhibition. [100] This is due to squalane being a branched hydrocarbon and thus possessing tertiary sites where autoxidation will predominately occur. From Figure 6.3 it can be seen heterolytic decomposition requires the hydrogen atom on the α -carbon to be transferred to the OH of the peroxide group, in order to form the ketone. However there are no hydrogen atoms α to the peroxide group for tertiary alkyl peroxides, so this decomposition cannot occur. Examining the heterolytic decomposition of a tertiary alkyl peroxide, Figure 6.4, it can be seen that this involves the dissociation of a carbon-carbon bond which is unfavourable with no examples present in the literature. This would suggest that once inside the reverse micelle core the mechanism must differ to what Bakunin implies.

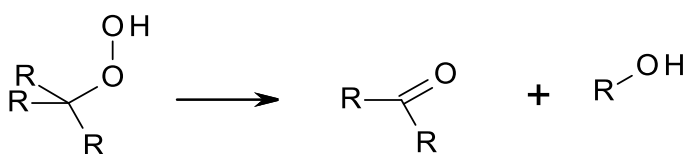


Figure 6.4: Heterolytic Decomposition of a Secondary Alkyl Peroxide into Non-Radical Products

Bakunin published work on the effect of reverse micelle structure on the performance of surfactant additives in automotive lubricants. [117] Bakunin proposes that incorporation of reverse micelles into a hydrocarbon media greatly influences the oxidation mechanism by the introduction of two new reaction phases an interface phase and a micelle phase, in addition to the traditional bulk hydrocarbon phase, Figure 6.5. [117] This theory is unique, in the field of lubricant autoxidation chemistry at least, as the rest of the literature on lubricant degradation treats the lubricant as a single non polar hydrocarbon phase.

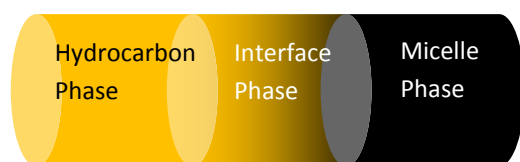


Figure 6.5: Bakunin's Proposed Three Phase System upon Addition of Reverse Micelles into a Non Polar Medium [117]

The three phase system proposed by Bakunin is not based on direct observation of reverse micelles but on the assumption that reverse micelles can markedly change the oxidation mechanism. Bakunin proposed that polar alkyl peroxides do not undergo the same decomposition mechanism in each phase. [117] The highly polar micelle core represents the micellar phase, with the main constituent being the polar head groups of the surfactant. [119] The interface phase provides stability to the system by facilitating the transport of components, typically alkyl peroxides, from the hydrocarbon phase to the micellar phase (and vice versa) and decomposition is suggested to go through either homolytically or heterolytically. This interface phase was suggested to comprise of the hydrophobic alkyl chains of the surfactant. In the bulk hydrocarbon phase it is assumed by Bakunin that alkyl peroxides undergo traditional bulk homolytic decomposition. [111]

To study the effect of added reverse micelle structure on additive efficiency Bakunin investigated the effect of the hydrophobic chain length of surfactants

on the formation of alkyl peroxides during the autoxidation of hexadecane at 170 °C. This was examined experimentally by incorporating sodium 1,4-bis(2-ethylhexoxy)-1,4-dioxobutane-2-sulfonate (AOT), Figure 6.6, reverse micelles with differing alkyl chain length into a solution of hexadecane, no AOT concentrations were provided in the paper. AOT was chosen by Bakunin due to it being the most widely used surfactant in reverse micelle studies and hence significant data is known for example critical micelle concentrations.

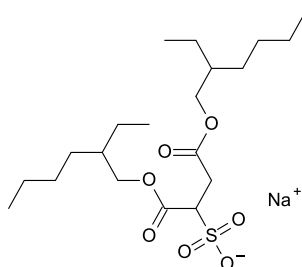


Figure 6.6: Sodium 1,4-bis(2-ethylhexoxy)-1,4-dioxobutane-2-sulfonate (AOT)

To study the effect of AOT reverse micelles on the oxidation of hexadecane, diethyldithiocarbamic acid (DTC), Figure 6.7, derivatives were employed in hexadecane. DTC is a polar molecule which is insoluble in the hydrocarbon media but becomes solubilised in AOT reverse micelle cores.

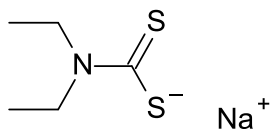


Figure 6.7: Sodium N,N-diethylcarbamodithioate (DTC- C₂)

AOT reverse micelles were used as the nanostructure by introducing above the critical micelle concentration, with DTC derivatives residing in the core. The critical micelle concentration is defined as the concentration of surfactant above which reverse micelle formation occurs with any additional surfactant going straight to micelle formation. The reactions were studying the effect of reverse micelles in the autoxidation of hexadecane at 170 °C. An increase in the inhibition period of 20 minutes, (10 minutes for hexadecane only to 30 minutes

for hexadecane in the presence of AOT micelles), was observed for the oxidation of hexadecane in the presence of AOT reverse micelles. There were also significant decreases in the rate of alkyl peroxide formation, again consistent with a lower rate of oxidation. A significant reduction in the inhibition period was reported upon addition of DTC to the formulation containing AOT micelles. Upon increasing the DTC hydrocarbon chain length from C2 to C12 resulted in decreased hydroperoxide formation.

An earlier theory for this effect is proposed by Bakunin suggesting that additive efficiency is highly dependent on the hydrophilic-lipophilic balance of the surfactant molecule, i.e. the balance between the degree of functional group polarity and the length of the hydrocarbon tail. [117] Paranego and Oganseova took this theory further and propose that it is the hydrocarbon tail of the surfactant and/or antioxidant which controls the antioxidant properties of the reverse micelle. [123]

The “Ideal” Antioxidant System

An “ideal” antioxidant system was proposed by Bakunin which combined a traditional bulk, hydrocarbon phase, antioxidant additive package with a reverse micelle also present in the bulk. [117] It was proposed that the traditional radical scavenging antioxidant will terminate the radical chains in the interface phase and it was suggested that the products would be “burned” in the reverse micelle core. There was no experimental evidence for this assumption.

Paranego also concurred on the proposal of an “ideal” antioxidant system, even though no experimental evidence has been shown. It was proposed that the concept of nanosized structures should allow for the creation of new and effective oxidation inhibitors for lubricants. [123] Paranego suggests that traditional antioxidants that act in the hydrocarbon phase can act in addition with the polar nucleus of the reverse micelles. [123] This is in contrast to Bakunin who suggests that the antioxidant will reside in the interface phase and not the bulk.

However, to date, it would appear that both Bakunin and Parenago have been unable to reach that goal. [117, 123]

Possible Experimental Evidence for “Ideal” Antioxidant System

Bakunin and Parenago have so far been unable to obtain their “ideal” antioxidant mechanism; however, it can be seen from a review of the literature that there are two reported works on the effectiveness of antioxidants in the presence of dispersants. Dispersants are known to form reverse micelles during normal operation mobilising oxidation products. Once the reverse micelles are formed then the proposals suggested by Bakunin could become valid.

Vipper et al reported a synergistic effect between succinimide dispersants and bisphenol antioxidant additives resulting in reduced rate of hydrocarbon oxidation. [82] They concluded that the synergism is the result of an increased level of protection between the two additives. In other words the additives are being consumed at a slower rate when in combination than when used separately. Vipper provided no chemical mechanism or analytical evidence for this action. However it could be further evidence towards Bakunin’s theory as the dispersant forms reverse micelles which then act as oxidation inhibitors. The addition of an antioxidant retards the rate of autoxidation which increases the length of the inhibition period further.

Later work by Alfadhli reports an increased effectiveness of a bisphenol antioxidant, 2,6-ditert-butyl-3-[(2,4-ditert-butyl-3-hydroxy-phenyl)methyl]phenol Figure 6.8 , in the presence of a succinimide dispersant. [83]

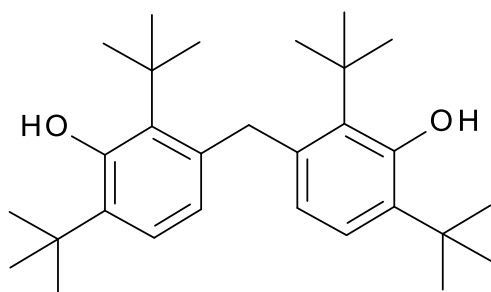


Figure 6.8: 2,6-ditert-butyl-3-[(2,4-ditert-butyl-3-hydroxyphenyl)methyl]phenol

This lead to increased oxidative stability of squalane samples containing these additives. The conclusion that Alfadhl reached was that the succinimide dispersant disperses the antioxidant more effectively into the lubricant and thus provides a greater level of protection against free radicals. This conclusion is different to that proposed by Bakunin who suggests that reverse micelles act as alkyl peroxide traps. However, there was no observational evidence for the action suggested by Alfadhl. [83]

Reverse Micelle Theory Summary

This section summarises the key observations and theories of the effect of reverse micelles on the autoxidation of hydrocarbon media from previous literature

Main Experimental Observations

- Bakunin and Paranego report decreased rate of oxidation during later stages of hexadecane and squalane autoxidation [100, 118, 122, 124]
- Methyl Orange becomes more soluble and displays increased baseline height during UV-VIS analysis in oxidising hexadecane or squalane [118]

- Decrease in alkylperoxide concentration reported in hexadecane samples containing AOT reverse micelles [123]
- No effect on the induction time reported in hexadecane samples containing AOT reverse micelles [123]

Main Theories and Proposals

- Reverse micelles form due to the agglomeration of polar material and/or addition of surfactant molecules [100, 118, 124]
- The presence of reverse micelles introduces two new reaction phases where oxidation mechanism differs.
 - Reverse micelle core where alkyl peroxides undergo heterolytic decomposition into non radical species [118]
 - Interface phase where alkyl peroxides can undergo heterolytic or homolytic decomposition [118]
- Reverse micelle core acts as an alkylperoxide trap effectively reducing the bulk concentration [100, 117-119, 124]
- Bakunin proposes that the effect of reverse micelles on additive efficiency could be highly dependent on the hydrophilic-lipophilic balance of the surfactant molecule [117]
- It was also suggested that reverse micelles can act in addition with a bulk antioxidant package, but with no evidence presented to date [117, 123]

6.1.2: Effect of Normal Micelles on the Efficiency of Antioxidants – The “Polar Paradox”

It could be seen in the work undertaken by Alfadhl and Vipper that antioxidants could be affected by the presence of reverse micelles. Therefore the literature review for this work was broadened to fields of study beyond liquid phase hydrocarbon autoxidation within the context of lubricant degradation to include

other areas where the effect of micelles on the efficiency of antioxidants has been reported.

From this review, the area of lipid oxidation in relation to food emulsions was seen to be quite active in the field of micelles and their effect on oxidation of lipid feedstocks. Of particular interest is the so called “polar paradox” which has been used to describe the behaviour of antioxidants in the field of lipid oxidation, without any clear mechanism to their action. This phenomena/paradox was first observed in the 1980’s when Porter reported that the relative effectiveness of phenolic antioxidants is highly dependent on the polarity of the reaction medium, either micellar (polar) or oil (non polar). [125, 126]

The work undertaken by Porter is in some ways chemically different to the work undertaken in this study or by Bakunin as Porter used normal micelles (oil in water) in his studies while the work presented in this thesis, along with Bakunin’s, studies reverse micelles (water in oil or more generally, polar in non-polar solvent). [102,111,119]

The Development of the “Polar Paradox”

It was observed that non-polar antioxidants are more effective in emulsified media (oil in water emulsions) than in dry oils which are homogeneous systems, with Porter the first to report this effect in 1989. [125] It has to be noted however that the “Polar Paradox” is an observation from experimental data and less of a paradox. Porter titled his observation as a “Polar Paradox”. The antioxidants that Porter studied ranged in polarity from the non-polar butylatedhydroxytoluene (BHT) Figure 6.9, increasing in polarity to the highly polar gallic acid, Figure 6.10.

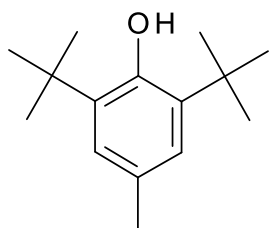


Figure 6.9: Butylatedhydroxytoluene (BHT)

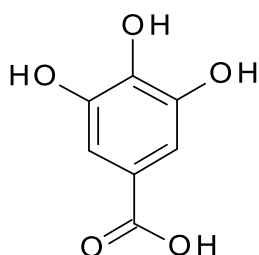


Figure 6.10: 3,4,5-Trihydroxybenzoic acid (Gallic Acid)

The work undertaken by Porter is different to the high temperature autoxidation studied by Bakunin. In his work Porter investigated the effect of air oxidation on dry, oil feedstock, and emulsified media, oil in water emulsion, at room temperature. The measure of oxidative stability was in relative effectiveness. Porter defined the relative effectiveness as the difference in the concentration of alkyl peroxides formed during the oxidation reaction with no antioxidant present and without

Porter reported that the non polar BHT was more effective in emulsified media (Oil suspended in soy lecithin) with a relative effectiveness of 16.7, in the dry oil (No soy lecithin) this was reduced to 0.5. [125] The polar Gallic acid, Figure 6.8, was reported to have a relative effectiveness of 0.5 in the emulsified media with the effectiveness increasing in the dry oil to a value of 2. Porter suggested that Gallic acid was more effective in non polar material. This difference in effectiveness suggests that the antioxidants are potentially affected by the reaction medium. In essence this is similar to Bakunins proposed “ideal

antioxidant” mechanism where non polar antioxidants are proposed to be more effective in the presence of reverse micelles. The work carried out by Porter and later workers could provide more evidence for the effectiveness of antioxidants in different environments.

Porter determined the relative effectiveness for a series of antioxidants in between the polarity range of BHT and Gallic acid and concluded that the antioxidants relative effectiveness in lipid oxidation is determined by the homogeneity of the reaction media and the polarity of the antioxidant, with non-polar antioxidants more effective in emulsified hydrocarbon media. The non-polar antioxidant will most likely reside in the oil core so the environment is similar to the hydrocarbon autoxidation mechanism where the antioxidant would be expected to reside in the bulk hydrocarbon phase.

Significant research has focused on gaining a better understanding of this paradox, and as a result this field has seen a significant level of interest. [127-140] A theory suggested for the increased effectiveness of non-polar antioxidants in emulsified media is based on the positioning of the phenolic antioxidant, Richards proposed that in the presence of a micelle non-polar antioxidants will be present in high concentrations at the interface phase, between the polar and non polar phases. [138] In this position any polar radical formed in the micelle will be scavenged by the antioxidant before entry into the emulsified media. This will reduce the concentration of radicals in the polar emulsion and reduce the rate of oxidative degradation. [138]

Effect of Reaction Medium on the “Polar Paradox”

In 2005 Chaiyasit et al reported on the effect of the reaction medium on antioxidants in order to provide a better understanding of the factors which control the “polar paradox”. [131] The study focussed on the effect of different antioxidants in emulsified media containing Brij micelles and dry oils.

The antioxidants chosen to study the effect of polarity were split into two classes either hindered phenol derivatives, (BHT, Figure 6.11 and 4-hydroxymethyl-2,6-ditertiarybutylphenol, Figure 6.12) or tocopherols (α tocopherol shown in Figure 6.13, and δ tocopherol shown in Figure 6.14).

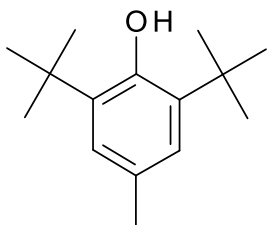


Figure 6.11: Butylatedhydroxytoluene (BHT)

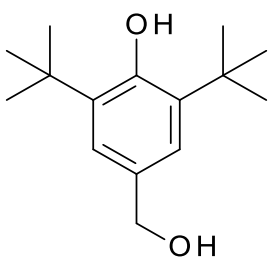


Figure 6.12: 4-Hydroxymethyl-2,6-ditertiarybutylphenol

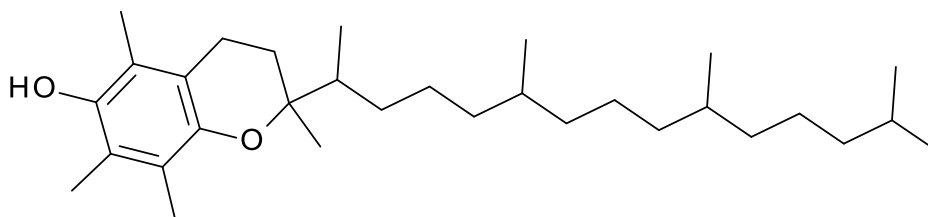


Figure 6.13: 2,5,7,8-Tetramethyl-2-(1,5,9,13-tetramethyltetradecyl)chroman-6-ol (α tocopherol)

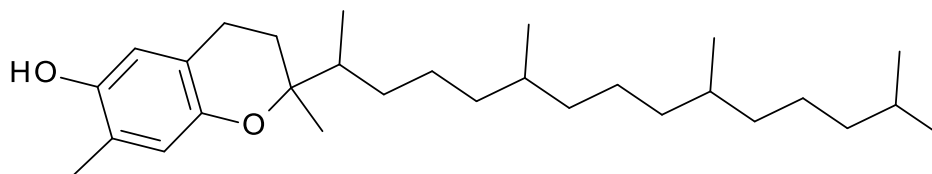


Figure 6.14: 2,7-Dimethyl-2-(1,5,9,13-tetramethyltetradecyl)chroman-6-ol (δ tocopherol)

The difference between the tocopherols is the degree of substitution on the benzene ring, δ -tocopherol only has one methyl group on the ring whilst α -tocopherol has three methyl groups, thus making δ -tocopherol the more polar antioxidant. In the case of the phenol derivatives BHT is the less polar of the two due to only one hydroxyl group present in the structure.

For the “polar paradox” to be observed in Chaiysaits work it was proposed that the non polar antioxidants should be more effective in the emulsified media (oil in water emulsions). This would relate to BHT and the α -tocopherol for the two different classes of antioxidant. The results which were actually published suggested otherwise, with no significant difference between the antioxidants upon increasing polarity, for both class of antioxidants. This contradicts the “polar paradox”. It has to be noted that this is unlike the majority of the work in this field; the difference in the polarity of the antioxidants used by Chaiysait did not vary significantly.

The difference between the two hindered phenol derivatives is largely due to polarity. So any difference in effectiveness could be suggested to be down to the polarity of the antioxidant. The two tocopherols differ by 2 methyl groups out of a total of 31. This would suggest that any difference between these antioxidants is not due to polarity but more likely the OH bond dissociation energy of the chosen antioxidant. Denisov reported that α -tocopherol has an OH bond dissociation energy of $341.5 \text{ kJ mol}^{-1}$ whilst the δ -tocopherol is $330.0 \text{ kJ mol}^{-1}$. [141] This is a difference of 11 kJ mol^{-1} between the two structures and is most likely to have a significant role in the effectiveness of the antioxidant. So

it is likely that Chaiyasits work is not controlled by polar effects but by thermodynamics and kinetics.

Contradictions in Field

This result from Chaiyasit is not isolated as there are several conflicting arguments which either support or do not support the “polar paradox” effects. [119,121,123,124,125,131,133,140-147] It has resulted in Shahidi concluding in his 2011 review that the “polar paradox” could be a small part of a much wider picture of oxidation of emulsified media and needs to be more extensively researched i.e., the theory may not only be related to lipid oxidation but could be applied to other systems. [142]

Critical Concentration of Antioxidants and the Effect on the “Polar Paradox”

Zhong suggested that polar antioxidants possess a critical concentration, indicated by the circle in Figure 6.15, where the polar and non-polar derivatives provide the same level of protection. [122] This was based on work undertaken studying the effect of concentration on the antioxidant activity. Zhong was investigating the effect of antioxidant polarity on the ability of the antioxidant to inhibit oxidation in non micelle media, stripped corn oil. This was in order to test the polar paradox observation.

If the polar paradox is being observed then the polar antioxidant should display higher levels of antioxidant activity in this non-polar medium, dry oil. The rate of oxidation was measured through the concentration of alkyl peroxides formed during the reaction. Zhong reported however that the antioxidants displayed differing characteristics an example of which is where the non-polar ascorbyl palmitate, Figure 6.16, was more effective than the polar ascorbic acid, Figure 6.17. [122]

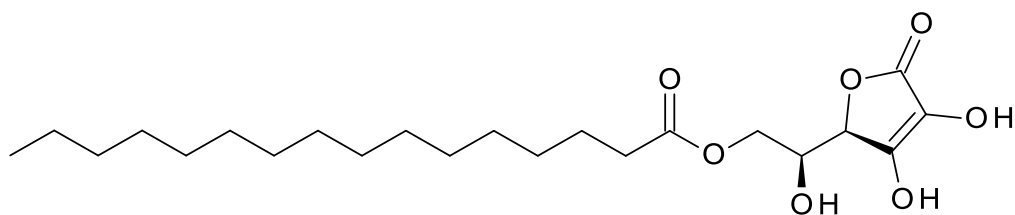


Figure 6.16: [(2S)-2-[(2R)-4,5-Dihydroxy-3-oxo-2-furyl]-2-hydroxy-ethyl] Hexadecanoate (ascorbyl palmitate)

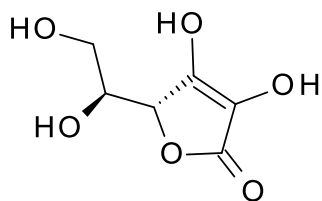


Figure 6.17: (2R)-2-[(1S)-1,2-Dihydroxyethyl]-3,4-dihydroxy-2H-furan-5-one (ascorbic acid)

A different trend was observed for 6-hydroxy-2,5,7,8-tetramethylchroman-2-carboxylic acid (Trolox®), Figure 6.18, where it was reported to be more effective than the non polar α -tocopherol in inhibiting the oxidation of the dry oil. Zhong proposes from these results that the polar paradox could in fact be concentration limited, in terms of the antioxidant, i.e. the polar paradox is not the effect of reaction medium on the effectiveness of antioxidants but determined by the concentration of antioxidant in the solution. [122]

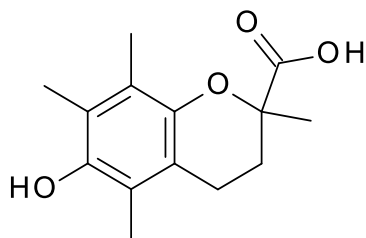


Figure 6.18: 6-Hydroxy-2,5,7,8-tetramethyl-chroman-2-carboxylic acid (Trolox®)

It can be seen in the data reported by Zhong that there are significant differences between the antioxidants in terms of their effectiveness, Figures 6.19-6.22. [122] The level of oxidation was determined by the level of inhibition which was calculated from the concentration of alkyl peroxides. The greatest increase in inhibition is reported for the ascorbic derivatives, Figure 6.19, where the non-polar ascorbyl palmitate had a 40% increase in inhibition over the polar derivative, ascorbic acid. It is not the results which are potentially in question but the bell shaped curve which is derived from these results. The bell shaped curve is derived from the degree of inhibition from Figures 6.19-22. It can be seen that only in Figures 6.19 and 6.20 that there are any significant differences in degree of inhibition between the non-polar and polar moiety. This would suggest that the bell shaped curve could be invalid.

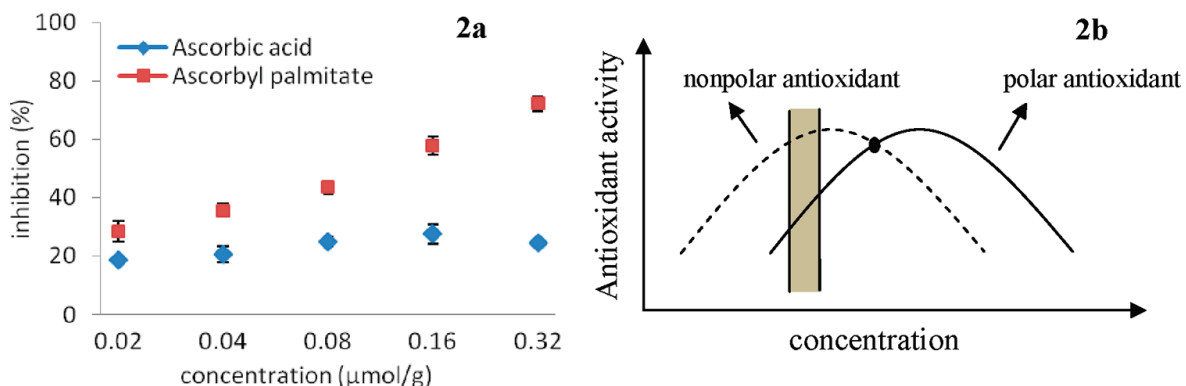


Figure 6.19: Antioxidant Activity of Ascorbic Acid and Ascorbyl Palmitate in Stripped Corn Oil [122]

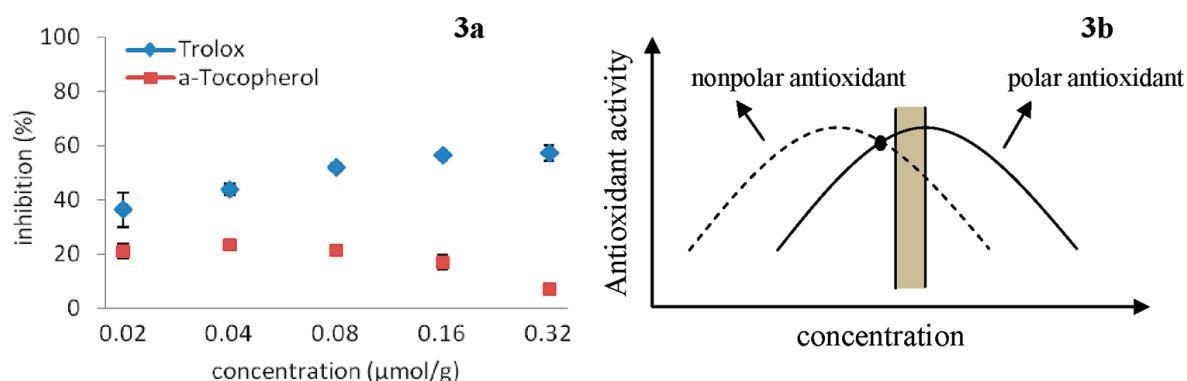


Figure 6.20: Antioxidant Activity of Trolox and α-Tocopherol in Stripped Corn Oil [122]

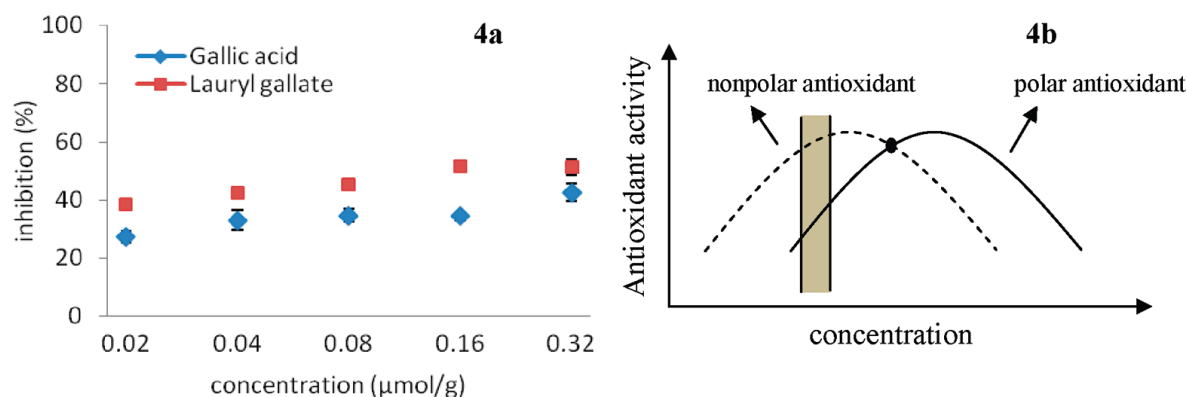


Figure 6.21: Antioxidant Activity of Gallic Acid and Lauryl Gallate in Stripped Corn Oil [122]

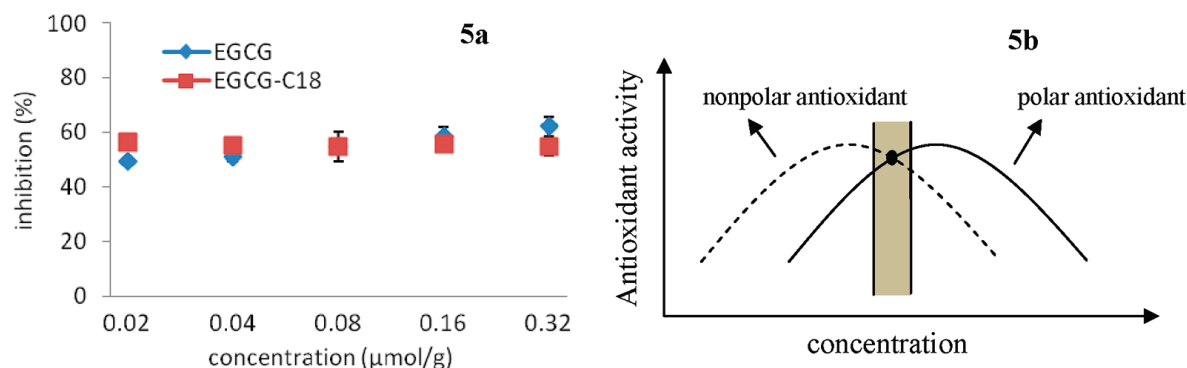


Figure 6.22: Antioxidant Activity of Epigallocatechin Gallate (EGCG) and EGCG-C18 in Stripped Corn Oil [122]

The data presented by Zhong has some shortcomings. Through Figures 6.19-6.22 the increase in antioxidant concentration is by a factor of 16. It can be seen that the concentration range seen in Figures 6.19-6.22 are extremely narrow. Therefore it is suggested that the representation of the data presented by Zhong is flawed and in essence the concentration range reported by Zhong covers the whole reported bell shaped curve. It is not only the presentation of data but Zhong's bell shaped curve is also in contradiction to that proposed by earlier work undertaken by Mahoney where it is suggested at high antioxidant concentration that activity reaches a maximum shown specifically in, Figure 6.23. [33]

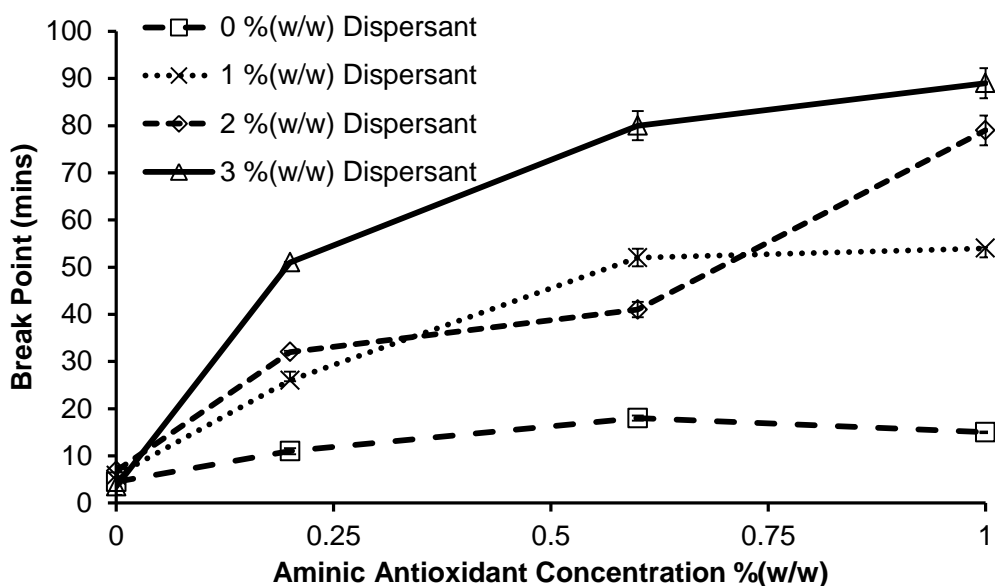


Figure 6.23: Example of Antioxidant Concentration Reaching Maximum Efficiency at 180 °C and O₂ Pressure of 1 Bar, see Chapter 3

From the results presented by Zhong it would seem that the results are actually following Mahoney's hypothesis. [122] An example of which is the antioxidant activity of EGCG, Figure 6.24, compared to EGCG-C18 where it is reported that both antioxidants have a similar level of inhibition over the concentration range, Figure 6.22.

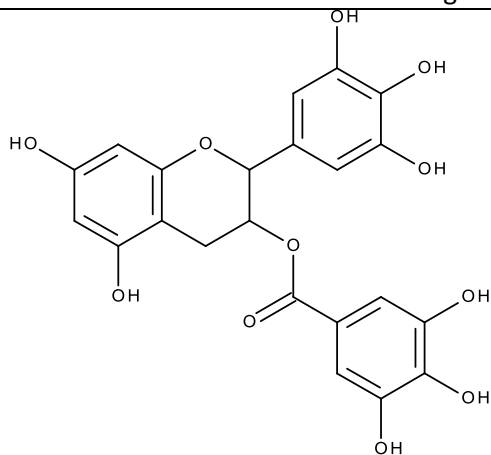


Figure 6.24: [5,7-Dihydroxy-2-(3,4,5-trihydroxyphenyl)chroman-3-yl] 3,4,5-trihydroxybenzoate (epigallocatechin gallate, EGCG)

Zhong suggests that this is the critical concentration where both antioxidants have the same level of activity. [128] However it could also be valid that through this concentration range the antioxidants in question have reached saturation point. The same conclusion could be given to the results presented for gallic acid and lauryl gallate, Figure 6.21.

The work presented in this thesis supports the theory of a maximum level of antioxidant activity and not that of a bell curve as suggested by Zhong. [128] In Figure 6.23 it can be seen that in the range of 0-1% (w/w) aminic antioxidant that the maximum period of inhibition was reached with 0.6% (w/w) aminic antioxidant in solution. The same level of inhibition was reached at the higher antioxidant concentration, 1% (w/w). This would suggest that the antioxidant activity does reach a plateau and provide an argument against Zhong's hypothesis that the polar paradox is concentration dependent.

Effect of Micelle Composition on the Rate of Oxidation

The most active group studying the effect of medium on the ability of antioxidants to inhibit oxidation has been the Decker group, where they have been attempting to gain a better understanding of this "polar paradox" phenomenon. [127, 130-133, 138, 143-147] This research is driven due to the recent move from saturated to polyunsaturated fats in many food products and

that, due to new REACH legislation, few new antioxidants are reaching the market. As a result there has been an increase in research activity into the effect of physical structures in bulk oils in order to use the current range of antioxidants more effectively. Decker et al. has seen the “polar paradox” as the best way to achieve this goal and has been studying the effects of micelle structure on the effectiveness of food grade antioxidants and the ability of micelles to inhibit oxidation.

In 2000 Silvestre published two papers on the effect of micelle structure on their ability to inhibit oxidation. This was achieved by altering the head group and tails of the surfactant and assessing the effect on the inhibition properties of the resultant micelle. [143, 146] The work by Silvestre could provide more evidence for what controls the effectiveness of micellar structure in the inhibition of oxidation.

It was concluded by Silvestre that the oxidation of oil in water emulsions is dependent on the size of the head group and in particular the strength of the interfacial membrane. [146] This work is based on two polyoxyethylene stearyl ether emulsions brij 76 , Figure 6.24, and brij 700, which are very similar in structure except for the size of the head group. Brij 700 contains 10 times more polyoxyethylene headgroups than Brij 76. It was reported that the emulsions containing Brij 700 reduced the rate of Fe^{2+} promoted decomposition of cumene hydroperoxide, while Brij 76 had little effect. This was proposed to be due to the increase in the size of the head group, and that the interfacial thickness plays an important role in the antioxidantancy of emulsified media.

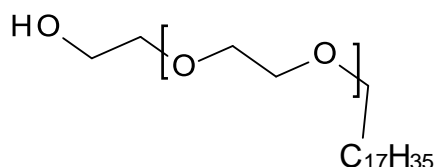


Figure 6.24: 2-Octadecoxyethanol (Brij 76)

In the same year Silvestre published work on the effect of the hydrophobic tail length on the oxidation of oil in water emulsions, i.e. altering the size of the micelle core. It was reported that the length of hydrophobic tail length had little or no effect on the rate of oxidation. [143] In Silvestre's work the rate of oxidation of two emulsions were compared (polyoxyethylene 10 stearyl (C16) ether emulsions and polyoxyethylene 10 lauryl (C10) ether). The rate of Fe^{2+} decomposition of cumene peroxide was effectively the same in both emulsion types. Silvestre proposes that hydrophobic chain length has little effect on the ability of the micelle to inhibit oxidation, in essence the size of the micelle core has little effect on the rate of oxidation.

The results published by Silvestre on the effect of chain length are unsurprising. During oxidation the feedstock becomes more polar and thus more likely to migrate into the polar water phase. Therefore changing the chain length would have little effect as the size of the micelle core does not control the rate of oxidation. The case for the hydrocarbon autoxidation is different. Bakunin proposes that the reverse micelle acts as a trap for polar material. Therefore systems with large reverse micelle cores present should result in greater protection against oxidation. Thus for hydrocarbon autoxidation the size of the micelle core plays a significant role in contrast to the "polar paradox".

"Polar Paradox" Summary

This section will summarise the key observations and theories of the "polar paradox"

Main Observations

- Antioxidants ability to inhibit lipid oxidation is dependent on reaction medium [125]
 - Non-polar antioxidants have been shown to be more effective in emulsified media, oil in water micelles [125]
 - Polar antioxidants have been shown to be more effective in dry oils [125]

- Not all researchers are in agreement with the above observation /effects or even mechanism to their action [127, 128, 131, 132, 137, 138]

Main Theories

- Two theories have been proposed as to the mechanism for this “polar paradox” observation
 - Non-polar antioxidants are more effective in emulsified media due to high concentrations at the interface phase of the micelle where oxidation is prevalent. [138]
 - Antioxidants have a critical concentration where the non-polar and polar derivatives are equally effective in the non-polar and emulsified media. Shahidi proposes that the antioxidants activity is concentration dependent which follows a bell curve. [128]

6.2: Similarities between Reverse Micelle Theory and the “Polar Paradox”

It can be seen from this review that micelles (both reverse and normal) can alter the rate of autoxidation when incorporated into a hydrocarbon solution. In the field of reverse micelles Bakunin reported a decrease in the rate of oxidation during the autoxidation of hexadecane and attributed this to the formation of reverse micelles, due to the agglomeration of polar oxidised hydrocarbons. [100] A mechanism was proposed by Bakunin where reverse micelles act as alkyl peroxide traps where they can undergo subsequent heterolytic decomposition to non-radical products.

In the field of normal micelles it has been observed that the ability of antioxidants to inhibit oxidation is dependent on the reaction media. This observation is termed the “polar paradox” and many groups have been actively researching this area. At present two theories have been proposed as to how

the observations in the “polar paradox” can be explained. Richards proposed that it is due to the positioning of the antioxidant whilst Zhong proposed that the “polar paradox” is due to a critical concentration where the antioxidant is equally effective in the emulsified and dry media. [122,132]

Taking the “polar paradox” and applying it to the reverse micelle situation, it can be seen that there are many similarities, in particular the role of micelles (reverse or normal) to influence rates of autoxidation. The mechanism proposed for the interaction of the antioxidant with micelles (normal or reverse) in both fields is similar in relation to the antioxidant having an affinity for the interfacial phase. It has been proposed that whilst in this position the antioxidants have the potential to scavenge radicals from the non polar micelle before entry into the polar bulk phase. [117, 138] For reverse micelles Bakunin suggests that the antioxidant terminates the radical chains in the interface phase of the reverse micelle, before entry into the reverse micelle core.

6.3: Relationship between the Work Presented in this Thesis and the Work in the Field

It can be seen that there are similarities between the work undertaken by Bakunin and the work presented in chapters 3 and 4 where the addition of dispersants greatly influenced the rate of squalane autoxidation. The mechanism proposed by Bakunin treats the reverse micelle as an alkyl peroxide trap, where once inside the reverse micelle core they can undergo heterolytic decomposition into non radical products. Bakunin's proposal is valid for straight chain hydrocarbons where heterolytic decomposition has been reported in the literature. The route of heterolytic decomposition inside the reverse micelle becomes invalid in the presence of branched hydrocarbons where there are no reported mechanisms in the literature. This is one of the major issues in the theory reported by Bakunin et al. [102, 113, 115, 117]

The next section of the chapter will outline a detailed mechanism for the hydrocarbon autoxidation mechanism in the presence of reverse micelles which aims to address some of the issues with the theory of Bakunin. This will in particular focus on the alkyl peroxide decomposition mechanism inside the reverse micelle core as this is one of the shortcomings of Bakunin's work when applied to the autoxidation of branched hydrocarbons. The mechanism can also be used to provide a more consistent mechanism for the "polar paradox" observations.

6.4: Micelle Mechanism with No Antioxidant

Summary of Key Experimental Observations from this Work

- Reduction in the rate of autoxidation observed in squalane samples containing 1% (w/w) dispersant, Figure 3.14
- No significant effect on the inhibition period upon addition of 1% (w/w) dispersant, Figure 3.14
- Reverse micelles suggested by use of UV-VIS analysis employing Nile red indicator in ethanol treated squalane samples containing dispersants

Previous chapters demonstrate that the introduction of reverse micelles, for example dispersants, can result in a noticeable increase in oxidative stability of hydrocarbons. It has previously been suggested that the reverse micelle can act as a trap for alkyl peroxides. [122] Alkyl peroxides are formed during the early stages of oxidation, steps 1-3 Figure 6.25, promoting the chain reaction mechanism. In the presence of reverse micelles the alkyl peroxide, due to its polarity (in comparison to the non-polar base oil), can be assumed to have a tendency to migrate to the polar micelle core (in sufficient concentration) as proposed by Bakunin et al. [102]

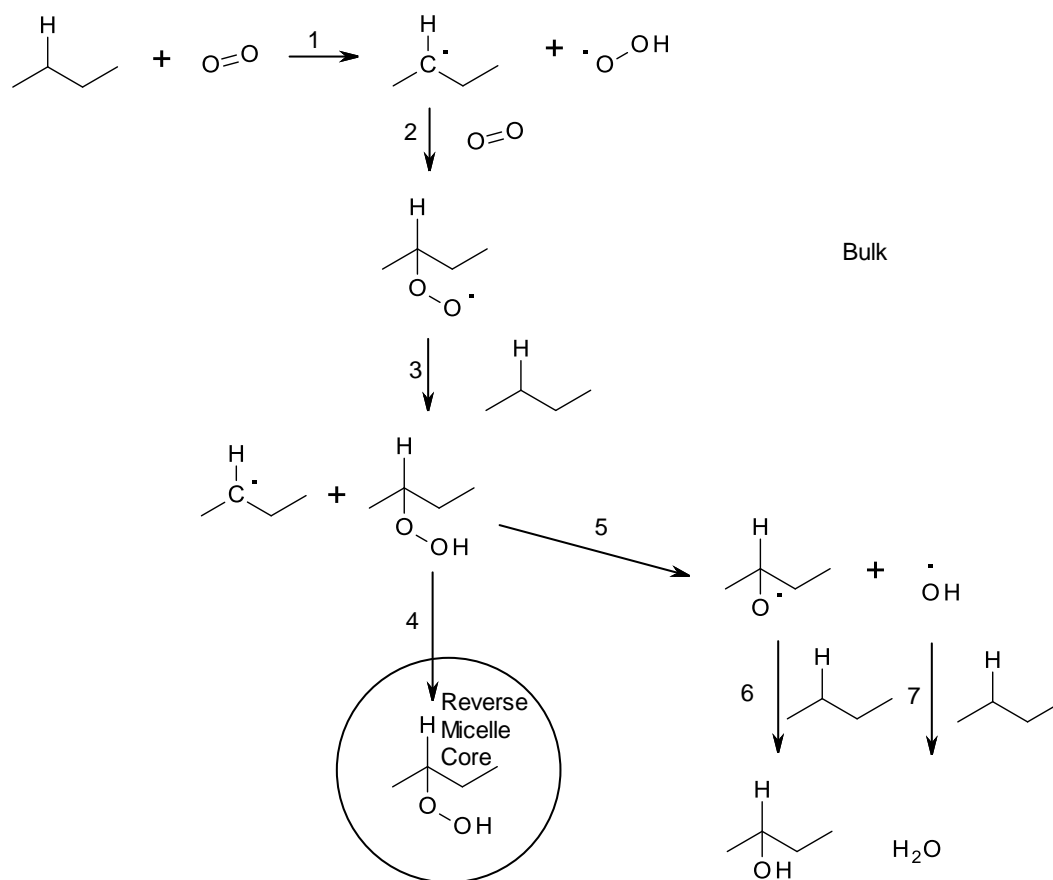


Figure 6.25: Reverse Micelle Autoxidation Mechanism

The mechanism for the autoxidation of hydrocarbons is dependent on the type of hydrogen sites that are present in the hydrocarbon structure. The weakest hydrogen site in the hexadecane structure is secondary sites ($-CH_2-$) and oxidation will predominately occur at these sites. [2, 13, 14] The resultant alkyl peroxide will be able to undergo heterolytic decomposition due to the ability of removing the remaining hydrogen on the carbon. [148] In comparison, in squalane the weakest carbon-hydrogen bonds are the tertiary sites (R_3C-H) which are present due to the branching of the alkane. As a consequence abstraction of the hydrogen from this tertiary site is the main route of autoxidation. [13] The resultant alkyl peroxide will have no aliphatic hydrogens less than two bonds apart. As such to undergo heterolytic decomposition a carbon carbon bond would need to be broken which is energetically

unfavourable. In the literature there are no papers suggesting the heterolytic decomposition of tertiary alkyl peroxides thus in this work it is assumed that the reverse micelles in essence work as alkyl peroxide traps.

Inside the reverse micelle core, as in the bulk phase, the alkyl peroxide will undergo decomposition due to the weak oxygen-oxygen bond dissociation energy to form alkoxy and hydroxyl radicals, Figure 6.26. When the alkyl peroxide present inside the reverse micelle core reach a high enough concentration then the radicals formed are likely to react further with the already oxidised material present in the reverse micelle core for instance other peroxides, Figure 6.26.

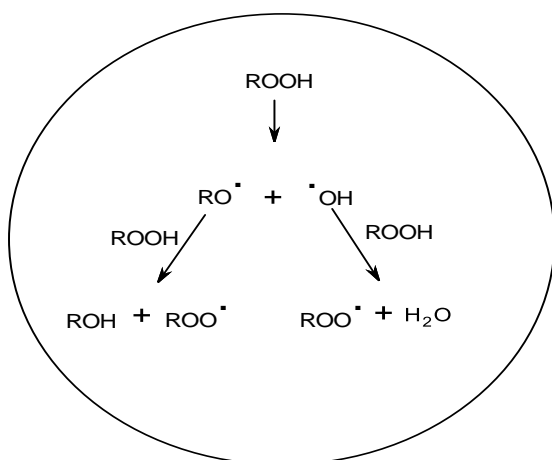


Figure 6.26: Alkyl Peroxide Decomposition inside a Peroxide Rich Environment i.e. Reverse Micelle [149]

This effectively reduces the secondary stages of the bulk autoxidation mechanism, by reducing the bulk alkyl peroxide concentration, where the alkyl peroxide can homolytically decompose to the alkoxy and hydroxyl radical, Figure 6.25 reaction 5, which react further with two more equivalents of squalane, Figure 6.25 reaction 6 & 7 to form the secondary oxidation products.

If we look at the overall reaction between the reverse micelle and bulk alkyl peroxide decomposition mechanism it can be seen why the rate of autoxidation

would be reduced. In the bulk three alkyl peroxides will decompose down into three alkoxy and three hydroxyl radicals, Figure 6.27.



Figure 6.27: Net Reaction for the Bulk Decomposition of Alkyl Peroxides

Both of these radicals are highly reactive and are likely to react further with squalane. In the reverse micelle alkyl peroxide-rich mechanism the products of alkyl peroxide decomposition is one alcohol and one water whilst two alkyl peroxy radicals are formed, Figure 6.28.



Figure 6.28: Net Reaction for the Reverse Micelle Decomposition of Alkyl Peroxide

The two alkyl peroxy radicals are less reactive than either the alkoxy or hydroxyl radicals and would reduce the rate of autoxidation in the presence of reverse micelles.

It can be proposed that in the presence of reverse micelles there will be a reduction in the rate of consumption of squalane due to the introduction of the alkyl peroxide trap which reduces the bulk alkyl peroxide concentration, Figure 6.25 reaction steps 1-4. This mechanism consumes two squalane molecules to form the alkyl peroxide, prior to micelle trapping and subsequent decomposition in the core. In comparison, four squalane molecules are consumed in the traditional homolytic decomposition mechanism, Figure 6.25 reaction steps 1-3,5-7. The proposed mechanism is very similar to that proposed by Bakunin in that reverse micelles act as alkyl peroxide traps. However they differ in the mechanism inside the reverse micelle core. Bakunin assumes that alkyl peroxides will undergo heterolytic decomposition into non radical products. What is proposed in this thesis is that alkyl peroxides decompose in the reverse

micelle core and undergo further reactions with alkyl peroxides and not the bulk oil.

6.5: Micelle Mechanism in the Presence of a Bulk Antioxidant

Summary of Key Experimental Observations from This Work

- Significant increase in the inhibition period of the ethanol treated squalane samples consisting primary antioxidant and dispersant, Figures 6.31 & 6.32
- Reverse micelles identified by use of UV-VIS analysis employing Nile red indicator in ethanol treated squalane samples containing dispersants and antioxidant
- Significant synergy observed between diphenyl aminic antioxidants and dispersants, Figure 6.23

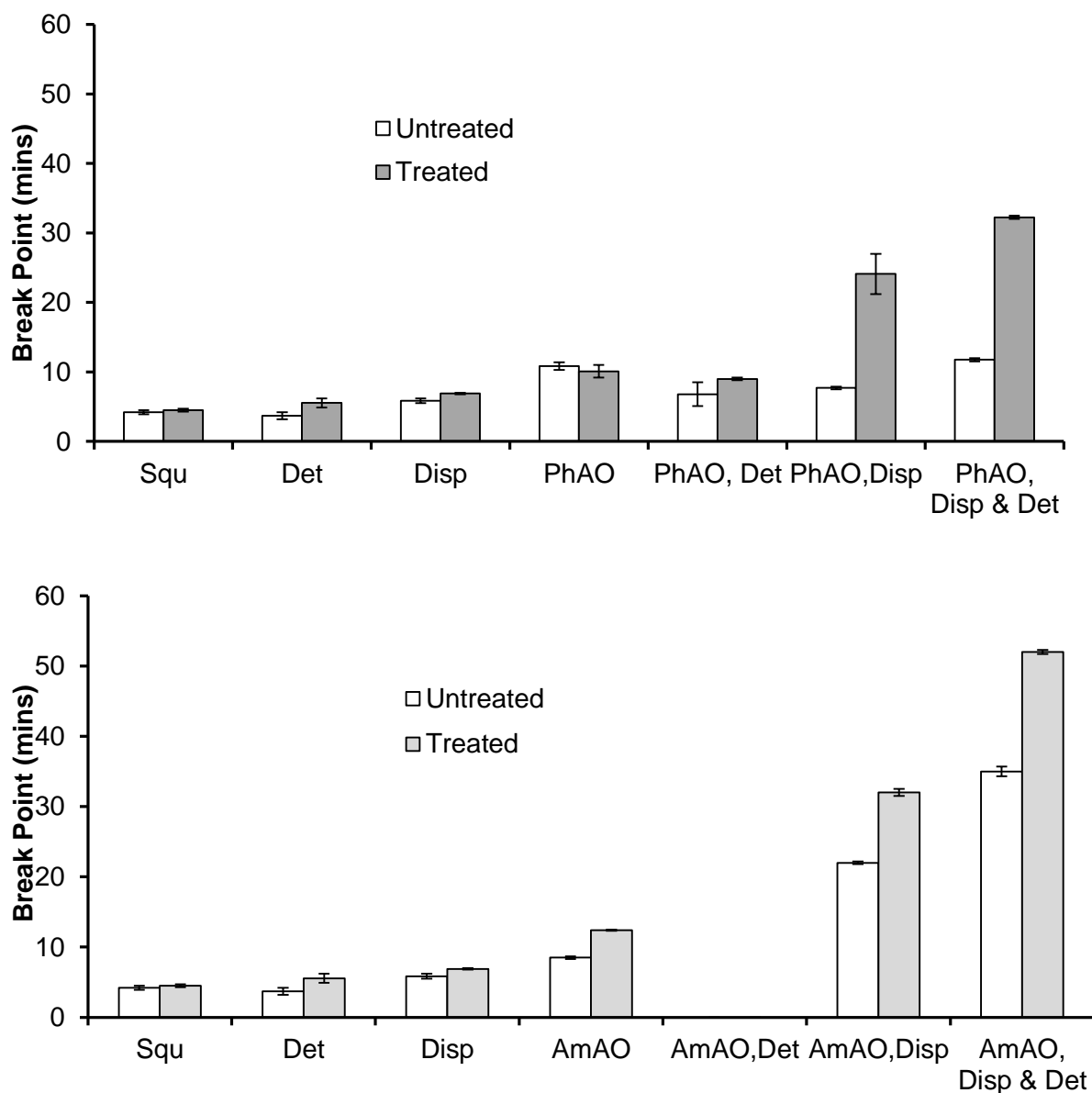


Figure 6.31 & 6.32: Effect of Ethanol on the Autoxidation of Squalane with 0.25% (w/w) Phenolic Antioxidant (PhAO), 0.3% (w/w) Aminic Antioxidant (AmAO), 1% (w/w) Dispersant (Disp) and 1% (w/w) Detergent (Det) at 180 °C and 1 Bar of O₂ (AmAO, Det Not Carried Out)

Antioxidants are incorporated into automotive lubricants to compete against the radical chain mechanism, Figure 6.33 reaction 3. This reduces the rate of alkyl peroxide formation during oxidation and hence increases the induction period of the lubricant. It was noted in the review of previous work that non-polar antioxidants are more effective in conjunction with normal micelles, this is the so

called “polar paradox”. It is also proposed by Bakunin that an ideal lubricant system should involve a bulk antioxidant system in conjunction with a reverse micelle. [119] In this work it can be seen that the ethanol treated squalane samples containing antioxidants and dispersants were significantly more stable to oxidation. It is the aim of this section to propose a mechanism which can explain the interactions between the primary antioxidant in the bulk hydrocarbon phase and a reverse micelle system.

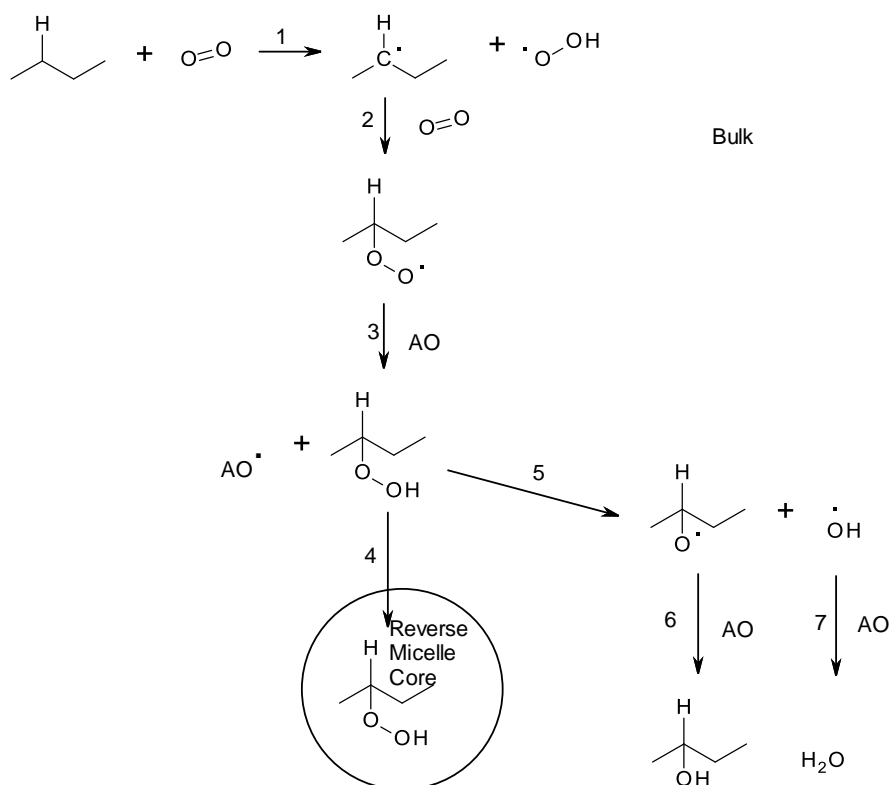


Figure 6.33: Reverse Micelle Autoxidation Mechanism in the Presence of an Antioxidant

It is assumed in this work that the antioxidant will reside in the non polar hydrocarbon phase where it can undergo traditional bulk oxidation chemistry reducing the rate of alkyl peroxide formation, due to it not taking part in reverse micelle formation. If the rate determining step of the reverse micelle inhibited reaction is indeed the formation of the alkyl peroxide an increased induction period should be observed upon addition of an antioxidant. This will be due to

the antioxidant competing against the radical chain mechanism and hence rate of hydrocarbon autoxidation is reduced. It is suggested here that the reverse micelle mechanism is unaltered and it is only the presence of the antioxidant in the bulk which reduces the rate of alkyl peroxide formation.

It is proposed here that the reverse micelle acts as an alkyl peroxide acceptor and only one equivalent of the antioxidant is consumed, Figure 6.33, reaction steps 1-4. Here the rate of antioxidant consumption will be significantly reduced in comparison to the rate expected via the traditional homolytic decomposition, where three equivalents are consumed. In the presence of an antioxidant the rate of alkyl peroxide formation is significantly reduced and this in turn with the reduced rate of antioxidant consumption relates to significant increases in the oxidative stability of the lubricant. The decomposition of the alkyl peroxide once inside the reverse micelle core follows the same mechanism as outlined for the mechanism with no antioxidant present.

Summary of Key Theories in Reverse Micelle and its Effect on Antioxidant

- The antioxidant is present in the bulk hydrocarbon phase.
- Antioxidants reduce the rate of alkyl peroxide formation.
- Alkyl peroxides migrate into the reverse micelle core and undergo the same mechanism as outlined in the mechanism where no antioxidant is present.

6.6: Summary of the Proposed Mechanism

The proposed mechanism can be used to describe the factor of three increase observed in the oxidative stability of a ethanol treated squalane sample containing phenolic antioxidant, dispersant and detergent, when compared with the untreated sample, Figure 6.31. It is assumed that the incorporation of reverse micelles consisting of dispersants into automotive lubricants (as a consequence of ethanol treatment) reduces the decomposition of alkyl

peroxides in the bulk oil, while the rate of bulk alkyl peroxide formation is reduced due to the bulk antioxidant. Alkyl peroxides migrate to the reverse micelle core where they undergo homolytic decomposition in the presence of already oxidised material. This is in contrast to the work undertaken by Bakunin who suggests that alkyl peroxides will undergo heterolytic decomposition into non radical products, which becomes invalid for branched hydrocarbons.

The proposed mechanism is not only applicable for the ethanol treated samples but for any sample containing surfactants. It can be seen in Figure 6.35, that squalane samples containing 1% (w/w) dispersant display a noticeable decrease in the rate of oxidative degradation but more importantly no change in the break point, Figure 6.35.

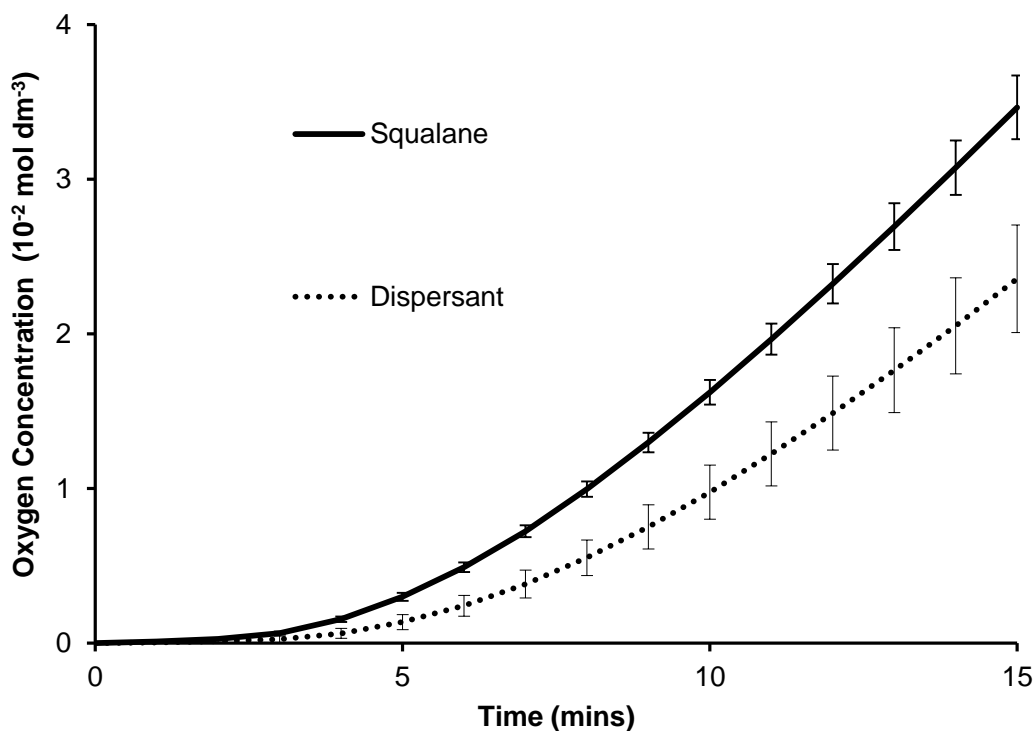


Figure 6.35: Effect of 1% (w/w) Dispersant on the Chemical Degradation of Squalane at 180 °C and 1 Bar of O₂

This can be attributed to the formation of reverse micelles during the reaction, in non-ethanol samples and the introduction of the reverse micelle reaction as outlined in chapter 3. The decrease in reaction rate is due to the dispersant reverse micelles effectively reducing the bulk alkyl peroxide concentration and hence decomposition. In this case there is no effect on break point between the dispersant containing sample and base oil sample. This is due to dispersant reverse micelles being formed during the reaction as they trap alkyl peroxides, i.e. the starting material can be classified as a homogeneous bulk oil it is only upon oxidation that reverse micelles are formed and the lubricant can be called heterogeneous, in effect dispersing the polar oxidised hydrocarbons. It is assumed that they are not present in the medium prior to oxidation.

In conclusion, it is assumed that the introduction of reverse micelles into a lubricant system reduces the bulk alkyl peroxide concentration effectively acting as alkyl peroxide traps. Inside the reverse micelle core the alkyl peroxides will undergo decomposition in the presence of already oxidised material. They do not undergo heterolytic decomposition as proposed by Bakunin.

6.7: Evidence for the Phenolic Antioxidant Being a Bulk Additive

The mechanism proposed above is based on the hypothesis that the majority of the phenolic antioxidant resides in the bulk oil not in the polar reverse micelle core. This section will gather evidence gained from previous chapters to ascertain the location of the antioxidant, in either the bulk, non polar phase or the more polar reverse micelles.

Nile red UV-VIS analysis provides evidence of the chemical environment in which the phenolic antioxidant resides, as described in chapters 4 & 5. The key characteristic of Nile red is the absorbance in the region of 480-520 nm. In this region Nile red shows two distinct absorbances which are dependent on the location of its location. Datta proposed that the absorbance at 480 nm is due to Nile red present in a hydrophobic environment, non micelle, with the absorbance

at 520 due to Nile red being present in a hydrophilic environment, reverse micelle core. [107] An attempt was made in earlier chapters to use the two absorbances for Nile red as an indication for reverse micelle formation, by calculating a non micelle:micelle (480:520 nm) peak height ratio in which values greater than one indicate that Nile red is in a non polar environment. This method is used as an indication of the presence of reverse micelle formation and is not intended to determine the concentration of reverse micelles in solution. It can be seen that upon ethanol treatment the phenolic antioxidant remains in a non-polar environment, due to the values of greater than one, Figure 6.36.

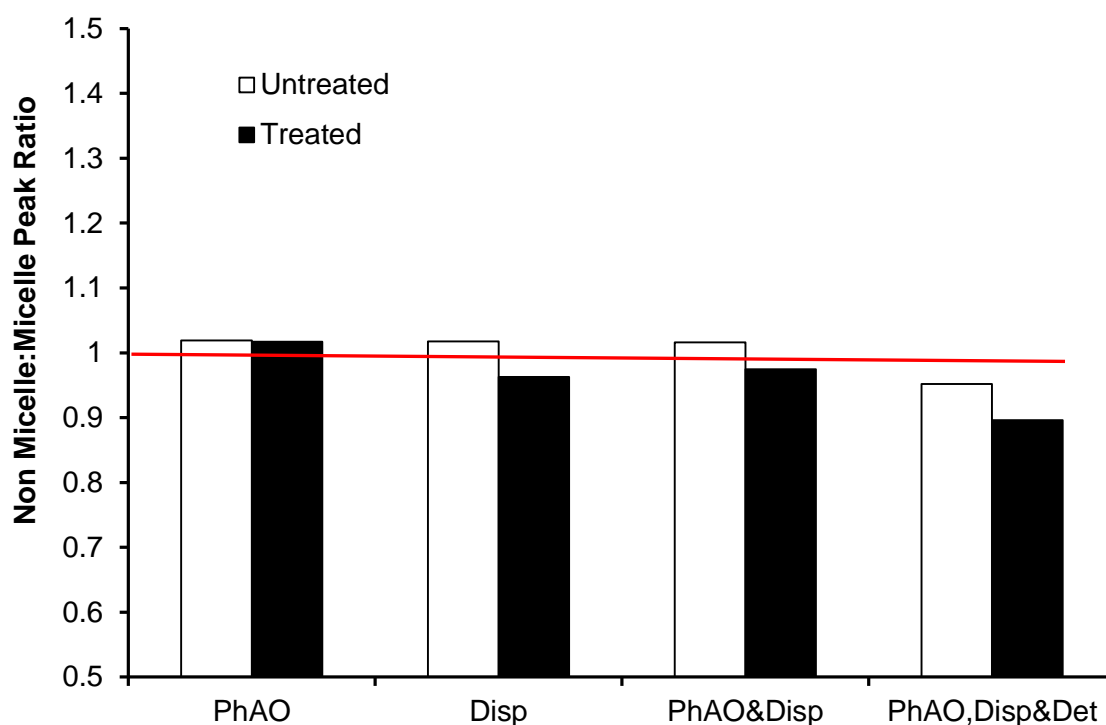


Figure 6.36: Effect of Phenolic Antioxidant (PhAO), Dispersant (Disp) and Detergent (Det) on Reverse Micelle Formation using Nile Red as a Marker in UV-VIS, using a Nile Red:Lubricant Ratio of 1:1x10⁶

This would indicate that the phenolic antioxidant does not form stable reverse micelles upon treatment with ethanol. There is also little or no difference upon the addition of a dispersant to an antioxidant and the dispersant only sample,

Figure 6.36. This should be expected if the phenolic antioxidant is not taking part in the formation of reverse micelles. If phenolic antioxidants were forming reverse micelles it would be expected that the reverse micelle value would be lower in the combined sample rather than in the dispersant only sample.

In earlier chapters the effect of reverse micelle formation on the oxidative stability of certain squalane formulations was presented, Figure 6.37. It can be seen that a general trend is observed that low reverse micelle ratio relates to an increased period of inhibition, Figure 6.37, suggesting that reverse micelles affect the oxidative stability of model lubricants.

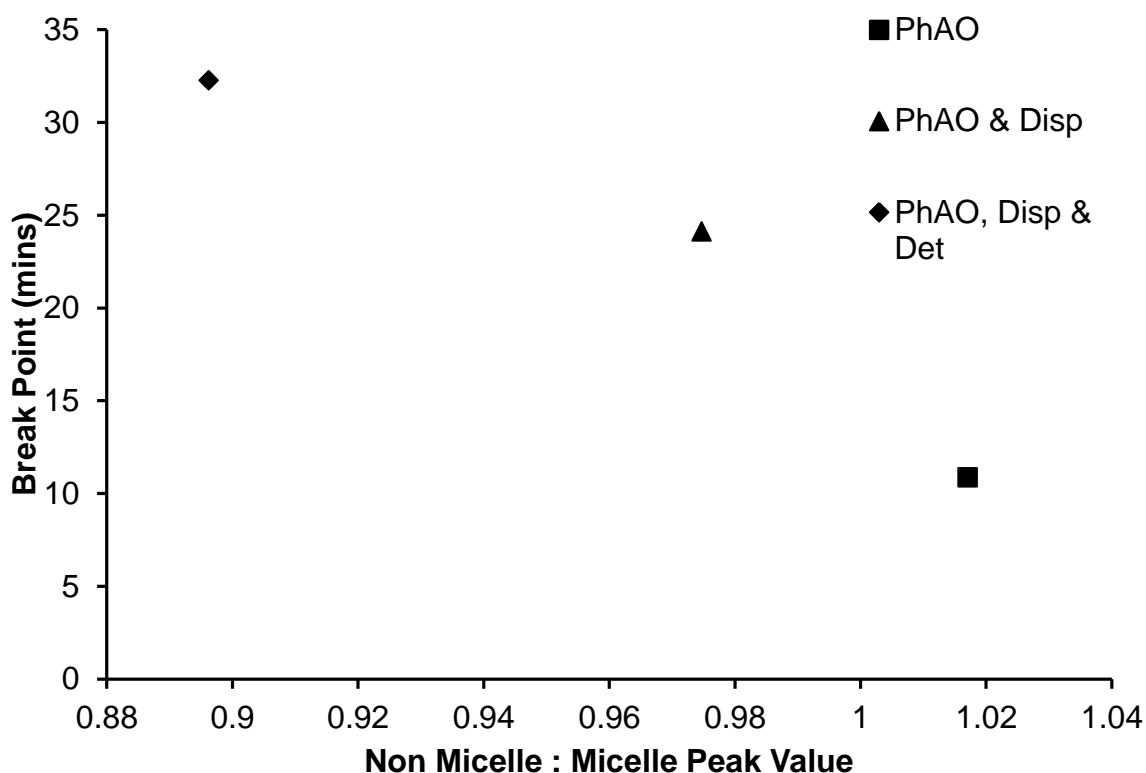


Figure 6.37: Effect of Reverse Micelle Formation on the Break Point of Ethanol Treated Squalane Samples Containing 1% (w/w) Dispersant (Disp), Detergent (Det) and 0.25% (w/w) Phenolic Antioxidant (PhAO) at 180 °C and 1 bar O₂

It can be seen in Figure 6.37 that with addition of a dispersant, triangle, the reverse micelle ratio is reduced slightly with a significant increase in the

oxidative stability of the lubricant. The increase in oxidative stability suggests that the dispersant reverse micelle interacts positively with the bulk antioxidant.

The decrease in reverse micelle ratio, going from phenolic antioxidant to dispersant with phenolic antioxidant, would suggest that the phenolic antioxidants does not take part in reverse micelle formation and could be considered a bulk additive. The majority of the chemical analysis suggests that surfactant reverse micelles are formed during the process of ethanol treatment. They act as oxidative inhibitors in their own right; however it is the addition of a bulk antioxidant that provides the synergistic effect. This supports Bakunin's hypothetical "ideal" lubricant.

6.8: How this Mechanism Compares to Existing Literature

It is generally accepted in the literature that the addition of micelles, normal and reverse, to a lubricant system will increase oxidative stability. They are also assumed to act in synergy with certain antioxidants and again this is apparent in both micelle types. The mechanism proposed in this work has tried to take findings from the key observations outlined in the introduction section and understand some of the areas which have been unanswered, i.e. the mechanism of alkyl peroxide decomposition in the reverse micelle and the effect of antioxidants in the presence of reverse micelles.

6.8.1: Comparisons to Bakunin's Work on Reverse Micelles

Bakunin has published work proposing that reverse micelles can act as alkyl peroxide traps effectively reducing their bulk concentration. Once the alkyl peroxide are present in the reverse micelle core Bakunin suggests they undergo heterolytic decomposition into non radical products. The reaction mechanism outlined in this work is in disagreement as to how the alkyl peroxides decompose inside the reverse micelle core.

The other point where the theories suggested by Bakunin and this work differ is the effect of the antioxidant on the oxidative stability of the lubricant. [117] It is

agreed in the work reported by Bakunin and in this work that antioxidants act synergistically with reverse micelles. There are however clear differences in the mechanism of this synergism. It is proposed by Bakunin that the antioxidant will be present in the interface phase where it effectively mediates the transport of radicals into the reverse micelle core.

It is hard to see why the antioxidant would provide a synergistic effect using Bakunin's suggested mechanism. If the majority of the antioxidant is present in the interface phase as is suggested than this would result in a reduction in the bulk concentration. This in turn reduces the ability of the antioxidant to protect the lubricant against the bulk radical chain mechanism. The consequences would be an increased rate of oxidative degradation and result in reverse micelles that display a pro-oxidant effect.

The mechanism proposed in this work has the antioxidant in the bulk where it can reduce the rate of alkyl peroxide production. The resultant alkyl peroxide can migrate to a reverse micelle core where it will agglomerate and undergo decomposition. Through this mechanism only one antioxidant equivalent is consumed to produce an alkyl peroxide compared to the three equivalents consumed in homogeneous media. The bulk antioxidant reduces the rate of alkyl peroxide formation due to the disruption of the chain mechanism. This in turn increases the lifetime of the reverse micelle to act as an oxidative inhibitor by increasing the time taken to reach the saturation point.

6.8.2: Can the Proposed Mechanism be Utilised to Understand the "Polar Paradox"

The effect of normal micelles on the rate of lipid oxidation has been extensively researched. The main conclusion is that the ability of the antioxidant in retarding the rate of oxidation is determined by the reaction medium, i.e. dry oil or emulsified media (oil in water emulsions). In particular they can affect the ability of the antioxidant to act against the oxidative degradation processes. Over the past 30 years this has been termed the "polar paradox" and has been used

extensively to examine the trends observed upon using the same antioxidant in differing media.

If one examines the current level of understanding given as to why non-polar antioxidants are more effective in slightly polar media a new theory using the knowledge gained in reverse micelles can also be suggested. The main hypothesis behind the polar paradox is that the antioxidant will be positioned where the oxidation is most prevalent. Now if this is the case, the antioxidant should be consumed at a faster rate as a result of a higher concentration of radicals in that area.

If the oxidisable substrate is taken into consideration a more plausible explanation can be found. In dry oils the substrate which is undergoing oxidation is the oil and therefore non polar antioxidants will effectively prevent oxidation.

In an emulsion where normal micelles are present, the non-polar antioxidant is assumed to reside in the micelle core. The rate of oxidation of the chosen oil in the micelle core is reduced as the peroxides formed as a result of oxidation are removed by transfer from the non polar core to the more polar environment. If one looks at the potential reaction mechanism it would hold similarities to the reverse micelle scheme. It is assumed in the micelle core that the alkyl peroxy radical formed as a result of oxidation consumes one equivalent of antioxidant to form the alkyl peroxide. Now the polarity of the peroxide has increased and has the potential to migrate out of the non-polar core into the polar solution. As a consequence the alkyl peroxide will undergo the secondary stages of oxidation in the polar solution away from the antioxidant. In the dry oil it is assumed that the peroxide will undergo the secondary stages of oxidation in the presence of antioxidants. As a consequence the non-polar antioxidant will provide greater protection against the chemical degradation of the oil in emulsified media as it is consumed at a far slower rate.

The mechanism proposed here differs to previous mechanisms in the literature. In the polar paradox it is assumed that the antioxidant will be present in the

interface phase trapping the polar radicals prior to entry into the polar medium. [138] Now this theory has one potential flaw based on the positioning of the antioxidant in the interface phase. This would suggest that it could still be susceptible to the bulk radicals formed in the secondary oxidation stages. If this is the case then the rate of antioxidant consumption should still be at a similar rate to the dry oil. In this work non-polar antioxidants have been shown to have an affinity for the non polar environment. As a consequence it is highly likely that they will be present in the micelle core, not the interface phase (as suggested in the literature). In the core the rate of oxidation is reduced due to the effective removal of the secondary stages of oxidation by the migration of the peroxide into the polar environment. This, in tandem with the reduced rate of oxidation upon introduction of a non-polar antioxidant, results in a more effective antioxidant in slightly polar media. In essence it is having an appreciation of the transfer of alkyl peroxides between phases which is the key to this mechanism.

6.9: Conclusions

The work presented so far in this thesis is in agreement with Bakunin who suggested that reverse micelles can decrease the rate of hydrocarbon autoxidation by acting as alkyl peroxide traps. This thesis has tried to question two of the main criticisms of the work undertaken by Bakunin. One of the criticisms is that Bakunin's analytical evidence is light. As can be seen in Chapter 5 this work employed a more suitable marker to identify reverse micelles, Nile red, and more substantial evidence. This chapter has dealt with the second criticism centring on the decomposition of the alkyl peroxide once inside the reverse micelle core. At present Bakunin proposes that the alkyl peroxide once inside the reverse micelle core decomposes heterolytically into non-radical products. As outlined in this chapter this conclusion is invalid for branched hydrocarbons for which the majority of the work presented in this thesis is based on.

In this chapter it can be seen that the main reverse micelle mechanism is in agreement with that proposed by Bakunin, Figure 6.25. This chapter has proposed a more plausible mechanism for the reaction of alkyl peroxides once inside the reverse micelle core, Figure 6.26. The mechanism suggests that reverse micelle cores are an alkyl peroxide rich environment and it is the decomposition of alkyl peroxides in this rich environment which provides a lower rate of autoxidation. Increased inhibition periods are observed upon addition of a bulk antioxidant which slows the rate of alkyl peroxide formation.

This mechanism has been critically evaluated against the current state of the art in both reverse and normal micelles. It has been applied to the “polar paradox” phenomena in lipid oxidation, something which has been very difficult for the past 30 years. Workers in the lipid oxidation field suggest that the antioxidant would reside in the interface phase whereas it is proposed here using the findings from reverse micelles that the antioxidant is in the non polar micelle core.

The main conclusion from this work is treating the autoxidation of base oils in the presence of dispersants as a single phase bulk oil mechanism is no longer appropriate. It can be seen in this work that the oxidation mechanism should now be described as a two phase mechanism, appreciating the ability of the micelles to act as an oxidative inhibitor. A particularly strong synergy is apparent between primary antioxidants and reverse micelles, which is due to the reduction in rate of formation of alkyl peroxides. It is only Bakunin and Parenago in this field which has appreciated a need to improve current methodologies which include the presence of reverse micelles. [100, 118, 121] Vipper and Alfadhl have presented similar results with no appreciation of the mechanism there conclusions being that the dispersant disperses the antioxidant. [81, 82, 83, 152]

Existing single phase chemical mechanisms need to be developed to incorporate the reaction mechanism outlined in this work. This conclusion of has already been obtained to a certain degree in the field of lipid oxidation with Decker, Porter, Frankel, Cuvelier and Shaidi all showing their contributions.

[125, 126, 128, 130, 131, 142, 143, 146, 150-153] It has taken a considerable time for it to be reached in this field. The reverse micelle has been identified and will have an effect on the oxidative properties of the lubricant; in essence this has opened a whole new area of additive chemistry with the introduction of reverse micelles into automotive lubricants.

7: Effect of 1-Methylnaphthalene on the Autoxidation of Squalane

Chapter Overview

The work in this chapter examines the effect of conventional crude oil derived fuel dilution on the oxidative stability of automotive lubricants, focusing on the chemical mechanism for the autoxidation of 1-methylnaphthalene, with validation by GC-MS, GPC and Gaussian 09w software. This mechanism will then be critically evaluated against previous work by Jensen. [45, 46]

7.1: Introduction

During typical operation of an automotive engine uncombusted fuel can dissolve in the lubricant in the piston assembly, before returning into the sump, as discussed earlier in this thesis. [19] Temperatures in the sump are relatively low (ambient to ca. 80 °C) and is the area of the engine where the lubricant spends the longest time. This compares to the combustion chamber where it is typically higher (110-160 °C). [7,24]

Fuel dilution is increased during the starting of the engine, particularly in winter, where the metal surfaces of the cylinder are cold leading to fuel accumulating in the lubricant in the sump in significant concentrations, [49, 50]. Values up to 13 % (v/v) in used oil samples being reported for gasoline engines. [50]

Whilst the fuel is in the lubricant it can undergo similar degradation reactions as the lubricant. Therefore, it has been of interest to investigate whether dilution by fuel in the sump has an effect on the chemical degradation of the lubricant. Any effect could alter the friction which could have consequences on the fuel consumption, atmospheric carbon dioxide emissions from the engine and the useable lifetime of the lubricant.

The majority of the work in this field employs expensive engine tests which give useful information but which typically do not provide detailed chemical analysis. An example of such work is by Pedersen where the effect of the lubricant on the

polycyclic aromatic hydrocarbon (PAH) emissions in the exhaust were undertaken. [52] During the work it was found that the lubricant acted as a PAH sink resulting in significant concentrations of PAH building up in the sump lubricant. This theory of the lubricant acting as a PAH sink was taken further by Brandenberger where the PAH concentration in the sump was found to be six times higher than in the exhaust gases. [53] The suggested theory is that non combusted PAH's are transported with the combustion gases, cool down in the ambient sump and accumulate in the sump lubricant, leading to the significant concentrations being observed. This work will model the effect of the simplest PAH, 1-methylnaphthalene on the oxidation of squalane at representative temperatures

In previous work, the effect of 1-methylnaphthalene on the autoxidation of hexadecane has been investigated in detail by Ingold, [45, 46] where it was suggested that 1-methylnaphthalene inhibited, but did not halt the reaction, the autoxidation of hexadecane i.e. did not act as an antioxidant. Ingold proposed that 1-methylnaphthalene have two potential reactions with peroxy radicals formed during oxidation, one which acts as an inhibitor while the other acts as a pro-oxidant. The pro-oxidant mechanism is due to the abstraction of a hydrogen atom from the methyl group on the methylnaphthalene, Figure 7.1 reaction 1, leading to the formation of the methylnaphthyl radical which will react further with oxygen and alkyl groups to form the typical oxidation products, Figure 7.1 reactions 3-6. [45]

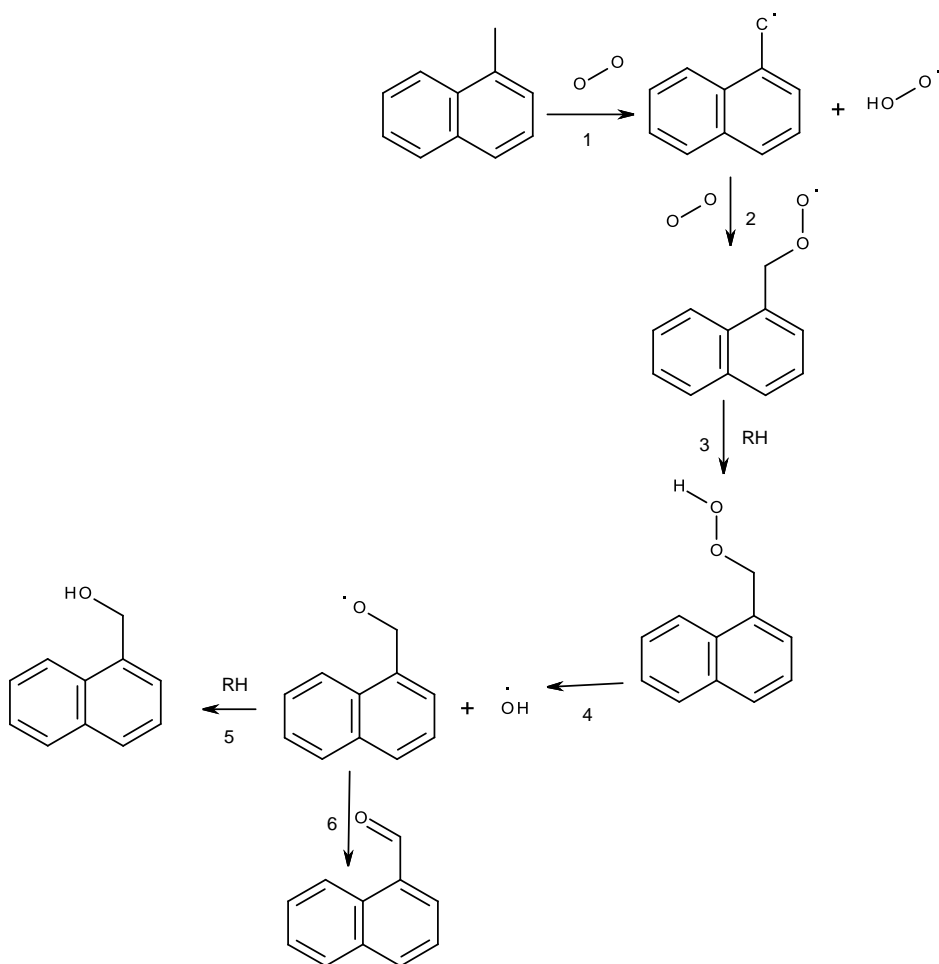


Figure 7.1: Autoxidation Mechanism of 1-methylnaphthalene Proposed by Ingold [45, 46]

The antioxidant mechanism proposed by Ingold involves the addition of alkyl peroxide radical to the β -position of the methylnaphthalene, which reacts further to give the phthalic anhydride and acid, Figure 7.2. The explanation given as to why this mechanism gave the antioxidant effect is due to the formation of the hydroperoxyl radical, Figure 7.2 reaction 2, which increases the 2nd order rate constant for the self and cross, Figure 7.3 & 7.4 proposed to be due to the (methyl)naphthoxyl radicals acting as effective alkyl peroxy chain termination reactions. [45]

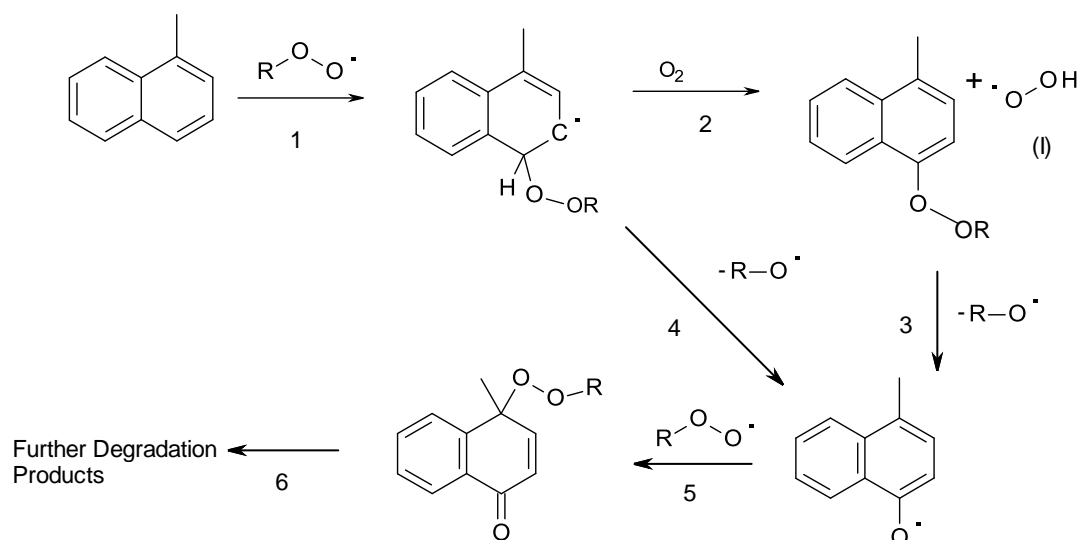


Figure 7.2: Mechanism for the Addition of the Alkyl Peroxide to the 1-methylnaphthalene [45 & 46]

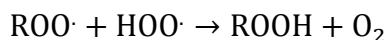


Figure 7.3: Hydroperoxyl-alkylperoxyl Cross Termination Reaction

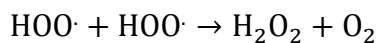


Figure 7.4: Hydroperoxyl-hydroperoxyl Termination Reaction

This chapter will investigate the effect of 1-methylnaphthalene on the autoxidation of a branched hydrocarbon, squalane, under representative temperatures and pressures, using a model bench top system. Product analysis will allow an evaluation of the mechanism that Ingold proposed and provide a greater understanding to the mechanism which gives 1-methylnaphthalene its antioxidant properties.

The work in this chapter differs from that undertaken by Ingold by using a temperature of 150 °C and employing different analysis techniques. In this work gel permeation chromatography was employed in addition to gas chromatography in the analysis of the oxidation products. Another difference is

that a branched hydrocarbon was used in this study whilst Ingold employed hexadecane.

7.2: Results and Discussion

7.2.1: Effect of 1-Methylnaphthalene on the Autoxidation of Squalane

Samples of squalane were diluted with 5% (v/v) 1-methylnaphthalene and oxidation runs were undertaken. It can be seen, Figure 7.5, that 1-methylnaphthalene has little significant effect on the induction time or the subsequent rate of squalane autoxidation at 150 °C with a gas flow rate of 0.1 dm³ min⁻¹. The error bars displayed in Figure 7.5 and subsequent Figures are the deviance from the mean of two or more runs. The data presented in Figures 7.5-7.7 are concentrations of squalane and 1-methylnaphthalene taken during the reaction and determined by GC.

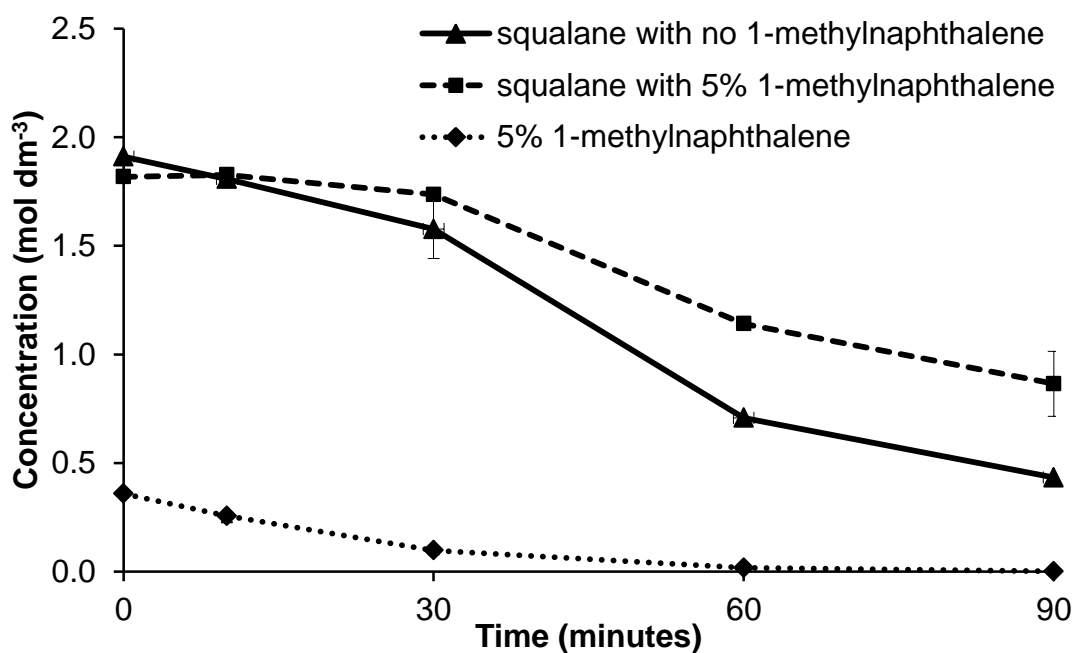


Figure 7.5: Effect of 5% (v/v) 1-methylnaphthalene on the Autoxidation of Squalane at 150 °C and an Oxygen Flow Rate of 0.1 dm³ min⁻¹ at a O₂ Pressure of 1 Bar

Through GC analysis of the volatile trap solution it was found to contain a significant concentration of 1-methylnaphthalene therefore suggesting that there was significant loss due to volatility. To overcome this problem the reaction was repeated but with a reduced gas flow rate of $0.03 \text{ dm}^3 \text{ min}^{-1}$, Figure 7.6.

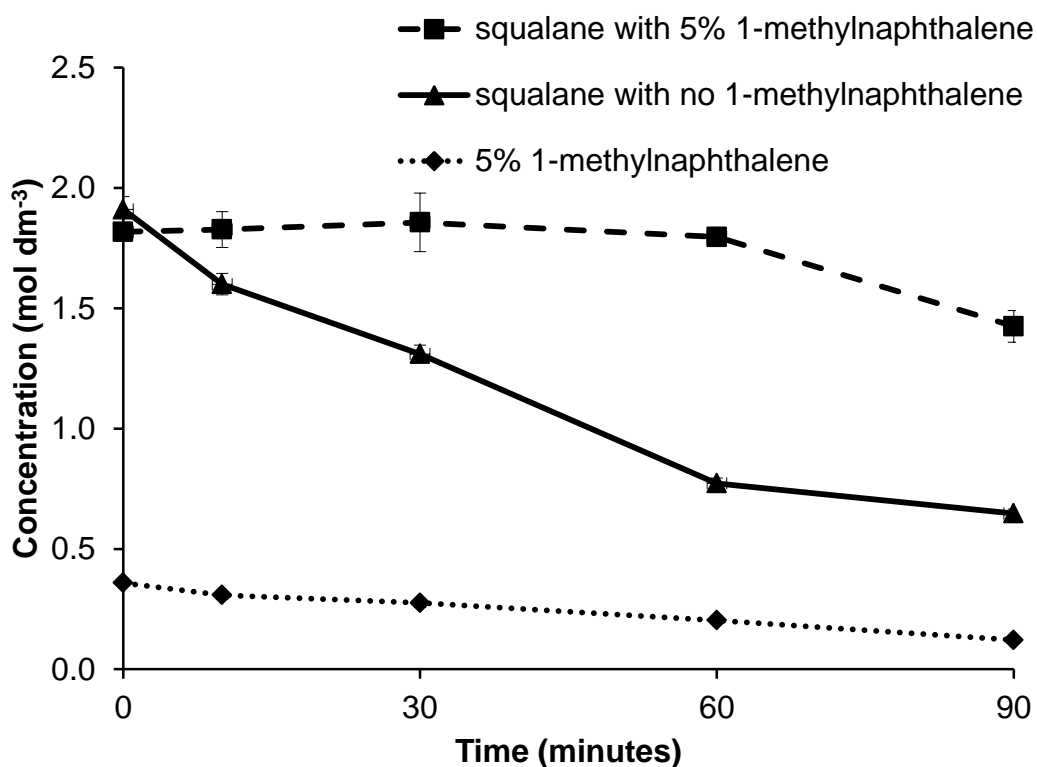


Figure 7.6: Effect of 5% (v/v) 1-methylnaphthalene on the Autoxidation of Squalane at 150 °C and an Oxygen Flow rate of $0.03 \text{ dm}^3 \text{ min}^{-1}$ at a O_2 Pressure of 1 Bar

By reducing the flow rate, the inhibitive period is increased by a factor of 2 (30 minutes). This would suggest that volatility is a significant problem and could be greater than the loss due to reaction.

The inhibitive properties of 1-methylnaphthalene were increased upon reducing the temperature to 130 °C. Squalane in the presence of 1-methylnaphthalene is stable to oxidation for a period of 240 minutes (4 hours) with an oxygen flow rate of $0.1 \text{ dm}^3 \text{ min}^{-1}$, Figure 7.7.

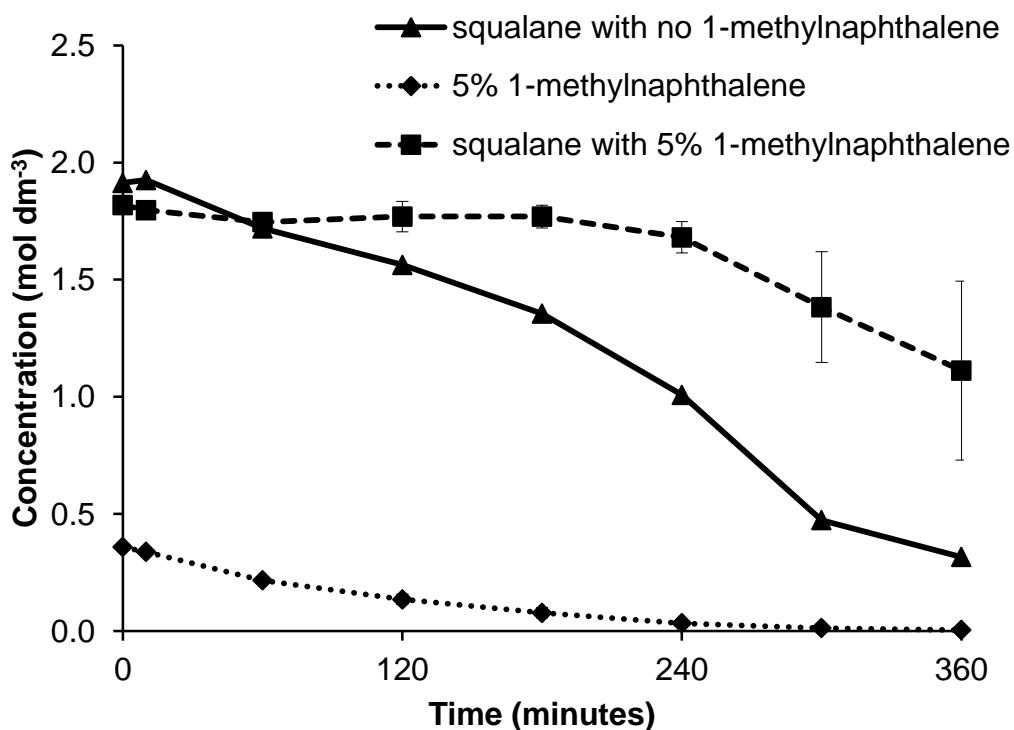


Figure 7.7: Effect of 5% (v/v) 1-methylnaphthalene on the Autoxidation of Squalane at 130 °C and a Oxygen Flow Rate of 0.1 dm³ min⁻¹ at an O₂ Pressure of 1 Bar

Again GC analysis of the two trap solutions provided evidence that volatility is still a significant issue at 130 °C. The reaction was repeated at a reduced flow rate, 0.03 dm³min⁻¹, where the induction period was increased by a factor of 1.5 (120 minutes), Figure 7.8. This shows whilst in a continuous flow reactor 1-methylnaphthalene is lost due to a physical process (volatility) and chemical process (oxidative degradation). Due to this point the observed rate of loss of 1-methylnaphthalene is not due entirely to reaction and hence cannot be used as a representation of its rate of reaction. The reaction rate constants for the oxidation of 1-methylnaphthalene at 150 °C were determined using two methods and presented in the appendix A.

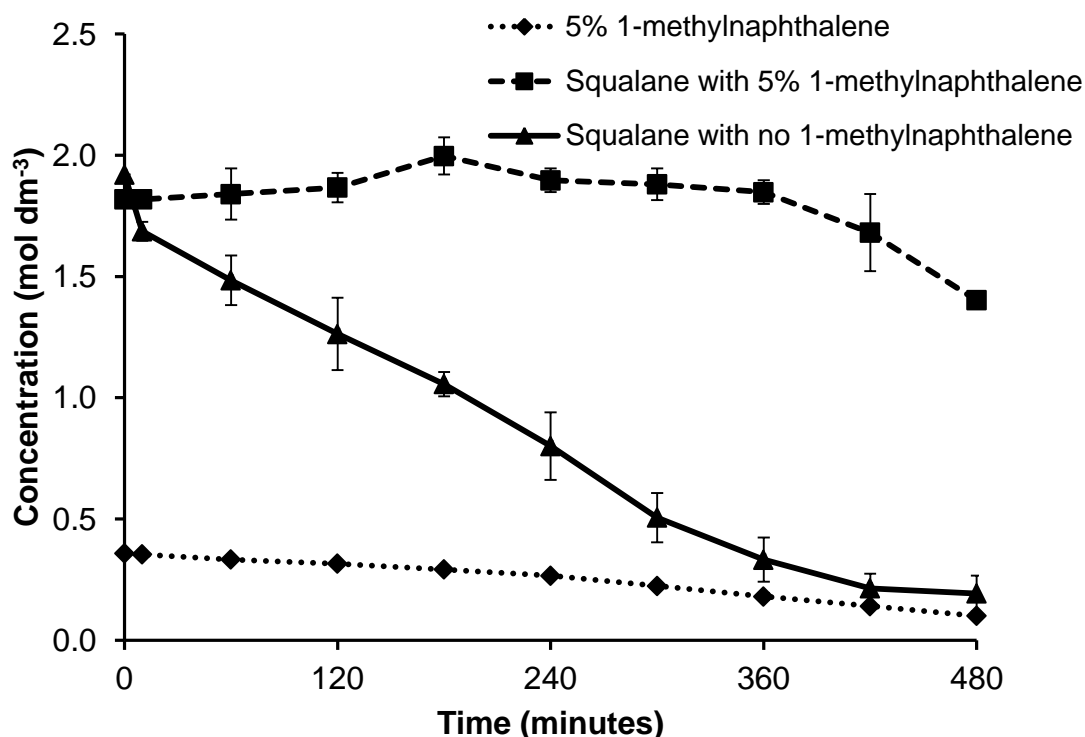


Figure 7.8: Effect of 5% (v/v) 1-methylnaphthalene on the Autoxidation of Squalane at 130 °C and an Oxygen Flow rate of 0.03 dm³ min⁻¹ at an O₂ Pressure of 1 Bar

7.2.2: Product Identification

1-methylnaphthalene can be seen to inhibit the autoxidation of hydrocarbon as earlier established by Ingold. [45] The reaction products were analysed by Gas Chromatography (GC) and Gel Permeation Chromatography, in particular aiming to identify products observed by Ingold. [45]

To aid identification of Ingold products standards were used. In the GC analysis products identified by Ingold were observed at very low concentrations however there were also new peaks identified however their concentrations were too low to identify on Gas Chromatography coupled with Mass Spectrometer. This was due to the volatility issues of 1-methylnaphthalene and the low reactive rate constant, see appendix, and to overcome this the reaction conditions were changed from a flow reaction to a sealed reaction. To eliminate the issue of volatility the reaction vessel was sealed and the rate of oxidation was measured

through changes in pressure. The sample was taken for analysis when oxygen was starting to be consumed. To aid product identification the substrate was 100% (v/v) 1-methylnaphthalene which ensured that no product peaks were masked by the base oil (squalane).

Three new products were identified in the GC-MS which were tentatively described as 1-methylnaphthalene dehydrodimers, Figures 7.9-7.11. It has to be noted that the intermediates observed by Ingold were identified in this work by use of standards in addition to the dehydrodimers.

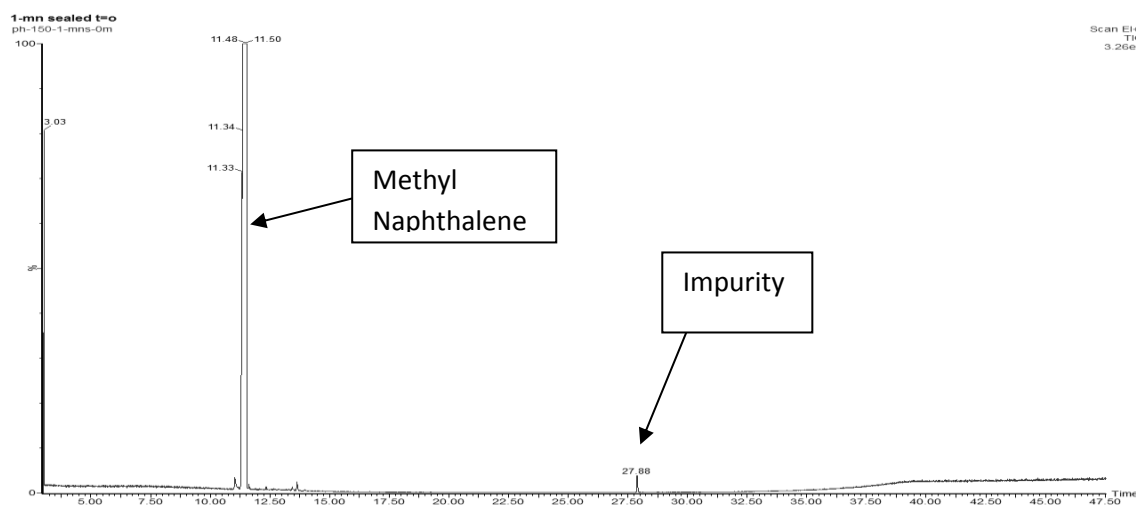


Figure 7.9: GC-MS(EI) Analysis of Starting Material at T=0, Performed on an Agilent DB5-HT Column (30m x 0.32mm)

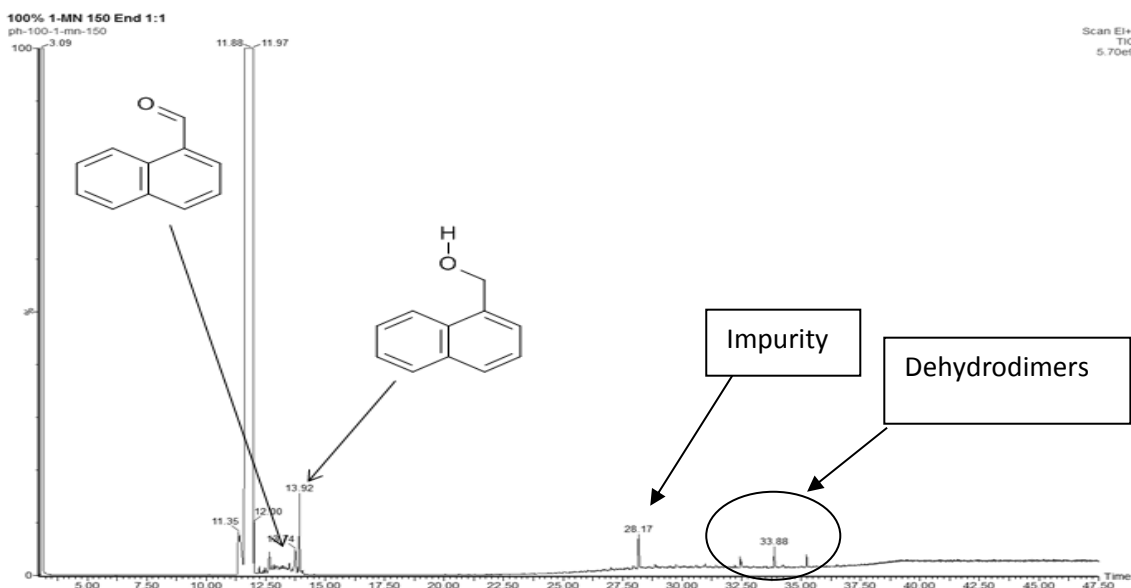


Figure 7.10: GC-MS(EI) Analysis of Oxidised 100% 1-methylnaphthalene at 150 °C and Sealed Reaction, Performed on an Agilent DB5-HT Column (30m x 0.32mm)

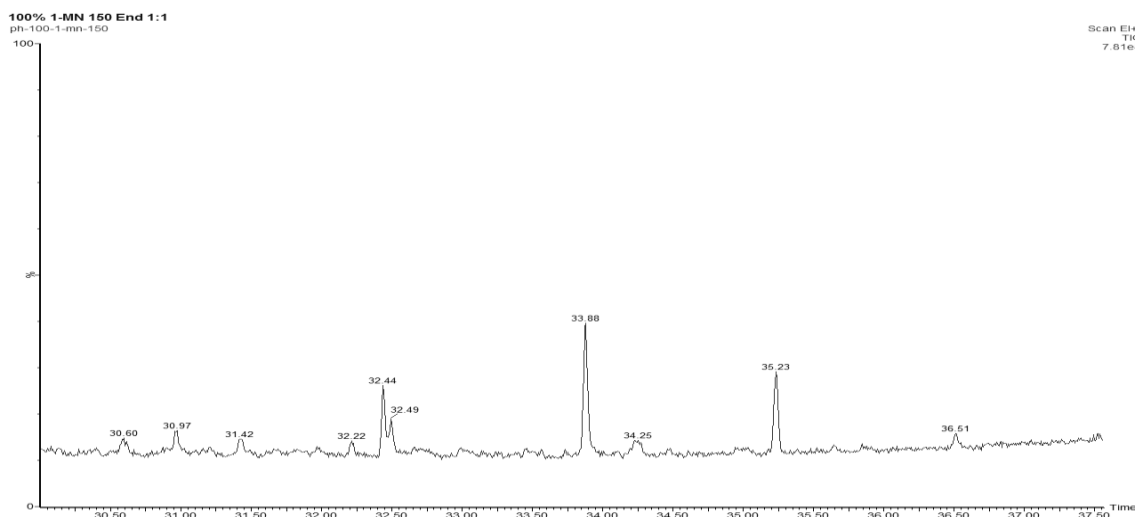


Figure 7.11: GC-MS(EI) Analysis of Oxidised 100% 1-methylnaphthalene after 240 Minutes at 150 °C in a Sealed Reaction at 1 Bar Pressure of O₂, Performed on an Agilent DB5-HT Column (30m x 0.32mm)

EI-MS fragmentation pattern of the product at 32-35 minutes is shown in Figure 7.12. Major ions are observed at m/z 281, 155 and 127. It is suggested here

that dehydrodimer formation would give rise to the peak at m/z 281. This is due to the characteristic M-1 peak which is apparent in the mass spectrometry analysis of 1-methylnaphthalene. The fragment which would give rise to the peak at m/z 155 is suggested to be from ethylnaphthalene, formed from the cleavage of the dehydrodimer at the methyl linkage. Loss of 28 going from m/z 155 – 127 is due to the loss of the ethyl group resulting in a charged naphthalene moiety. The identification of the fragments provides some evidence for dehydrodimer formation.

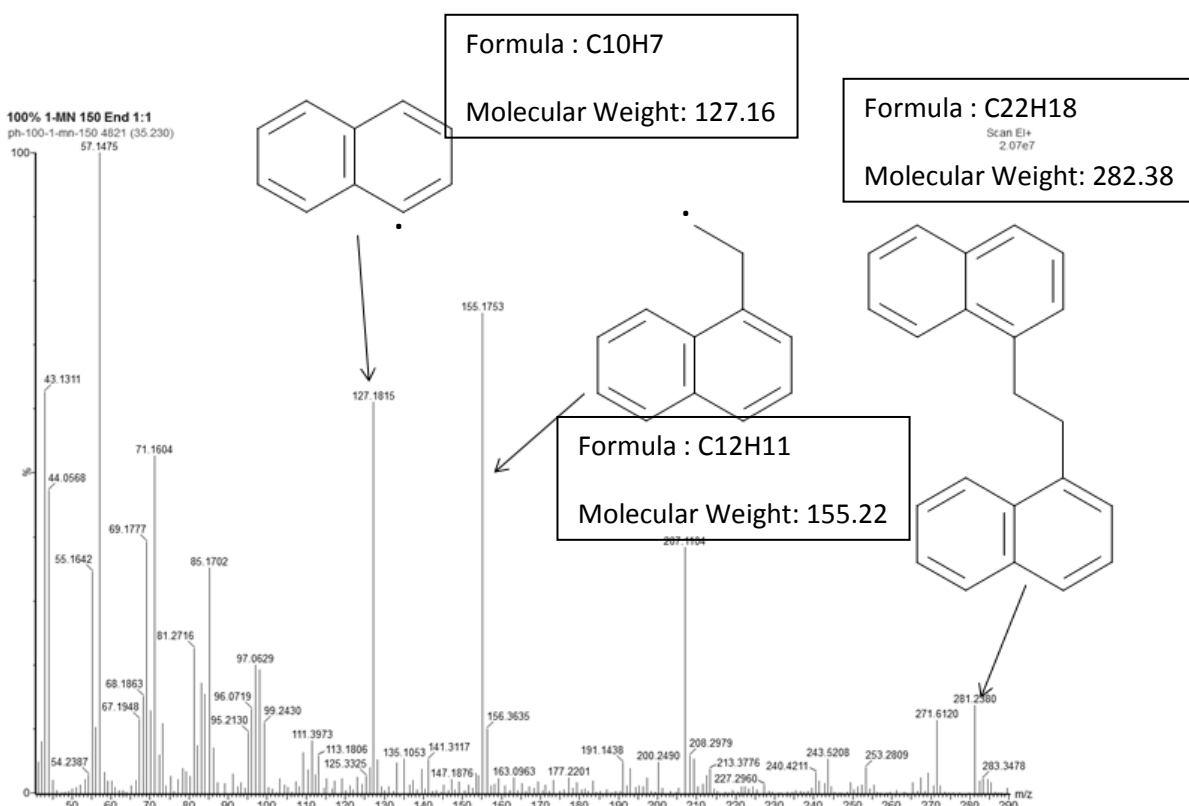


Figure 7.12: GC-MS(EI) Fragmentation Pattern of Peak with Retention Time 35 Minutes Proposed to be a 1-methylnaphthalene Dehydrodimer, Performed on an Agilent DB5-HT Column (30m x 0.32mm)

The possible mechanism for the formation of 1-[2-(1-naphthyl)ethyl]naphthalene is shown in Figures 7.13.

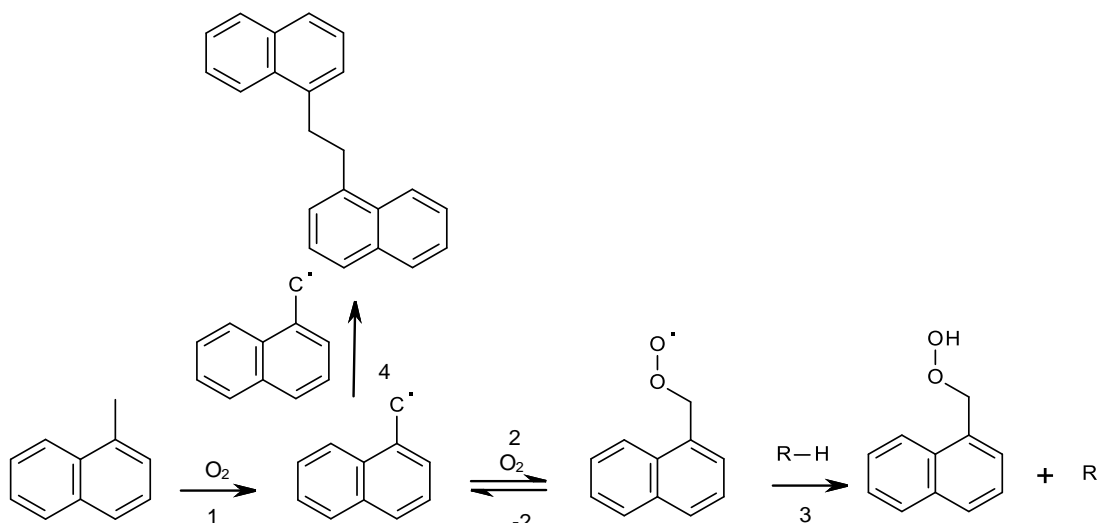


Figure 7.13: Proposed Mechanism for the Formation of 1-[2-(1-naphthyl)ethyl]naphthalene in the Autoxidation of 1-methylnaphthalene

It has to be noted that the 1-methylnaphthyl radical is resonance stabilised so there is likely to be more possible structures than that suggested above. Also the reaction was undertaken in a sealed system so the formation of methylnaphthalene dehydromers could be due to pyrolysis, high temperature heating under an inert atmosphere, rather than due to autoxidation. However these peaks were identified in GC analysis but at far lower concentrations.

The formation of the dehydromers was also examined through Gel Permeation Chromatography (GPC) with UV-VIS diode array detector analysis of the oxidised samples in the presence of squalane using a flow reactor. The starting material, Figure 7.14, has a peak with a retention time of 9.5 minutes and is attributed to 1-methylnaphthalene.

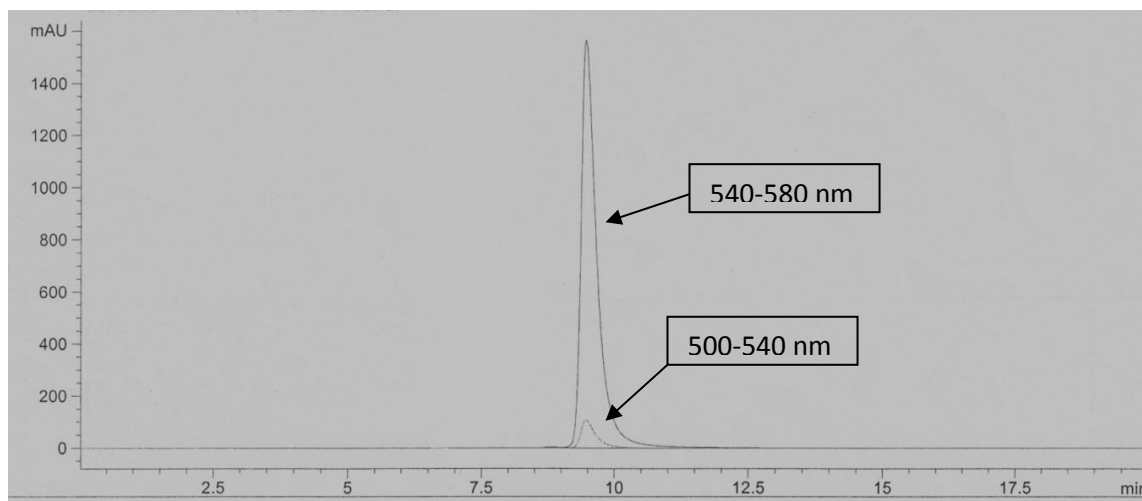


Figure 7.14: GPC Analysis of Squalane with 5% (v/v) 1-methylnaphthalene Prior to Oxidation (t=0)

By the end of the reaction two new product peaks were identified with retention times of 6.5 and 8.5 minutes, Figure 7.15. The product peak at 6.5 minutes was assigned to the products of squalane oxidation by comparison to a squalane only reaction.

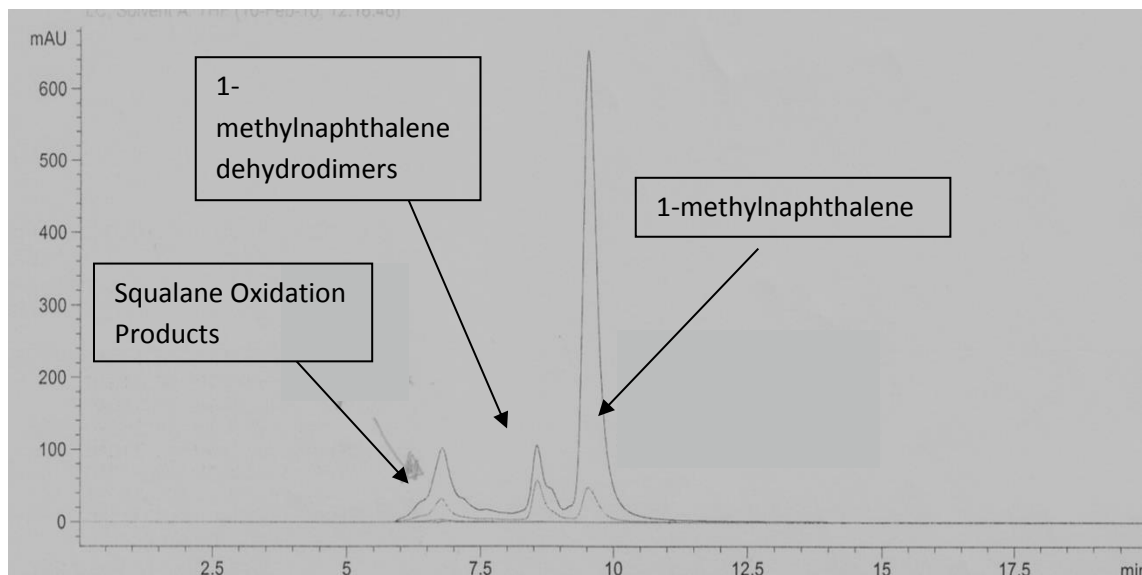


Figure 7.15: GPC Analysis of Squalane with 5% (v/v) 1-methylnaphthalene after 90 Minutes at a Temperature of 150 °C and a Gas Flow Rate of 0.1 dm³ min⁻¹

The product peak at 8.5 minutes is attributed to the oxidation of 1-methylnaphthalene and relates to a mass of 250 ± 5 using appropriate polystyrene standards, Figure 7.16, and was observed in all the oxidised 1-methylnaphthalene samples. It is also apparent that the product peak has a much stronger absorbance in the region between 500-540 nm. This would suggest that the product is delocalised through the link of the dimer.

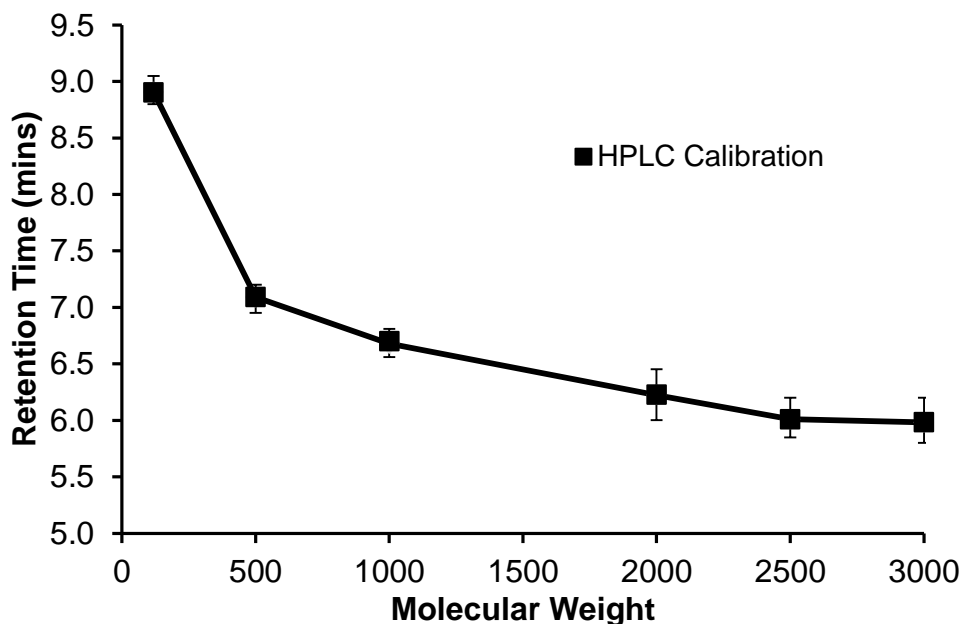


Figure 7.16: GPC Polystyrene Standard Weight Calibration Curve Run on a Phenomenex Phenogel 50Å Column (300 x 4.6mm) with a Tetrahydrofuran Flow Rate of $0.350 \text{ ml min}^{-1}$

This mass is what would be expected if dehydrodimers were being formed during the reaction but not the structure given in Figure 7.13. It has to be noted that in this instance GPC is qualitative and not quantitative as in GC. Therefore the peak area in GPC relates directly to the strength of the chromophore and is not an indication to the quantity in the sample.

7.3: Possible 1-Methylnaphthalene Autoxidation Mechanism

From the proposed mechanism, Figure 7.13, it can be seen why the formation of dehydrodimers would lead to increased stability to oxidation. Take the formation of the dehydrodimer as an example, Figure 7.13 reactions 1, & 5-6. The mechanism for its formation consumes and removes two naphthyl radicals from the autoxidation mechanism. This reduces the rate of oxidative degradation as the radical chain mechanism is disrupted. It has to be noted that this mechanism is only likely to be significant if the experimental temperatures are above the ceiling temperature of reactions 2 and 8 in Figure 7.13. The ceiling temperature is defined as the temperature at which the forwards and backwards reactions are in equilibrium resulting in a reaction rate constant of 1. This would induce R-OO bond dissociation and result in a long lived carbon centred methylnaphthyl radical which can then have the potential to form dehydrodimers. Ab-initio thermocalculations were performed to determine the ceiling temperature for the 1-methylnaphthylperoxy radical.

7.4: Ab-initio Thermocalculations of Ceiling Temperatures

The experimental work reported earlier in this chapter and by Ingold show 1-methylnaphthalene to act as an oxidative inhibitor, effectively inhibiting the autoxidation of squalane, while present in solution, at temperatures of 130-150 °C. Product identification for this work suggests formation of a 1-methylnaphthalene dehydrodimer, Figure 7.13 reaction 2, which has not been noted in previous work, in addition to the typical oxidation products, i.e. naphthaldehyde and 1-naphthalenemethanol. To explain the phenomena of 1-methylnaphthalene dehydrodimer formation at 150 °C the thermochemistry of O₂ addition to the 1-methylnaphthyl radical and other hydrocarbons were calculated.

7.4.1: Ceiling Temperature Determination

The thermodynamic calculations which are presented later in this chapter can be used to determine equilibrium constants for specific reactions. It is proposed in this chapter that the addition of oxygen to an alkyl radical will be reversible. This is based on the assumption that the resultant R-OO bond is relatively weak and at high temperatures could dissociate back into oxygen and the carbon centred alkyl radical.



The equilibrium constant for the addition of oxygen to the alkyl radical can be expressed for example using molar concentrations $[X]$ (as $[X]/[X]^\ominus$, where $[X]^\ominus = 1 \text{ mol dm}^{-3}$) and the equilibrium constant K_c is using subscript "c" for the concentration, Equation 7.1.

$$K_c = \frac{[R - OO]}{[R^*][O_2]}$$

Equation 7.1: Equilibrium Constant for the Addition of Oxygen to a Alkyl Peroxy Radical

The ceiling temperature is defined as the temperature at which the rates of the forward and reverse reactions are equal ($K_{rr} = K_{-rr}$), so the equilibrium constant for the addition of oxygen to an alkyl radical will be unity ($K = k_{rr}/k_{-rr} = 1$), and above which the reverse reaction is favourable.

Ceiling temperatures can be calculated as previously stated for oxidation studies by Benson, Equation 7.5. [155] This equation is derived from the Gibbs free energy law, Equation 7.2.

$$\Delta G = \Delta H^\ominus - T_c \Delta S^\ominus$$

Equation 7.2: Gibbs Free Energy Equation

At equilibrium the gibbs free energy should be zero, Equation 7.3.

$$\Delta G = 0$$

Equation 7.3: Gibbs Free Energy at Equilibrium

Substituting Equation 7.1 into Equation 7.2 gives Equation 7.4.

$$0 = \Delta H^\phi - T_c \Delta S^\phi$$

Equation 7.4: Gibbs Free Energy Equation at Equilibrium

Rearranging Equation 7.4 provides an equation by which the ceiling temperature can be calculated, Equation 7.5.

$$T_c = \frac{\Delta H^\phi}{\Delta S^\phi}$$

Equation 7.5: Calculation to Determine Ceiling Temperature

It can be seen from Equation 7.5, that the enthalpy (ΔH) and entropy (ΔS) of the reaction are required to be known. These values have not been measured for methylnaphthalene, so they were calculated for this work with density functional theory (DFT) using Gaussian 09w. DFT is a computational quantum mechanical modelling method to investigate the electronic structure of many body systems. It works by finding the lowest energy state and calculating the thermochemical values from that structure. Gaussian 09w is a computer program used for computational chemistry and which one of its functions is to calculate DFT.

7.4.2: Gaussian Method Development

Prediction of the thermochemical values in this work was obtained using Gaussian Software 09w. [95] The level of theory was determined based on the BDE calculations which provided the lowest mean absolute deviation (MAD) between calculations and experimental values for a group of molecules similar to methylnaphthyl peroxide.

7.4.3: Testing the Model for the Level of Theory

To determine the most appropriate computational method to study the thermochemical properties of 1-methylnaphthalene pre-testing of two DFT

methods, B3LYP [156] and B3PW91[157, 158], were performed using a number of basis sets. This was achieved by calculating the R-OO and R-H bond dissociation energies of an alkane (ethane), alkene (propene), and a substituted aromatic (toluene), Equations 7.6 & 7.7, which were compared to experimental values to provide a mean absolute deviation (M.A.D.), Table 7.1 and 7.2.

$$BDE(R-OO\cdot) = \Delta H_f(R-OO) - (\Delta H_f(R) + \Delta H_f(O_2))$$

Equation 7.6: Calculation to Determine R-OO Bond Dissociation Energy

$$BDE(R-H) = (\Delta H_f(R) + (\Delta H_f(H)) - \Delta H_f(R-H))$$

Equation 7.7: Calculation to Determine R-H Bond Dissociation Energy

Table 7.1: R-OO Bond Dissociation Energies of C₂H₅-OO, C₃H₅-OO and (C₆H₅)CH₂OO Calculated using Different Methods and Basis Sets Based on Published Experimental Values. [159] Values in Brackets Display the Deviance From the Mean

Method and basis set	Bond Dissociation Energy (kJ mol ⁻¹)			M.A.D.
	C ₂ H ₅ -OO	C ₃ H ₅ -OO	(C ₆ H ₅)CH ₂ -OO	
DFT B3PW91 6311G (d)	122.3 (26.1)	50.1 (25.9)	66.4 (23.5)	25.2
DFT B3PW91 6311G ++(d)	123.6 (24.8)	50.8 (25.2)	69.0 (20.9)	23.6
DFT B3PW91 6311G (3df)	123.4 (25.0)	51.4 (24.6)	67.0 (22.9)	24.2
DFT B3PW91 6311G ++(3df)	124.2 (24.2)	51.6 (24.4)	68.4 (21.5)	23.4
DFT B3LYP 6311G ++(3df)	125.8 (22.6)	122.1 (46.1)	68.3 (21.6)	30.1
Experimental	148.4 ± 7.9	76 ± 9.1	89.6 ± 4.4	

Table 7.2: R-H Bond Dissociation Energies of C₂H₅-H, C₃H₅-H and (C₆H₅)CH₂-H Calculated using Different Methods and Basis Sets Based on Published Experimental Values. [85, 159-161] Values in Brackets Display the Deviance From the Mean

Method and basis set	Bond Dissociation Energy (kJ mol ⁻¹)			M.A.D.
	C ₂ H ₅ -H	C ₃ H ₅ -H	(C ₆ H ₅)CH ₂ -H	
DFT B3PW91 6311G (d)	405.9 (4.1)	345.3 (26.7)	357.9 (2.9)	11.2
DFT B3PW91 6311G ++(d)	403.8 (6.2)	344.3 (27.7)	356.9 (1.9)	11.9

DFT B3PW91 6311G (3df)	403.7 (6.3)	343.2 (28.8)	355.5 (0.5)	11.9
DFT B3PW91 6311G ++(3df)	402.0 (8.0)	342.6 (29.4)	354.7 (0.3)	11.6
DFT B3LYP 6311G ++(3df)	406.3 (3.7)	412.2 (40.2)	353.6 (2.4)	15.4
Experimental	410 ± 4	372 ± 12	355 ± 3	

Based on the results from Table 7.2 the chosen method for calculating the R-OO BDE was the DFT B3PW91 6-311G ++(3df) where the mean absolute deviation was calculated approximately as 23.4 kJ mol⁻¹ with a range of 2.9 kJ mol⁻¹.

7.4.4: Thermochemical Calculations of Selected 1-methylnaphthalene Adducts

The calculated ΔH and ΔS values for the C-H bond and the C-OO bond on the methyl moiety of 1-methylnaphthalene are shown in Table 7.3.

Table 7.3: Thermochemical Data for 1-methylnaphthalene Calculated Using Gaussian 09w Running the DFT B3PW91 6-311G ++(3df) Method and Basis Set

Bond	ΔH (kJ mol ⁻¹)	ΔS (kJ mol ⁻¹ k ⁻¹)
(C ₁₀ H ₇)CH ₂ -H	-350.49 ±5.51	-0.116
(C ₁₀ H ₇)CH ₂ -OO	-56.19 ±23.40	-0.147

It can be seen that the R-H bond, -350.49 kJ mol⁻¹, is significantly stronger than that for the corresponding R-OO, -56.19 kJ mol⁻¹. The entropy changes for both bonds are negative which suggest that this reaction is spontaneous at standard temperature and pressure.

It is apparent that the B3PW91 method underestimates the R-OO bond dissociation energy by 23 – 25 kJ mol⁻¹, Table 7.2. As a consequence a compensation factor was introduced and for the DFT B3PW91 6-311G ++(3df) method it equated to 23.4 kJ mol⁻¹ with the deviation equalling 2.9 kJ mol⁻¹, Equation 7.8.

$$BDE(R - OO) = \text{Calculated } (R - OO)BDE + 23.4 \text{ kJ mol}^{-1}$$

Equation 7.8: Compensation Factor for BDE (R-OO) Determination using Gaussian 09w

7.4.5: Ceiling Temperature Calculation

R-OO bond formation on the Methyl Moiety

The values in Table 7.3 can be employed to determine the ceiling temperature of Figure 7.17, employing Equation 7.5.

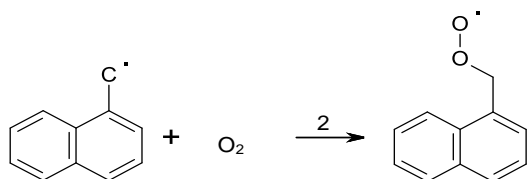


Figure 7.17: Formation of the methylnaphthylperoxyl Radical

Table 7.4: Estimated Ceiling Temperature for Reaction $R + O_2 \longrightarrow R-OO$ Employing the DFT B3PW91 6-311G ++(3df) Method

Molecule	ΔH^θ Experimental (kJ Mol ⁻¹)	ΔS^θ (kJ Mol ⁻¹ K ⁻¹)	$T_c(K)$	$T_c(^{\circ}C)$	Graph Labels
(C ₁₀ H ₇)CH ₂ -OO•	-79.6 ± 2.3**	-0.147	542 ± 12	269 ± 12.	Square
(C ₆ H ₅)CH ₂ -OO•	-89.6 ± 4.38	-0.139	645 ± 26	371 ± 25	Triangle
C ₂ H ₅ -OO•	-148.4 ± 7.86	-0.161	922 ± 42	649 ± 42	Diamond
C ₃ H ₅ -OO•	-76.0 ± 9.12	-0.145	524 ± 48	251 ± 48	Cross

* Calculated using the DFT B3PW91 6-311G ++(3df) method including the compensation factor

** Corrected to include the compensation factor employed in the enthalpy calculations

The ceiling temperatures calculated in Table 7.4 are presented graphically in Figure 7.18. Here it can be seen that there is a clear trend ($R^2 = 0.9885$) and from the gradient it can be seen to cross the intercept at a very low temperature (122.77 K).

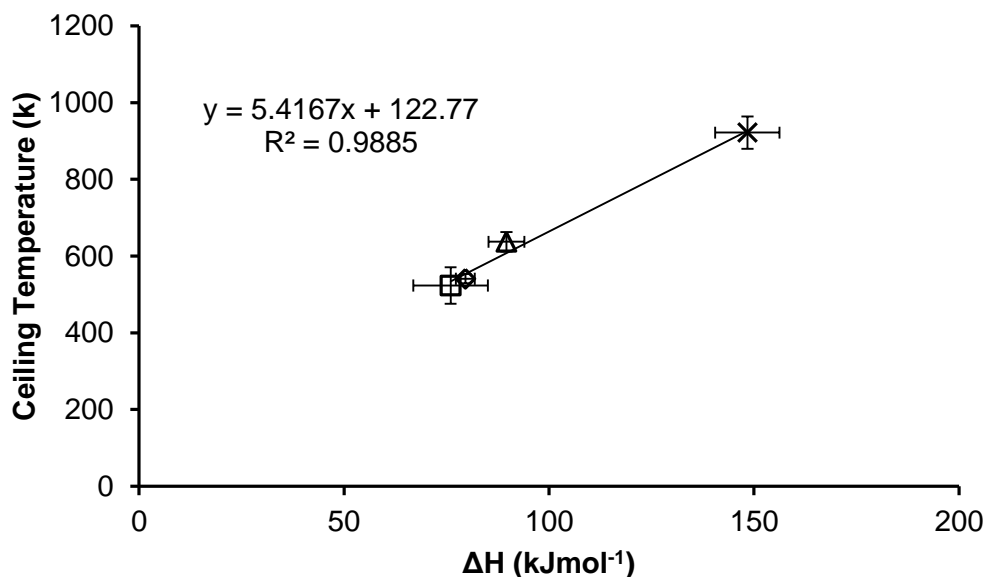


Figure 7.18: Ceiling Temperatures of 1-methylnaphthalene (Square), Toluene (Triangle), Allyl (Diamond) and Ethane (Cross) Calculated using the DFT B3PW91 6-311G ++ (3df) Method

The estimated ceiling temperature for R-OO bond formation on the methyl moiety of 1-methylnaphthalene was calculated as 269 ± 12 °C, Table 7.4. This therefore suggests that the reaction is not reversible in the temperature range employed in this study, 130-150 °C, and does not support the proposed reaction mechanism where the antioxidant potential of 1-methylnaphthalene is provided through the formation of dehydrodimers and is initially proposed through analytical data.

R-OO Bond Formation on the Para Position

The methyl centred methylnaphthyl radical, Figure 7.13 reaction 1, can take the form of two resonance structures (there are others), Figure 7.19 reaction 5. This resonance structure places the radical onto the para position of the naphthalene moiety. The ceiling temperature for the addition of oxygen to the para position on the naphthalene moiety, Figure 7.19 reaction 8, was also calculated. This should give an indication of the effect that resonance stability has on the ceiling

temperature. Thermochemical calculations were undertaken to determine the ΔH and ΔS for this resonance structure, the computed values are shown in Table 7.5.

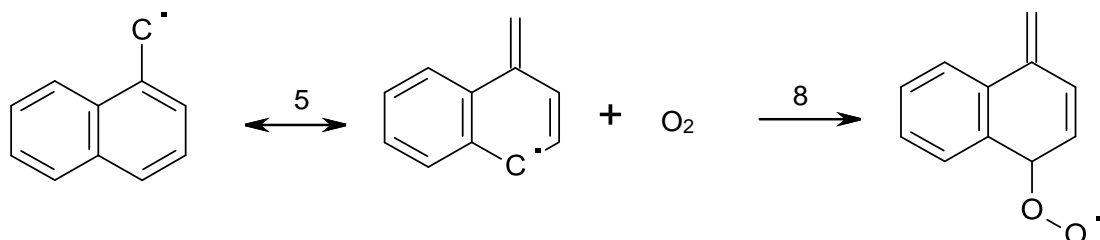


Figure 7.19: Oxygen Addition to the Para Resonance Structure of 1-methylnaphthalene

Table 7.5: Thermochemical Data for the Para Resonance 1-methylnaphthyl Structure Calculated using Gaussian 09w Running the DFT B3PW91 6-311G ++(3df) Method and Basis Set

Bond	ΔH (kJ mol ⁻¹)	ΔS (kJ mol ⁻¹ k ⁻¹)
p-C ₁₁ H ₉ -O ₂	-26.4 ± 2.3	-0.143

The ceiling temperature for the addition of oxygen to the para position of the naphthalene moiety is shown in Table 7.6.

Table 7.6: Estimated Ceiling Temperature for Reaction R + O₂ → R-OO Employing the DFT B3PW91 6-311G ++(3df) Method

Molecule	ΔH^θ Experimental (kJ Mol ⁻¹)	ΔS^θ (kJ Mol ⁻¹ K ⁻¹)	T _c (K)	T _c (°C)
(C ₅ H ₄)CH- OOC ₃ H ₂ CH ₂ **	-49.4 ± 2.3	-0.143	345 ± 12	72 ± 12

* Calculated using the DFT B3PW91 6-311G ++(3df) method including the compensation factor

** Corrected to include the compensation factor employed in the enthalpy calculations

The estimated ceiling temperature for the addition of oxygen to the para radical was calculated to be 345 ± 12 K or 72 ± 12 °C, which is significantly lower than the experimental conditions employed in this study and suggests that oxygen addition to the para position of the naphthalene moiety is unlikely to occur. This low estimated ceiling temperature is not unexpected. It can be seen that aromaticity is lost upon formation of the R-OO bond in the para position. The loss of aromaticity is not favoured and in conjunction with the relatively weak bond formed (In comparison to the R-H bond) results in the low ceiling temperature. It would suggest that this resonance structure is stable to oxidation and can be termed oxidatively inert. This supports the idea of 1-methylnaphthalene dehydrodimer formation.

From the estimated ceiling temperatures it is suggested that the aromatic ring determines the rate of oxidation due to the formation of the oxidatively stable resonance structure.

Comparison to Established Work

Previous studies by Ingold on the autoxidation of methylnaphthalene suggest radical addition to the para position of the aromatic ring is the most likely cause for the antioxidant properties. [45, 46] The theory proposed was that this is due to the promotion of the self and cross coupling termination reactions, which remove peroxides from the bulk oil and reduce the rate of oxidation.

The work undertaken in this study differs slightly to that by Ingold. It is not the conclusion by which this work differs from Ingolds as they are both in agreement that the naphthalene ring provides the oxidative stability to 1-methylnaphthalene. The proposed mechanism is where the two pieces of work differ.

The thermochemical calculations undertaken in this study suggest an alternative mechanism to that proposed earlier by Ingold. It can be seen that the addition of oxygen to the para position of the naphthalene moiety has an estimated ceiling temperature of 72 ± 12 °C, Table 7.6. As a consequence bond formation on the para position is highly unlikely at the temperatures employed in this study and that undertaken by Ingold. The para radical is most likely to either undergo resonance stabilisation to form the methyl radical or combine with another naphthyl radical to form a dehydrodimer of 1-methylnaphthalene. Experimental analysis has provided evidence for the formation of the dehydrodimer as well as the expected methyl oxidation products 1-naphthalenemethanol and 1-naphthaldehyde. In this work it could be said that the para radical is in essence oxidatively inert and it is this which provides the antioxidancy. By oxidatively inert it is meant that the radical is in a position by which further oxidation is unlikely to occur.

These two bodies of work are in agreement that it is the aromatic ring which has the greatest contribution to 1-methylnaphthalenes high level of oxidative stability. It is also in agreement that the methyl moiety has little effect on the oxidative stability of 1-methylnaphthalene.

7.4.6: 1-Ethynaphthalene as a Model for Polyalkylated Naphthalene Base Oils

In this chapter 1-methylnaphthalene has been employed as a model fuel component but it can also be a model for alkylnaphthalene base oils. This is of interest as these base oils are known to be more stable to oxidation compared to their branched hydrocarbon and polyalphaolefin alternatives. [162] Thermocalculations were undertaken to determine the peroxy bond formation ceiling temperature for 1-ethynaphthalene, Figure 7.20. This was chosen to investigate the effect of increased alkyl chain length on the ceiling temperature.

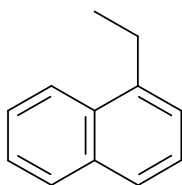


Figure 7.20: 1-ethylnaphthalene

Thermochemical calculations were undertaken to determine the ΔH and ΔS for a secondary hydrogen on the ethyl moiety, the computed values are shown in Table 7.7.

Table 7.7: Thermochemical data for 1-ethylnaphthalene Calculated using Gaussian 09w Running the DFT B3PW91 6-311G ++(3df) Method and Basis Set

Bond	ΔH (kJ mol ⁻¹)	ΔS (kJ mol ⁻¹ k ⁻¹)
(C ₁₀ H ₇)C(HCH ₃)-H	-348 ±6	-0.133
(C ₁₀ H ₇)C(HCH ₃)-OO (Figure 7.21, 10)	-73 ±23	-0.168

The ceiling temperature for the addition of oxygen to the two resonance structures of the secondary ethylnaphthyl radical, Figure 7.25, are shown in Table 7.8.

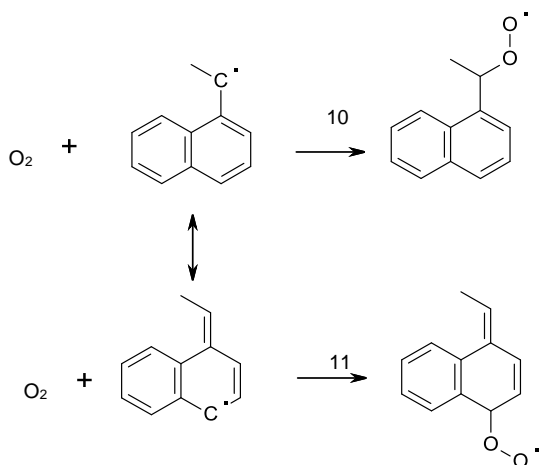


Figure 7.25: R-OO Bond Formation on the Two Resonance Structures of 1-ethylnaphthalene

Table 7.8: Estimated Ceiling Temperature for Reaction $R + O_2 \longrightarrow R-OO$ Employing the DFT B3PW91 6-311G ++(3df) Method

Reaction	ΔH^θ Calculated (kJ Mol ⁻¹)	ΔS^θ (kJ Mol ⁻¹ K ⁻¹)	T _c (K)	T _c (°C)
10	-96 ± 2*	-0.168	434 ± 11	300 ± 11
11	-41 ± 2*	-0.195	210 ± 12	-63 ± 12

* Calculated using the DFT B3PW91 6-311G ++(3df) method including the compensation factor

It can also be seen that with the carbon centred radical on the para position of the aromatic ring makes the radical in essence inert to oxidation at this position.

7.5: Conclusions

The effect of conventional fuel dilution has been studied in squalane using a bench top continuous flow reactor operating in the temperature range of 130-150 °C. It can be seen that the chosen fuel component, 1-methylnaphthalene, inhibited the oxidation of squalane.

Addition of 5% (v/v) 1-methylnaphthalene to squalane resulted in a lubricant which had no significant alteration in the break point at 150 °C and a gas flow rate of 0.1 dm³ min⁻¹. The oxidative stability was increased by a factor of 2 (30 minutes) upon reducing the gas flow rate to 0.03 dm³ min⁻¹. This was attributed to the reduction in the rate of volatile loss of 1-methylnaphthalene. It was concluded that the rate of reaction of 1-methylnaphthalene is so low that the period of inhibition is determined by the rate of volatile loss.

Product identification highlighted the possibility of dehydrodimer formation and thermochemical calculations were undertaken to determine the ceiling

temperature on the two resonance structures. Both the estimated ceiling temperatures were sufficiently low enough for R-OO bond dissociation to occur. However the para resonance structure had a significantly lower ceiling temperature (72 ± 12 °C) and it is therefore assumed that the aromatic ring controls the rate of methylnaphthalene oxidation and this is in agreement with Ingold. [151, 163]

8: Summary and Conclusions

Chapter Overview

This chapter will highlight the key conclusions from this thesis, and also suggest key future work, focussing on the effect of reverse micelles on automotive lubricant degradation.

8.1: Conclusions

The main conclusion from this thesis is that reverse micelles have been identified and can be shown to inhibit the autoxidation of hydrocarbons as has been highlighted in chapters 3-5. The mode to the action is through the transfer of alkyl peroxide into a reverse micelle core away from the bulk oil phase. When in the core alkyl peroxides undergo decomposition in the presence of already oxidised products resulting in less reactive radicals being produced as outlined in chapter 6. This mechanism is in contrast to that proposed by Bakunin who suggests that the alkyl peroxides will undergo heterolytic decomposition in the micelle core. This is invalid for branched hydrocarbons.

The significance of this result is that formulations are getting tighter with increasing pressure to reduce ZDDP content. From the results presented in this thesis it can be seen significant increases in the oxidative stability of the lubricant can be obtained without altering the formulation by ethanol treatment. There is also the possibility of increasing the effectiveness of aminic antioxidants by incorporating higher levels of surfactant. Therefore it is concluded that heterogeneity of lubricant formulations plays a significant role in its effectiveness. By taking into consideration the migration of alkyl peroxides into reverse micelle cores significant increases in lubricant stability can be made.

8.2: Recommendations for Future Work

There are many potential avenues for future research in the area of reverse micelles and the subsequent effect on oxidation. These include altering the type of dispersant and changing the bulk additive package. Key avenues which could be followed are outlined below.

8.2.1: Effect of Surfactant on Reverse Micelle Formation

This work was limited to studying only one surfactant and its effect on reverse micelle formation. In reality industry employ many types of surfactants which could display different effects on lubricant degradation.

It is therefore suggested to further this field that there is a requirement to increase the range of surfactants studied. By screening more surfactants more information on the properties which control the oxidative inhibition properties can be gained. As shown earlier there is a body of work in lipid oxidation which in practise could be applied to this field. This would provide significant shortcuts and allow this new technology to be fully implemented in automotive lubricants.

8.2.2: Effect of Altering the Bulk Additive Package

It is suggested in this work that the autoxidation of automotive lubricants is a heterogeneous mechanism, which takes into account both the surfactant and the bulk additive package. The previous section proposed future work which could be carried out by altering the surfactant. However significant improvements can be made by optimization of the bulk additive package.

It is suggested in this work that the rate determining step of the reverse micelle oxidation mechanism is the rate of alkyl peroxide formation. If this is reduced then the micelle will longer to reach the saturation point. This is easily achieved by altering the antioxidant used in the lubricant system. In this study the number of bulk additives employed was relatively low with only three types of

antioxidant being employed. While this approach provided the support for this theory it would be beneficial to increase the number and types of additives employed as it can be seen that the ability of antioxidants to inhibit oxidation is greatly affected in a reverse micelle system. This was unfortunately beyond the scope of this project but would provide more information on the bulk additive reverse micelle interactions.

8.2.3: More Robust Imaging Methods

In this work the identification of reverse micelles was achieved through standard UV-VIS (for ethanol treated samples) and confocal microscopy (for ethanol diluted samples). Dynamic light scattering (DLS) is a technique which provides information on the size and distribution of small particles suspended in a solution. DLS employs a monochromatic laser source that will scatter upon bombardment of small particles. From the level and degree of scattering the size of the particles can be determined and the distribution is applied by assuming that Brownian motion is obeyed. It is suggested that any future work should investigate the size and distribution by a light scattering method.

Appendix

A.1: Volatile Loss and Lifetime of 1-Methylnaphthalene

To determine the volatile species being lost from the reactor, GC analyses were undertaken on the gas trap solution. It became apparent when comparing the cold trap solution of the reaction with 5% (v/v) 1-methylnaphthalene with the reaction with no 1-methylnaphthalene addition, that 1-methylnaphthalene was a major component. This provided some questions as to whether the observed loss of 1-methylnaphthalene from the reactor was due to a chemical reaction or just due to volatility. Two methods were employed to characterize the volatile loss; the first method calculated the volatile loss through calculating the vapour pressure. The second method investigated the rate of loss of 1-methylnaphthalene from the reactor under an inert atmosphere, nitrogen.

A.1.1: Determination of Volatile Loss by Calculation

The volatile loss was calculated by use of equations A1.1, A1.2 and A1.3 and assuming pseudo first order kinetics, with the enthalpy of vaporisation (ΔH_{vap}) of 1-methylnaphthalene being 45.5 kJmol^{-1} .

$$k_v = \frac{p_{vap}}{RT} \cdot \frac{1}{\text{Molar Density}} \cdot \frac{F}{V}$$

k_v	Pseudo first order rate constant for volatile loss
p_{vap}	Vapour pressure of 100% liquid
R	Gas constant
T	Temperature
<i>Molar Density</i>	Molar density of liquid
F	Gas flow rate
V	Volume of liquid in reactor

Equation A1.1: Equation for k_v , rate constant for the volatile loss

$$p = p^* e^{-x} \quad x = \frac{\Delta_{vap}H}{R} \left(\frac{1}{T} - \frac{1}{T^*} \right)$$

P	Known vapour pressure
p^*	Unknown vapour pressure
$\Delta_{vap}H$	Enthalpy of vaporization
R	Gas constant
T	Temperature of known vapour pressure
T^*	Temperature of unknown vapour pressure

Equation A1.2: Clausius Clapeyron equation for calculating vapour pressure dependence on temperature

$$[Conc]_t = [Conc]_0 e^{-k_v t}$$

$[Conc]_t$	Concentration at time t
$[Conc]_0$	Initial concentration
k_v	Rate constant for the volatile loss
t	Time

Equation A1.3: Calculation of concentration of 1-methylnaphthalene due to volatility loss assuming pseudo first order kinetics

From comparing the expected volatile loss against the observed loss (determined by experiment) it can be seen that the observed loss appears greater than the calculated volatile loss, Figures A1.1 (at 150 °C) and A1.2 (at 130 °C).

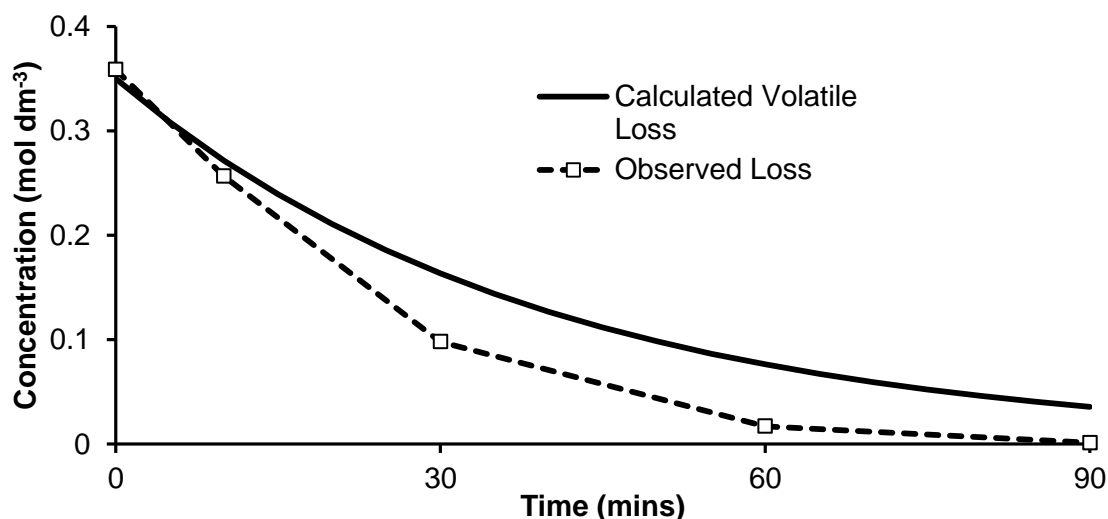


Figure A1.1: Calculated volatile loss of 1-methylnaphthalene compared to observed experimental loss of 1-methylnaphthalene at 150 °C with an O₂ flow rate of 0.1 dm³ min⁻¹ at a O₂ pressure of 1 bar

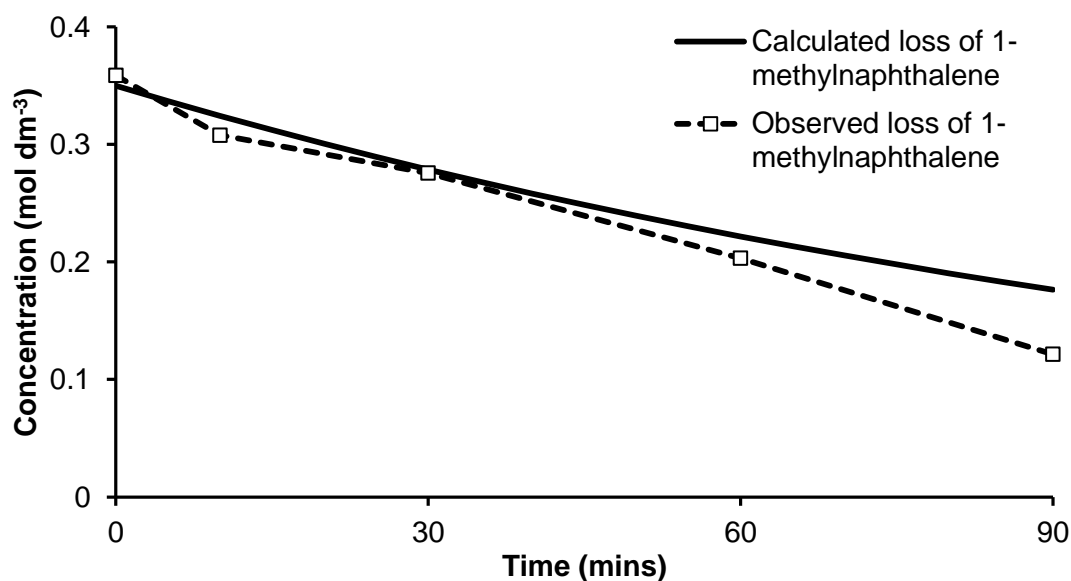


Figure A1.2: Calculated volatile loss of 1-methylnaphthalene compared to observed experimental loss of 1-methylnaphthalene at 130 °C with an O₂ flow rate of 0.1 dm³ min⁻¹ at a O₂ pressure of 1 bar

To quantify calculated loss due to volatility Figures A1.3 and A1.4 were produced, which display pseudo first order plots for both the observed loss and the expected volatile loss at the two temperatures under investigation.

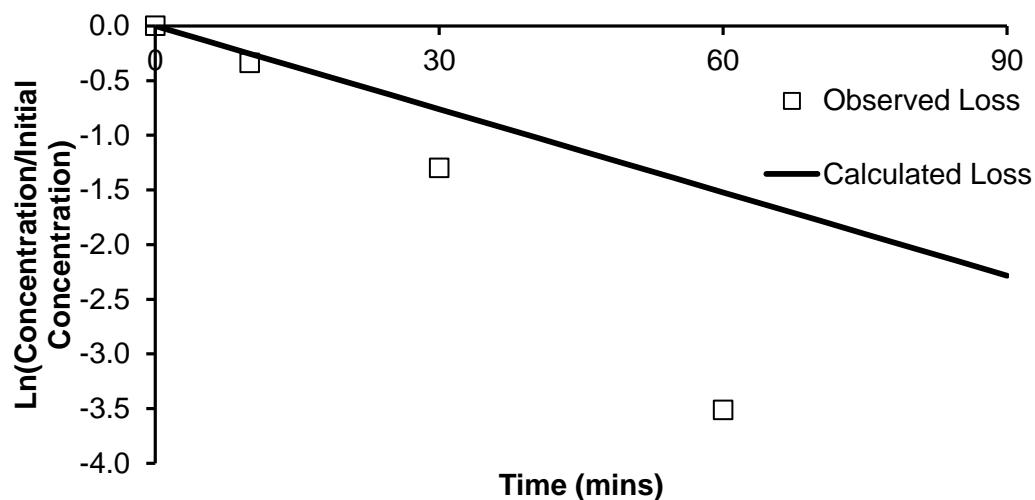


Figure A1.3: First order plot of the observed loss of 1-methylnaphthalene with the volatile loss at 150 °C, 0.1 dm³min⁻¹ and 1 bar absolute

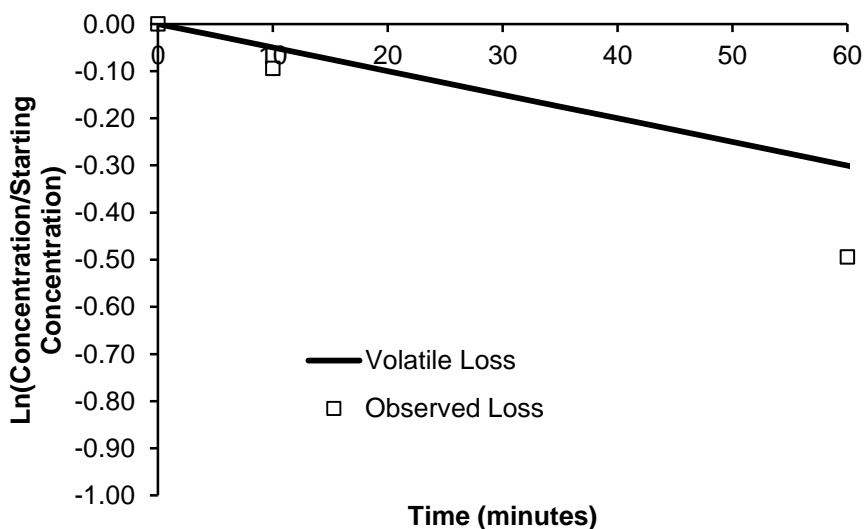


Figure A1.4: First order plot of the observed loss of 1-methylnaphthalene with the volatile loss at 130 °C, 0.1 dm³min⁻¹ and 1 bar absolute

By determining the rate constant for the observed loss, k_{obs} , and the calculated volatile loss, k_v , the rate at which 1-methylnaphthalene is reacting, k_r , can be derived, using equation A1.3.

$$k_r = k_{Obs} - k_v$$

k_r	Rate of reaction
k_{Obs}	Rate of observed loss
k_v	Rate of volatile loss

Equation A1.3: Calculation of K_r

From the gradients of Figures A1.3 and A1.4 k_{Obs} and k_v can be calculated and are shown in Table A1.1 along with the data from the tests undertaken at 130 and 150 °C.

Table A1.1: Calculation of rate of reaction k_r

Temperature (°C)	Gas Flow Rate (dm ³ min ⁻¹)	k_{Obs} (secs ⁻¹) x10 ⁻⁴	k_v (secs ⁻¹) x10 ⁻⁴	k_r (secs ⁻¹) x10 ⁻⁴	Half Life for reaction (Hours)
150	0.1	4.2±0.6	2.1	2.1±0.6	1.0
150	0.03	1.6±0.3	0.7	0.9±0.3	2.1
130	0.1	1.1±0.2	0.8	0.3±0.2	7.7
130	0.03	0.7±0.05	0.3	0.4±0.03	4.8

The calculations in Table 7.1 suggest that the rate of volatile loss of 1-methylnaphthalene is far greater than the reactive loss. It is also apparent that at temperatures below 150 °C the rate of reactive loss is so low that it becomes insignificant and therefore the inhibition properties of 1-methylnaphthalene are

due entirely to volatility. Therefore it can be concluded that the antioxidant potential of 1-methylnaphthalene is highly dependent on the rate of volatile loss. To ensure the calculated techniques are accurate they were compared to an experimental technique.

A.1.2: 1-Methylnaphthalene Volatility under an Inert Atmosphere at 150 °C

The test undertaken to investigate the reaction of squalane with 5% 1-methylnaphthalene, at 150 °C with a gas flow rate of $0.1 \text{ dm}^3\text{min}^{-1}$, was repeated but under a nitrogen atmosphere, as shown in Figure A1.5. From this method the loss of 1-methylnaphthalene from the reactor should only be due to volatility and therefore be the true rate of volatile loss. The value of k_v , from this inert gas method, can then be compared with the k_v 's derived from the previous method and the k_{obs} from the oxidation reactions. This allows the rate constant for the reaction at 150 °C to be found and to test the reliability of the calculated method.

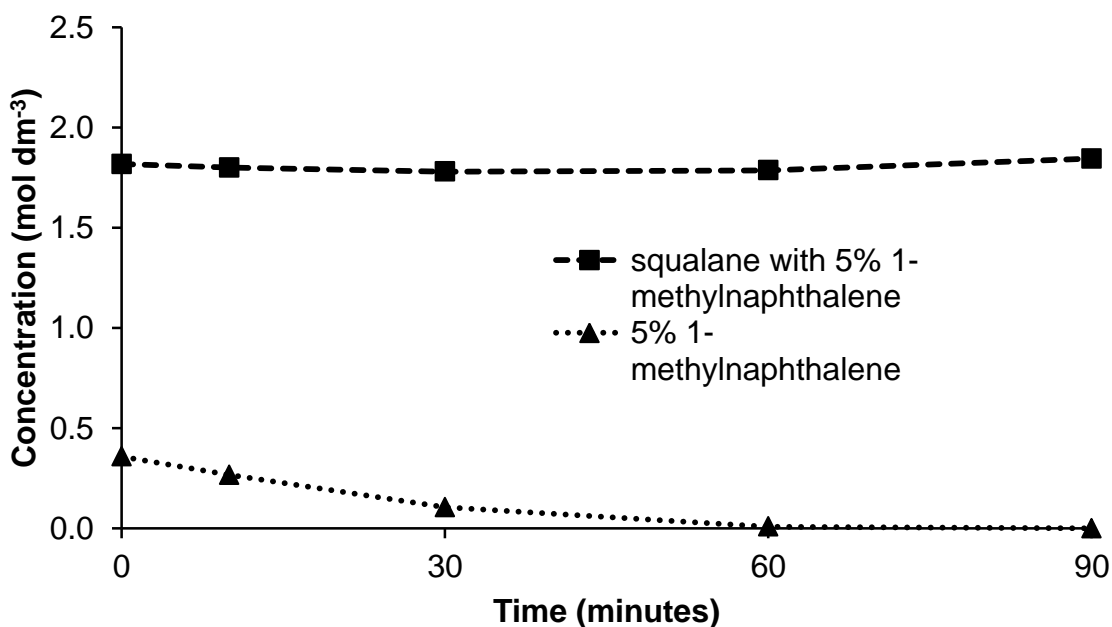


Figure A1.5: Effect on squalane concentration of 5% 1-methylnaphthalene dilution at 150 °C with $0.1 \text{ dm}^3\text{min}^{-1}$ N_2 flow rate at 1 bar absolute

From Figure A1.5 it is apparent that in a nitrogen atmosphere 1-methylnaphthalene is being lost from the reactor, by comparison there is virtually no loss of squalane and this loss of can only be due to volatility. If the k_{obs} for 1-methylnaphthalene is the same for the reaction under nitrogen and oxygen, then it could be assumed that there is no chemical loss being observed at 150 °C and at a gas flow rate of 0.1 dm³min⁻¹.

It can be seen from Figure A1.6 that by plotting the difference between the rate of loss of 1-methylnaphthalene under oxygen and nitrogen, the rate constant can be calculated from the gradient. By this method the pseudo first order reaction rate constant of 1-methylnaphthalene at 150 °C was found to be $(0.5 \pm 0.3) \times 10^{-4}$ seconds⁻¹.

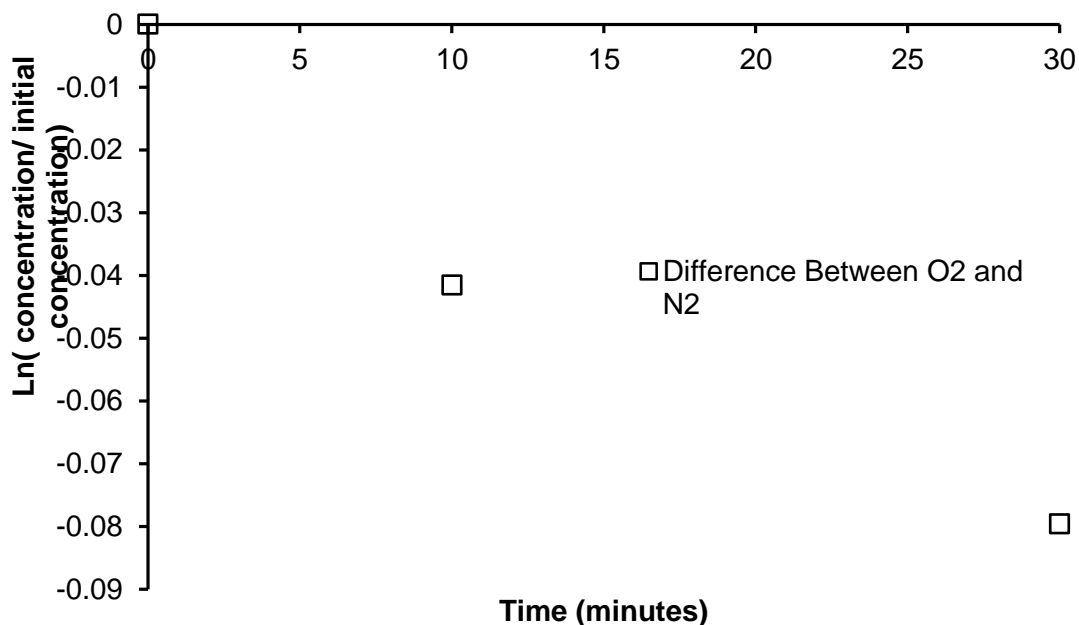


Figure A1.6: Difference in the rate of loss of 1-methylnaphthalene under an nitrogen atmosphere with the loss observed under an oxygen atmosphere at 150 °C, 0.1 dm³min⁻¹ and 1 bar absolute

Due to the positive value of k_r obtained it can be assumed that a reaction is occurring, even though at a very reduced rate, the next logical step is to

compare the k_r derived by this method with the previous method employed for determining the volatile loss of 1-methylnaphthalene, Table A1.2.

Table A1.2: Comparison of the two methods employed to calculate the rate constant for the volatile loss of 1-methylnaphthalene at 150 °C and a gas flow rate of 0.1 dm³ min⁻¹

Method	k_{obs} (secs⁻¹) x10⁻⁴	k_v (secs⁻¹) x10⁻⁴	k_r (secs⁻¹) x10⁻⁴	Reaction Half Life (Hours)
Calculated volatility	4.2±0.6	2.1	2.1±0.6	1.0
Effect of inert Gas	4.2±0.6	3.7 ±0.6	0.5±0.6	3.9

It can be seen from Table A1.2 that the two methods employed to determine and quantify the volatile loss are in reasonable agreement, providing similar k_r values of (0.5 – 2.1)x10⁻⁴ seconds⁻¹. Even though there are variations between the methods it is still evident that a reaction is occurring as discussed in chapter 7.

This analysis was also undertaken at a lower flow rate 0.03 dm³ min⁻¹. From Figure A1.7, the k_r value for the reaction at 0.03 dm³ min⁻¹ can be calculated employing the method outlined earlier at the higher flow rate, through calculating the gradient.

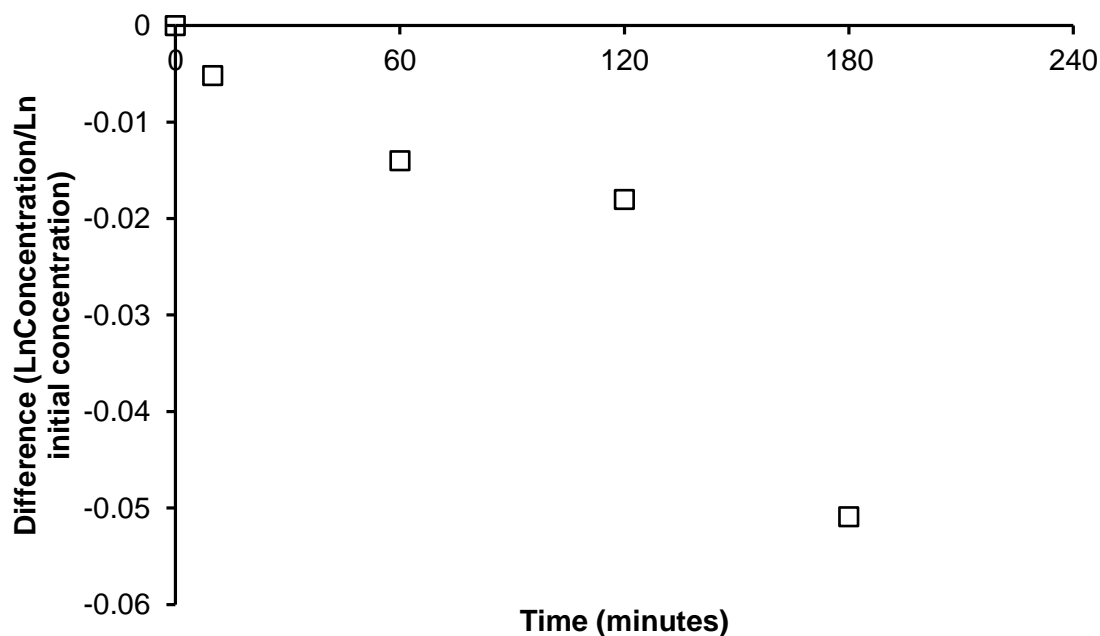


Figure A1.7: Plot of the difference in the rate of loss of 1-methylnaphthalene under an nitrogen atmosphere with the loss observed under an oxygen atmosphere at 150 °C, 0.03 dm³ min⁻¹ and 1 bar absolute

From Figure A1.7, it can be confirmed that a reaction is occurring with a rate constant of $(0.3 \pm 0.01) \times 10^{-4}$ seconds⁻¹, and this is in suitable agreement with the calculated method, Table A1.3.

Table A1.3: Comparison of the two methods employed to calculate the rate constant for the volatile loss of 1-methylnaphthalene at 150 °C and a gas flow rate of 0.1 dm³ min⁻¹

Method	k_{obs} (secs ⁻¹) $\times 10^{-4}$	k_v (secs ⁻¹) $\times 10^{-4}$	k_r (secs ⁻¹) $\times 10^{-4}$	Reaction Half Life (Hours)
Calculated volatility	1.6±0.3	1.3	0.3±0.3	6.4
Effect of inert Gas	1.6±0.3	1.3	0.3±0.3	6.4

As expected, by lowering the flow rate of the gas through the reactor the volatile loss is reduced while the reactive loss is unaffected. By comparing the two methods, Tables A1.2 & A1.3, of calculating the rate constant for the reaction, it can be seen that they are in agreement that a reaction is occurring. The duration was dependent on the rate of volatile loss. Therefore it can be concluded that at 150 °C the pseudo first order rate constant for the reaction of methylnaphthalene in squalane is $(0.3-2.1) \times 10^{-4} \text{ seconds}^{-1}$, and therefore at this temperature with this apparatus it is dominated by volatile loss of 1-methylnaphthalene.

While 1-methylnaphthalene is in the reactor it can be seen that it is effective in inhibiting the oxidation of squalane, this can be seen in figures 7.5-7.7. The reaction rate constant and the reactive half life suggests that if no volatile loss was occurring 5% (v/v) 1-methylnaphthalene would be an effective inhibitor with a calculated half life of approximately 6.4 hours at 150 °C. It can be seen from the k_{obs} of the reaction at 150 °C and an oxygen flow rate of $0.1 \text{ dm}^3\text{min}^{-1}$ that the observed half life will be 0.36 hours. As the rate constant for the volatile loss is significantly higher than the reactive rate constant it can be said that the duration of the inhibiting effect is due to the rate of volatile loss of 1-methylnaphthalene from the reactor resulting in the lower observed half life.

A2: Effect of 2nd Generation Bio-fuel on Automotive Lubricant Degradation

Chapter Overview

This chapter utilises methodologies developed earlier in the thesis to evaluate the compatibility of three 2nd generation bio-fuels (2,5-dimethylfuran, bio-butanol and ethyl pentanoate) with current automotive lubricants. The two issues of concern are the fuels residence time in the sump, after its dilution into the lubricant, and the solubility of the fuel in the model base lubricant. The aim of this chapter is to determine whether current lubricant technologies are suitable for use with these new fuels.

A2.1: Introduction

The current state of the art manufacturing processes for 1st generation bio-fuels, ethanol and methyl esters, are unsustainable due to competition against food supplies and the consequent relatively low scalability of production. There are also problems regarding compatibility with current engine and lubricant technologies. This has required automotive engine manufacturers to redesign their engines for use with bio-ethanol,[163] which has had consequences for the rate of introduction of ethanol into the mainstream gasoline fuel market. In order to overcome these problems it is predicted that 2nd generation processes need to be developed to allow bio-fuels to become a viable alternative to traditional gasoline.[58]

At present 1st generation bio-ethanol is manufactured from the fermentation of maize (e.g. USA) and/or sugar cane (e.g. Brazil) with the biomass source highly dependent on the country of origin.[58, 61] 2nd generation processes differ in that they utilize parts of the crop which are not used for food to produce the fuel. An example of this process is the lignocellulosic bio process that employs the stalk of the food crop to produce the fuel and hence does not compete with the

food process. Lignocellulosic techniques for the manufacture of bio-ethanol and 2,5-dimethylfuran have been reported in the literature. [61, 164] The current level of technology does not produce sufficient volumes of fuel to replace current 1st generation bio-fuels. However, OPEC predicts that 2nd generation bio-fuels could account for over 50% of the bio-fuels market by 2022. As a result, this area has seen a significant surge in popularity from the major oil producing companies. The particular point of interest investigated here is the compatibility of 2nd generation bio-fuels with automotive lubricants and engine components.

In this chapter the compatibility of three 2nd generation bio-fuels and model automotive lubricants will be assessed. The three bio-fuels chosen are 2,5-dimethylfuran, figure A2.1, butanol, figure A2.2, and ethyl pentanoate (ethyl valerate), figure A2.3. Solubility of the fuel in the lubricant and its loss due to volatility are the two key parameters studied. The aim is to use techniques outlined earlier in this thesis to study the compatibility of suggested 2nd generation bio-fuels and propose successful candidates.

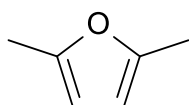


Figure A2.1: 2,5-dimethylfuran

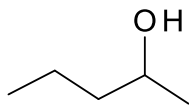


Figure A2.2: butanol

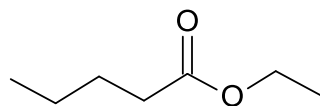


Figure A2.3: ethyl valerate

A2.2: Results

A2.2.1: Calculated Loss of 2nd Generation Bio-Fuels Due to Volatility at 150 °C

For this study the volatile loss of the fuel at low piston ring pack temperatures was calculated by the use of equation A1.2 for the conditions shown in Table A2.1. This allows the fuels residence time in the lubricant to be determined. The residence time is defined in this chapter as the period of time that the fuel is present in the lubricant and can affect the chemical degradation of the lubricant.

Table A2.1: Model reaction details used to calculate the rate of volatile loss of the model fuel component

Temperature	150 °C
Pressure	1 Bar
Gas Flow Rate	0.03 dm ³ min ⁻¹
Sump Fuel Dilution	5%(v/v)

By modelling low piston ring pack conditions (flow rate of 0.03 dm³ min⁻¹ at 150 °C) the calculated volatile loss of 2,5-dimethylfuran was found to be significantly faster than for 1-methylnaphthalene. This resulted in an extremely short residence time of 15 minutes, as shown in Figure A2.4. Due to this high rate of volatile loss it is assumed that 2,5-dimethylfuran will have only a low concentration in the engine sump lubricant.

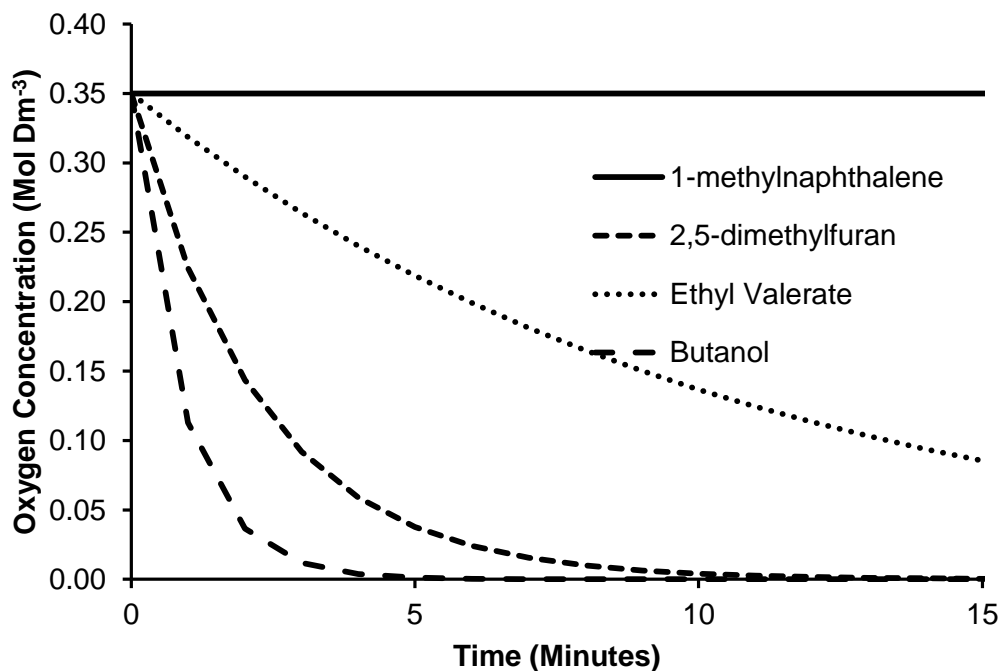


Figure A2.4: The calculated volatile loss of 2,5-dimethylfuran, ethyl valerate, butanol and 1-methylnaphthalene at 150 °C and a gas flow rate of 0.03 dm³ min⁻¹

In comparison, using the same calculations and conditions ethyl valerate has a relatively longer residence time at low piston ring pack conditions, as presented in Figure A2.4, however the rate of volatile loss is still significant. After 15 minutes the concentration of ethyl valerate present in the lubricant reduced to 14% of the starting concentration. It has to be appreciated that the temperature employed in this model represents the low end of the temperature range of the piston ring pack and as such it is highly unlikely that ethyl valerate will have an effect on the lubricant in the piston ring pack region of the engine assembly. This is based on the assumption that the modelled conditions are relatively mild in comparison to normal operating conditions where temperatures and gas flow rates are significantly higher. As a consequence the volatile loss of ethyl valerate should increase dramatically under normal operating conditions resulting in a negligible lubricant residence time.

The calculated residence time for butanol under low piston ring pack conditions was 10 minutes. This therefore suggests that volatility is still a significant issue, as shown in Figure A2.4. It is assumed due to the low temperature employed in this model that butanol like ethyl valerate will have little or no impact on the chemical degradation of the lubricant in the piston ring pack area of the engine assembly due to the relatively mild model conditions employed in this study.

A2.2.2: Calculated Loss of 2nd Generation Bio-Fuels due to Volatility at 100 °C

Figure A2.4 has shown that the three bio-fuels investigated possess extremely short lubricant residence times when low piston ring pack temperatures are modelled. It is possible that at lower temperatures, i.e. sump lubricant, the bio-fuels could exert some influence on the chemical degradation processes. At these temperatures the fuels could have the potential to affect the oxidative stability of the lubricant, either by affecting the radical chain mechanism or through altering the distribution of the additive package. The analysis is extended in this section where the residence times of the fuels under investigation are determined at a model high sump temperature. The data used is that presented in Table A2.2 and the results determined by the use of equation A1.1.

Table A2.2: Model reaction details used to calculate the rate of volatile loss of the model fuel component

Temperature	100 °C
Pressure	1 Bar
Gas Flow Rate	0.03 dm ³ min ⁻¹
Sump Fuel Dilution	5%(v/v)

Under model high sump temperature conditions (flow rate of 0.03 dm³ min⁻¹ at 100 °C) the calculated lifetime of 2,5-dimethylfuran in the sump lubricant is 15 minutes, figure A2.5, with the rate of volatile loss slightly reduced resulting in a

small concentration present after 15 minutes. It is assumed that 2,5-dimethylfuran will not have the potential to affect the lubricants degradation at this high sump temperature due to the rate of loss due to volatility still being far greater than the potential reactive loss.

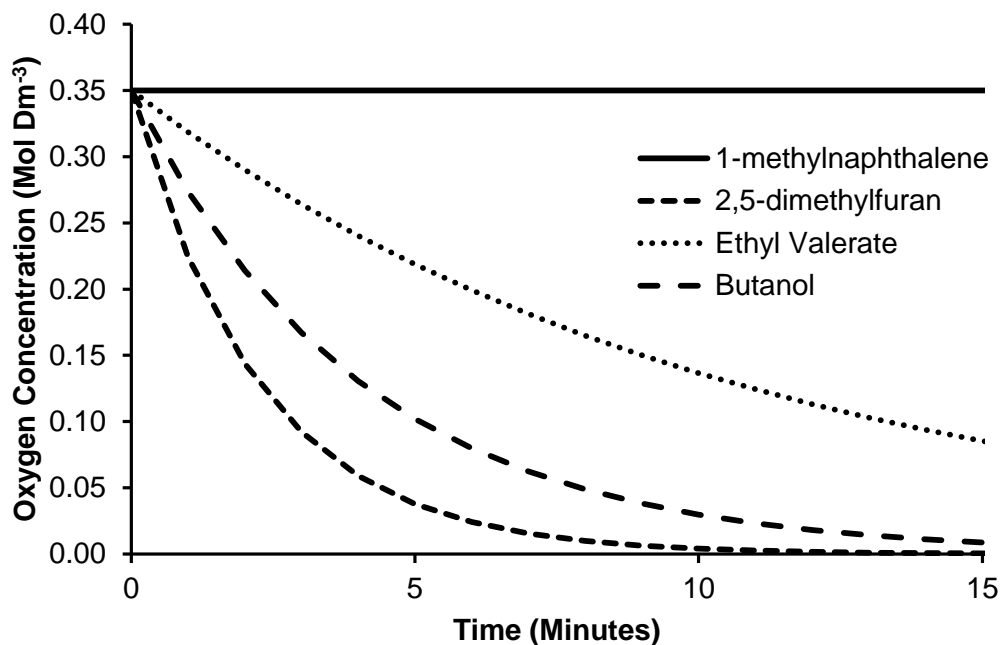


Figure A2.5: The calculated volatile loss of 2,5-dimethylfuran, ethyl valerate, butanol and 1-methylnaphthalene at 100 °C and a gas flow rate of 0.03 dm³ min⁻¹

An increased sump residence time is also calculated for ethyl valerate, as shown in Figure A2.5. This is greater than the corresponding time for 2,5-dimethylfuran. After 15 minutes the concentration of ethyl valerate present in the lubricant has dropped to 70% of the initial concentration. This would suggest that ethyl valerate dilution could have the potential to affect the degradation of the automotive lubricant in the sump at lower temperatures. However as the rate of lubricant degradation due to oxidation reduces as the temperature decreases the effect is assumed to be negligible.

A residence time of 15 minutes was calculated using same equation A1.1 for butanol at high sump temperatures, figure A2.5. This relates to an increase of 5 minutes as a consequence of reducing the temperature by 50 °C. It is still highly unlikely that butanol is present in the lubricant for a sufficient period to significantly affect the chemical degradation mechanism of the lubricant.

A2.3: Discussion

Table A2.3: Calculated pseudo first order rate constant for the volatile loss of the fuel component at a flow rate of 0.03 dm³min⁻¹

	k_v @ 150 °C (min ⁻¹)	k_v @ 100 °C (min ⁻¹)
2,5-dimethylfuran	0.445	0.149
ethyl valerate	0.094	0.026
butanol	1.131	0.246
1-methylnaphthalene	2.7×10^{-6}	5.7×10^{-7}
ethanol	0.421	0.110

The calculated rate constants for the volatile loss of the three bio-fuels are significant, table A2.3. In comparison to earlier calculated data for 1-methylnaphthalene it can be seen that all the 2nd generation fuels studied are significantly more volatile, table A2.3. It was earlier determined that the volatile loss of 1-methylnaphthalene is the rate determining factor for its ability to act as an antioxidant. Therefore it can be assumed that the three bio-fuels should have little or no effect on the automotive lubricant, due to their increased volatility.

This is confirmed by plotting the calculated volatile losses for the three bio-fuels against 1-methylnaphthalene, figures A2.4 and A2.5. It is the case for all three bio-fuels that the rate of loss due to volatility is too significant and likely too great to affect the chemical degradation processes.

As a consequence of the calculated results subsequent bench top reactions were not undertaken on the 2nd generation bio-fuels to assess their effect on the autoxidation of squalane. This was based on the assumption that the volatile loss was too great and that at the temperatures where oxidation is thought to be

prevalent the fuel will be in the gas phase. As a result the fuels are assumed not to have an effect on the liquid chemical degradation of the lubricant.

The situation can alter if the engine is run frequently in the cold and does not reach operating temperature.[19] As a consequence, the concentration of fuel in the sump lubricant could increase to significant levels and be present for a period of time if the vehicle was out of use for an extended period. [50, 98] The 2nd generation bio-fuels are unlikely to affect the rate of lubricant degradation due to oxidation as the reactions occur at far greater temperatures where the fuel will be present in the gas phase. However it could still have an effect as in the case with ethanol in altering the additive package and affecting certain oxidative properties of the lubricant once the fuel has been removed from the lubricant.

It can be seen in previous chapters (chapters 4-6) that the ability of the fuel to alter the distribution of the additive package is highly dependent on the polarity of the fuel. If the fuel is sufficiently polar it can form an unstable emulsion upon dilution into the lubricant system and as a consequence alter the distribution of the additive package. For the three bio-fuels considered in this chapter the fuel/lubricant immiscibility was tested with the most polar model lubricant (95% (w/w) squalane, 0.25% (w/w) phenolic antioxidant, 1% (w/w) dispersant and 1% (w/w) detergent) used in chapters 3-6 was diluted with 5% (v/v) 2nd generation bio-fuel. The sample was then subjected to the same mixing regime as employed in chapter 4.

Scattering was present in the 2,5-dimethylfuran diluted sample, figure A2.12 however this is assumed to have a negligible effect on the automotive lubricant. This is based on the assumption that employing the same mixing regime, ethanol dilution caused the lubricant to form an unstable emulsion, water in oil suspension. It was only after the subsequent ethanol treatment process, i.e. ethanol treatment, that a single well defined scatter pattern was observed in the lubricant. The scatter pattern in the 2,5-dimethylfuran diluted sample is more representative to that of an ethanol treated sample.



Figure A2.12: Laser scattering of butanol treated squalane sample containing 0.25% (w/w) Phenolic Antioxidant, 1% (w/w) Dispersant and 1% (w/w) Detergent



Figure A2.13: Laser scattering of ethyl valerate treated squalane sample containing 0.25% (w/w) Phenolic Antioxidant, 1% (w/w) Dispersant and 1% (w/w) Detergent



Figure A2.14: Laser scattering of 2,5-dimethylfuran treated squalane sample containing 0.25% (w/w) Phenolic Antioxidant, 1% (w/w) Dispersant and 1% (w/w) Detergent

A2.4: Conclusions

It can be seen that 2nd generation bio-fuels have little effect on the chemical degradation of the lubricant. This conclusion was reached through calculating the volatile loss of the fuels employing optimised conditions. It was found that the residence time in the lubricant was significantly shorter than that observed for 1-methylnaphthalene. The bio-fuels were also completely soluble in the most polar squalane sample containing 1% (w/w) dispersant, 1% (w/w) detergent and 0.25% (w/w) phenolic antioxidant and it is therefore assumed not to alter the lubricants additive package. It is therefore concluded that in this bench top evaluation, 2nd generation bio-fuels are likely to have little or no effect on the lubricants oxidative stability.

Abbreviations

1-MN	1-methylnaphthalene
AmAO	Aminic Antioxidant
AO	Antioxidant
AOT	Sodium 1,4-bis(2-ethylhexoxy)-1,4-dioxobutane-2-sulfonate
ATR	Attenuated Total Reflection
BDE	Bond Dissociation Energy
BHT	Butylated Hydroxy Toluene
B3LYP	Becke, Three-parameter, Lee-Yang-Parr
B3PW91	Becke, Three-parameter, Perdew and Wang's 1991
B3P86	Becke, Three-parameter, Perdew 86
BPV86	Becke, Three-parameter, Vosco 86
Brij 76	2-octadecoxyethanol
CO	Carbon Monoxide
CO ₂	Carbon Dioxide
DAD	Diode Array Detector
Det	Detergent
DFT	Density Functional Theory
Disp	Dispersant
Dm ⁻³	Litres
DTC	Sodium N,N-diethylcarbamodithioate
ECN	Effective Carbon Number
EI	Electron Impact
EtOH	Ethanol
FID	Flame Ionisation Detector
GC	Gas Chromatography
GC-FID	Gas Chromatography with Flame Ionisation Detector
GC-MS	Gas Chromatography-Mass Spectroscopy
GPC	Gel Permeation Chromatography
ΔH	Enthalpy
KV	Kinematic Viscosity
MW	Mass Weight
mins	Minutes
Mol	Moles
PhAO	Phenolic Antioxidant
RH	Alkyl
R·	Alkyl radical
ROO·	Peroxy Radical
ROOH	Alkyl Peroxide
ΔS	Entropy
Squ	Squalane
THF	Tetrahydrofuran
T _c	Ceiling Temperature
Trolox	6-hydroxy-2,5,7,8-tetramethyl-chromane-2-carboxylic acid
UV-VIS	Ultraviolet-Visible Spectroscopy
(v/v)	Weight by Volume

(w/w) Weight by Mass
ZDDP Zinc Dialkyl-Dithio-Phosphate

References

1. European Commission, Roadmap to a Single European Transport Area - Towards a competitive and resource efficient transport system, **2011**: p. 171.
2. Jensen, R.K., S. Korcek, L.R. Mahoney, and M. Zinbo, *J Am Chem Soc*, **1981**. 103(7): p. 1742-1749.
3. European Union, *Regulation (EC) No 715/2007 of The European Parliament and of the Council of 20 June 2007*. 2007, Journal of the European Union. p. 16.
4. Korcek, S., J. Sorab, M.D. Johnson, and R.K. Jensen, *Ind Lub Trib*, **2000**. 52(5): p. 209-220.
5. Taylor, R.I. and R.C. Coy, *Proc Inst Mech Eng Part J-J Eng Trib*, **2000**. 214(J1): p. 1-15.
6. Colyer, C.C.a.G., W.C., *Detergents and Dispersants*. 2 ed. Chemistry and Technology of Lubricants, ed. R.M.a.O. Mortier, S.T. 1997, London: Blackie Academic and Professional.
7. Taylor, R.I. and P.G. Evans, *J Eng Trib*, **2004**. 218(J): p. 185-200.
8. Taylor, R.I., R. Mainwaring, and R.M. Mortier, *Proc Inst Mech Eng Part J-J Eng Trib*, **2005**. 219(J5): p. 331-346.
9. ACEA, *Service fill oils for Gasoline Engines light duty Diesel Engines Engines with after Treatment Devices and Heavy Duty Diesel Engines*, in *ACEA European Oil Sequences*. 2010: Brussels. p. 14.
10. Inoue, K., Ogura, H., Igawa, S. and Takeda, K., *Effects of Lubricant Composition on Wear in Methanol-Fueled SI Engines*, in *International Fuels and Lubricants Meeting and Exposition*. 1993, SAE: Philadelphia.
11. Sillion, B., *Actual Chim.*, **2003**(10): p. 3-9.
12. Blau, P.J., *A Review of Sub-Scale Test Methods to Evaluate the Friction and Wear of Ring and Liner Materials for Spark- and Compression Ignition Engines*. 2001, U.S. Department of Energy.
13. Stark, M.S., J.J. Wilkinson, J.R.L. Smith, A. Alfadhil, and B.A. Pochopien, *Ind Eng Chem Res*, **2010**. 50(2): p. 817-823.
14. Blaine, S. and P.E. Savage, *Ind Eng Chem Res*, **1992**. 31(1): p. 69-75.
15. Owens. E.C., H.W. Marbach., E. Frame. and T. Ryan, *The Effects of Alcohol Fuels on Engine Wear*. **1980**, US Army Fuels and Lubricants Research Laboratory., DOI 10.4271/800857
16. Mahoney, L.R., K. Otto, S. Korcek, and M.D. Johnson, *Ind Eng Chem Prod Res Dev*, **1980**. 19(1): p. 11-15.
17. Spilners, I.J. and J.F., Hedenburg, Effect of Fuel and Lubricant Composition on Engine Deposit Formation, in *Symposium on Chemistry of Engine Combustion Deposits Presented before the Division of Petroleum Chemistry, Inc.* 1981, American Chemical Society: Atlanta.
18. Marbach, H.W., E.A. Frame, E.C. Owens, and D.W. Naegeli (1981) *The Effects of Alcohol Fuels and Fully Formulated Lubricants on Engine Wear*. DOI: 811199.

19. Winborn, L.D. and P.J. Shayler, *Proceedings of the Institution of Mechanical Engineers Part D-J Aut Eng*, **2001**. 215(D10): p. 1117-1130.
20. Stark, M.S., R.J. Gamble, C.J. Hammond, H.M. Gillespie, J.R. Lindsay Smith, E. Nagatomi, M.Priest, C.M. Taylor, R.I. Taylor and D.J. Waddington, *Trib Lett*, **2005**. 19(3): p.163-168
21. Marbach, H.W., E. Frame, E. Owens, D. Naegeli, *The Effects of Lubricant Composition on S.I. Engine Wear with Alcohol Fuels, US Army Fuels and Lubricants Research Laboratory*, DOI: 10.4271/831702.
22. Yasutomi, S., Y. Maeda, and T. Maeda, *Ind Eng Chem Prod Res Dev*, **1981**. 20(3): p. 530-536.
23. Gulwadi, S.D., *Tribology Transactions*, **2000**. 43(2): p. 151-162.
24. Moritani, H. and Y. Nozawa, *Oil Degradation in the second land region of Gasoline Engine Pistons.*, , R&D Review of Toyota CRDL, **2004**, 38(3): p. 36-43.
25. Morgan, J.D., *J. Chem. Soc.*, **1919**. 115: p. 94-104.
26. Bates, S.C., *Combust. Flame*, **1991**. 85(3-4): p. 331-352.
27. Fox, M.F., D.J. Picken, M.C.R. Symons, and A.L. Thomson, *Trib Int*, **1997**. 30(6): p. 417-422.
28. Blaine, S. and P.E. Savage, *Ind Eng Chem Res*, **1991**. 30(9): p. 2185-2191.
29. Blaine, S. and P.E. Savage, *Ind Eng Chem Res*, **1991**. 30(4): p. 792-798.
30. Saville, S.B., F.D. Gainey, S.D. Cupples, M.F. Fox, and D.J. Picken, *SAE International*, **1988**, SAE 881586.
31. Larsen, R.G., R.E. Thorpe and F.A. Armfield, *Ind Eng Chem Prod Res Dev*, **1942**. 34: p. 183-193.
32. George, P., E.K. Rideal, and A. Robertson, *Proc Roy Soc Lond Ser-A Mat Phys Sci*, **1946**. 185(1002): p. 288-309.
33. Mahoney, L.R., *Angew Chem Int Edit*, **1969**. 8(8): p. 547-555.
34. Jensen, R.K., S. Korcek, L.R. Mahoney, and M. Zinbo, *J Am Chem Soc*, **1979**. 101(25): p. 7574-7584.
35. Bordwell, F.G. and M.J. Bausch, *J. Am. Chem. Soc.*, **1986**. 108(8): p. 1979-1985.
36. Lide, D.R., *CRC Handbook of Chemistry and Physics*. 86 ed. 2005-2006: CRC.
37. Min, D.B., D. Ticknor, and D. Schweizer, *J Am Oil Chem Soc*, **1982**. 59(9): p. 378-380.
38. Jerzykiewicz, M., I. Cwielag, and W. Jerzykiewicz, *J Chem Technol Biot*, **2009**. 84(8): p. 1196-1201.
39. King, R.W., *J. Expo. Anal. Environ. Epidemiol.*, **1992**. 2(1): p. 9-22.
40. Bates, J.R., F.W. Rose, S.S. Kurtz, and I.W. Mills, *Ind. Eng. Chem.*, **1942**. 34: p. 147-152.
41. Griffiths J.F., B.J.A., *Flame and Combustion*. 3rd ed. 1996: Blackie Academic and Professional.
42. Coleman, L.E., *J I Petrol*, **1973**. 59(568): p. 154-163.
43. Chertkov, Y.B., E.A. Kunina, and T.I. Kirsanova, *J Appl Chem-USSR+*, **1980**. 53(7): p. 1245-1250.

44. Stark, M.S., *Identification and Quantification of Persistent Aromatic Free Radicals and Other Aromatic Species in Degraded Engine Lubricant*, in *STLE*. 2008: Cleveland, Ohio.
45. Igarashi, J., R.K. Jensen, J. Luszyk, S. Korcek, and K.U. Ingold, *J Am Chem Soc*, **1992**. 114(20): p. 7727-7736.
46. Igarashi, J., J. Luszyk, and K.U. Ingold, *J Am Chem Soc*, **1992**. 114(20): p. 7719-7726.
47. Shaddix, C.R., K. Brezinsky, and I. Glassman, *Combust Flame*, **1997**. 108(1-2): p. 139-157.
48. Ehrhardt, M.G., M.C. Bicego, and W.R. Weber, *J Photoch Photobio A*, **1997**. 108(2-3): p. 253-259.
49. Shayler, P.J. and C. Belton, *P I Mech Eng D-J Aut*, **1999**. 213(D2): p. 161-174.
50. Boons, M., *The Impact of E85 Use on Lubricant Performance*, 2008 SAE International Powertrains, Fuels and Lubricants Congress, **June 2008**.
51. Lieberzeit, P.A., G. Glanznig, A. Leidl, G. Voigt, and F.L. Dickert, *IEEE Sens J*, **2006**. 6(3): p. 529-535.
52. Pedersen, P.S., J. Ingwersen, T. Nielsen, and E. Larsen, *Environ Sci Technol*, **1980**. 14(1): p. 71-79.
53. Brandenberger, S., M. Mohr, K. Grob, and H.P. Neukomb, *Atmos Environ*, **2005**. 39(37): p. 6985-6994.
54. Reardon, M.R., L. Allen, E.C. Bender, and K.M. Boyle, *J Forensic Sci*, **2007**. 52(3): p. 656-663.
55. Cracknell, R.F. and M.S. Stark, *Influence of Fuel Properties on Lubricant Oxidative Stability: Part 2 - Chemical Kinetics Modelling*. **2005**, SAE 2007-01-0003.
56. Yoshida, T.W. and H. Watanbe, *Synthetic Oils*, **1987**: International Patent Number: 4714794.
57. Chrysler, M.C., *Chrysler's Plan for short-term and long term viability.*, in *Senate Committee on Banking, Housing and Urban Affairs*. 2008: Washington. p. 14.
58. Ford, M.C., *Ford Motor Company Buisness Plan*, in *Senate Banking Committee*. 2008: Washington. p. 33.
59. General Motors, C., *Restructuring Plan for Long-Term Viability*, in *Senate Banking Committee and House of Representatives Financial Services Committee*. 2008, GM Corporation: Washington. p. 37.
60. Wheals, A.E., L.C. Basso, D.M.G. Alves, and H.V. Amorim, *Trends Biotechnol*, **1999**. 17(12): p. 482-487.
61. Moreira, J.R. and J. Goldemberg, *Energy Policy*, **1999**. 27(4): p. 229-245.
62. Demirbas, A., *Energy Sources Part B-Economics Planning and Policy*, **2007**. 2(3): p. 311-320.
63. Wang, M., J. Wang, and J.X. Tan, *Energy Sources Part A-Recovery Utilization and Environmental Effects*, **2011**. 33(7): p. 612-619.
64. Powell, T., Hofstra University, *Racing Experiences With Methanol and Ethanol-Based Motor-Fuel Blends*. **1975**, DOI: 10.4271/750124.

65. Cunningham, L.J., *Method and compositions for reducing wear in engines combusting ethanol-containing fuels*, US Patent Number, US2008/0086936 A1
66. Lozano, P., D. Pioch, and G. Vaitilingom, *Jpc-Journal of Planar Chromatography-Modern Tlc*, **1999**. 12(3): p. 228-229.
67. Chui, G.K. and D.H.T. Millard, *Development and Testing of Crankcase Lubricants for Alcohol Fueled Engines*. **1981**, DOI: 10.4271/811203.
68. Schwartz, S.E., *Laboratory studies of the effects of methanol fuel on engine oil and iron.*, in *International symposium on alcohol fuels technology*. 1984: Ottawa, Ontario, Canada.
69. Naegeli, D.W., *Combustion-Associated Wear in Alcohol-Fueled Spark Ignition Engines.*, **1989**, DOI: 10.4271/891641
70. Shah, R., E. Klaus, and J.L. Duda, *Lub Eng*, **1996**. 52(10): p. 753-761.
71. Shah, R.J., J.L. Duda, and J. Perez, *Effect of alcohol fuels on lubricants: Oxidative and lubricity properties*, in *Abstracts of Papers of the American Chemical Society*. 1997. p. 125-130.
72. Kahlweit, M., R. Strey, and G. Busse, *J Phys Chem*, **1991**. 95(13): p. 5344-5352.
73. Besser, C., C. Schneidhofer, N. Dörr, F. Novotny-Farkas, and G. Allmaier, *Trib Int*, **2012**. 46(1): p. 174-182.
74. Scanlon, J.T. and D.E. Willis, *J. Chromatogr. Sci.*, **1985**. 23(8): p. 333-340.
75. Howard, J.A., K. Adamic, and K.U. Ingold, *Can J Chem*, **1969**. 47(20): p. 3793-&.
76. Howard, J.A. and K.U. Ingold, *Can J Chem*, **1967**. 45(8): p. 785-&.
77. Burn, A.J., R. Cecil, and V.O. Young, *J I Petrol*, **1971**. 57(558): p. 319-&.
78. Spikes, H., *Trib Lett*, **2004**. 17(3): p. 469-489.
79. Varlamov, V.T. and E.T. Denisov, *Russ Chem Bull*, **1987**. 36(8): p. 1607-1612.
80. Becker, R. and A. Knorr, *Lubr. Sci.*, **1996**. 8(2): p. 95-117.
81. Sharma, B.K., J.M. Perez, and S.Z. Erhan, *Energy & Fuels*, **2007**. 21(4): p. 2408-2414.
82. Vipper, A.B., *Lubri Sci*, **2004**. 16(2): p. 169-182.
83. Alfadhil, A., *PhD Thesis*, **2009**: p. 175-176.
84. Barnes, A.M., K.D. Bartle, and V.R.A. Thibon, *Trib Int*, **2001**. 34(6): p. 389-395.
85. Burn, A.J., *Tet*, **1966**. 22(7): p. 2153-2161.
86. Topolovec-Miklozic, K., T. Forbus, and H. Spikes, *Trib Lett*, **2007**. 26(2): p. 161-171.
87. Somayaji, A. and P.B. Aswath, *Trib Trans*, **2009**. 52(4): p. 511-525.
88. Palacios, J.M., *Trib Int*, **1986**. 19(1): p. 35-39.
89. Suominen Fuller, M.L., L. Rodriguez Fernandez, G.R. Massoumi, W.N. Lennard, M. Kasrai, and G.M. Bancroft, *Trib Lett*, **2000**. 8(4): p. 187-192.
90. Aktary, M., M.T. McDermott, and G.A. McAlpine, *Trib Lett*, **2002**. 12(3): p. 155-162.
91. Yin, Z., M. Kasrai, M. Fuller, G.M. Bancroft, K. Fyfe, and K.H. Tan, *Wear*, **1997**. 202(2): p. 172-191.

92. Martin, J.M., C. Grossiord, T. Le Mogne, S. Bec, and A. Tonck, *Trib Int*, **2001**. 34(8): p. 523-530.
93. Dato, A.N.G., M.F. Fox, D. Dowson, M. Priest, D. Dalmaz, and A.A. Lubrecht, *Trib Int Eng*, **2003**. 41: p. 517-522.
94. Naidu, S.K., E.E. Klaus, and J.L. Duda, *Ind Eng ChemProd Res Dev*, **1986**. 25(4): p. 596-603.
95. Gaussian 09, Revision **A.1**, M. J. Frisch, G. W. Trucks, H. B. Schlegel, G. E. Scuseria, M. A. Robb, J. R. Cheeseman, G. Scalmani, V. Barone, B. Mennucci, G. A. Petersson, H. Nakatsuji, M. Caricato, X. Li, H. P. Hratchian, A. F. Izmaylov, J. Bloino, G. Zheng, J. L. Sonnenberg, M. Hada, M. Ehara, K. Toyota, R. Fukuda, J. Hasegawa, M. Ishida, T. Nakajima, Y. Honda, O. Kitao, H. Nakai, T. Vreven, J. A. Montgomery, Jr., J. E. Peralta, F. Ogliaro, M. Bearpark, J. J. Heyd, E. Brothers, K. N. Kudin, V. N. Staroverov, R. Kobayashi, J. Normand, K. Raghavachari, A. Rendell, J. C. Burant, S. S. Iyengar, J. Tomasi, M. Cossi, N. Rega, J. M. Millam, M. Klene, J. E. Knox, J. B. Cross, V. Bakken, C. Adamo, J. Jaramillo, R. Gomperts, R. E. Stratmann, O. Yazyev, A. J. Austin, R. Cammi, C. Pomelli, J. W. Ochterski, R. L. Martin, K. Morokuma, V. G. Zakrzewski, G. A. Voth, P. Salvador, J. J. Dannenberg, S. Dapprich, A. D. Daniels, Ö. Farkas, J. B. Foresman, J. V. Ortiz, J. Cioslowski, and D. J. Fox, Gaussian, Inc., Wallingford CT, 2009.
96. Gately, D., *Japan and the World Economy*, **1993**. 5(4): p. 295-320.
97. Shukla, D.S., A.K. Gondal, and P.C. Nautiyal, *Wear*, **1992**. 157(2): p. 371-380.
98. Shukla, D.S. and P.C. Nautiyal, *Laboratory studies on the effect of methanol fuel on engine wear and lubricant degradation*. **1991**, Indian Institute of Petroleum, Dehradun, India.
99. Sorab, J. and G.K. Chui, *Rheological Characterization of Lubricant Methanol Water Emulsions*, in *International Fuels and Lubricants Meeting and Exposition*. **1992**, SAE: San Francisco, DOI: 922283
100. Moritani, H., M. Yoshiyuki, and N. Masahiko, *JSAE Review*, **1994**. 15(3): p. 242-244.
101. French, R. and P. Malone, *Fluid Phase Equilibria*, **2005**. 228: p. 27-40.
102. Bakunin, V.N., G.N. Kuzmina, and O.P. Parenago, *Pet Chem*, **1997**. 37(2): p. 93-98.
103. Finzi, L. and D.D. Dunlap, *Polarized Light Microscopy*, in *eLS*. **2001**, John Wiley & Sons, Ltd.
104. Paddock, S., *Mol Bio*, **2000**. 16(2): p. 127-149.
105. Barnett, C.E., *J Phys Chem*, **1942**. 46(1): p. 69-75.
106. Kraiwattanawong, K., H.S. Fogler, S.G. Gharfeh, P. Singh, W.H. Thomason, and S. Chavadej, *Energy & Fuels*, **2009**. 23: p. 1575-1582.
107. Pozharski, E.V., L. McWilliams, and R.C. MacDonald, *Anal Bio*, **2001**. 291(1): p. 158-162.
108. Richardson, E.G., *Proc Phys Soc*, **1943**. 55: p. 0048-0063.
109. Brown, W.J., T.R. Sullivan, and P. Greenspan, *Histochem Cell Biol*, **1992**. 97(4): p. 349-354.
110. Cser, A., K. Nagy, and L. Biczók, *Chem Phys Lett*, **2002**. 360(5-6): p. 473-478.

111. Datta, A., D. Mandal, S.K. Pal, and K. Bhattacharyya, *J Phys Chem-US B*, **1997**. 101(49): p. 10221-10225.
112. Fowler, S.D. and P. Greenspan, *J Histochem Cytochem*, **1985**. 33(8): p. 833-6.
113. Greenspan, P. and P. Lou, *Int J Biochem*, **1993**. 25(7): p. 987-991.
114. Greenspan, P., E.P. Mayer, and S.D. Fowler, *J Cell Biol*, **1985**. 100(3): p. 965-973.
115. Jose, J. and K. Burgess, *J Org Chem*, **2006**. 71(20): p. 7835-7839.
116. Krishna, M.M.G., *J Phys Chem A*, **1999**. 103(19): p. 3589-3595.
117. Nagy, K., S. Gokturk, and L. Biczok, *J Phys Chem A*, **2003**. 107(41): p. 8784-8790.
118. Sackett, D.L. and J. Wolff, *Anal Biochem*, **1987**. 167(2): p. 228-234.
119. Bakunin, V.N., G.N. Kuz'mina, and O.P. Parenago, *Lubr Scie*, **2004**. 16(3): p. 255-266.
120. Bakunin, V.N., Z.V. Popova, E.Y. Oganeseva, G.N. Kuz'mina, V.V. Kharitonov, and O.P. Parenago, *Pet Chem*, **2001**. 41(1): p. 37-42.
121. Oganeseva, E.Y., V.N. Bakunin, E.G. Bordubanova, G.N. Kuz'mina, and O.P. Parenago, *Pet Chem*, **2005**. 45(4): p. 268-274.
122. Oganeseva, E.Y., E.G. Bordubanova, G.N. Kuz'mina, V.N. Bakunin, and O.P. Parenago, *Pet Chem*, **2009**. 49(4): p. 311-316.
123. Oganeseva, E.Y., E.G. Bordubanova, Z.V. Popova, V.N. Bakunin, G.N. Kuz'mina, and O.P. Parenago, *Pet Chem*, **2004**. 44(2): p. 99-105.
124. Parenago, O.P., G.N. Kuz'mina, V.N. Bakunin, R.G. Shelkova, and T.A. Zaimovskaya, *Pet Chem*, **1995**. 35(3): p. 210-218.
125. Parenago, O.P., G.N. Kuz'mina, V.N. Bakunin, and E.Y. Oganeseva, *Russ J Gen Chem*, **2009**. 79(6): p. 1390-1399.
126. Parenago, O.P., G.N. Kuz'mina, and V.N. Bakunin, *Problems of inhibiting the high-temperature oxidation of hydrocarbons*, in *Additives'97 - Additives in Petroleum Refinery and Petroleum Product Formulation Practice, Proceedings*, A. Kovacs, Editor. 1997, Hungarian Chemical Soc: Budapest. p. 81-88.
127. Porter, W.L., E.D. Black, and A.M. Drolet, *J Agri Food Chem*, **1989**. 37(3): p. 615-624.
128. Porter, W.L., M.G. Simic, and M. Karel, *Autoxidation in Food and Biological Systems*, Plenum Publishing Corporation, **1980**. p.295.
129. Laguerre, M.I., L.J. López Giraldo, J. Lecomte, M.-C. Figueroa-Espinoza, B. Bareì, J. Weiss, E.A. Decker, and P. Villeneuve, *J Agri Food Chem*, **2009**. 57(23): p. 11335-11342.
130. Zhong, Y. and F. Shahidi, *J Agri Food Chem*, **2011**. 60(1): p. 4-6.
131. Bondet, V., M.E. Cuvelier, and C. Berset, *J Am Oil Chem Soc*, **2000**. 77(8): p. 813-818.
132. Chaiyasit, W., R.J. Elias, D.J. McClements, and E.A. Decker, *Crit Rev Food Sci*, **2007**. 47(3): p. 299-317.
133. Chaiyasit, W., D.J. McClements, and E.A. Decker, *J Agric Food Chem*, **2005**. 53(12): p. 4982-4988.
134. Chen, B., A. Han, M. Laguerre, D.J. McClements, and E.A. Decker, *Food & Function*, **2011**. 2(6).

135. Chen, B.C., A. Han, D.J. McClements, and E.A. Decker, *J Agric Food Chem*, **2010**. 58(22): p. 11993-11999.
136. Frankel, E.N., *J Sci Food Agric*, **1991**. 54(4): p. 495-511.
137. Heins, A., D. McPhail, T. Sokolowski, H. Stöckmann, and K. Schwarz, *Lipids*, **2007**. 42(6): p. 573-582.
138. Kasaikina, O.T., V.D. Kortenska, Z.S. Kartasheva, G.M. Kuznetsova, T.V. Maximova, T.V. Sirota, and N.V. Yanishlieva, *Colloid Surface A*, **1999**. 149(1-3): p. 29-38.
139. Laguerre, M.I., L.J. López Giraldo, J.r.m. Lecomte, M.-C. Figueroa-Espinoza, B. Baréa, J. Weiss, E.A. Decker, and P. Villeneuve, *J Agric Food Chem*, **2010**. 58(5): p. 2869-2876.
140. Richards, M.P., W. Chaiyasit, D.J. McClements, and E.A. Decker, *J Agric Food Chem*, **2002**. 50(5): p. 1254-1259.
141. Yuji, H., J. Weiss, P. Villeneuve, L.J. López Giraldo, M.-C. Figueroa-Espinoza, and E.A. Decker, *J Agric Food Chem*, **2007**. 55(26): p. 11052-11056.
142. Zhu, X., K.M. Schaich, X. Chen, D. Chung, and K.L. Yam, *Food Res Int*, **2012**. 47(1): p. 1-5.
143. Chaiyasit, W., M.P.C. Silvestre, D.J. McClements, and E.A. Decker, *J Agric Food Chem*, **2000**. 48(8): p. 3077-3080.
144. Cho, Y.-J., D.J. McClements, and E.A. Decker, *J Agric Food Chem*, **2002**. 50(20): p. 5704-5710.
145. Nuchi, C.D., P. Hernandez, D.J. McClements, and E.A. Decker, *J Agric Food Chem*, **2002**. 50(19): p. 5445-5449.
146. Silvestre, M.P.C., W. Chaiyasit, R.G. Brannan, D.J. McClements, and E.A. Decker, *J Agric Food Chem*, **2000**. 48(6): p. 2057-2061.
147. Chen, B., D.J. McClements, D.A. Gray, and E.A. Decker, *Food Chem.*, **2012**. 132(3): p. 1514-1520.
148. Cuvelier, M.E., V. Bondet, and C. Berset, *J Am Oil Chem Soc*, **2000**. 77(8): p. 819-823.
149. Cuvelier, M.E., L. Lagunes-Galvez, and C. Berset, *J Am Oil Chem Soc*, **2003**. 80(11): p. 1101-1105.
150. Frankel, E.N., S.-W. Huang, J. Kanner, and J.B. German, *J Agric Food Chem*, **1994**. 42(5): p. 1054-1059.
151. Sasaki, K., J. Alamed, J. Weiss, P. Villeneuve, L.J. López Giraldo, J. Lecomte, M.-C. Figueroa-Espinoza, and E.A. Decker, *Food Chem*, **2010**. 118(3): p. 830-835.
152. Stöckmann, H., K. Schwarz, and T. Huynh-Ba, *J Am Oil Chem Soc*, **2000**. 77(5): p. 535-542.
153. Panya, A., M. Laguerre, J. Lecomte, P. Villeneuve, J. Weiss, D.J. McClements, and E.A. Decker, *J Agric Food Chem*, **2010**. 58(9): p. 5679-5684.
154. Peña, A.A. and C.A. Miller, *Adv Colloid Interface Sci*, **2006**. 123-126: p. 241-257.
155. Oehlke, K., A. Heins, H. Stöckmann, and K. Schwarz, *Food Chem*, **2010**. 118(1): p. 48-55.
156. Shahidi, F. and Y. Zhong, *J Agric Food Chem*, **2011**. 59(8): p. 3499-3504.

157. Denisova, T. and E. Denisov, *Russ. Chem. Bull.*, **2008**. 57(9): p. 1858-1866.
158. Benson, S.W. and P.S. Nangia, *Acc of Chem Res*, **1979**. 12(7): p. 223-228.
159. Ingold, K.U., *ChemRev*, **1961**. 61(6): p. 563-589.
160. Vipper, A.B. and V.A. Tarasov, *Synergistic Effect of Succinimide and Bisphenol Additives*. *Russ. Chem. Bull.*, **1998**. 47(9): p. 300-303
161. Frankel, E.N. and A.S. Meyer, *J Sci Food Agric*, **2000**. 80(13): p. 1925-1941.
162. Chaiyasit, W., C. Stanley, H. Strey, D. McClements, and E. Decker, *Food Biophysics*, **2007**. 2(2): p. 57-66.
163. Benson, S.W., *J. Am. Chem. Soc.*, **1965**. 87(5): p. 972-979.
164. Chandra, A. and T. Uchimaru, *Int J Mol Sci*, **2002**. 3(4): p. 407-422.
165. Pratt, D.A., J.H. Mills, and N.A. Porter, *J Am Chem Soc*, **2003**. 125(19): p. 5801-5810.
166. Pratt, D.A. and N.A. Porter, *Org Lett*, **2003**. 5(4): p. 387-390.
167. Kranenburg, M., M.V. Ciriano, A. Cherkasov, and P. Mulder, *J Phys Chem A*, **2000**. 104(5): p. 915-921.
168. Fenter, F.F., B. Nozière, F. Caralp, and R. Lesclaux, *Int J Chem Kin*, **1994**. 26(1): p. 171-189.
169. Knyazev, V.D. and I.R. Slagle, *J Phys Chem A*, **1998**. 102(10): p. 1770-1778.
170. Hourani, M.J., E.T. Hessell, R.A. Abramshe, and J. Liang, *TribTrans*, **2007**. 50(1): p. 82-87.
171. Ingold, K.U., *Acc Chem Res*, **1969**. 2(1): p. 1-9.
172. Tandon, A., A. Kumar, P. Mondal, P. Vijay, U.D. Bhangale, and D. Tyagi, *Brit Jour Env Cli Cha*, **2011**. 1(2): p. 28-43.
173. Roman-Leshkov, Y., C.J. Barrett, Z.Y. Liu, and J.A. Dumesic, *Nature*, **2007**. 447(7147): p. 982-U5.